METHODS FOR IMPROVING THE SAFETY OF FLUOROPYRIMIDINE ANTICANCER DRUGS

Bart A.W. Jacobs

METHODS FOR IMPROVING THE SAFETY OF FLUOROPYRIMIDINE ANTICANCER DRUGS

Methodes ter verbetering van de veiligheid van de anti-kanker geneesmiddelen behorende tot de groep van fluoropyrimidines
(met een samenvatting in het Nederlands)

Proefschrift

ter verkrijging van de graad van doctor aan de Universiteit Utrecht op gezag van de rector magnificus, prof.dr. G.J. van der Zwaan, ingevolge het besluit van het college voor promoties in het openbaar te verdedigen op woensdag 30 november 2016 des middags te 2.30 uur

door

Bart Albertus Wilhelmus Jacobs
geboren op 27 september 1985 te Winssen

PROMOTOREN

Prof. dr. J.H.M. Schellens
Prof. dr. J.H. Beijnen

COPROMOTOR

dr. B. Nuijen

TABLE OF CONTENTS

PREFACE

The fluoropyrimidine capecitabine is an important anti-cancer drug for the treatment of several solid tumours. The European Commission approved the drug in 2001 for the treatment of metastatic colorectal cancer. In the following years, capecitabine became subsequently available for the treatment of metastatic breast cancer, adjuvant colon cancer and advanced gastric cancer.

Capecitabine is a pre-pro-drug of 5-fluorouracil (5-FU). A major advantage of capecitabine over intravenous (IV) 5-FU therapy is the availability of oral tablet formulations, which allows patients to take capecitabine at home. Moreover, capecitabine was found to be at least as effective as IV 5-FU therapy and demonstrated a favourable safety profile [1–4]. Therefore, oral capecitabine treatment largely replaced IV 5-FU therapy.

Metabolic pathway of capecitabine

Capecitabine tablets are preferably ingested within 30 minutes after a meal, since all pivotal clinical studies were conduced following this procedure. Although the administration of food has shown to delay the capecitabine absorption rate and to reduce the maximum plasma concentrations and the area under the plasma concentration-time curve of capecitabine, it does not lead to significantly reduced plasma exposure in 5-FU [5]. Therefore, the effect of food was considered clinically irrelevant [6]. Following absorption, capecitabine is enzymatically converted within the liver to the intermediate metabolites 5'-deoxy-5-fluorocytidine (dFCR), 5'-deoxy-5-fluoro-uridine (dFUR) and 5-FU [6]. These reactions are catalysed by the enzymes carboxylesterase, cytidine deaminase and thymidine phosphorylase (TP), respectively [6,7]. Intratumoral TP expression is relatively high, which also enables conversion of dFUR to 5-FU within tumour tissue [8,9]. The average maximum capecitabine, dFCR, dFUR and 5-FU plasma concentrations are observed approximately 1-1.5 hours after capecitabine intake [5,10,11]. Around 80% of the formed 5-FU is rapidly catabolized to inactive metabolites [12]. The first step of 5-FU catabolism is regulated by the enzyme dihydropyrimidine dehydrogenase (DPD), which catalyses the conversion of 5-FU into dihydro-5-fluorouracil (FUH_2) [12]. FUH_2 is further catabolised to other inactive metabolites and eventually renally excreted [6,12]. Only a small fraction of 5-FU is eventually intracellularly anabolized to molecules that possess anti-cancer properties by inhibition of DNA and RNA synthesis. The main route of inhibition of DNA synthesis is achieved by blocking the enzyme thymidylate synthase (TS), an enzyme that is important for *de novo* DNA synthesis [13].

Tolerability of capecitabine

The safety profile of capecitabine is generally acceptable. Nevertheless, approximately 25% of the patients experience severe treatment-induced toxicity, of which vomiting, diarrhoea, stomatitis and hand-foot syndrome are most common [1–4,14]. About 12% of patients treated with capecitabine require hospital admission for treatment-induced toxicity [2,14]. Treatment-related death occurs in approximately 1% of the patients [15].

Since capecitabine is frequently used, the absolute number of patients experiencing treatment-induced toxicity is substantial.

A well-recognized cause of severe fluoropyrimidine-induced toxicity is DPD deficiency. Deficiency in the enzyme DPD leads to reduced 5-FU degradation, which, in turn, leads to increased systemic 5-FU exposure [16]. Some polymorphisms in the gene encoding DPD, *DPYD*, are associated with DPD deficiency and fluoropyrimidine-induced toxicity. In particular, the *DPYD**2A allele and the c.1679T>G, c.1236G>A, c.2846A>T mutations have been associated with an increased risk of severe toxicity [17–19]. Fluoropyrimidine dose reductions have been recommended for patients carrying these mutations [17,20].

Although genotyping analysis has been shown useful for the identification of patients at risk of severe fluoropyrimidine-induced toxicity, the combined sensitivity of genotyping analysis concerning the four polymorphisms in *DPYD* remains low [19]. Besides, most patients are heterozygous carriers of a *DPYD* risk allele and also carry one functional allele. Consequently, not all patients who carry a mutation in *DPYD* mutation are poor metabolizers of 5-FU and some of these patients do not require upfront dose modifications.

Since highly sensitive biomarkers are unavailable, identification of patients who are at risk of severe fluoropyrimidine-induced toxicity remains challenging. There are, however, alternative methods for the identification of DPD deficiency by assessing the DPD phenotype instead of the *DPYD* genotype. The most often applied DPD phenotyping method is based on *ex vivo* quantification of DPD activity in human peripheral blood mononuclear cells (PBMCs) [21]. DPD activity in PBMCs correlates with systemic clearance of 5-FU [22] and has been associated with fluoropyrimidine-induced toxicity [21,23,24]. Other DPD phenotyping approaches are based on quantification of plasma levels of the endogenous DPD substrate uracil and the reaction product dihydrouracil [25], and assessment of uracil clearance after administration of an uracil loading dose [26]. Although the applicability of DPD phenotype markers is promising, optimization of bioanalytical assays is warranted in order to apply DPD phenotyping assays in clinical practise [25,27]. Besides the enzyme DPD, multiple other enzymes are important for activation and inactivation of capecitabine and 5-FU. Exploring the role of phenotypic markers of other enzymes within the capecitabine pathway could attribute to better identification of patients at risk of toxicity. Additional research is necessary to investigate the role of phenotyping assays for improving fluoropyrimidine treatment safety.

Circadian rhythmicity

Previous studies have demonstrated that the enzyme DPD might be subject to circadian rhythmicity [28,29]. A circadian rhythm in the target enzyme TS has also been proposed [30]. Circadian rhythmicity in these two enzymes might have consequences for the catabolism and pharmacodynamics of 5-FU. Moreover, this might influence the safety and efficacy of fluoropyrimidine treatment. A previous study performed by Levi et al. demonstrated that the time of IV 5-FU administration influences treatment safety and efficacy. In their study, nocturnal 5-FU administration was found to be less toxic and

more effective than constant-rate 5-FU infusion [31]. It was expected that the favourable efficacy and tolerability profile of chronomodulated 5-FU administration was the result of relatively high DPD activity and relatively low TS activity during the night [31,32]. In current clinical practise, however, fluoropyrimidine treatment schedules that are adapted to circadian rhythmicity in DPD and TS activity have not been implemented yet. These so called chronotherapeutic regimens remain controversial, since translational data supporting fluoropyrimidine chronotherapy are inconsistent [28,29,33].

Pharmacokinetics of capecitabine and metabolites

Several clinical studies have been performed in which the pharmacokinetics of capecitabine and metabolites were evaluated [6]. Most of the pharmacokinetic analyses were performed for capecitabine and each metabolite independently using non-compartmental analysis [6]. Non-compartmental analysis is, however, not ideal for the estimation of inter-patient and intra-patient variability in the capecitabine and metabolite pharmacokinetics. Investigation of capecitabine and metabolite pharmacokinetics using non-linear mixed effects modeling would be more appropriate for estimation of these variabilities. Additional pharmacokinetic research is needed in order to provide better understanding of capecitabine and metabolite pharmacokinetics. Moreover, non-linear mixed effects modeling allows for investigation of covariate effects, such as DPD deficiency, on 5-FU exposure after the intake of capecitabine tablets.

Previous pharmacokinetic studies did, however, demonstrate that capecitabine, dFCR, dFUR and 5-FU are completely cleared from human plasma approximately six hours after ingestion of capecitabine tablets [10,11]. Given the recommended capecitabine dosing schedule of twice daily administration, there is an expected gap in capecitabine and 5-FU plasma exposure of approximately six hours within each dosing interval. Importantly, continuous administration of 5-FU has been shown to improve treatment tolerability and efficacy compared to bolus administration of intravenous 5-FU treatment [34]. The currently available capecitabine tablet formulations more closely resemble the pharmacokinetic profile of 5-FU after bolus instead of continuous intravenous administration. Therefore, it is expected that the currently available capecitabine formulation might not possess the pharmacokinetic properties for most optimal treatment efficacy and safety. The availability of an extended-release formulation of capecitabine could overcome these limitations by facilitating more continuous exposure to capecitabine and 5-FU. This, in turn, might lead to improved treatment safety and efficacy.

AIMS OF THIS THESIS

Although capecitabine was introduced 15 years ago, it remains the mainstay for treatment of gastro-intestinal and breast cancer. In 2014, 11,993 patients in the Netherlands were treated with this drug [35]. The total number of capecitabine prescriptions in the Netherlands in 2014 was 78,069 [35], which was the highest number over the last five years.

This thesis includes several studies that have been performed in order to: (1) develop and validate phenotypic assays that might contribute to improved identification of patients at risk of toxicity, (2) improve the current knowledge of capecitabine pharmacokinetics and pharmacodynamics, and (3) explore the pharmacology of alternative capecitabine tablet formulations and chronomodulated treatment regimens.

The general aim of these studies was to obtain a better insight into capecitabine pharmacology and to explore opportunities for improved capecitabine tolerability.

THESIS OUTLINE

The development and validation of phenotypic assays is described in the first part of this thesis. **Chapter 1** and **chapter 2** are focussed on the development of two different phenotypic methods for assessing DPD activity in human plasma and PBMCs, respectively. In **chapter 3**, the development and validation of a phenotypic assay of TP activity in PBMCs is described.

The second part of this thesis presents translational and clinical studies in which the developed phenotypic methods have been applied. **Chapter 4** is focussed on circadian rhythmicity in DPD and TS activity in human volunteers. In **chapter 5**, we studied the effect of liver resection on DPD activity in patients with colorectal liver metastases. The roles of genotypic variability in the gene encoding TS, *TYMS*, and phenotypic variability in TS activity on fluoropyrimidine treatment safety are described in **chapter 6**.

The third part of this thesis includes pharmacokinetic studies of capecitabine and metabolites. **Chapter 7** describes a population pharmacokinetic model of capecitabine and four metabolites pharmacokinetics, in which the effect of the *DPYD**2A mutation on 5-FU elimination has been included. A phase 0 clinical trial of candidate extended-release formulations of capecitabine is presented in **chapter 8**. In **chapter 9**, we present an exploratory study of the intracellular pharmacokinetics of an active metabolite in patients who were treated with capecitabine.

The fourth part is focused on optimization of capecitabine therapy using an alternative capecitabine dosing strategy. An interim analysis of a phase I study of chronomodulated capecitabine therapy is described in **chapter 10**.

The results of all studies described in this thesis are summarized and put into a perspective in the **conclusions and perspectives** section.

REFERENCES

1. Hoff PM, Ansari R, Batist G, Cox J, Kocha W, Kuperminc M, et al. Comparison of oral capecitabine versus intravenous fluorouracil plus leucovorin as first-line treatment in 605 patients with metastatic colorectal cancer: results of a randomized phase III study. J Clin Oncol 2001;19:2282–92.

2. Van Cutsem E, Twelves C, Cassidy J, Allman D, Bajetta E, Boyer M, et al. Oral capecitabine compared with intravenous fluorouracil plus leucovorin in patients with metastatic colorectal cancer: results of a large phase III study. J Clin Oncol 2001;19:4097–106.

3. Twelves C, Wong A, Nowacki MP, Abt M, Burris H, Carrato A, et al. Capecitabine as adjuvant treatment for stage III colon cancer. N Engl J Med 2005;352:2696–704.

4. Kang Y-K, Kang W-K, Shin D-B, Chen J, Xiong J, Wang J, et al. Capecitabine/cisplatin versus 5-fluorouracil/cisplatin as first-line therapy in patients with advanced gastric cancer: a randomised phase III noninferiority trial. Ann Oncol 2009;20:666–73.

5. Reigner B, Verweij J, Dirix L, Cassidy J, Twelves C, Allman D, et al. Effect of food on the pharmacokinetics of capecitabine and its metabolites following oral administration in cancer patients. Clin Cancer Res 1998;4:941–8.

6. Reigner B, Blesch K, Weidekamm E. Clinical pharmacokinetics of capecitabine. Clin Pharmacokinet 2001;40:85–104.

7. Judson IR, Beale PJ, Trigo JM, Aherne W, Crompton T, Jones D, et al. A human capecitabine excretion balance and pharmacokinetic study after administration of a single oral dose of ^{14}C-labelled drug. Invest New Drugs 1999;17:49–56.

8. Miwa M, Ura M, Nishida M, Sawada N, Ishikawa T, Mori K, et al. Design of a novel oral fluoropyrimidine carbamate, capecitabine, which generates 5 fluorouracil selectively in tumours by enzymes concentrated in human liver and cancer tissue. Eur J Cancer 1998;34:1274–81.

9. Schüller J, Cassidy J, Dumont E, Roos B, Durston S, Banken L, et al. Preferential activation of capecitabine in tumor following oral administration to colorectal cancer patients. Cancer Chemother Pharmacol 2000;45:291–7.

10. Budman DR, Meropol NJ, Reigner B, Creaven PJ, Lichtman SM, Berghorn E, et al. Preliminary studies of a novel oral fluoropyrimidine carbamate: capecitabine. J Clin Oncol 1998;16:1795–802.

11. Mackean M, Planting A, Twelves C, Schellens J, Allman D, Osterwalder B, et al. Phase I and pharmacologic study of intermittent twice-daily oral therapy with capecitabine in patients with advanced and/or metastatic cancer. J Clin Oncol 1998;16:2977–85.

12. Heggie GD, Sommadossi JP, Cross DS, Huster WJ, Diasio RB. Clinical pharmacokinetics of 5-fluorouracil and its metabolites in plasma, urine, and bile. Cancer Res 1987;47:2203–6.

13. Longley DB, Harkin DP, Johnston PG. 5-fluorouracil: mechanisms of action and clinical strategies. Nat Rev Cancer 2003;3:330–8.

14. Cassidy J, Twelves C, Van Cutsem E, Hoff P, Bajetta E, Boyer M, et al. First-line oral capecitabine therapy in metastatic colorectal cancer: A favorable safety profile compared with intravenous 5-fluorouracil/leucovorin. Ann Oncol 2002;13:566–75.

15. Mikhail SE, Sun JF, Marshall JL. Safety of capecitabine: a review. Expert Opin Drug Saf 2010;9:831–41.

16. van Kuilenburg ABP, Häusler P, Schalhorn A, Tanck MWT, Proost JH, Terborg C, et al. Evaluation of 5-fluorouracil pharmacokinetics in cancer patients with a c.1905+1G>A mutation in DPYD by means of a Bayesian limited sampling strategy. Clin Pharmacokinet 2012;51:163–74.

17. Deenen MJ, Meulendijks D, Cats A, Sechterberger MK, Severens JL, Boot H, et al. Upfront Genotyping of DPYD*2A to Individualize Fluoropyrimidine Therapy: A Safety and Cost Analysis. J Clin Oncol 2016;34:227–34.

18. Terrazzino S, Cargnin S, Del Re M, Danesi R, Canonico PL, Genazzani AA. DPYD IVS14+1G>A and 2846A>T genotyping for the prediction of severe fluoropyrimidine-

related toxicity: a meta-analysis. Pharmacogenomics 2013;14:1255–72.

19. Meulendijks D, Henricks LM, Sonke GS, Deenen MJ, Froehlich TK, Amstutz U, et al. Clinical relevance of DPYD variants c.1679T>G, c.1236G>A/HapB3, and c.1601G>A as predictors of severe fluoropyrimidine-associated toxicity: a systematic review and meta-analysis of individual patient data. Lancet Oncol 2015;16:1639–50.

20. Henricks LM, Lunenburg CA, Meulendijks D, Gelderblom H, Cats A, Swen JJ, et al. Translating DPYD genotype into DPD phenotype: using the DPYD gene activity score. Pharmacogenomics 2015:1–10.

21. van Kuilenburg AB, Haasjes J, Richel DJ, Zoetekouw L, Van Lenthe H, De Abreu RA, et al. Clinical implications of dihydropyrimidine dehydrogenase (DPD) deficiency in patients with severe 5-fluorouracil-associated toxicity: identification of new mutations in the DPD gene. Clin Cancer Res 2000;6:4705–12.

22. Fleming RA, Milano G, Thyss A, Etienne MC, Renée N, Schneider M, et al. Correlation between dihydropyrimidine dehydrogenase activity in peripheral mononuclear cells and systemic clearance of fluorouracil in cancer patients. Cancer Res 1992;52:2899–902.

23. Van Kuilenburg ABP, Meinsma R, Zoetekouw L, Van Gennip AH. Increased risk of grade IV neutropenia after administration of 5-fluorouracil due to a dihydropyrimidine dehydrogenase deficiency: High prevalence of the IVS14+1G>A mutation. Int J Cancer 2002;101:253–8.

24. Milano G, Etienne MC, Pierrefite V, Barberi-Heyob M, Deporte-Fety R, Renée N. Dihydropyrimidine dehydrogenase deficiency and fluorouracil-related toxicity. Br J Cancer 1999;79:627–30.

25. Sistonen J, Büchel B, Froehlich TK, Kummer D, Fontana S, Joerger M, et al. Predicting 5-fluorouracil toxicity: DPD genotype and 5,6-dihydrouracil:uracil ratio. Pharmacogenomics 2014;15:1653–66.

26. van Staveren MC, Theeuwes-Oonk B, Guchelaar HJ, van Kuilenburg ABP, Maring JG. Pharmacokinetics of orally administered uracil in healthy volunteers and in DPD-deficient patients, a possible tool for screening of DPD deficiency. Cancer Chemother Pharmacol 2011;68:1611–7.

27. van Staveren MC, Jan Guchelaar H, van Kuilenburg ABP, Gelderblom H, Maring JG. Evaluation of predictive tests for screening for dihydropyrimidine dehydrogenase deficiency. Pharmacogenomics J 2013:1–7.

28. Jiang H, Lu J, Ji J. Circadian rhythm of dihydrouracil/uracil ratios in biological fluids: a potential biomarker for dihydropyrimidine dehydrogenase levels. Br J Pharmacol 2004;141:616–23.

29. Harris BE, Song R, Soong SJ, Diasio RB. Relationship between dihydropyrimidine dehydrogenase activity and plasma 5-fluorouracil levels with evidence for circadian variation of enzyme activity and plasma drug levels in cancer patients receiving 5-fluorouracil by protracted continuous infusion. Cancer Res 1990;50:197–201.

30. Bjarnason GA, Jordan RC, Wood PA, Li Q, Lincoln DW, Sothern RB, et al. Circadian expression of clock genes in human oral mucosa and skin: association with specific cell-cycle phases. Am J Pathol 2001;158:1793–801.

31. Lévi F, Zidani R, Misset J. Randomised multicentre trial of chronotherapy with oxaliplatin, fluorouracil, and folinic acid in metastatic colorectal cancer. Lancet 1997;350:681–6.

32. Lévi F, Okyar A, Dulong S, Innominato PF, Clairambault J. Circadian timing in cancer treatments. Annu Rev Pharmacol Toxicol 2010;50:377–421.

33. Van Kuilenburg AB, Poorter RL, Peters GJ, Van Gennip AH, Van Lenthe H, Stroomer AE, et al. No circadian variation of dihydropyrimidine dehydrogenase, uridine phosphorylase, beta-alanine, and 5-fluorouracil during continuous infusion of 5-fluorouracil. Adv Exp Med Biol 1998;431:811–6.

34. Meta-analysis Group In Cancer. Efficacy of intravenous continuous infusion of fluorouracil compared with bolus administration in advanced colorectal cancer. J Clin Oncol 1998;16:301–8.

35. GIP / Zorginstituut Nederland. Aantal gebruikers 2010-2014 voor ATC-subgroep L01BC06 : Capecitabine 2014. www.gipdatabank.nl.

PART 1

DEVELOPMENT AND VALIDATION
OF PHENOTYPING METHODS

CHAPTER 1

DEVELOPMENT AND VALIDATION OF A RAPID AND SENSITIVE UPLC-MS/MS METHOD FOR DETERMINATION OF URACIL AND DIHYDROURACIL IN HUMAN PLASMA

Bart A.W. Jacobs, Hilde Rosing, Niels de Vries, Didier Meulendijks, Linda M. Henricks, Jan H.M. Schellens, Jos H. Beijnen

ABSTRACT

Quantification of the endogenous dihydropyrimidine dehydrogenase (DPD) substrate uracil (U) and the reaction product dihydrouracil (UH$_2$) in plasma might be suitable for identification of patients at risk of fluoropyrimidine-induced toxicity as a result of DPD deficiency. In this paper, we describe the development and validation of a rapid and sensitive ultra-performance liquid chromatography – tandem mass spectrometry (UPLC-MS/MS) assay for quantification of U and UH$_2$ in human plasma.

Analytes were extracted by protein precipitation, chromatographically separated on an Acquity UPLC® HSS T3 column with gradient elution and analyzed with a tandem mass spectrometer equipped with an electrospray ionization source. U was quantified in the negative ion mode and UH$_2$ in the positive ion mode. Stable isotopes for U and UH$_2$ were used as internal standards.

Total chromatographic run time was 5 min. Validated concentration ranges for U and UH$_2$ were from 1 to 100 ng/mL and 10 to 1000 ng/mL, respectively. Inter-assay bias and inter-assay precision for U were within ±2.8% and ≤12.4%. For UH$_2$, inter-assay bias and inter-assay precision were within ±2.9% and ≤7.2%. Adequate stability of U and UH$_2$ in dry extract, final extract, stock solution and plasma was demonstrated. Stability of U and UH$_2$ in whole blood was only satisfactory when stored up to 4 hours at 2-8°C, but not at ambient temperatures.

An accurate, precise and sensitive UPLC-MS/MS assay for quantification of U and UH$_2$ in plasma was developed. This assay is now applied to support clinical studies with fluoropyrimidine drugs.

INTRODUCTION

Chemotherapeutic agents belonging to the group of fluoropyrimidines are the mainstay for treatment of colorectal, breast and gastric cancer. Fluoropyrimidine-based chemotherapeutic regimens usually involve administration of intravenous 5-fluorouracil (5-FU) or its orally available pre-prodrug capecitabine. After oral administration, capecitabine is rapidly and almost completely absorbed via the gastrointestinal tract and converted to 5-FU through a three-step enzymatic cascade. Approximately 80% of 5-FU is catabolized to inactive metabolites by the enzyme dihydropyrimidine dehydrogenase (DPD) [1–3]. A small fraction of 5-FU follows a complex route of intracellular metabolism, which eventually leads to formation of active metabolites. The active metabolites are misincorporated in RNA and DNA and inhibit the enzyme thymidylate synthase, thereby inducing cell death.

Clinical application of fluoropyrimidines is seriously limited by poorly predictable treatment-related toxicity. Approximately 15-30% of patients who are treated with fluoropyrimidines will suffer from severe ($\geq$ National Cancer Institute Common Toxicity Criteria grade 3) toxicity [4]. Treatment-related death is observed in approximately 0.5-1% of patients [5].

Several studies have been performed to examine the relationship between fluoropyrimidine-induced toxicity and DPD phenotype. The most often applied phenotyping approach is based on *ex vivo* quantification of DPD activity in peripheral blood mononuclear cells (PBMCs) [6–8]. The DPD activity in PBMCs has been associated with systemic clearance of 5-FU [9] and fluoropyrimidine-induced toxicity [10–12]. Although promising, determination of DPD activity in PBMCs is laborious, expensive and requires the use of radioisotopes, thereby limiting the clinical applicability of this method.

An alternative and promising DPD phenotyping approach is quantification of the endogenous DPD substrate uracil (U) and the reaction product dihydrouracil (UH_2). Several bioanalytical methods for quantification of U and UH_2 in plasma [13–25], urine [14,26–31], and saliva have been described [32]. The reported bioanalytical methods are based on high performance liquid chromatography (HPLC) coupled with ultraviolet spectrophotometry [15–17,20–24,32,33], or tandem mass spectrometry (MS/MS) [13,14,17,19,25–30], or employ gas chromatography – MS/MS [31]. Clinical relevance of U and UH_2 levels has most often been studied using the plasmatic matrix. Pre-therapeutic UH_2/U plasma ratios showed good correlation with clearance of 5-FU [34,35] and fluoropyrimidine-induced toxicity [18,34,36–38]. Therefore, upfront determination of U and UH_2 levels in plasma is an attractive and promising approach for improved identification of patients at risk of fluoropyrimidine-induced toxicity.

Previously described bioanalytical methods for U and UH_2 in plasma require extensive sample pre-treatment consisting of protein precipitation followed by liquid/liquid extraction [13,14,19–25,39], or the use of solid phase extraction [16–18], and sometimes long analytical run times (30-90 min) [16,17,20–24]. Furthermore, method validation was shown to be challenging because blank, U and UH_2 free, plasma is not available. Most described methods have therefore been validated using bovine serum albumin as

1

a surrogate matrix for plasma or were validated using the standard addition method [13,14,16,17,19,24,25], which hampers adequate examination of matrix effects and assay sensitivity, respectively. Sistonen et al. reported that ranges of U and UH_2 plasma levels were highly variable among published studies, and suggested that this could, at least partly, be attributed to variability in method development and validation [36]. Altogether, these results indicate that development of an accurate, sensitive and robust assay for U and UH_2 in plasma is not straightforward.

Our aim was to develop and validate a rapid and sensitive bioanalytical method for quantification of U and UH_2 in human plasma. We applied ultra-performance liquid chromatography (UPLC) - MS/MS for optimal chromatographic separation, short run time and adequate sensitivity and selectivity. This method is the first to describe sample pre-treatment only by protein precipitation. Validation experiments were performed using both the original matrix and dialyzed (blank) human plasma. The applicability of the developed method is demonstrated by the quantitative analysis of U and UH_2 in plasma samples.

MATERIALS AND METHODS
Chemicals

U and UH_2 were purchased from Toronto Research Chemicals (North York, ON, Canada). $^{15}N_2$-labeled U and Phosphate Buffered Saline (PBS) were purchased from Sigma (St. Louis, MO, USA). $^{13}C_4,^{15}N_2$-labeled UH_2 was obtained from Cambridge Isotope Laboratories (Andover, MA, USA). UPLC-grade acetonitrile, methanol, formic acid and water were purchased from Biosolve Ltd (Valkenswaard, The Netherlands). Distilled water was purchased from B. Braun Medical (Melsungen, Germany). Dimethylsulfoxide (DMSO) was obtained from Merck (Darmstadt, Germany). Control human heparinized plasma was purchased from Bioreclamation (Hicksville, NY, USA).

Preparation of calibration standards and quality control samples

Stock solutions, which were used for preparation of calibration standards, containing 1 mg/mL of U and UH_2, were prepared in DMSO for both analytes. Separate stock solutions for quality control (QC) samples were prepared with U and UH_2 diluted in DMSO, also at concentrations of 1 mg/mL. Working solutions were obtained by diluting U and UH_2 stock solutions with water. For the internal standards, separate stock solutions containing the stable isotopes U-$^{15}N_2$, and UH_2-$^{13}C_4$-$^{15}N_2$ were prepared at concentrations of 1 mg/mL in DMSO. An internal standard working solution was prepared by diluting stock solutions in 0.1% (v/v) formic acid in water up to concentrations of 1,000 and 10,000 ng/mL for U-$^{15}N_2$ and UH_2-$^{13}C_4$-$^{15}N_2$ respectively. All stock and working solutions were stored at -20°C.

Blank matrix was obtained by removing endogenous U and UH_2 from control human plasma. Therefore, control human plasma was dialyzed using Slide-A-Lyzer Dialysis Cassettes with a molecular weight cut-off of 2 kDa (Thermo Fisher Scientific, Rockford,

IL, USA). Dialysis was performed by placing dialysis cassettes, which were filled with 12 mL control human plasma, in 2 L of 0.01 M PBS in distilled water under magnetic stirring at room temperature. After 0.5, 2, and 4 hours, the PBS solution was discarded and replaced by 2 L of fresh PBS. Dialysis continued overnight and the obtained blank plasma was used for preparation of calibration and QC samples. After preparation, the blank plasma was stored at -70°C.

For preparation of calibration standards, a volume of 15 µL each working solution was added to 285 µL blank control plasma. Calibration standards containing U and UH_2 were freshly prepared at concentrations of 1, 2.5, 10, 40, 80 and 100 ng/mL for U and 10, 25, 100, 400, 800 and 1000 ng/mL for UH_2. QC samples were freshly prepared by adding 15 µL of QC working solutions to 285 µL blank control plasma. Concentrations at QC lower limit of quantification (LLoQ), low, mid and high levels were 1, 3, 25 and 75 ng/mL for U and 10, 30, 250 and 750 ng/mL for UH_2, respectively.

Sample pre-treatment

A volume of 20 µL internal standard working solutions was added to 300 µL of plasma (or control dialyzed plasma in case of calibration standards and QC samples). Plasma proteins were precipitated by adding 900 µL of methanol:acetonitrile (50:50, v/v). After a 10 s vortex spin, samples were shaken for 10 min at 1250 rpm. Next, the samples were centrifuged at 14,000 g for 10 min at room temperature. Clear supernatants were collected and evaporated under a gentle stream of nitrogen gas at 40°C. After approximately 45 minutes, dry extracts were obtained. The dry extracts were reconstituted with 100 µL of 0.1% (v/v) formic acid in water, vortex-mixed for 10 s, and were centrifuged at 14,000 g for 10 min at 4°C. Clear final extracts were transferred to 96-well plates (350 µL; Waters, Milford, MA, USA). A volume of 5 µL was injected into the UPLC-MS/MS system.

Liquid chromatography and mass spectrometry

U and UH_2 plasma concentrations were determined using an Acquity UPLC system (Waters, Milford, MA, USA) coupled to a QTrap 5500 triple quadrupole spectrometer (Sciex, Framingham, MA, USA). Chromatographic separation was achieved on an Acquity UPLC HSS T3 column (150 x 2.1 mm ID, particle size 1.8 µm; Waters, Milford, MA, USA). The temperature within the autosampler was set to 5°C and the column temperature was maintained at 30°C. Mobile phase A consisted of 0.1% (v/v) formic acid in UPLC-grade water and mobile phase B was 0.1% (v/v) formic acid in UPLC-grade acetonitrile. Gradient elution was applied at a flow rate of 0.3 mL/min. The following gradient was used: 0% B from 0-3.0 min, 0-90% B from 3.0-3.2 min, 90% B from 3.2-3.7 min, 0% B from 3.7-5 min. The Qtrap 5500 mass spectrometer was equipped with a turbo spray ion source and operated in the negative ion mode for detection of U and in the positive ion mode UH_2. The analytes were detected in multiple reaction monitoring (MRM) mode. An overview of applied mass spectrometer settings, including analyte specific settings, is shown in Table 1. Analyst software (Sciex; version 1.5.2) was used to control the UPLC-MS/MS system and for data processing.

1

Table 1. Mass spectrometer settings for the analysis of uracil and dihydrouracil in human plasma.

Detector parameters	Setting			
Ion source	Turbo Ion Spray			
Ionization modes	Negative for U and positive for UH_2			
Ion spray voltages	-4500 / 5000 V			
Entrance potential	-10 / 10 V			
Temperature	700°C			
Gas 1 (nebulizer)	50 a.u.			
Gas 2	50 a.u.			
Collision gas	6 a.u.			
Curtain gas	40 a.u.			
Analyte specific parameters	U	IS U	UH_2	IS UH_2
Parent ion (m/z)	110.9	112.9	114.9	120.9
Product ion (m/z)	42.0	43.0	55.0	58
Declustering potential (V)	-75	-75	86	86
Collision energy (V)	-16	-16	15	15
Collision cell exit potential (V)	-19	-19	10	10
Dwell time (ms)	75	75	75	75
Typical retention time (min)	2.80	2.80	2.65	2.65

Abbreviations: a.u., arbitrary units; IS, internal standard; U, uracil; UH_2, dihydrouracil

Validation procedures

Linearity

Calibration standards (six non-zero calibration standards, a blank standard and a standard exclusively spiked with internal standard) were prepared in duplicate in dialyzed control human plasma in three independent analytical runs. For both analytes, the linear regression of the peak area ratio (analyte/internal standard) versus the concentration was weighted $1/x^2$. Calibration concentrations were back-calculated from the calibration lines. Subsequently, deviations from the nominal concentrations were determined. Back-calculated concentrations should not deviate from nominal concentrations by more than ±20% at the LLoQ level and ±15% for higher concentrations [40,41].

Accuracy and precision

In three consecutive analytical runs, five replicates of QC samples were prepared in dialyzed control human plasma at QC LLoQ, low, medium and high concentrations and analyzed. Inter-assay bias and inter-assay precision were calculated in order to examine accuracy and precision of this bioanalytical assay. Inter- and intra-assay accuracies were considered acceptable in case bias was within ±20% at the LLoQ level and ±15% for other QC concentrations. Inter- and intra-assay precisions ≤20% were considered adequate at the LLoQ level and ≤15% for other concentrations [40,41].

Carry-over

Carry-over was assessed in duplicate within one analytical run by analyzing peak responses in double blank QC samples after injection of the highest calibration sample. The response in double blank samples should not be greater than 20% of the peak response of U and UH_2 at the LLoQ level and 5% of the response of the internal standards [40,41].

Sample preparation for assessing matrix factor, recovery, and selectivity

The analytes U and UH_2 are naturally present in human plasma at concentrations of approximately 10 ng/mL and 100 ng/mL, respectively [36]. However, the stable isotopes U-$^{15}N_2$ and UH_2-$^{13}C_4$-$^{15}N_2$ are not occurring in human plasma and have similar chemical properties to U and UH_2. Therefore, control human plasma was spiked with U-$^{15}N_2$ and UH_2-$^{13}C_4$-$^{15}N_2$ and quantified using U and UH_2 as internal standards for examination of matrix factor, recovery and selectivity. For these purposes, working solutions containing the stable isotopes U-$^{15}N_2$ and UH_2-$^{13}C_4$-$^{15}N_2$ were prepared in water. Samples were prepared by adding 15 µL of these working solutions to 285 µL non-dialyzed heparinized control human plasma (QC-IS samples). Concentrations at the QC-IS low and high level were 3 and 75 ng/mL for U-$^{15}N_2$ and 30 and 750 ng/mL for UH_2-$^{13}C_4$-$^{15}N_2$. Calibration standards containing U-$^{15}N_2$ and UH_2-$^{13}C_4$-$^{15}N_2$ were freshly prepared at concentrations of 1, 2.5, 10, 40, 80 and 100 ng/mL for U-$^{15}N_2$ and 10, 25, 100, 400, 800 and 1,000 ng/mL for UH_2-$^{13}C_4$-$^{15}N_2$. An internal standard working solution was prepared with U and UH_2 at concentrations of 1,000 and 10,000 ng/mL, respectively. Addition of this internal standard working solution to QC-IS samples resulted in U and UH_2 levels that greatly exceeded endogenous U and UH_2 levels, thereby avoiding the introduction of a bias in the quantification of U-$^{15}N_2$ and UH_2-$^{13}C_4$-$^{15}N_2$ in these samples. Sample pre-treatment was according to the procedure described above.

Matrix factor and recovery

Matrix effects were investigated at QC-IS low and high levels in triplicate using the same batch of human control plasma. The absolute matrix factor was determined by calculating the ratio of the peak area in the presence of matrix ions to the peak area in absence of matrix. Samples without matrix ions consisted of neat solutions in 0.1% formic acid in water with analyte concentrations at QC-IS low and high level. For samples including matrix ions, dry extracts of blank control plasma were spiked with the same neat solutions. The relative matrix factor was determined by dividing the matrix factor of the analytes through the matrix factors of the corresponding internal standards.

Overall and protein precipitation (PP) recovery were determined at QC-IS low and high levels in triplicate. The PP recovery was calculated by comparing peak areas of processed samples with peak areas of blank control samples that were reconstituted with neat solutions of analytes (representing 100% recovery). Overall recovery was determined by comparing analyte peak areas of processed samples with peak areas of analyte in absence of matrix ions.

The relative standard deviation (RSD) values of relative matrix factor and PP recovery should be ≤15% [40,41].

Selectivity

Six different batches of human heparinized control plasma were spiked at QC-IS low level. Selectivity was evaluated by determining endogenous interferences for U-^{15}N$_2$ and UH$_2$-^{13}C$_4$-^{15}N$_2$ in double blank samples in relation to peak responses of QC-IS low samples. Endogenous interference should be equal to or less than 15% of the peak area of QC-IS low samples.

Stability

The stability of U and UH$_2$ stock solutions was examined after storage for 148 days at -20°C. Short-term stability in plasma was determined in triplicate by analyzing QC-IS low and high samples after a storage period of 4 hours at ambient temperatures. Long-term stability in plasma was assessed by re-analysis of study samples. These study samples were collected from patients who participated in a phase I clinical study that was approved by the Ethics Committee of the Antoni van Leeuwenhoek Hospital, Amsterdam, The Netherlands. After initial analysis, five samples with concentrations close to QC low and medium levels were selected for re-analysis after storage for 93 days at -70°C. Stability of U and UH$_2$ in whole blood was examined for 0.5, 1, 2, 4 and 6 hours at ambient temperatures or 2-8°C. For this purpose, peripheral blood was collected from three volunteers in heparinized tubes. Stability in dry extract and final extract were determined after storage of five QC samples at low and high level for 5 days at 2-8°C. Stability of analytes was considered acceptable if 85-115% of the initial concentration was recovered.

RESULTS AND DISCUSSION

Assay development

Sample pre-treatment and analytical run time had to be adequate and efficient for rapid and high-throughput quantification of U and UH$_2$ in human plasma. The most frequently described sample pre-treatment procedure for determination of U and UH$_2$ consists of ammonium sulfate precipitation followed by liquid-liquid extraction with a mixture of ethyl acetate and isopropanol [14]. This two-step pre-treatment has been shown to be adequate, but limits high sample throughput because it is rather laborious. In order to accelerate and simplify sample pre-treatment, a procedure consisting of protein precipitation with a mixture of methanol and acetonitrile (50:50, v/v) was successfully applied. The methanol:acetonitrile mixture was added to plasma with a ratio of 3:1. After protein precipitation, clear supernatants were quickly evaporated under a stream of nitrogen, reconstituted in mobile phase A, and transferred to a 96-well plate. The use of 96-well plates allowed for analysis of large batches of samples.

The analytes U and UH$_2$ (Figure S1) are highly polar. In order to obtain adequate analyte retention, an analytical column that remains stable at highly aqueous mobile

phase conditions is warranted. Others have shown that chromatographic separation of U and UH_2 was challenging. Sparidans et al. and Büchel et al. used a reversed-phase Atlantis dC18 column (Waters) and obtained adequate peak separation only when the column was cooled with ice or maintained at 5°C, respectively [13,26]. We applied reversed-phase chromatography and used the Acquity UPLC® HSS T3 column. Using this analytical column, and gradient elution with 0.1% formic acid in water and 0.1% formic acid acetonitrile, adequate analyte retention and separation were obtained, without the need of refrigeration of the column. Total analytical run time was only 5 minutes and typical retention times of U and UH_2 were 2.80 and 2.65 minutes. Flow injection analysis was applied for optimization of the source settings and the analyte-specific conditions. In order to obtain largest signal-to-noise ratios, the mass spectrometer was utilized in the negative ion mode for quantification of U and in the positive ion mode for quantification of UH_2. Optimized detector and analyte specific settings are presented in Table 1. Representative chromatograms of a blank QC sample, QC LLoQ sample and study sample are shown in Figure 1. Chromatographic analysis of the study sample demonstrated peaks at 2.2 and 2.9 min in the chromatograms for U and UH_2, respectively (Figure 1). These peaks were not present in the chromatograms of the QC samples. The compounds that elute at 2.2 and 2.9 min were possibly removed from control plasma during the dialysis procedure, which could explain why the peaks do not appear in the chromatograms of the QC samples.

Assay validation

Linearity

The assay was linear over a concentration range of 1-100 ng/mL for U and 10-1000 ng/mL for UH_2. Correlation coefficients of the calibration curves were 0.998 or higher for U and 0.995 or higher for UH_2. The average slope of the U calibration curve was 0.0131 with a RSD of 9.4%. For UH_2, the average slope of the calibration curve was 0.00177 with a RSD of 3.5%. Intersects of the U and UH_2 calibration curves were within ±0.00312 and ±0.00181, respectively. Deviations of back-calculated concentrations from nominal concentrations were between -2.0 and 1.6% for U with RSD values ≤7.1%. Regarding UH_2, deviations of back-calculated concentrations were between -2.0 and 3.2% with RSD values ≤10.3%. Relative differences between the back-calculated and nominal concentrations are shown in Figure S2. The acceptance criteria concerning linearity were met for both analytes.

Accuracy and precision

The results regarding inter-assay bias and precision are summarized in Table 2. Intra-assay biases were within -1.3 and 5.7% at the QC LLoQ level and within ±7.3% at the higher QC levels. Intra-assay precisions were within 5.3 and 19.7% at the QC LLoQ level and ≤7.4% at the higher QC levels. One measure for U at QC LLoQ was considered an outlier based on the Dixon's Q test for outliers and excluded from the analysis. The results met the predefined criteria for adequate accuracy and precision.
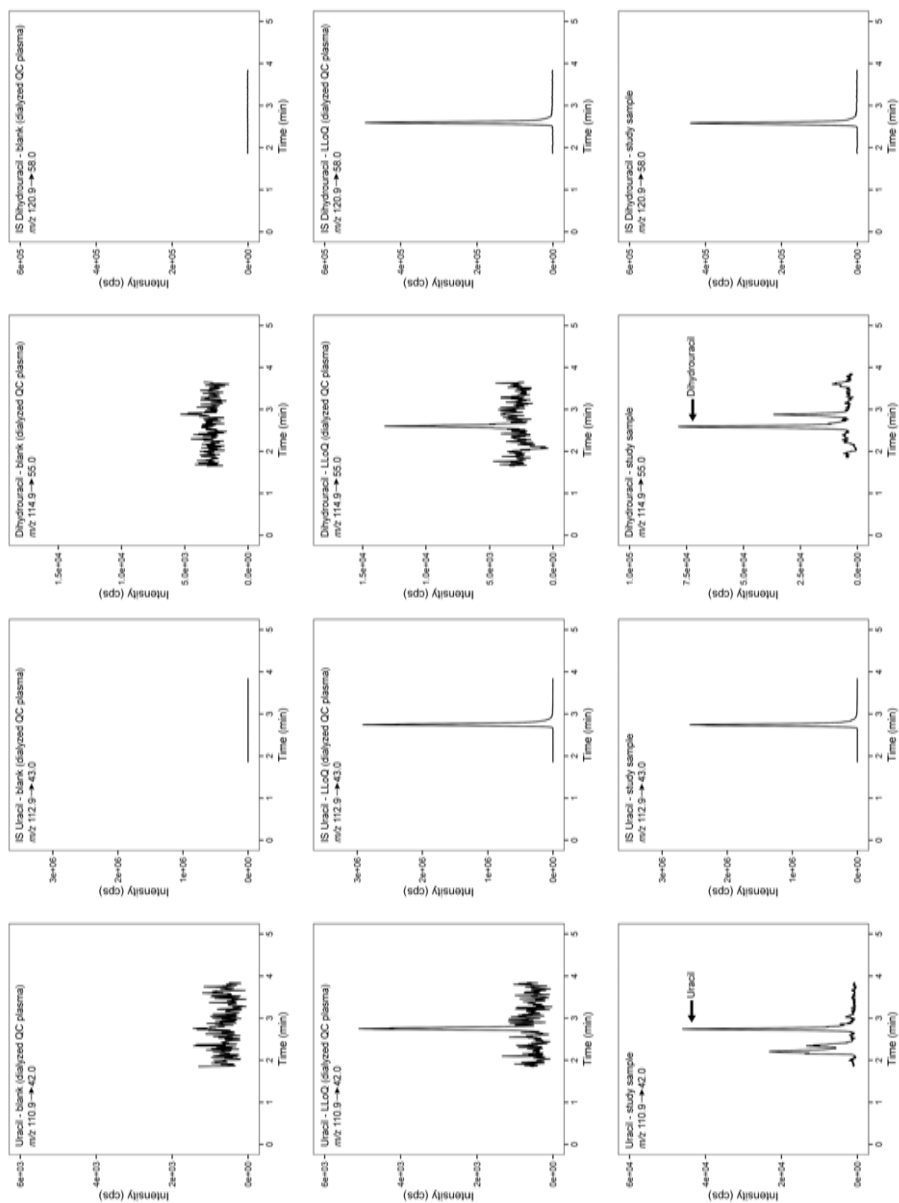
Figure 1. Representative chromatograms of uracil (U) and dihydrouracil (UH$_2$) and internal standards (IS) for blank (dialyzed) samples, quality control (QC) LLoQ sample and study sample. The U and UH$_2$ plasma concentrations in the study sample were 11.7 ng/mL and 113 ng/mL, respectively.

1

Table 2. Assay performance data for the analysis of uracil and dihydrouracil in human plasma at validated quality control concentration levels.

Analyte	QC	Nominal concentration (ng/mL)	Average measured concentration (ng/mL)	Inter-assay bias (%)	Inter-assay precision (%)	Number of replicates
U	LLoQ	1	1.02	1.9	12.4	14[§]
	Low	3	3.07	2.2	5.4	15
	Medium	25	24.8	-0.9	5.6	15
	High	75	77.1	2.8	5.1	15
UH$_2$	LLoQ	10	10.3	2.9	7.2	15
	Low	30	29.6	-1.3	6.4	15
	Medium	250	257	2.8	4.3	15
	High	750	771	2.8	5.4	15

Abbreviations: QC, quality control; U, uracil; UH$_2$, dihydrouracil; LLoQ, lower limit of quantification
§ One value was considered a statistical outlier using the Dixon's Q test and excluded from the analysis.

Carry-over

Carry-over for U was ≤9.8% of the signal at the corresponding LLoQ and for no carry-over was observed for UH$_2$. For U-^{15}N$_2$ and UH$_2$-^{13}C$_4$-^{15}N$_2$, carry-over was ≤0.2% and ≤0.1%, respectively. It was concluded that the carry-over test fulfilled the predefined criteria.

Matrix factor and recovery

Table 3 shows the results of matrix factor and recovery analyses. The results indicate that U-^{15}N$_2$ and UH$_2$-^{13}C$_4$-^{15}N$_2$ are subject to ion suppression, and that the role of matrix effects is effectively minimized by the internal standards U and UH$_2$. Moreover, these results show that ion suppression for U and UH$_2$ was observed in the same extent as for the stable isotopes. Therefore, the effect of ion suppression on quantification of U and UH$_2$ in human plasma samples can be minimized by the use of internal standards U-^{15}N$_2$ and UH$_2$-^{13}C$_4$-^{15}N$_2$.

Mean PP recovery for U-^{15}N$_2$ and UH$_2$-^{13}C$_4$-^{15}N$_2$ ranged between 97.0% and 114% (Table 3). Relatively low overall recovery of both U-^{15}N$_2$ and UH$_2$-^{13}C$_4$-^{15}N$_2$ is the result of ion suppression (Table 3), since there was a pronounced matrix effect identified.

The RSD values of relative matrix factor and PP recovery were ≤7.9% and ≤5.6%, respectively, and fulfilled predefined criteria.

Selectivity

Endogenous interferences did not exceed 0.3% of the peak area of U-^{15}N$_2$ at the QC-IS low level. There was no endogenous interference detected for UH$_2$-^{13}C$_4$-^{15}N$_2$. Based on these data, selectivity for the stable isotopes was considered acceptable.

Table 3. Matrix factor and recovery for stable isotopes of uracil and dihydrouracil.

Analyte[s]	Nominal concentration	Absolute matrix factor	RSD (%)	Relative matrix factor	RSD (%)	Protein precipitation recovery (%)	RSD (%)	Overall recovery (%)	RSD (%)
U-^{15}N$_2$	3	0.476	6.7	0.856	6.5	97.9	5.3	46.2	5.7
	75	0.456	1.0	0.906	7.0	100	0.8	45.4	0.4
UH$_2$-^{13}C$_4$-^{15}N$_2$	30	0.724	6.0	1.00	7.9	97.9	5.6	70.7	1.7
	750	0.686	2.2	0.893	3.0	114	1.7	78.1	2.2

Abbreviations: RSD, relative standard deviation; U, uracil; UH$_2$, dihydrouracil
§ Uracil and dihydrouracil are naturally present in control human plasma. Therefore, control human plasma was spiked with the stable isotopes U-^{15}N$_2$ and UH$_2$-^{13}C$_4$-^{15}N$_2$, and quantified using U and UH$_2$ as internal standards.

Selectivity for U and UH_2 could not be determined because these analytes are endogenous compounds and present in the matrix. Dialyzed control human plasma is free of U and UH_2. However, during the preparation of dialyzed control plasma, molecules with a molecular weight below 2 kDa are eliminated from the matrix. Consequently, molecules that potentially interfere with quantification of U and UH_2 could be diminished by dialysis of the control human plasma. The use of dialyzed control human plasma was therefore not considered a suitable matrix for determination of selectivity of this assay for U and UH_2.

Stability

Results of stability experiments are shown in Table 4. Both U and UH_2 were stable at -20°C for at least 148 days. These analytes also showed adequate stability in dry extracts and final extracts that were stored at 2-8°C for 5 days. Short-term stability of U and UH_2 in plasma was examined by spiking the stable isotopes $U\text{-}^{15}N_2$ and $UH_2\text{-}^{13}C_4\text{-}^{15}N_2$ at QC-IS low and high levels. After 4 hours at ambient temperatures, there was no significant change in $U\text{-}^{15}N_2$ and $UH_2\text{-}^{13}C_4\text{-}^{15}N_2$ levels detected. Therefore, it can be concluded that also U and UH_2 have acceptable stability in plasma for at least 4 hours at ambient temperatures. Long-term stability of U and UH_2 in plasma was examined by re-analysis of study samples. Both analytes showed adequate stability in plasma that was stored at -70°C for 93 days. All five samples that were re-analyzed for stability assessment at the QC low level for U and QC medium level of UH_2 showed a relative change to initial measurement that was within ±15%. Four out of five samples that were selected for long-term stability assessment for U at QC medium level and UH_2 at the QC low level showed a deviation that was within ±15%.

Stability of U and UH_2 in whole blood was determined both at ambient temperatures and at 2-8°C. The concentration of U in plasma showed a large and variable percent increase from baseline after storage of whole blood at ambient temperatures (Figure S3). Increase in U plasma levels was 13.8 ± 5.0% after storage of whole blood for 4 hours at 2-8°C and was 21.2 ± 2.1% after storage for 6 hours. The relative increase in UH_2 plasma levels was less affected by storage of whole blood at both temperature conditions (Figure S3). After storage of whole blood for 6 hours, relative change in UH_2 plasma levels were -6.9 ± 4.9% at 2-8°C and 9.8 ± 12.2% at ambient temperatures. Thus, stability of UH_2 seems most adequately assured when whole blood was stored at 2-8°C. It can be concluded that whole blood should not be stored longer than 4 hours at 2-8°C for acceptable analysis of both U and UH_2 plasma levels. Storage of whole blood at ambient temperatures is discouraged.

These findings are in line with findings of Coudoré et al., who reported increased U and UH_2 plasma levels after storage of whole blood at ambient temperatures [19]. Increased levels of U and UH_2 that were found after storage of whole blood at ambient temperatures could be the result of *ex vivo* metabolism. The precursor of U, uridine, is present in human plasma [42], and is converted to U by uridine phosphorylase, an enzyme that is known to be expressed by many cell types, among which PBMCs [43].

Table 4. Stability data for uracil and dihydrouracil.

Analyte	Condition	Matrix	Initial concentration (ng/mL)	Observed concentration (ng/mL)	Deviation (%)	RSD (%)
U	-20°C, 148 days	Stock solution	1.00×10^6	0.96×10^6	-3.9	7.1
	Ambient, 4 hours	Plasma	3.00	3.00	0.0	5.5
			75.0	72.2	-3.8	3.7
	-70°C, 93 days§	Plasma	11.8	11.8	-0.5	N/A
			29.6	27.5	-7.3	N/A
	2-8°C, 5 days	Dry extract	3.00	3.01	0.4	6.2
			75.0	76.9	2.5	4.9
	2-8°C, 5 days	Final extract	3.00	3.02	0.6	8.2
			75.0	75.3	0.4	4.3
UH_2	-20°C, 148 days	Stock solution	1.00×10^6	1.05×10^6	4.9	2.1
	Ambient, 4 hours	Plasma	30.0	28.7	-4.4	6.8
			750	759	1.2	3.9
	-70°C, 93 days§	Plasma	82.0	73.1	-10.1	N/A
			282	257	-8.8	N/A
	2-8°C, 5 days	Dry extract	30.0	32.1	6.9	3.3
			750	751	0.2	6.0
	2-8°C, 5 days	Final extract	30.0	31.3	4.5	4.3
			750	733	-2.3	2.8

Abbreviations: RSD, relative standard deviation; N/A, not applicable; U, uracil; UH_2, dihydrouracil
§ Five study samples with initial U and UH_2 levels close to QC Low and QC Medium levels were selected and re-analyzed after storage at -70°C for 93 days. The deviation from the initial measured concentrations is shown.

In turn, formed U could be converted to UH_2 by DPD that is expressed by leukocytes and platelets [44]. Thus, *ex vivo* metabolism could lead to increased levels of UH_2 after storage of whole blood at ambient temperatures. Alternatively, U and UH_2 might be released by blood cells or transporter proteins during storage of whole blood at ambient temperatures, which could lead to increased UH_2 plasma levels.

CLINICAL APPLICABILITY

The described assay is currently applied for the analysis of U and UH_2 plasma levels to support a pharmacological phase I clinical study of chronomodulated capecitabine therapy in patients (http://www.trialregister.nl, study identifier: NTR4639). Figure 2 shows the measured U and UH_2 plasma concentrations in a patient with colorectal cancer that participated in this study after oral administration of 900 mg capecitabine. As shown in this figure, the U and UH_2 plasma levels were within the validated ranges. Both U and UH_2 levels decreased within the first hour after administration of capecitabine, followed by an increase and subsequent stabilization. These changes in U and UH_2 plasma levels could be caused by competition between U and UH_2 and capecitabine metabolites for
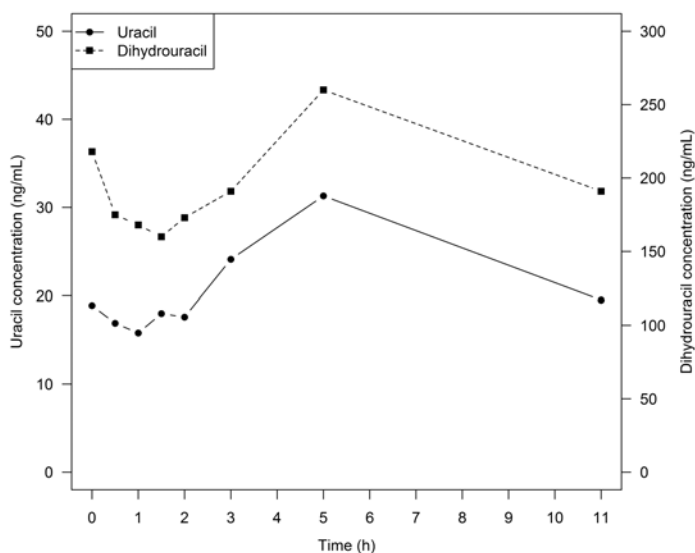
Figure 2. Plasma concentrations of uracil and dihydrouracil in a patient with colorectal cancer following administration of 900 mg of capecitabine at the 7th day of treatment.

the same enzymes. However, more research is obviously needed to draw solid conclusions on this. The described assay is also applied in a large retrospective study and a prospective study (http://www.clinicaltrials.gov, study identifier: NCT02324452) to assess the clinical implications of U and UH_2 plasma levels for identification of patients who are DPD deficient and at risk of developing severe fluoropyrimidine-induced toxicity.

CONCLUSION

An accurate, precise, robust and sensitive UPLC-MS/MS assay for quantification of U and UH_2 in plasma was developed and validated. Sample pre-treatment consists only of protein precipitation, which together with short chromatographic run time, enables fast sample analysis. The validated concentration ranges are 1-100 ng/mL for U and 10-1000 ng/mL for UH_2. Stable isotopes were used as internal standards for both analytes, enabling examination of matrix factor, recovery and selectivity without using an artificial plasma matrix. Moreover, these stable isotopes are essential for correction of matrix effects. Selectivity was not evaluated for U and UH_2. Stability of U and UH_2 in whole blood was adequate at 2-8°C, but not at ambient temperatures. Examined assay validation parameters fulfilled the acceptance criteria of the US Food and Drug Administration and the European Medicines Agency guidelines for method validation [40,41]. The developed method allows fast and reliable quantitative analysis of U and UH_2 in plasma samples.

1

REFERENCES

1. Heggie GD, Sommadossi JP, Cross DS, Huster WJ, Diasio RB. Clinical pharmacokinetics of 5-fluorouracil and its metabolites in plasma, urine, and bile. Cancer Res 1987;47:2203–6.

2. Thorn CF, Marsh S, Carrillo MW, McLeod HL, Klein TE, Altman RB. PharmGKB summary: fluoropyrimidine pathways. Pharmacogenet Genomics 2011;21:237–42.

3. Judson IR, Beale PJ, Trigo JM, Aherne W, Crompton T, Jones D, et al. A human capecitabine excretion balance and pharmacokinetic study after administration of a single oral dose of 14C-labelled drug. Invest New Drugs 1999;17:49–56.

4. Twelves C, Wong A, Nowacki MP, Abt M, Burris H, Carrato A, et al. Capecitabine as adjuvant treatment for stage III colon cancer. N Engl J Med 2005;352:2696–704.

5. Mikhail SE, Sun JF, Marshall JL. Safety of capecitabine: a review. Expert Opin Drug Saf 2010;9:831–41.

6. Pluim D, Jacobs BAW, Deenen MJ, Ruijter AEM, van Geel RMJM, Burylo AM, et al. Improved pharmacodynamic assay for dihydropyrimidine dehydrogenase activity in peripheral blood mononuclear cells. Bioanalysis 2015;7:519–29.

7. Pluim D, Jacobs BAW, Krähenbühl MD, Ruijter AEM, Beijnen JH, Schellens JHM. Correction of peripheral blood mononuclear cell cytosolic protein for hemoglobin contamination. Anal Bioanal Chem 2013;405:2391–5.

8. Van Kuilenburg AB, Van Lenthe H, Tromp A, Veltman PC, Van Gennip AH. Pitfalls in the diagnosis of patients with a partial dihydropyrimidine dehydrogenase deficiency. Clin Chem 2000;46:9–17.

9. Fleming RA, Milano G, Thyss A, Etienne MC, Renée N, Schneider M, et al. Correlation between dihydropyrimidine dehydrogenase activity in peripheral mononuclear cells and systemic clearance of fluorouracil in cancer patients. Cancer Res 1992;52:2899–902.

10. Van Kuilenburg ABP, Meinsma R, Zoetekouw L, Van Gennip AH. Increased risk of grade IV neutropenia after administration of 5-fluorouracil due to a dihydropyrimidine dehydrogenase deficiency: High prevalence of the IVS14+1G>A mutation. Int J Cancer 2002;101:253–8.

11. Milano G, Etienne MC, Pierrefite V, Barberi-Heyob M, Deporte-Fety R, Renée N. Dihydropyrimidine dehydrogenase deficiency and fluorouracil-related toxicity. Br J Cancer 1999;79:627–30.

12. van Kuilenburg AB, Haasjes J, Richel DJ, Zoetekouw L, Van Lenthe H, De Abreu RA, et al. Clinical implications of dihydropyrimidine dehydrogenase (DPD) deficiency in patients with severe 5-fluorouracil-associated toxicity: identification of new mutations in the DPD gene. Clin Cancer Res 2000;6:4705–12.

13. Büchel B, Rhyn P, Schürch S, Bühr C, Amstutz U, Largiadèr CR. LC-MS/MS method for simultaneous analysis of uracil, 5,6-dihydrouracil, 5-fluorouracil and 5-fluoro-5,6-dihydrouracil in human plasma for therapeutic drug monitoring and toxicity prediction in cancer patients. Biomed Chromatogr 2013;27:7–16.

14. Jiang H, Jiang J, Hu P, Hu Y. Measurement of endogenous uracil and dihydrouracil in plasma and urine of normal subjects by liquid chromatography-tandem mass spectrometry. J Chromatogr B Anal Technol Biomed Life Sci 2002;769:169–76.

15. van Staveren MC, Theeuwes-Oonk B, Guchelaar HJ, van Kuilenburg ABP, Maring JG. Pharmacokinetics of orally administered uracil in healthy volunteers and in DPD-deficient patients, a possible tool for screening of DPD deficiency. Cancer Chemother Pharmacol 2011;68:1611–7.

16. Déporte R, Amiand M, Moreau A, Charbonnel C, Campion L. High-performance liquid chromatographic assay with UV detection for measurement of dihydrouracil/uracil ratio in plasma. J Chromatogr B Analyt Technol Biomed Life Sci 2006;834:170–7.

17. Svobaite R, Solassol I, Pinguet F, Ivanauskas L, Brès J, Bressolle FMM. HPLC with UV or mass spectrometric detection for quantifying

endogenous uracil and dihydrouracil in human plasma. Clin Chem 2008;54:1463–72.

18. Kristensen MH, Pedersen P, Mejer J. The value of dihydrouracil/uracil plasma ratios in predicting 5-fluorouracil-related toxicity in colorectal cancer patients. J Int Med Res 2010;38:1313–23.

19. Coudoré F, Roche D, Lefeuvre S, Faussot D, Billaud EM, Loriot M-A, et al. Validation of an ultra-high performance liquid chromatography tandem mass spectrometic method for quantifying uracil and 5,6-dihydrouracil in human plasma. J Chromatogr Sci 2012;50:877–84.

20. Garg MB, Sevester JC, Sakoff JA, Ackland SP. Simple liquid chromatographic method for the determination of uracil and dihydrouracil plasma levels: a potential pretreatment predictor of 5-fluorouracil toxicity. J Chromatogr B Analyt Technol Biomed Life Sci 2002;774:223–30.

21. Remaud G, Boisdron-Celle M, Hameline C, Morel A, Gamelin E. An accurate dihydrouracil/ uracil determination using improved high performance liquid chromatography method for preventing fluoropyrimidines-related toxicity in clinical practice. J Chromatogr B Analyt Technol Biomed Life Sci 2005;823:98–107.

22. Ciccolini J, Mercier C, Blachon M-F, Favre R, Durand A, Lacarelle B. A simple and rapid high-performance liquid chromatographic (HPLC) method for 5-fluorouracil (5-FU) assay in plasma and possible detection of patients with impaired dihydropyrimidine dehydrogenase (DPD) activity. J Clin Pharm Ther 2004;29:307–15.

23. Gamelin E, Boisdron-Celle M, Larra F, Robert J. A Simple Chromatographic Method for the Analysis of Pyrimidines and their Dihydrogenated Metabolites. J Liq Chromatogr Relat Technol 1997;20:3155–72.

24. Hahn RZ, Galarza AFA, Schneider A, Antunes MV, Schwartsmann G, Linden R. Improved determination of uracil and dihydrouracil in plasma after a loading oral dose of uracil using high-performance liquid chromatography with photodiode array detection and porous graphitic carbon stationary phase. Clin Biochem 2015, [Epub ahead of print].

25. César IC, Cunha-Júnior GF, Duarte Byrro RM, Vaz Coelho LG, Pianetti GA. A rapid HPLC-ESI-MS/MS method for determination of dihydrouracil/uracil ratio in plasma: evaluation of toxicity to 5-flurouracil in patients with gastrointestinal cancer. Ther Drug Monit 2012;34:59–66.

26. Sparidans RW, Bosch TM, Jörger M, Schellens JHM, Beijnen JH. Liquid chromatography-tandem mass spectrometric assay for the analysis of uracil, 5,6-dihydrouracil and beta-ureidopropionic acid in urine for the measurement of the activities of the pyrimidine catabolic enzymes. J Chromatogr B Analyt Technol Biomed Life Sci 2006;839:45–53.

27. van Lenthe H, van Kuilenburg AB, Ito T, Bootsma AH, van Cruchten A, Wada Y, et al. Defects in pyrimidine degradation identified by HPLC-electrospray tandem mass spectrometry of urine specimens or urine-soaked filter paper strips. Clin Chem 2000;46:1916–22.

28. Hartmann S, Okun JG, Schmidt C, Langhans CD, Garbade SF, Burgard P, et al. Comprehensive detection of disorders of purine and pyrimidine metabolism by HPLC with electrospray ionization tandem mass spectrometry. Clin Chem 2006;52:1127–37.

29. Sun Q. Urine Pyrimidine Metabolite Determination by HPLC Tandem Mass Spectrometry. Methods Mol Biol 2016;1378:237–42.

30. Schmidt C, Hofmann U, Kohlmüller D, Mürdter T, Zanger UM, Schwab M, et al. Comprehensive analysis of pyrimidine metabolism in 450 children with unspecific neurological symptoms using high-pressure liquid chromatography-electrospray ionization tandem mass spectrometry. J Inherit Metab Dis 2005;28:1109–22.

31. Hofmann U, Schwab M, Seefried S, Marx C, Zanger UM, Eichelbaum M, et al. Sensitive method for the quantification of urinary pyrimidine metabolites in healthy adults by gas chromatography-tandem mass spectrometry. J Chromatogr B Analyt Technol Biomed Life Sci 2003;791:371–80.

32. Carlsson G, Odin E, Gustavsson B, Wettergren Y. Pretherapeutic uracil and dihydrouracil levels in

1

saliva of colorectal cancer patients are associated with toxicity during adjuvant 5-fluorouracil-based chemotherapy. Cancer Chemother Pharmacol 2014, [Epub ahead of print].

33. Kristensen MH, Weidinger M, Bzorek M, Pedersen PL, Mejer J. Correlation between thymidylate synthase gene variants, RNA and protein levels in primary colorectal adenocarcinomas. J Int Med Res 2010;38:484–97.

34. Gamelin M, Boisdron-Celle M, Guérin-Meyer V, Delva R, Lortholary A, Genevieve F, et al. Correlation between uracil and dihydrouracil plasma ratio, fluorouracil (5-FU) pharmacokinetic parameters, and tolerance in patients with advanced colorectal cancer: A potential interest for predicting 5-FU toxicity and determining optimal 5-FU dosage. J Clin Oncol 1999;17:1105–10.

35. Jiang H, Lu J, Jiang J, Hu P. Important role of the dihydrouracil/uracil ratio in marked interpatient variations of fluoropyrimidine pharmacokinetics and pharmacodynamics. J Clin Pharmacol 2004;44:1260–72.

36. Sistonen J, Büchel B, Froehlich TK, Kummer D, Fontana S, Joerger M, et al. Predicting 5-fluorouracil toxicity: DPD genotype and 5,6-dihydrouracil:uracil ratio. Pharmacogenomics 2014;15:1653–66.

37. Zhou ZW, Wang GQ, Wan D Sen, Lu ZH, Chen YB, Li S, et al. The dihydrouracil/uracil ratios in plasma and toxicities of 5-fluorouracil-based adjuvant chemotherapy in colorectal cancer patients. Chemotherapy 2007;53:127–31.

38. Boisdron-Celle M, Remaud G, Traore S, Poirier A, Gamelin L, Morel A, et al. 5-Fluorouracil-related severe toxicity: a comparison of different methods for the pretherapeutic detection of dihydropyrimidine dehydrogenase deficiency. Cancer Lett 2007;249:271–82.

39. Maring JG, Schouten L, Greijdanus B, de Vries EGE, Uges DRA. A simple and sensitive fully validated HPLC-UV method for the determination of 5-fluorouracil and its metabolite 5,6-dihydrofluorouracil in plasma. Ther Drug Monit 2005;27:25–30.

40. Committee for Medicinal Products for Human Use and European Medicines Agency. Guide to bioanalytical method validation. European Medicines Agency, London, UK. 2011.

41. US Food and Drug Administration. FDA Guidance for Industry: Bioanalytical Method Validation. US Department of Health and Human, MD, USA. 2013.

42. Traut TW. Physiological concentrations of purines and pyrimidines. Mol Cell Biochem 1994;140:1–22.

43. Temmink OH, de Bruin M, Laan AC, Turksma AW, Cricca S, Masterson AJ, et al. The role of thymidine phosphorylase and uridine phosphorylase in (fluoro)pyrimidine metabolism in peripheral blood mononuclear cells. Int J Biochem Cell Biol 2006;38:1759–65.

44. Van Kuilenburg AB, van Lenthe H, Blom MJ, Mul EP, Van Gennip AH. Profound variation in dihydropyrimidine dehydrogenase activity in human blood cells: major implications for the detection of partly deficient patients. Br J Cancer 1999;79:620–6.

SUPPLEMENTARY FIGURES
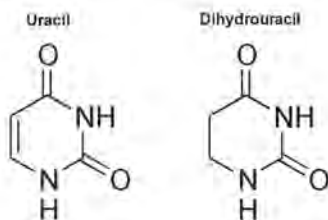
Figure S1. Chemical structures of uracil and dihydrouracil.
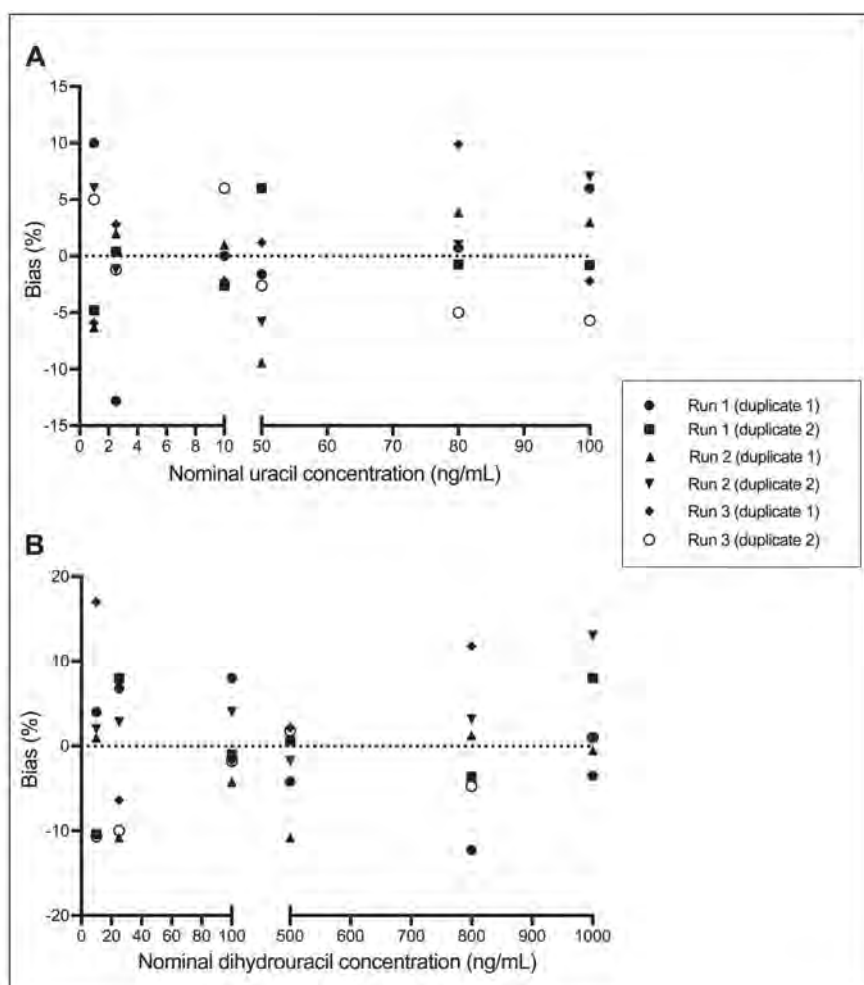
Figure S2. Relative difference between the back-calculated and nominal uracil (A) and dihydrouracil (B) concentrations of the calibration standards in three independent analytical runs.

1
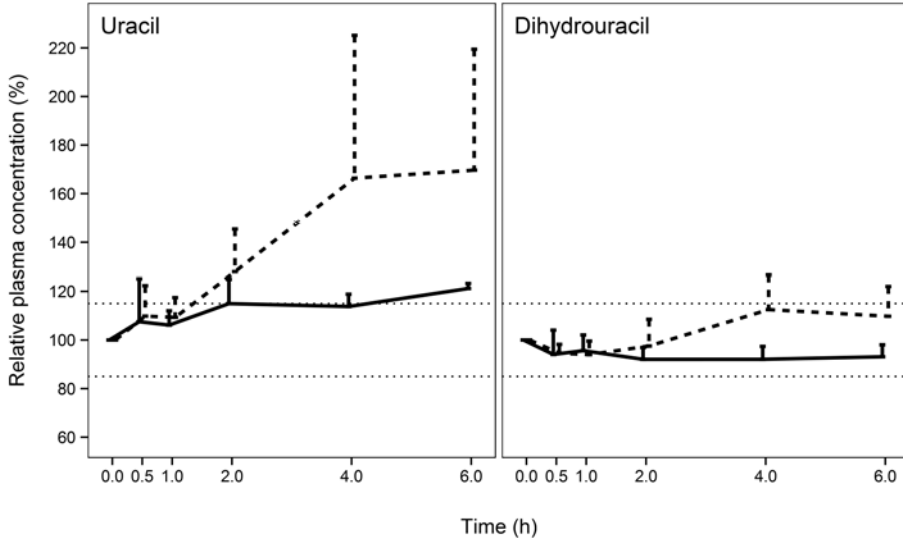
Figure S3. Stability of uracil and dihydrouracil in whole blood at ambient temperatures (dashed lines) and 2-8°C (solid lines). Whole blood was obtained from 3 healthy volunteers. Average uracil and dihydrouracil plasma concentrations are shown relatively to initial values. Error bars represent standard deviations. Dotted lines represent 15% deviation from the initial value.

CHAPTER 2

IMPROVED PHARMACODYNAMIC ASSAY FOR DIHYDROPYRIMIDINE DEHYDROGENASE ACTIVITY IN PERIPHERAL BLOOD MONONUCLEAR CELLS

Dick Pluim, Bart A. W. Jacobs, Maarten J. Deenen, Anneloes E. M. Ruijter,
Robin M. J. M. van Geel, Artur M. Burylo, Didier Meulendijks,
Jos H. Beijnen, Jan H. M. Schellens

2

ABSTRACT

Background

Dihydropyrimidine dehydrogenase (DPD) activity determination in peripheral blood mononuclear cells of DPD deficient patients was hitherto inaccurate due to hemoglobin (Hb) contamination. We developed an improved method for accurate measurement of DPD activity in patients.

Results

DPD activity was determined by high performance liquid chromatography with online radio-isotope detection using liquid scintillation counting. Hb was determined spectrophotometrically. Method accuracy and precision were significantly improved by using cumulative area of all peaks as internal standard. PBMC lysates from DPD deficient patients were highly contaminated with on average 23.3% (range 2.7 – 51%) of Hb resulting in up to twofold underestimated DPD activity. DPD activities were corrected for Hb contamination. The method was validated and showed good long-term sample stability.

Conclusion

This method has increased specificity allowing accurate identification of DPD deficient patients.

INTRODUCTION

Dihydropyrimidine dehydrogenase (DPD) catalyzes the reduction of the pyrimidine bases uracil and thymine into 5,6-dihydrouracil and 5,6-dihydrothymine, respectively [1]. DPD also facilitates the rate-limiting step in the metabolism of the anti-cancer drug 5-fluorouracil (5-FU). Approximately 85% of the administered 5-FU is metabolized into inactive metabolites by DPD. Because reduced DPD activity results in a higher exposure to 5-FU, patients with a complete or partial DPD deficiency who are treated with 5-FU or capecitabine are at high risk for developing severe, and sometimes fatal, fluoropyrimidine-induced toxicity [2-4].

Severe fluoropyrimidine related toxicity due to decreased DPD activity can be caused by point mutations, such as c.1905+1G>A (IVS 14 + 1G>A, *DPYD*2A*) in the 5' splicing site of intron 14, c.2846A>T, or c.1679T>G [5]. So far, an additional 50 polymorphisms spread over the entire *DPYD* coding region have been identified [6], but their clinical relevance is uncertain. Other genetic and epigenetic regulations such as promoter hypermethylation or variations in transcriptional factor expression may play a critical role in *DPYD* expression [7,8]. In addition, also non-genetic causes, such as drug-drug interactions and circadian variations might explain the large inter-patient variability in DPD activity [9].

For these reasons, phenotypic testing of DPD activity is likely to be a more sensitive way to detect DPD deficiency in patients compared to genetic screening for *DPYD* polymorphisms alone. In fact, recent studies using phenotypic screening have evidenced reduced DPD enzyme activity in between 36 - 71% of the patients with fluoropyrimidine-induced severe toxicities [10]. Phenotypic screening for DPD deficiency is most often performed in peripheral blood mononuclear cells (PBMCs) [11]. Only radio-isotope based DPD activity assays can be adequately sensitive to detect complete DPD deficiency [12,13]. However, several technical challenges limit the applicability of these methods. The original method by van Kuilenburg *et al.* [14,15] is based on the conversion of [^{14}C]-thymine into [^{14}C]-dihydrothymine with subsequent detection by high performance liquid chromatography and on-line liquid scintillation counting (HPLC-LSC). This method is relatively expensive and requires a laborious and hazardous purification process. Second, precision of the method is likely to be less than optimal due to experimental errors which are not corrected for. In addition, previous studies reported highly variable red colorization of PBMC lysates [16]. Recently, we demonstrated that the accuracy of the DPD activity was strongly affected by this hemoglobin (Hb) contamination in PBMC lysates, by 20.3% (range 1- 59%, n = 12) [17]. We evidenced that this contamination is exclusively caused by Hb and introduced a simple spectrophotometrical method for the quantification of Hb in PBMC lysates.

Here we developed and validated an improved radio-isotopic method for the quantification of DPD activity in human PBMCs using the substrate [^{3}H]-thymine, eliminating the need of hazardous [^{14}C]-thymine. We based our DPD activity method on the method first reported by van Kuilenburg *et al.* [14,15], with modifications.

DPD activity was quantified using the peak area of the DPD enzyme reaction product [³H]-dihydrothymine (DHT). We demonstrate, that DPD activity can also be quantified using the area of the substrate [³H]-thymine. This opens the possibility for determining DPD activity in e.g. liver extracts and other tissues containing, in contrast to PBMCs, DHT metabolizing enzymes.

We improved method precision and accuracy by using the ratio between the average total peak area of five negative controls and total sample peak area to compensate for experimental errors in measurement of DPD activity.

Our improved method was used for the determination of DPD activity in PBMCs from eight patients experiencing severe capecitabine-induced toxicity in order to establish the effect of Hb contamination on the accuracy of DPD phenotyping. Lastly, since data on long-term storage stability of these samples is missing, we performed stability experiments and validated different storage conditions to allow batch analysis of stored samples.

MATERIALS AND METHODS

Reagents and chemicals

Ficoll-paque™PLUS was obtained from General Electric Healthcare (Little Chalfont, UK). Phosphate buffered saline (PBS) was purchased from GIBCO BRL (Gaithersburg, MD, USA). Complete® EDTA-free Protease Inhibitor was from Roche (Woerden, the Netherlands). Ammonium chloride (NH_4Cl), sodium bicarbonate ($NaHCO_3$), ethylenediaminetetraacetate (EDTA), β-nicotinamide adenine dinucleotide phosphate (NADPH), dipotassium hydrogenphophate (K_2HPO_4), potassium dihydrogenphosphate (KH_2PO_4), magnesium chloride hexahydrate ($MgCl_2.6H_2O$), dithiotreitol (DTT-DL), and thymine were purchased from Sigma (St. Louis, MO, USA). [³H-methyl]-thymine (1.85 – 2.59 TBq/mmol) was purchased from Moravek (Brea, CA, USA). Ultima Flow M was from Canberra Packard (Meriden, CT, USA). Cofactor solution consisted of 2.5 mM NADPH in water, and was stored in 500 µl aliquots at -80 °C. PBS Complete® buffer consisted of 17.5 mM K_2HPO_4 pH 7.4 and 2 mM DTT-DL in PBS supplemented with 1 Complete® EDTA-free Protease Inhibitor tablet per 10 ml, and was stored in 1 ml aliquots at -20 °C. Thymine mix consisted of 123 µM thymine, 2 µM [³H-methyl]-thymine and 12.5 mM $MgCl_2$ in water, and was stored at -20 °C. Reaction mix was freshly prepared on ice each day shielded from light by aluminium foil, and consisted of a 1:1 (v/v) mixture of cofactor solution and thymine mix.

Method development

PBMC isolation and cytosolic lysate preparation

PBMCs were isolated immediately after blood collection using Ficoll gradient centrifugation [18,19]. Briefly, 8 ml of heparinized blood was mixed with an equal volume of PBS at room temperature (RT) and carefully layered on top of a 12.5 ml Ficoll layer in a 50 ml tube. After centrifugation at 720g for 20 min at RT, the PBMC layer was transferred to a new 50 ml tube, washed with 50 ml of ice-cold PBS, and centrifuged at 500g for 10 min at 4°C. The PBS buffer wash and centrifugation procedure was done twice and each

time the supernatant was discarded. Next, the pellet was suspended in 1 ml of ice-cold PBS and transferred to a 1.5 ml cryo vial. After centrifugation at 500g for 5 min at 4°C, the supernatant was discarded and the PBMC pellet was snap frozen in liquid nitrogen and subsequently stored at -80°C.

PBMC lysates were prepared by resuspending the stored PBMC pellet in 100 µl of ice-cold PBS Complete® buffer after defrosting on ice and applying 15 pulses with a Branson 250 tip sonicator (Branson, Danbury, CT, USA) at power input setting level 3 with a 50% duty cycle. After centrifugation at 11,000g for 20 min at 4°C, 95 µl of supernatant was transferred to a clean 1.5 ml vial on ice for immediate determination of protein content and DPD activity.

Protein assay

Protein concentrations in the PBMC lysates were determined using the Bio-Rad protein assay kit (Bio-Rad, Hercules, CA, USA). Briefly, 5 µl of PBMC lysate was diluted with 45 µl of MilliQ water (Millipore, Billerica, MA, USA). Five bovine serum albumin standards were prepared in concentrations ranging from 32.5 to 500 mg/ml. In duplicate, 10 µl of diluted lysate and the standard curve were transferred to a clear 96-well flat bottom plate. After the addition of 200 µl dye solution, the plate was incubated for 15 min at RT and subsequently the absorption was measured at 590 nm using an EL340 microplate reader (Bio-Tek, Winooski, VT, USA).

Determination of and correction for hemoglobin content

Hemoglobin concentration was determined spectrophotometrically at 413 nm with a Nanodrop1000 spectrophotometer (Thermo Scientific, Ashville, NC, USA) in ten-fold diluted PBMC lysate [17]. Next, the corrected protein concentration in the PBMC lysate was calculated by subtracting the contaminating Hb concentration from the total protein concentration. DPD activity was expressed relative to the protein concentration after correction for Hb.

DPD activity assay

The assay was based on the method by van Kuilenburg *et al.* [14,15], with several modifications. Substrate for the DPD reactions was 12.5 µM of [³H]-thymine, as compared to 25 µM of [¹⁴C]-thymine in the original protocol. For optimal DPD activity determination PBMC lysates should be diluted into triplicates with ice-cold PBS complete buffer to protein concentrations that are approximately 0.5 mg/mL. By doing so, the odds, that thymine conversion is above the upper limit of the linearity range is reduced, and thymine conversion is most probably above the limit of quantification. DPD reactions were originally started one sample at a time by mixing PBMC lysates and reaction mix after pre-equilibration at 37°C in a water bath. We, however, initiated the DPD reactions in batch by transfer to a 37°C water bath after preparation of all samples on ice by mixing 20 µl of ice-cold reaction mix with 80 µl of ice-cold PBMC lysate or negative control. Next,

samples were incubated for 60 min at 37°C, in accordance with the original protocol. We terminated the reactions by boiling for 3 min at 100°C, which replaced termination by perchloric acid used in the original protocol. Next, denatured proteins were removed by centrifugation at 11,000g for 5 min at 4°C, in accordance with the original protocol. Subsequently, an amount of 90 µl of clear supernatant was transferred to a vial for analysis of sample by reversed phase HPLC.

High performance liquid chromatography analysis

Separation and quantification of [^{3}H]-thymine and the reaction product [^{3}H]-DHT was performed using HPLC (Beckman Coulter, CA, USA). A C18 HDO Uptisphere® column (Interchim, Montluçon Cedex, France), particle size 5 µm, 150 x 4.6 mm was used at RT at an eluent flow of 0.8 ml/min, which was mixed 1:1 (v,v) with Ultima-Flow M for on-line tritium radioisotope detection (Packard Instrument Co, CT, USA). The mobile phase consisted of 100% eluent A (50 mM KH_2PO_4 pH 4.5, and 1.0% (% v,v) MeOH) during the first 20 min, followed by 100% eluent B (50 mM KH_2PO_4 pH 4.5, and 40% (% v,v) MeOH) during the next 10 min. Then, the column was re-equilibrated for 5 min using 100% eluent A.

Calculation of DPD activity

Formulas 1 and 2 were used for calculation of the DPD activity (nmol/mg/h) using the [^{3}H]-DHT and [^{3}H]-thymine peak, respectively:

$$((A_1 - A_2) * A_3 * nmol\ T) / (A_4 * A_5 * mg * t) \tag{1}$$

$$((nmol\ T - (A_6 * A_3 * nmol\ T) / (A_4 * A_5))\ (mg * t) \tag{2}$$

A_1 = area of the DHT peak in the sample in counts per minute (cpm)
A_2 = average area of the DHT peaks in the 5 negative control samples (cpm)
A_3 = average area of the sum of all peaks in the 5 negative control samples (cpm)
A_4 = average area of all thymine peaks in the 5 negative control samples (cpm)
A_5 = sum of the area of all peaks in the sample (cpm)
A_6 = area of the thymine peak in the sample in counts per minute (cpm)
$nmol\ T$ = input level of thymine (= 1.27 nmol)
mg = amount of Hb corrected protein (mg)
t = incubation time in hours (h)
all peaks = the sum of the peak areas of DHT, thymine, and all background peaks

Method validation

DPD enzyme kinetics

The effect of concentration of the cofactor NADPH on DPD activity was determined in threefold in samples containing 0, 0.05, 0.1, 0.25, 0.5, 1.25, and 2.5 mM of NADPH, 100 µg of PBMC lysate protein, and 12.5 µM of thymine in a total volume of 100 µl.

To determine at which concentration of thymine the method would discriminate best between DPD poor and extensive metabolizers, the Michaelis-Menten constant (K_m) and maximum DPD enzyme velocity (V_{max}) were determined in blood obtained from a genetically-confirmed partial DPD-deficient (*DPYD*2A,* heterozygous) volunteer, and in PBMCs from a patient who was wild type for all tested mutations. The K_m and V_{max} were determined in triplicate in samples containing 0, 0.25, 2.5, 5.0, and 25 μM of total thymine (thymine + [^{3}H]-thymine), 2.5 mM of NADPH, and 100 μg of PBMC lysate protein in a total volume of 100 μl.

Specificity and limit of detection

Five negative control samples containing 80 μl PBS complete and 20 μl RM were assessed during each batch analysis. The limit of detection of the DPD method was defined as the DPD activity (nmol/h) that resulted in a DHT peak area that was equal to the average DHT background signal from these five negative control samples plus three times the standard deviation (SD). The specificity of the DPD reaction was determined in triplicate from the effect on DPD activity of 200 and 1000 nM of the specific DPD inhibitor gimeracil [20] in samples containing 80 μg of PBMC lysate protein obtained from a healthy volunteer. The 50% inhibitory concentration of gimeracil was earlier estimated to be 95 nM [20].

Linearity and lower limit of quantification

The linearity and lower limit of quantification (LLOQ) were determined in triplicate in samples spiked with 5, 9.3, 19, 29, 40, 48, 60, 79, 100, 100, 120, and 140 μg of pooled PBMC lysate protein from six healthy volunteers. This results in samples with the same average relative DPD activity (nmol/h/mg), but with different absolute DPD activities (nmol/h) and thymine conversions. DPD activities were determined using the peak areas of thymine and DHT with and without using the total sample peak area as internal standard. The DPD activity determined at the highest linear spike level was defined as nominal. The LLOQ and linear range were defined as the protein input level or protein input range, respectively, at which DPD activity could be determined with a precision of ≤ 20%, and an accuracy of 80 – 120% of the nominal DPD activity.

Within- and between-day precision

Samples containing 20, 60 or 100 μg of PBMC lysate protein were measured in triplicate on 7 consecutive days. The between-day (BDP) and within-day precision (WDP) were calculated by one-way analysis of variance (ANOVA) for each spike level using the run day as classification variable using the software package SPSS v15.0 for windows (Chicago, USA). The day mean square (DayMS), error mean square (ErrMS) and the grand mean (GM) of the observed cell concentrations across run days were used. The WDP% and BDP% for each spike level was calculated using the formulas:

WDP% = (ErrMS)$^{0.5}$ / GM x 100%   (3)

BDP% = [(DayMS − ErrMS)/n]$^{0.5}$ / GM x 100%   (4)

(where n is the number of replicates within each run).

Clinical applicability

To test the clinical applicability of the assay, we determined DPD activity in PMBCs from 19 healthy volunteers and 8 cancer patients who experienced severe capecitabine-induced toxicity (grade III/IV). Volunteers were aged ≥ 18 years of age (median age 28.7; range 22.9 – 39.8), not known with cancer, not treated with investigational or other drugs within 30 days before start of the study, and who had not undergone surgery within the past six months. Patients (4 female/4 male) had not been on treatment for at least 4 weeks before peripheral blood was drawn. Blood from each subject was drawn between 9:00 and 10:00 am into a 10 ml heparin blood tube for DPD activity determination, and a 5 ml EDTA blood tube for pharmacogenetic analysis. An amount of 3 ml of EDTA blood was used for isolation of genomic DNA using the QIAamp DNA mini kit (Qiagen, Inc. Valencia, CA). Polymorphisms for *DPYD* IVS14+1G>A (*DPYD*2A*), c.496A>G, c.1236G>A, c.2194G>A, c.2846A>T, c.1601G>A, and c.1679T>G were determined using real-time PCR (RT-PCR) assays using allele-specific TaqMan probes (Applied Biosystems, Bleijswijk, The Netherlands), and polymorphisms for *DPYD* 1627A>G were determined by sequencing [21].

The study received approval from the institutional medical ethical review board and subjects provided whole blood after written informed consent.

Stability

The stability of DPD activity in PBMCs, isolated from whole blood of a healthy volunteer stored *ex vivo* at RT for 0, 0.5, 1, 2 and 3 h, was determined in triplicate. In addition the stability of DPD activity in PBMC lysates stored for 0, 2, 3, 5, 6, 24 and 28 h on ice was determined in triplicate. For assessment of the long-term storage stability, 32 ml of blood was drawn in 8 ml heparinized blood tubes from each of 6 healthy volunteers. After isolation, according to the previously described method, PBMC suspensions were pooled and divided over 24 cryo-vials. After centrifugation, supernatants were removed and PBMC dry pellets were stored at -80°C. At the same time, aliquots of 500 µl of 2.5 mM NADPH were prepared in water and stored at -80°C. DPD activity was assessed in triplicate after storage of PBMC dry cell pellets and NADPH for 0, 1, 7, 14, 45, 120, 180, and 1020 days. For testing of the long-term storage stability, NADPH was thawed on ice in the dark and discarded after use. In a separate experiment, the effect of 3 repeated freeze/thaw cycles on NADPH stability was assessed in triplicate by determination of DPD activity in freshly prepared PBMC lysates from a single batch of PBMC dry cell pellets. Furthermore, we determined the stability of processed samples in the HPLC autosampler during 0, 24, 48 and 72 h of storage at RT.

Statistical Analysis

Statistical evaluation was performed using Student's *t*-test, unless indicated otherwise. DPD activities in PBMCs from healthy volunteers were tested for normal Gaussian distribution using the Kolmogorov-Smirnov test. DPD deficiency was defined as a DPD deficiency was defined as a DPD activity within the lower quartile (25th percentile) determined by quartile analysis of DPD activities in the control population. Analysis was performed with the Statistical Package for the Social Sciences (SPSS, Chicago, USA).

RESULTS

Method development

The original method of Van Kuilenburg was based on [14C]-thymine as substrate for DPD. Our DPD activity method is based on [3H]-thymine for cost and safety reasons. The cost of an equal amount of [3H]-thymine is approximately seven times less than the cost of [14C]-thymine. [3H]-thymine is also less dangerous as indicated by the annual limit of intake that is forty times higher than for [14C]-thymine [22].

Furthermore, the original method uses 25 μl of perchloric acid for reaction termination. This, however, lowers the pH-values of the final samples to below the advised working range of most HPLC columns, which strongly reduces column life-span. Therefore, in our method the DPD reactions are terminated by boiling for 3 min. The retrieval of [3H]-thymine and [3H]-DHT, after 3 min of boiling as compared to termination by perchloric acid, was not significant different at 102% ± 3.5% and 99.5% ± 4.9%, respectively. An additional 2 min of boiling did not significantly affect the retrieval of [3H]-thymine and [3H]-DHT, which were 98.4% ± 5.3% and 98.9% ± 4.1%, respectively.

The separation of DHT and thymine by HPLC was optimised by testing different eluents A containing 0, 0.5, 1.0, 1.5 and 2.0 (% v,v) of methanol. Complete baseline separation of DHT from thymine was only achieved using eluent A containing 1% of methanol (Fig. 1). Immediately after purchase the [3H]-thymine stock contained 5% of unknown compounds eluting between 2 and 7 min, and 4% of [3H]-DHT eluting at 12.5 min, respectively (Fig.1).

The radiochemical purity of the [3H]-thymine stock further deteriorated at 1% per month resulting in an increase of the area of the peaks between 2 and 7 min. However, [3H]-DHT content remained stable at about 4%.

Method validation

DPD enzyme kinetics

The dependence of the DPD reaction on the NADPH concentration is depicted in Fig. 2A. The K_m and V_{max} were 4.3 μM and 8.24 nmol/mg/h, respectively, as calculated from the Eadie-Hofstee plot (Fig. 2B). DPD activity did not significantly increase at NADPH concentrations above 125 μM.

The substrate dependency of the DPD reaction is depicted in Fig. 3A. V_{max} for the extensive and poor metabolizer were 9.96 and 3.51 nmol/mg/h, and K_m was 1.11 and
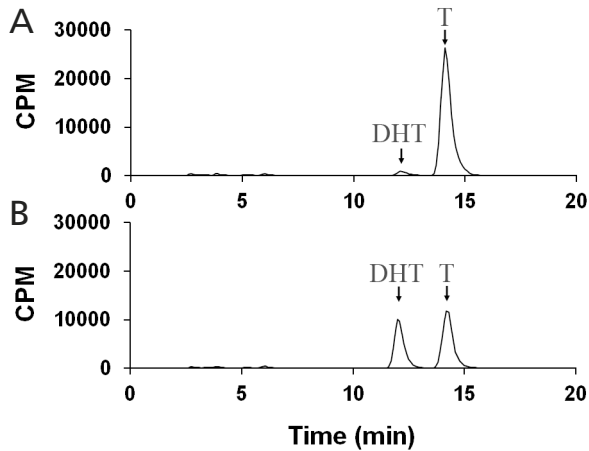
Figure 1. HPLC-liquid scintillation counting chromatograms of (A) a negative control sample; and (B) a dihydropyrimidine dehydrogenase reaction, performed with 100 μg of peripheral blood mononuclear cell lysate protein. The [³H]-dihydrothymine and [³H]-thymine peaks were indicated as DHT and T, respectively. Liquid scintillation detector response was in counts per minute. Abbreviations: DHT, dihydrothymine; T, Thymine.
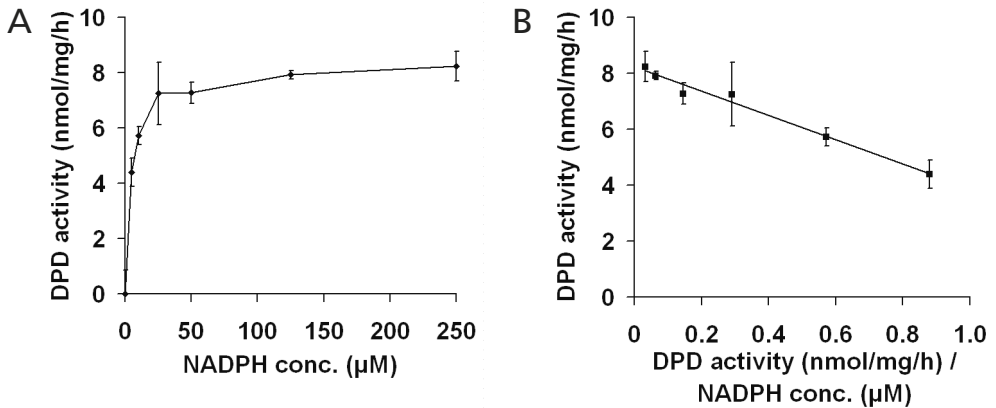
Figure 2. Effect of NADPH concentration on dihydropyrimidine dehydrogenase activity in peripheral blood mononuclear cell lysate from a healthy volunteer. Data are shown as (A) Michaelis–Menten; and (B) Eadie–Hofstee plots. Results are expressed as means ±S.D. of three different samples. Abbreviations: NADPH, β-nicotinamide adenine dinucleotide phosphate; DPD, dihydropyrimidine dehydrogenase.

0.97 μM, respectively, as determined from the Eadie-Hofstee plot (Fig. 3B). DPD activity did not significantly increase at thymine concentrations above 5 μM, which indicates saturation of DPD enzyme activity. Based on this, we decided to perform all subsequent DPD reactions with 12.5 μM of total thymine (~10 times Km), which theoretically results in only 8% reduction of enzyme activity after 50% of substrate is consumed [23].
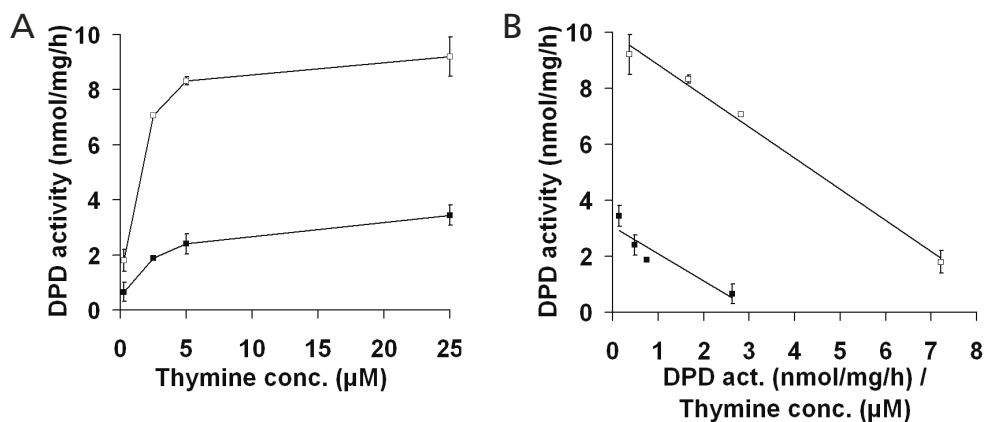
Figure 3. Enzyme kinetics of the dihydropyrimidine dehydrogenase activity in peripheral blood mononuclear cell lysate from a genetically-determined partial DPD-deficient (*DPYD*2A*) volunteer (), and in lysate from a subject who was wild type for *DPYD*2A* (, extensive metabolizer). Data are shown as Michaelis-Menten (A) and Eadie-Hofstee plots (B). Results are expressed as means ± S.D. of three different samples. Abbreviations: DPD, dihydropyrimidine dehydrogenase; WT, wild-type.

Specificity

The lower limit of detection of the method determined from five background control samples was 16.25 pmol DHT, which corresponds to 1.3% of the total thymine input of 1267 pmol per sample. The DPD reaction was inhibited by 67% and 96% using 200 and 1000 nM of gimeracil, respectively.

Linearity and lower limit of quantification

The nominal DPD activity using the DHT peak and internal standard correction was 8.12 ± 0.28 nmol/mg/h (Table 1). The linear range was from 9.3 to 120 µg PBMC lysate (Fig. 4) corresponding with a thymine conversion of 6.1 ± 0.3% to 77.1 ± 3.8%, respectively. At the LLOQ of 9.3 µg accuracy and precision were 102.3 and 13.4%, respectively. Internal standard correction had no effect on the linear range, however average precision improved from 5.0% to 3.1%.

The DPD activity method using the thymine peak and internal standard correction was 8.18 ± 0.35 nmol/mg/h (Table 1). The linear range was from 40 to 120 µg PBMC lysate (Fig. 4) corresponding with a thymine conversion of 23.7 ± 1.2% to 74.6 ± 2.7%, respectively. At the LLOQ of 40 µg accuracy and precision were 97.4% and 3.6%, respectively. Internal standard correction extended the lower part of the linear range from 60 to 40 µg of PBMC lysate protein and improved the average precision from 9.3% to 4.3%. Furthermore, internal standard correction reduced the difference in mean DPD activity between both methods from a significant 12% (p = 0.003) to a nonsignificant 0.8%.

Table 1. LLOQ mean dihydropyrimidine dehydrogenase activity, precision, and linear range of thymine conversion of the dihydropyrimidine dehydrogenase activity assay based on either thymine reduction, dihydrothymine formation, with or without the use of IS correction

	Thymine based		DHT based	
	- IS	+ IS	- IS	+ IS
Mean (±SD) DPD act.[†] (nmol/mg/h)	7.62 ± 0.57	8.18 ± 0.35	8.57 ± 0.44	8.12 ± 0.28
LLOQ (µg)[‡]	60	40	9.3	9.3
linear range (µg)[‡]	60 - 120	40 - 120	9.3 - 120	9.3 - 120
linear thymine conversion range (%)	37.1 ± 1.2	23.7 ± 1.0	6.6 ± 1.0	6.1 ± 0.8
	−73.5 ± 3.0	−74.6 ± 2.7	−80.5 ± 5.1	−77.1 ± 3.8

[†] Mean DPD activity over the linear range.
[‡] Amount of peripheral blood mononuclear cell lysate protein.
Abbreviations: Act, activity; DHT, dihydrothymine; DPD, dihydropyrimidine dehydrogenase; IS, internal standard.
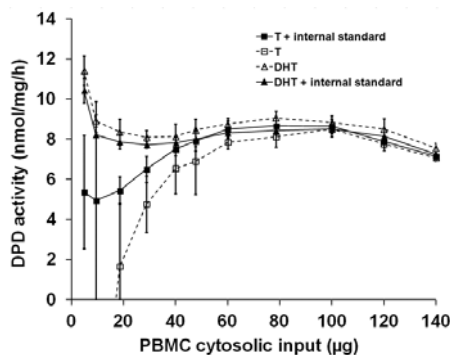
Figure 4. Correlation between the amount of peripheral blood mononuclear cells lysate protein and the dihydropyrimidine dehydrogenase activity calculated using the thymine peak and dihydrothymine peak. Both calculations were performed with or without using the total peak area as an IS for correction of experimental errors. Results are expressed as means ±S.D. of three different samples. Abbreviations: DHT, dihydrothymine; DPD, dihydropyrimidine dehydrogenase; IS, internal standard; PBMC, peripheral blood mononuclear cell; T, thymine.

Within- and between-day precision

DPD activity based on DHT with internal standard correction was determined at 20, 40, and 60 µg of PBMC lysate protein input. The average DPD activity was 8.5 ± 0.4 nmol/mg*h. BDP was 4.2, 3.8, and 5.1 % and WDP was 4.7, 3.6 and 2.4% at 20, 40, and 60 µg of PBMC lysate protein input, respectively.

DPD activity based on thymine with internal standard correction was 8.3 ± 0.5 nmol/mg*h. BDP was 6.3, 4.8, and 4.7 % and WDP was 4.0, 2.9 and 5.4% at 20, 40, and 60 µg of PBMC lysate protein input, respectively.

Internal standard correction had no significant effect on BDP, however WDP was significantly improved by on average 46% ($p = 0.004$) and 34% ($p = 0.01$) using the DHT and thymine based methods, respectively.

Stability

The stability of samples at different stages of processing was assessed under various storage conditions (Table 2). Whole blood was stored on ice for 3 h prior to PBMC isolation and subsequent lysate preparation, which resulted in stable DPD activity levels. In addition, PBMC lysates could be stored on ice for 24 h without a significant deterioration in DPD activity. Long term storage of PBMC dry cell pellets and 2.5 mM of NADPH at -80°C was possible for at least 1020 days without significant reduction of DPD activity. We noticed, however, a significantly lower DPD activity after 30 days of storage of the NADPH solution at -20°C (p = 0.018, data not shown). NADPH stored at -80°C was stable for 2 freeze/thaw cycles, however, a significant 11% (p= 0.023, data not shown) decrease in DPD activity was noticed after 3 freeze/thaw cycles. DPD activity was stable in final extracts which were stored within the HPLC autosampler for up to 72 h at RT.

Clinical applicability of DPD phenotyping

The average DPD activity before and after Hb correction in the healthy volunteers was 8.0 ± 2.6 (range 5.0 – 11.8, n= 19) and 9.6 ± 2.2 nmol/mg/h (range 6.0 – 14.0, n = 19), respectively. No significant difference was found between the average Hb contamination of 19.4% (range 2.0 – 54.3) and 23.3% (range 2.7 – 51, n = 8) in PBMC lysates from healthy volunteers and patients, respectively. An amount of 3 ml of EDTA blood was used for isolation of genomic DNA using the QIAamp DNA mini kit (Qiagen, Inc. Valencia, CA). Polymorphisms for *DPYD* IVS14+1G>A (*DPYD*2A*), c.496A>G, c.1236G>A, c.2194G>A, c.2846A>T, c.1601G>A, and c.1679T>G were determined using real-time PCR (RT-PCR) assays using allele-specific TaqMan probes (Applied Biosystems, Bleijswijk, The Netherlands), and polymorphisms for *DPYD* 1627A>G were determined by sequencing [21].

The findings with respect to DPD activity measurements in cancer patients, their *DPYD* genotypes, and the experienced toxicity are presented in Table 3. DPD deficiency was found in seven out of eight patients (88%) if no correction for Hb contamination was applied. However, two out of these seven patients (29%) with higher than average Hb contamination levels (31% and 34%, respectively) were shown to have normal DPD activity levels after correction for Hb. The lowest DPD activity was found in patient 6 who was heterozygous for the IVS14+1G>A (*DPYD*2A*) polymorphism. We measured DPD deficiency in two out of three patients that tested negative for any tested genetic *DPYD* mutation. The other three DPD deficient patients had point mutations at c.1627A>G, c.1236G>A, and c.496A>G.

DISCUSSION

We developed a simple, accurate and precise method for the determination of DPD activity in PBMCs. The method was substantially simplified by using commercially available [3H]-thymine without additional HPLC removal of remaining traces of [3H]-DHT. The method showed to be highly specific for DPD, since 200 and 1000 nM of the specific DPD inhibitor gimeracil inhibited the DPD reaction by 67% and 96%, respectively. This

Table 2. Stability of dihydropyrimidine dehydrogenase activity in samples at different processing stages under various storage conditions[†].

Processing stages	Storage temperature (°C)	Storage period	Initial DPD activity (nmol/mg/h)	Measured DPD activity (nmol/mg/h)	Change (%)
whole blood	RT	3 h	5.17 ± 0.18	4.78 ± 0.13	- 7.6
PBMC cytosolic lysate	0	28 h	9.10 ± 0.70	8.01 ± 0.35	- 11.9
PBMC dry pellet	-80	1020 d	4.99 ± 0.31	4.91 ± 0.39	2.5
autosampler	RT	72 h	4.54 ± 0.10	4.61 ± 0.16	1.5

[†] Results for initial and measured dihydropyrimidine dehydrogenase activity are the average of three replicate measurements ±SD.
Abbreviations: DPD, dihydropyrimidine dehydrogenase; PBMC, peripheral blood mononuclear cell; RT, room temperature.

Table 3. Summary of patients suspected of experiencing capecitabine induced toxicity[†].

Patient # (Gender (f/m) / Age (years))	Treatment regimen (conventional capecitabine dose)	Grade 3 – 4 CAP related toxicities	DPD activity[‡] (nmol/mg/h) +/- (SD)	DPD activity[§] (nmol/mg/h) +/- (SD)	DPYD Polymorphism(s)
1 (f / 39)	CAP (1000 mg/m² BID)	Mucositis	3.80 (0.07)[i]	7.56 (0.10)[i]	1627A>G (heterozygous)
2 (f / 71)	EP + CIS + CAP (500 mg/m² BID)	Mucositis	5.68 (0.27)[i]	8.61 (0.39)[iii]	1236G>A (heterozygous)
3 (f / 73)	CAPOX (1000 mg/m² BID)	Mucositis	10.06 (0.08)[ii]	10.56 (0.11)[ii]	None detected
4 (f / 61)	CAPOX (1000 mg/m² BID)	Mucositis	5.51 (0.12)[i]	6.05(0.13)[i]	2194G>A 496A>G (heterozygous)
5 (m / 69)	CAP + RT (825 mg/m² BID)	Diarrhea	3.37 (0.16)[i]	4.36 (0.21)[i]	None detected
6 (m / 65)	CAP (1000 mg/m² BID)	Yes (type unknown)	3.51 (0.05)[i]	4.23 (0.06)[i]	IVS14+1G>A (heterozygous)
7 (m / 67)	CAPOX (1000 mg/m² BID)	Mucositis	4.75 (0.17)[i]	5.64 (0.21)[i]	None detected
8 (m / 56)	CAP + OX + Doc (850 mg/m² BID)	Mucositis Neutropenia	6.94 (0.81)[i]	10.03 (1.03)[iii]	2194G>A (heterozygous)

[†]Measured dihydropyrimidine dehydrogenase (DPD) activities were compared with DPD activity in healthy volunteers (n = 19).
[‡]DPD activity before Hb correction.
[§]DPD activity after Hb correction.
[i,ii]indicates whether a measured DPD activity is within the first or second quartile (25 percentile) of the reference population (n = 19).
Abbreviations: BID, twice daily; RT, radiotherapy; CAP, capecitabine; EP, epirubicine; CIS, cisplatin; OX, oxaliplatin; Doc, Docetaxel; Hb, hemoglobin; DPD, dihydropyrimidine dehydrogenase.

level of inhibition of DPD by gimeracil is in line with the 50% inhibitory concentration of 95 nM [20].

Method accuracy and precision were significantly improved by using the ratio of the average total peak area of five controls and total peak area of samples as internal standard to correct for experimental errors. After applying this internal standard correction DPD activities calculated based on thymine and DHT were the same over the linear ranges of 40 – 120, and 9.3 - 120 µg of PBMC lysate, respectively. The DHT based method had the highest sensitivity with a lower limit of quantification of 9.3 µg PBMC lysate, which corresponds to an amount of 500.000 PBMCs. The WDP and BDP precisions were both well within the limit of 15% which is common for analytical assays [24]. Our innovative way of using the cumulative area of all peaks in the chromatogram as internal standard can also be applied for the development and optimization of other HPLC-based radioassays. We demonstrated the clinical applicability of our improved method in eight cancer patients. Although DPD activity was determined in PBMCs, which is used as a surrogate marker for systemic 5-FU catabolising capacity, the results provide information that could explain the observed capecitabine-induced toxicities such as mucositis, diarrhea, and neutropenia in these patients. Earlier studies already demonstrated a highly significant correlation between DPD activity in PBMCs and liver cells [11], illustrating that DPD activity in PBMCs is a valid marker for systemic DPD activity.

All patients treated with fluoropyrimidine anti-cancer agents in the Antoni van Leeuwenhoek Hospital are prospectively screened for *DPYD* IVS14+ 1G>A (*DPYD*2A*) prior to start of treatment. Although this strategy proves to significantly reduce the incidence of severe toxicity in mutation carriers and is cost-effective [25], there are many more polymorphisms in *DPYD* that may result in fluoropyrimidine-induced severe toxicity [6]. By phenotyping DPD activity, the consequences of all possible polymorphisms in *DPYD* are taken into account.

The results from this case series show the importance of correction of DPD activity for Hb contamination in PBMC lysates. We and others [16,17] have reported about wide inter-individual variability in red colorization of PBMCs isolated by Ficoll. Recently, we evidenced that the origin of this red color was Hb instead of intact RBCs [17]. As expected, we found an equal mean amount and range of Hb contamination in PBMC lysates from volunteers and patients. Importantly, we found that above average Hb contamination can result in significant underestimation of DPD activity and consequently lead to misidentification of DPD deficient patients. In our case series, two out of seven patients were wrongfully identified as being DPD deficient. The chance of underestimating DPD activity is, of course, higher in samples containing above average Hb contamination. After Hb correction five out of eight (= 63%) patients were identified as DPD deficient. Patient 6 with a *DPYD*2A* mutation was DPD deficient with the lowest DPD activity, which is in line with literature [26]. Patients 1, 4, and 8 were DPD deficient and had mutations at c.1627A>G, c.2194G>A + c.496A>G, and c.2194G>A, respectively. However, the association of these mutations with DPD deficiency is questionable [5]. Interestingly, patient 2 had the c.1236G>A mutation, but no DPD deficiency. Although this mutation

has been associated with severe toxicity, little is known about the effect of this mutation on DPD activity [5,27]. Three patients screened wild type for all tested mutations. However, two of these patients were found to be DPD deficient, which indicates that other genetic alterations in *DPYD* might be involved and confirms the added value of DPD phenotyping compared with genetic screening alone. The limitation of these observations is of course the small sample size of the case series. Other factors, such as co-medication, epigenetic factors and polymorphisms within other genes were not taken into account. To determine whether upfront phenotyping of DPD activity has any clinical implications, and if this is possibly linked to other polymorphisms in *DPYD*, a well-powered controlled clinical trial is warranted, a study, which will be performed at the Antoni van Leeuwenhoek hospital.

CONCLUSION

We developed and validated an improved method for the determination of DPD activity in PBMCs isolated from whole blood. The method is simple, sensitive, precise, and robust. We showed long-term stability of samples, thereby making the method suitable for batch analysis. Importantly, this DPD activity method is more accurate than previously developed methods, due to the application of an internal standard and by correcting for highly variable levels of Hb contamination that are found in Ficoll isolated PBMCs lysates. We have successfully applied our method in a volunteer study for determining the circadian rhythm of DPD activity, as described earlier [28], in PBMC (for submission). Our method has increases precision and accuracy, enabling better identification of DPD deficient patients in the clinical setting.

FUTURE PERSPECTIVE

We believe that this improved method for establishing DPD deficiency can help in the identification of DPD deficient patients with increased specificity. Furthermore, false positive identification of DPD deficient patients due to above average hemoglobin contamination of the PBMC lysates can possibly be prevented using our method. This may prevent the treating physician from lowering the dose of fluoropyrimidine anti-cancer agent based on wrongfully identified DPD deficiency, which can negatively affect treatment outcome.

2

REFERENCES

1. Yen JL, McLeod HL. Should DPD analysis be required prior to prescribing fluoropyrimidines? Eur J Cancer 2007;43:1011–6.

2. Milano G, Etienne MC, Pierrefite V, Barberi-Heyob M, Deporte-Fety R, Renée N. Dihydropyrimidine dehydrogenase deficiency and fluorouracil-related toxicity. Br J Cancer 1999;79:627–30.

3. Johnson MR, Diasio RB. Importance of dihydropyrimidine dehydrogenase (DPD) deficiency in patients exhibiting toxicity following treatment with 5-fluorouracil. Adv Enzyme Regul 2001;41:151–7.

4. van Kuilenburg ABP. Dihydropyrimidine dehydrogenase and the efficacy and toxicity of 5-fluorouracil. Eur J Cancer 2004;40:939–50.

5. Rosmarin D, Palles C, Church D, Domingo E, Jones A, Johnstone E, et al. Genetic markers of toxicity from capecitabine and other fluorouracil-based regimens: Investigation in the QUASAR2 study, systematic review, and meta-analysis. J Clin Oncol 2014;32:1031–9.

6. Ciccolini J, Gross E, Dahan L, Lacarelle B, Mercier C. Routine dihydropyrimidine dehydrogenase testing for anticipating 5-fluorouracil-related severe toxicities: hype or hope? Clin Colorectal Cancer 2010;9:224–8.

7. Zhang X, Li L, Fourie J, Davie JR, Guarcello V, Diasio RB. The role of Sp1 and Sp3 in the constitutive DPYD gene expression. Biochim Biophys Acta 2006;1759:247–56.

8. Etienne MC, Lagrange JL, Dassonville O, Fleming R, Thyss A, Renée N, et al. Population study of dihydropyrimidine dehydrogenase in cancer patients. J Clin Oncol 1994;12:2248–53.

9. Mercier C, Ciccolini J. Profiling dihydropyrimidine dehydrogenase deficiency in patients with cancer undergoing 5-fluorouracil/capecitabine therapy. Clin Colorectal Cancer 2006;6:288–96.

10. Ciccolini J, Mercier C, Evrard A, Dahan L, Boyer J, Duffaud F, et al. A rapid and inexpensive method for anticipating severe toxicity to fluorouracil and fluorouracil-based chemotherapy. Ther Drug Monit 2006;28:678–85.

11. Ostapowicz A, Dołęgowska B. Review of methods for determination of dihydropyrimidine dehydrogenase and possible application in screening previous chemotheraphy with 5-fluorouracil. Przegląd Lek 2012;69:694–7.

12. van Staveren MC, Guchelaar HJ, van Kuilenburg ABP, Gelderblom H, Maring JG. Evaluation of predictive tests for screening for dihydropyrimidine dehydrogenase deficiency. Pharmacogenomics J 2013;13:389-95.

13. van Kuilenburg ABP, van Lenthe H, Zoetekouw L, Kulik W. HPLC-electrospray tandem mass spectrometry for rapid determination of dihydropyrimidine dehydrogenase activity. Clin Chem 2007;53:528–30.

14. Van Kuilenburg ABP, Van Lenthe H, Van Gennip AH. Identification and tissue-specific expression of a NADH-dependent activity of dihydropyrimidine dehydrogenase in man. Anticancer Res 1996;16:389–94.

15. Van Kuilenburg ABP, Van Lenthe H, Tromp A, Veltman PC, Van Gennip AH. Pitfalls in the diagnosis of patients with a partial dihydropyrimidine dehydrogenase deficiency. Clin Chem 2000;46:9–17.

16. Jansen RS, Rosing H, Schellens JHM, Beijnen JH. Protein versus DNA as a marker for peripheral blood mononuclear cell counting. Anal Bioanal Chem 2009;395:863–7.

17. Pluim D, Jacobs BAW, Krähenbühl MD, Ruijter AEM, Beijnen JH, Schellens JHM. Correction of peripheral blood mononuclear cell cytosolic protein for hemoglobin contamination. Anal Bioanal Chem 2013;405:2391–5.

18. Böyum A. Isolation of mononuclear cells and granulocytes from human blood. Isolation of monuclear cells by one centrifugation, and of granulocytes by combining centrifugation and sedimentation at 1 g. Scand J Clin Lab Invest Suppl 1968;97:77–89.

19. Böyum A. Isolation of leucocytes from human blood. A two-phase system for removal of red cells with methylcellulose as erythrocyte-aggregating agent. Scand J Clin Lab Invest Suppl 1968;97:9–29.

2

20. Matt P, van Zwieten-Boot B, Calvo Rojas G, Ter Hofstede H, Garcia-Carbonero R, Camarero J, et al. The European Medicines Agency review of Tegafur/Gimeracil/Oteracil (Teysuno™) for the treatment of advanced gastric cancer when given in combination with cisplatin: summary of the Scientific Assessment of the Committee for medicinal products for human use. Oncologist 2011;16:1451–7.

21. Deenen MJ, Tol J, Burylo AM, Doodeman VD, de Boer A, Vincent A, et al. Relationship between single nucleotide polymorphisms and haplotypes in DPYD and toxicity and efficacy of capecitabine in advanced colorectal cancer. Clin Cancer Res 2011;17:3455–68.

22. ICRP Publication 61: Annual Limits on Intake of Radionuclides by Workers Based on the 1990 Recommendations, Elsevier, 1991.

23. Scopes RK. Enzyme Activity and Assays. John Wiley & Sons Ltd, West Sussex, United Kingdom, 2002.

24. Chandran S, Singh RSP. Comparison of various international guidelines for analytical method validation. Pharmazie 2007;62:4–14.

25. Deenen MJ, Cats A, Sechterberger M, Severens J, Smits PHM, Bakker R, et al. Safety, pharmacokinetics (PK), and cost-effectiveness of upfront genotyping of DPYD in fluoropyrimidine therapy. J Clin Oncol 2011:29(suppl; abstract 3606).

26. Offer SM, Fossum CC, Wegner NJ, Stuflesser AJ, Butterfield GL, Diasio RB. Comparative functional analysis of DPYD variants of potential clinical relevance to dihydropyrimidine dehydrogenase activity. Cancer Res 2014;74:2545–54.

27. van Kuilenburg ABP, Meijer J, Mul ANPM, Meinsma R, Schmid V, Dobritzsch D, et al. Intragenic deletions and a deep intronic mutation affecting pre-mRNA splicing in the dihydropyrimidine dehydrogenase gene as novel mechanisms causing 5-fluorouracil toxicity. Hum Genet 2010;128:529–38.

28. Wood PA, Du-Quiton J, You S, Hrushesky WJM. Circadian clock coordinates cancer cell cycle progression, thymidylate synthase, and 5-fluorouracil therapeutic index. Mol Cancer Ther 2006;5:2023–33.

C H A P T E R   3

DEVELOPMENT AND VALIDATION OF A QUANTITATIVE METHOD FOR THYMIDINE PHOSPHORYLASE ACTIVITY IN PERIPHERAL BLOOD MONONUCLEAR CELLS

Bart A.W. Jacobs, Dick Pluim, Pia van der Laan, Anna Tzani,
Jos H. Beijnen, Jan H.M. Schellens

ABSTRACT

The enzyme thymidine phosphorylase (TP) is important for activation of capecitabine and 5-fluorouracil. Assessment of TP phenotype might be suitable for identification of patients at risk of fluoropyrimidine-induced toxicity. In this paper, we describe the development and validation an assay for TP activity in peripheral blood mononuclear cells (PBMCs). The assay was based on *ex vivo* conversion of the TP substrate thymidine to thymine. The amount of thymine formed was determined by high-performance liquid chromatography – ultraviolet detection (HPLC-UV) with 5-bromouracil as internal standard. Lymphocytes and monocytes were purified from isolated PBMCs to examine cell-specific TP activity. TP activity in PBMCs demonstrated Michaelis-Menten kinetics. The lower limit of quantification was 2.3 µg PBMC protein and assay linearity was demonstrated up to 22.7 µg PBMC protein. Within-day and between-day precisions were $\leq 9.2\%$ and $\leq 6.0\%$, respectively. Adequate stability TP activity was demonstrated after long-term storage of PBMC dry pellets and lysates at -80 °C. In monocytes, TP activity was approximately 3 times higher than in lymphocytes. Clinical applicability was demonstrated in samples that were collected from five cancer patients. A simple, precise and sensitive HPLC-UV assay for quantification of TP activity in PBMCs was developed that can be applied for clinical research.

3

INTRODUCTION

Capecitabine is an orally available pre-prodrug of 5-fluorouracil (5-FU) that is used for treatment of colorectal, gastric and breast cancer. After administration, capecitabine is rapidly absorbed and enzymatically converted to subsequently 5'-deoxy-5-fluorocytidine (dFCR) and 5'-deoxy-5-fluorouridine (dFUR) [1–5]. Conversion of dFUR to 5-FU is catalyzed by thymidine phosphorylase (TP) [6]. Because of relatively high TP expression, formation of 5-FU preferentially occurs within tumor and liver tissue [4,7,8]. Approximately 80% of 5-FU is catabolized to inactive metabolites by the enzyme dihydropyrimidine dehydrogenase (DPD) and about 1-3% of 5-FU is intracellularly anabolized to active metabolites. The metabolite 5-fluoro-2'-deoxyuridine-5'-monophosphate (FdUMP) possesses the highest anticancer potency. This metabolite inhibits the enzyme thymidylate synthase (TS), which leads to disrupted DNA synthesis and cell death [9]. Formation of FdUMP also depends on TP, since TP catalyzes intracellular conversion of 5-FU to 5-fluoro-2-deoxyuridine (FdUrd), which, in turn, is converted to FdUMP by thymidine kinase. The activation pathway of capecitabine is illustrated in Figure 1.

About 10-30% of the patients treated with capecitabine develop severe, sometimes even lethal, toxicity [10]. Recent studies by us and others showed that some single nucleotide polymorphisms (SNPs) in the gene encoding DPD (*DPYD*) are associated with capecitabine-induced toxicity [11,12]. Genotyping for relevant SNPs in *DPYD* alone, however, has limited sensitivity for identification of patients at risk of severe toxicity [12].

Recently, a single nucleotide mutation (*1412C>T,* rs11479) in the gene for TP (*TYMP*) was found to be associated with relatively high expression of TP and capecitabine-induced diarrhea and hand-foot syndrome in patients [13,14]. *In vitro* studies have demonstrated that the cytotoxic effects of the TP substrate dFUR are increased after upregulation of TP [15]. Furthermore, upregulation of TP has been found in tumor tissue of patients after treatment with docetaxel, adriamycin and epirubicin [16,17]. Studies of xenograft models and *in vitro* experiments also demonstrated TP induction after exposure to vorinostat, vinorelbine, lidamycin and X-ray irradiation [18–21]. Based on these findings, it seems likely that the availability of a marker for the TP phenotype could attribute to the identification of patients at risk of capecitabine-induced toxicity. Since TP activity seems to be affected by other treatments, the ideal TP phenotype marker should allow for longitudinal assessments of TP activity.

Peripheral blood mononuclear cells (PBMCs) are extensively used as a source of surrogate tissue for quantification of a phenotype marker [6, 7]. Collection of PBMCs is minimally invasive and can be repeated at several time points in order to assess treatment effects. A method for phenotyping TP activity in total leukocytes has previously been described [22]. This method is based on quantification of the amount of thymine formed after *ex vivo* incubation with the TP substrate thymidine. Importantly, TP activity significantly differed among leukocyte subpopulations [23]. The PBMC population mainly consists of lymphocytes and a small percentage of monocytes. Therefore, the PBMC population is more homogenous than the total leukocyte population and is possibly less distorted by alterations in relative sample composition.
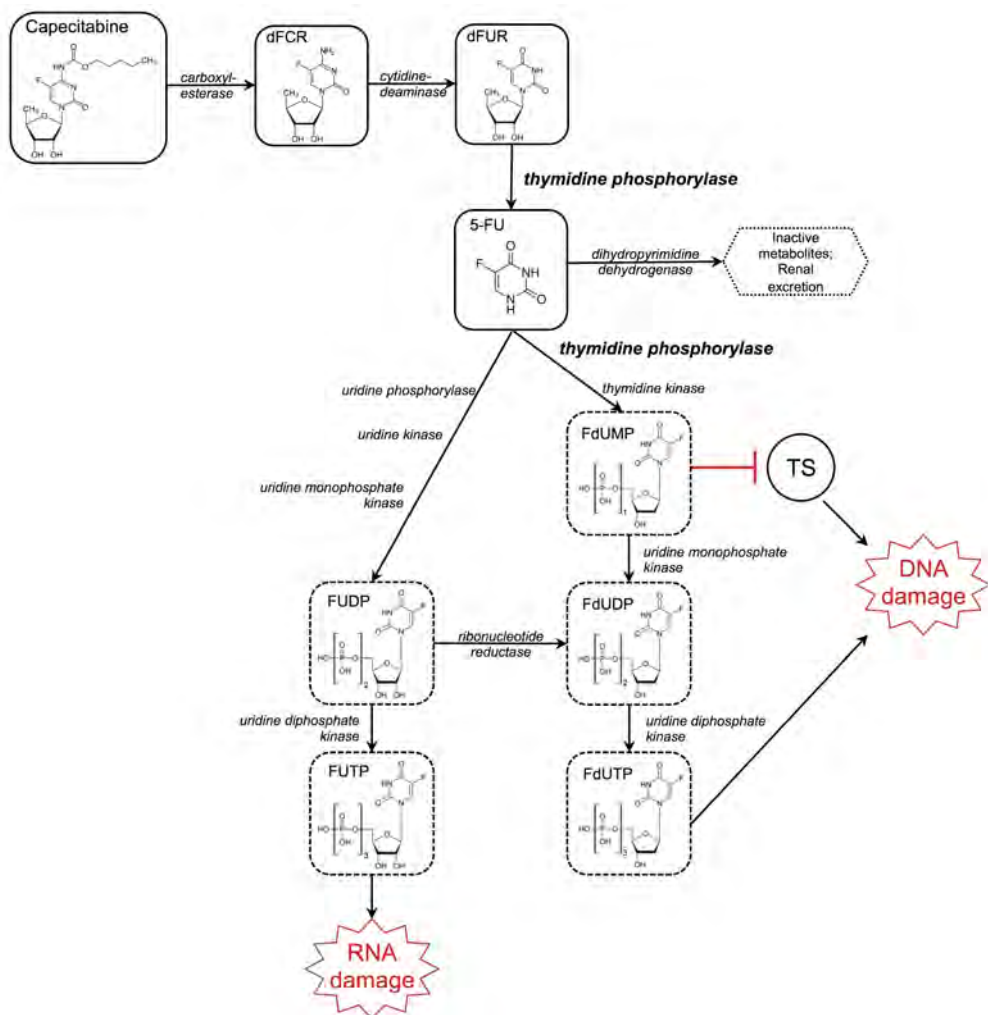
Figure 1. Activation pathway of capecitabine. The role of thymidine phosphorylase is highlighted in bold. Abbreviations: dFCR, 5'-deoxy-5-fluorocytidine; dFUR, 5'-deoxy-5-fluorouridine; 5-FU, 5-fluorouracil, FdUMP, 5-fluoro-2'-deoxyuridine-5'-monophosphate; TS, thymidylate synthase; FUDP, 5-fluorouridine-5'-diphosphate; FUTP, 5-fluorouridine-5'-triphosphate; FdUDP, 5-fluoro-2'-deoxyuridine-5'-diphosphate; FdUTP, 5-fluoro-2'-deoxy-5'-triphosphate

The primary objective was to develop and validate a simple assay for quantification of TP activity in PBMCs (TPA$_{pbmc}$). In addition, we explored the TP activity in the purified lymphocytes and monocytes.

3

MATERIALS AND METHODS

Chemicals

Thymidine, thymine, 5-bromouracil (5-BU), dithiothreitol (DTT), potassium dihydrogenphosphate (KH_2PO_4), dipotassium hydrogenphosphate (K_2HPO_4), high-performance liquid chromatography (HPLC)-grade methanol, bovine serum albumin (BSA) and Hoechst33258 were purchased from Sigma (St. Louis, MO, USA). The water used for the experiments was Milli-Q grade (Millipore, Billerica, MA, USA). Ficoll-paque™ PLUS was obtained from General Electric Healthcare (Little Chalfont, UK). Phosphate buffered saline (PBS) was purchased from Gibco BRL (Gaithersburg, MD, USA). Perm/Wash™ was obtained from Becton Dickinson (Heidelberg, Germany) and formaldehyde was purchased from Merck (Darmstadt, Germany). Magnetic antibody cell sorting (MACS) columns, anti-CD14 microbeads, anti-CD45 fluorescein isothiocyanate (FITC), anti-CD14 allophycocyanin (APC) were obtained from Miltenyi (Bergisch Gladbach, Germany).

Isolation of PBMCs

Heparinized blood (8 mL) was mixed with an equal volume PBS. Isolation of PBMCs was achieved using Ficoll density gradient centrifugation at 720g for 20 min at room temperature. The leukocyte layer containing PBMCs was transferred to a clean 50 mL tube, washed with PBS and centrifuged at 1000g for 10 min at 4 °C. Then, PBMCs were washed twice with PBS, centrifuged at 500g for 10 min at 4 °C and transferred to a 1.5 mL cryovial. After centrifugation, supernatant was removed and the PBMCs were snap-frozen in liquid nitrogen and stored at -80 °C until further processing.

Sample preparation for TP activity measurement

After defrosting, PBMCs were resuspended in 300 μL assay buffer (35 mM potassium phosphate, 1 mM DTT; pH 7.4) and divided into three 100 μL aliquots that were independently processed. Samples were sonicated for 15 pulses using a Branson 250 tip sonicator (Branson, Danbury, USA) that was set on program 3 and 50% duty. PBMC cytosolic lysate was isolated after centrifugation at 11,000g for 20 min at 4 °C. Protein concentration was determined using the Bradford assay (Bio-Rad protein assay kit, Bio-Rad, Hercules, CA, USA) [24]. The amount of hemoglobin contamination in PBMC cytosolic lysate was quantified and subtracted from the total PBMC cytosolic protein [25].

TP enzyme activity assay

The assay was based on a method for TP activity of the total leukocyte population, with modifications [22]. TPA$_{pbmc}$ was expressed by the amount of thymine formed after incubation of the TP substrate thymidine. Incubation started when PBMC cytosolic lysate was added to 2 mM thymidine in assay buffer in a total reaction volume of 500 μL. Three negative control samples consisting of 2 mM thymidine in assay buffer were freshly prepared for each run. Samples were incubated for 1 hour at 37 °C. Directly after incubation, 50 μL of the ice-cold internal standard solution (100 μg/mL 5-BU in Milli-Q

water) was added and the reaction was terminated by placing the samples on a heat block for 4 min at 100 °C. After centrifugation at 11,000g for 5 minutes at 4°C, clear supernatant was transferred to a glass vials and a volume of 60 μL was injected into the HPLC system coupled with ultraviolet detection (HPLC-UV).

HPLC-UV analysis

Thymine and 5-BU concentrations were quantified using an UltiMate 3000 HPLC-UV system (Dionex, Sunnyville, CA, USA). Chromatographic separation was achieved on an Interchrom C$_{18}$ column (150 x 4.6 mm ID, particle size 5 μm; Interchim, Montluçon Cedex, France). The autosampler and the column were at room temperature. Eluent A consisted of 50 mM KH$_2$PO$_4$ (pH 4.5) and 1.0% (v/v) methanol in water and eluent B consisted of 50 mM KH$_2$PO$_4$ (pH 4.5) and 40% (v/v) methanol in water. The following gradient was used: 20% B from 0-8 min, 20-100% B from 8-9 min, 100% B from 9-14 min, 20% B from 14-20 min. The flow rate was 0.8 mL/min. Thymine and 5-BU were quantified at 265 nm. An external calibration curve was prepared in duplicate with thymine concentrations ranging from 0.76 to 500 μM. The amount of thymine in the negative control samples was subtracted from the amount of thymine in study samples. Chromeleon software (Dionex, Sunnyville, CA, USA; version 6.8) was used to control the HPLC-UV system and for data processing.

Method validation

TP enzyme kinetics

The influence of thymidine concentration on TPA$_{pbmc}$ was investigated by running the assay with 0.98, 1.95, 3.9, 7.8, 15.6, 31.2, 62.5, 125, 250, 500 and 1000 μM thymidine. For all reactions, the amount of PBMC cytosolic protein was 10 μg. Non-linear regression, using the Michealis-Menten equation, was performed to determine the V_{max} and K_m. A linearized model of Michealis-Menten, the Eadie-Hofstee model, was used for data visualization.

Assay linearity and the lower limit of quantification (LLoQ) were determined by running the assay with 0.9, 2.3, 4.5, 9.1, 18.2 and 22.7 μg of PBMC cytosolic protein. Linear regression of TPA$_{pbmc}$ versus protein input was performed. TPA$_{pbmc}$ values were back-calculated from the regression line and deviations from the measured TP activities were determined. Back-calculated TPA$_{pbmc}$ should not deviate from the observed TPA$_{pbmc}$ by more than ±20% at the LLoQ level and ±15% for higher protein input levels. Assay precision of ≤20% at the LLoQ level and ≤15% at the higher cytosolic protein input levels was considered acceptable.

Time dependency of the TP reaction was assessed in samples that were incubated for 15, 30, 60, 90, 120 and 210 minutes at 37 °C using 12.5 μg PBMC cytosolic protein. The effect of temperature on TPA$_{pbmc}$ was assessed by running the assay at 0, 25, 37, 50, 60 and 70 °C with 10 μg of PBMC cytosolic protein. Samples were equilibrated for 15 minutes at the different temperatures before thymidine was added. Kinetics of TP was assessed using pooled PBMCs from three healthy volunteers.

Within-day and between-day precision

Within-day precision (WDP) and between-day precision (BDP) were determined from quantification of TPA_{pbmc} in 5 consecutive analytical runs. PBMCs of one healthy volunteer were aliquoted in 5 cryovials and stored at -80 °C. On each day, one sample was thawed, prepared and analyzed in triplicate using 5 and 15 µg of PBMC cytosolic protein for the enzymatic reaction. One-way analysis of variance (ANOVA) with run day as classification variable was performed in order to calculate WDP and BDP [24]. Assay precision was considered acceptable in case WDP and BDP were <15%.

Stability

The stability of TPA_{pbmc} was examined after storage of whole blood for 4 and 24 hours at room temperature and for 4 hours on ice-water. Long-term stability of TPA_{pbmc} was assessed after storage of PBMC dry pellets and PBMC cytosolic protein lysates for 60 days at −80 °C. The stability of processed samples in the HPLC autosampler was assessed after 24 hours of storage at room temperature. Assay buffer and thymidine (50 mM) stock solution were stored for 2 months at −20 °C, before the effect on TPA_{pbmc} was determined. Stability of TPA_{pbmc} was considered acceptable if 85-115% of the initial activity was obtained.

Clinical applicability

Clinical applicability of the developed assay was assessed by quantification of TPA_{pbmc} in patient samples. The samples were collected from cancer patients who participated in a phase I clinical study of chronomodulated capecitabine therapy (http://www.trialregister.nl, study identifier: NTR4639). From each patient, 4 mL of blood was drawn within 3 days prior to treatment with capecitabine (screening sample), at the 7th day of capecitabine treatment and at the end of treatment. Immediately after blood collection, PBMCs were isolated and stored as dry pellets at −80 °C until further processing. The study was approved by the Ethics Committee of the Antoni van Leeuwenhoek Hospital, Amsterdam, The Netherlands.

TP activity PBMC subpopulations

Isolation of monocytes and lymphocytes

TP activities in the monocyte and lymphocyte subpopulations were explored in samples that were obtained from six healthy volunteers. PBMCs were isolated from 24 mL of heparinized blood using Ficoll density gradient. After washing the PBMCs three times with PBS, the cells were resuspended in 1 mL of beads buffer (BB) that consisted of 0.5% BSA and 2 mM EDTA in PBS. A total of 15×10^6 PBMCs were used for separation and isolation of the monocyte and lymphocyte subpopulations. The remaining PBMCs were used for assessment of TP activity in the total PBMC population. A volume of 8 µL of anti-CD14 microbeads, which was used for positive selection of monocytes, was added to the 15×10^6 PBMCs in a total volume of 200 µL and incubated for 30 minutes at

room temperature. After incubation, PBMCs were washed three times with 1 mL BB in order to remove unbound anti-CD14 microbeads. The PBMCs were resuspended in 500 µL BB and the cell suspension was loaded on a MACS column for magnetic enrichment. The lymphocytes, which are CD14-negative, were collected by rinsing the MACS column three times with 500 µL BB. After removal from the magnetic field, the column was flushed twice with 1 mL of BB in order to elute the monocytes. The samples were centrifuged at 1000g for 4 min at 4 °C. After centrifugation, the supernatant was removed, leaving 100 µL buffer on the pellets. Sample purity was assessed by analyzing 5 µL of each sample by flow cytometry. The isolated monocytes, lymphocytes and the sample containing the total PBMC population were washed twice with PBS and once with TP assay buffer, before the TP activity was assessed. Differences in TP activity among monocytes, lymphocytes and total PBMC populations were assessed by one-way analysis of variance and Tukey's post-hoc tests.

Flow cytometry analysis

Fluorescence-activated cell sorting (FACS) analysis was performed to assess the amount of monocytes and lymphocytes in the processed samples. From each sample, a 5µL aliquot was fixed in 1 mL of 2% formaldehyde in BB (v/v) for 15 minutes at room temperature. The samples were centrifuged for 4 minutes at 1000g at 4°C and washed twice with 1 mL BB. After discarding the supernatant, 1 mL of Perm/Wash™ was added and the samples were inverted 10 times, followed by centrifugation at 1000g for 4 minutes at 4 °C. Supernatants were carefully removed, leaving 100 µL on the cell pellets. The cells were stained with 3 µL anti-CD45-FITC, 1.5 µL anti-CD14-APC and Hoechst33258. After incubation for 1 hour at room temperature, the cells were washed twice with 1 mL Perm/Wash™. Samples were centrifuged at 1000g for 4 minutes at 4 °C and supernatants were removed, leaving 100 µL on the cell pellets. A volume of 300 µL BB was added. Flow cytometry was performed with a CyAn ADP Analyzer (Beckman Coulter, Brea, CA, USA). Summit software (Dakota Cytomation, Fort Collins, CO, USA; version 4.3) was used for data analysis.

Statistics

Statistical analyses were performed using Prism 6 (GraphPad, La Jolla, CA, USA). *P*-values ≤ 0.05 were considered statistically significant.

RESULTS
Method development

Quantification of TPA$_{pbmc}$ was achieved by determining the amount of thymine formed after incubation of thymidine in the presence of PBMC cytosolic protein and the co-factor phosphate. We used a previously optimized method for isolation of PBMC cytosolic lysate [24,26]. For the current method, we adapted the same procedures for processing PBMCs.

In order to quantify DPD activity in PBMCs, we previously established a HPLC method for chromatographic separation of thymine and dihydrothymine [26]. The same HPLC column was used for the current assay. We used 5-BU as an internal standard because this substance closely resembles the physicochemical properties of thymine. The proportion of eluent B was titrated up to a level that allowed for adequate separation of thymine and 5-BU. Typical retention times for thymine and 5-BU were 6.6 and 7.8 min, respectively. Thymidine eluted after 12.1 min and was not quantified during the HPLC-UV analysis, since the reduction in thymidine levels after incubation with PBMC cytosolic lysate was relatively small and could not be accurately quantified. The chromatogram of a sample that was processed with 20 μg of PBMC cytosolic protein without thymidine and internal standard did not reveal interfering peaks at the retention times of thymine and 5-BU (Figure 2A). A small peak was observed at the expected retention time of thymine in a sample that only contained 2 mM thymidine in assay buffer (Figure 2B). There was no thymine peak in the sample that only contained PBMC cytosolic protein and 5-BU (Figure 2C). The chromatogram of a representative study sample that was incubated with 15 μg PBMC cytosolic protein resulted in a relatively large increase of the thymine peak (Figure 2D). Because of the background signal in control samples of 2 mM thymidine in assay buffer (Figure 2B), three negative control samples were freshly prepared for each analytical run. The average thymine concentration in the background samples was subtracted from the thymine levels in the study samples.

Method validation

TP enzyme kinetics

The kinetics of TPA_{pbmc} with varying thymidine concentrations is illustrated in Figure 3. TPA_{pbmc} clearly demonstrated Michaelis-Menten kinetics. The estimated V_{max} and K_m were 1278 nmol/mg/h (95% confidence interval (CI) = 1255-1301 nmol/mg/h) and 78.1 μM (95% CI = 73.2-83.0 μM), respectively.

The amount of thymine increased linearly between 2.3 and 22.7 μg of PBMC cytosolic protein that was used for the enzymatic reaction (Figure 4A). At the LLoQ level of 2.3 μg protein input level, the average (± s.d.) thymine concentration was 6.78±0.13 nM and highly exceeded thymine levels in blank control samples (1.61±0.02 nM). Assay accuracy and precision were 94.4% and 2.8% at the LLoQ level. At protein input levels of 4.5, 9.1, 18.2 and 22.7 μg, the accuracy and precision ranged between 98.8-107.5% and 1.6-3.6%, respectively.

There was a linear association between the amount of thymine formed and the duration of incubation (Figure 4B). TPA_{pbmc} was highly temperature-dependent and peaked at 60 °C (Figure 4C). Incubation at this temperature resulted in a 3-fold increase of TPA_{pbmc} compared to incubation at 37 °C. There was no significant TPA_{pbmc} observed at 70 °C.

Within-day and between-day precision

Average TPA_{pbmc} in samples spiked with 5 and 15 μg of PBMC cytosolic protein were 910 nmol/mg/h and 916 nmol/mg/h, respectively. The WDP and BDP of the TP assay were
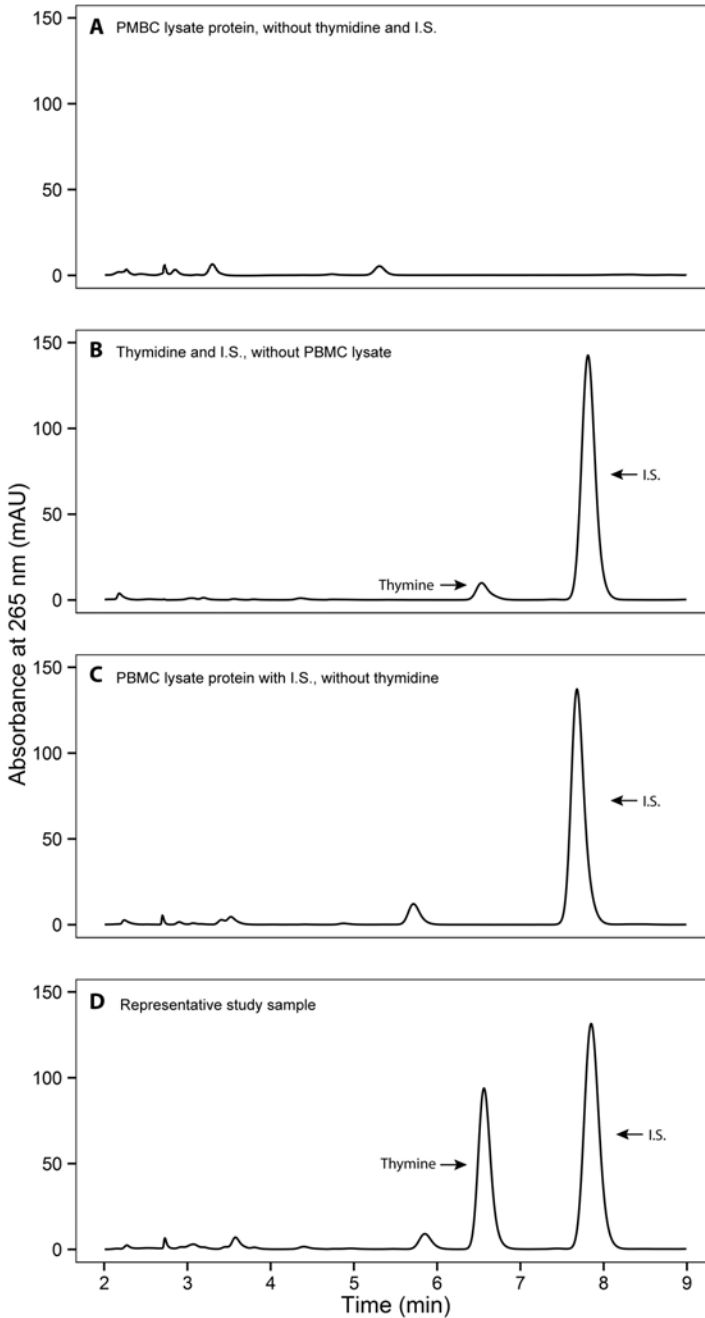
Figure 2. Representative chromatograms of thymine and the internal standard 5-bromouracil in A) a negative control sample of 20 μg peripheral blood mononuclear cells cytosolic protein in assay buffer B) a negative control sample 2 mM thymidine and internal standard C) a control sample of 20 μg peripheral blood mononuclear cell lysate protein and internal standard D) a study sample incubated with 15 μg of cytosolic protein and 2 mM thymidine in assay buffer. Abbreviations: PBMC, peripheral blood mononuclear cells; I.S., internal standard
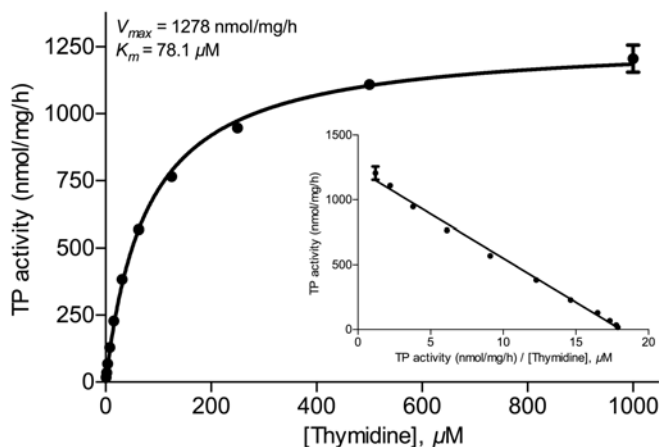
Figure 3. The effect of thymidine concentration on thymidine phosphorylase activity in peripheral blood mononuclear cells that were pooled from 3 volunteers. Data are visualized by a Michaelis-Menten and linearized (Eadie-Hofstee) plot (insert). Results are expressed by the average ± s.d. of three samples. Abbreviations: TP, thymidine phosphorylase; V_{max}, maximum enzyme velocity; K_m, Michaelis-Menten constant

8.1% and 4.6% in samples that were spiked with 5 µg protein. For samples spiked with 15 µg, the WDP and BDP were 9.2 % and 6.0 %.

Stability

Results of stability experiments are shown in Table 1. TPA_{pbmc} was stable in whole blood that was stored for 24 hours at room temperature. Storage of whole blood for 4 hours on ice-water resulted in significant reduction of TPA_{pbmc}. Long-term stability of PBMC dry pellets and cytosolic lysates was demonstrated for at least 6 months at -80 °C. There was no significant change in TPA_{pbmc} after storage of assay buffer and thymidine stock solutions for two months at -20 °C. Furthermore, re-injection analysis showed that final extracts were adequately stored in the HPLC autosampler for at least 24 hours at room temperature.

Clinical applicability

Figure 5 illustrates the TPA_{pbmc} of five patients. These analyses demonstrated the feasibility of quantification of TPA_{pbmc} in samples that were collected from cancer patients. TPA_{pbmc} demonstrated between-subject variability but did not seem to be altered after seven days of capecitabine treatment or at the end of treatment.

TP activity in monocyte and lymphocyte subpopulations

The TP activities in monocytes, lymphocytes and PBMCs of six volunteers are shown in Figure 6. Average (± s.d.) TP activity in monocytes was 2710±490 nmol/mg/h and in lymphocytes 906±134 nmol/mg/h ($P<0.001$). The average TPA_{pbmc} was 1286±190

3
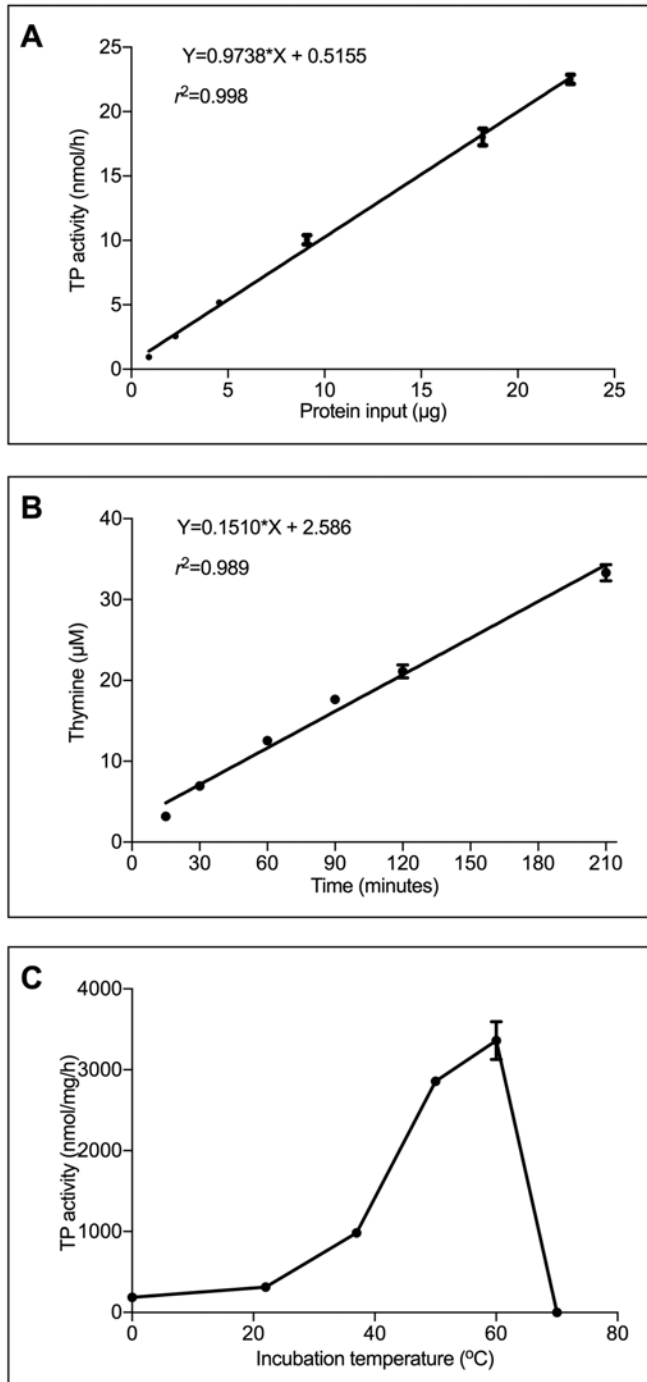
Figure 4. Linearity of thymidine phosphorylase activity in peripheral blood mononuclear cells with protein input (A) incubation time (B) and the effect of incubation temperature (C). Thymidine phosphorylase activity was determined in pooled samples from three volunteers. Results are expressed by the average ± s.d. of three samples. Abbreviation: TP, thymidine phosphorylase

Table 1. Stability of thymidine phosphorylase activity in peripheral blood mononuclear cells at different processing stages and storage conditions.

Component	Condition	Initial TP activity (nmol/mg/h)	Measured TP activity (nmol/mg/h)	Deviation (%)	CV (%)
Whole blood	Ice-water, 4 hours	1020	792	-22.3	9.7
Whole blood	Ambient, 4 hours	1020	987	-3.2	5.9
Whole blood	Ambient, 24 hours	1020	1015	-0.5	2.0
PBMC dry pellet	-80 °C, 6 months	934	856	-8.4	5.5
PBMC cytosolic lysate	-80 °C, 6 months	950	871	-8.3	4.1
Re-injection stability (final extract)	Ambient, 24 hours	1020	1060	3.9	5.9
Assay buffer	-20 °C, 2 months	1129	1118	-1.0	3.8
Thymidine stock solution	-20 °C, 2 months	1041	1118	7.4	3.8

Abbreviations: TP, thymidine phosphorylase; CV, coefficient of variation; PBMC, peripheral blood mononuclear cell

nmol/mg/h and was significantly different from TP activity in lymphocytes and monocytes ($P<0.01$). Purity of the monocyte and lymphocyte populations ranged between 93.5-98.6%. The percentage of monocytes in the total PBMC fractions ranged between 14.8-21.9%.

DISCUSSION

The primary aim was to develop and validate a simple and accurate method for the quantification of TPA_{pbmc}. We successfully developed a method that is based on *ex vivo* conversion of the TP substrate thymidine to the reaction product thymine. By applying the widely available HPLC-UV technique, this method can be implemented in most laboratories. The use of the internal standard 5-BU helps to reduce variation due to sample preparation.

We found a small background signal at the retention time of thymine in the chromatogram of a sample of 2 mM thymidine. The thymine background signal was not noticeable in samples that did not contain the thymidine stock solution. Most probably, thymine is an impurity in the thymidine dry powder, which is ≥99% pure, and directly causes the background signal. By quantifying the amount of thymine in three negative control samples, thymine background signals can be easily quantified and corrected for in study samples.

Validation experiments showed that assay linearity was observed for PBMC cytosolic protein levels between 2.3 – 22.7 µg. Within this range, assay accuracy and precision met
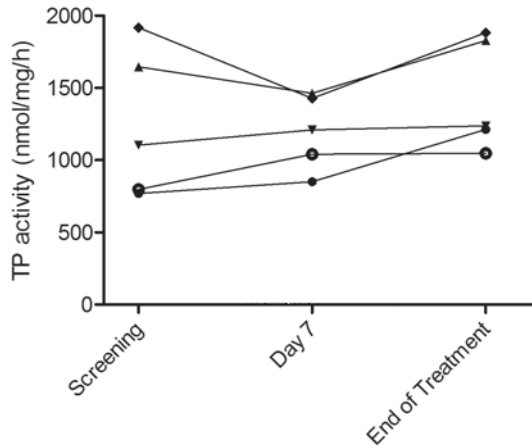
Figure 5. Thymidine phosphorylase activity in peripheral blood mononuclear cells of five cancer patients before treatment (Screening) with capecitabine, on the 7th day of capecitabine treatment and at the end of treatment. The patients participated in a phase I clinical trial of chronomodulated capecitabine therapy. Abbreviation: TP, thymidine phosphorylase
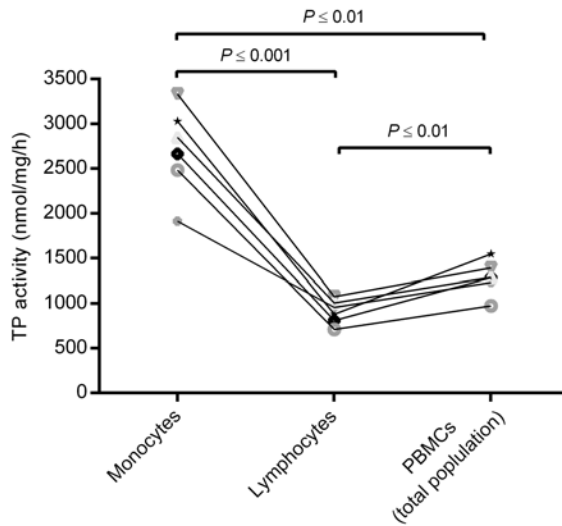
Figure 6. Thymidine phosphorylase activity in purified monocytes, purified lymphocytes and peripheral blood mononuclear cells of six volunteers. Abbreviation: TP, thymidine phosphorylase

the predefined criteria and were considered acceptable. Using only 2.3 µg PBMC cytosolic protein, the amount of thymine formed highly exceeds background levels. The minimum amount of PBMC protein needed for quantification of TPA$_{pbmc}$ can be extracted from approximately 125,000 cells, which can already be isolated from about 0.1 mL of whole blood. Since only a limited amount of blood is required, the developed assay can be easily implemented for sequential quantification of TPA$_{pbmc}$ in cancer patients. Clinical

applicability of the assay was confirmed by the quantification of TPA_{pbmc} in five patients that were sampled at 3 time points during the treatment course.

The estimated K_m was 78.1 µM and is comparable to the previously determined K_m of TP activity in the total leukocyte population [22]. It can be anticipated that a thymidine concentration of 2 mM, which corresponds to approximately ~25 times the estimated K_m, saturation of the TP enzymes occurs. Therefore, a thymidine concentration of 2 mM can be considered adequate for quantification of TP in PBMCs. The V_{max} of TP activity is approximately 3-fold higher in PBMCs compared to TP activity in total leukocytes [22].

Assay precision was tested using 5 and 15 µg PBMC protein. These protein input levels were at the lower and higher end, respectively, of the established linear range. For both protein input levels, the within-day and between-day precision met the predefined criteria for adequate precision. Therefore, we conclude that the assay shows good precision within the validated linear range of protein input levels.

Changes in temperature highly affect TPA_{pbmc}. Shaw et al. previously found that incubation at a temperature slightly above 40 °C increases the conversion of thymidine to thymine compared to samples that were incubated at 37 °C [27]. We also determined TPA_{pbmc} at temperatures above 40 °C and found the highest TPA_{pbmc} at 60 °C. Incubation at 50 °C already resulted in a relatively large increase of TPA_{pbmc} compared to incubation at 37 °C. It could be that denaturation of TP occurs at a temperature close to 70 °C. In order to obtain reliable and reproducible results, it is of major importance to keep the incubation temperature constant. We choose to maintain the incubation temperature at 37 °C because this best resembles the *in vivo* physiological conditions, and may better predict the role of TP inducers or inhibitors on TP activity.

In addition, future experiments might be performed to study the role of TP inducers or inhibitors on TP activity. Such experiments normally require incubation at a temperature that resembles the *in vivo* situation.

Other assays have been described for quantification of TP activity of the total leukocyte population [22,28]. Leukocyte subpopulations, however, showed high variability in TP activity [23]. A more homogenous population, like PBMCs, is most probably more appropriate for longitudinal observation of TP activity than the total leukocyte population. The PBMC fraction consists for 70 – 90% of lymphocytes and for 10-30% of monocytes. We found that TP activity was ~3 times higher in monocytes than in lymphocytes. Other researchers previously found that monocytes also possess higher DPD activity in comparison with lymphocytes [29]. Although the proportion of monocytes in PBMCs is relatively low, changes in the sample composition with respect to the relative amount of monocytes could affect the TP activity. Our analysis by flow cytometry provides a simple way for monitoring the amount of monocytes in the PBMC samples and their potential effect on TPA_{pbmc}

In conclusion, we successfully developed and validated a simple, accurate and precise assay for quantification of TPA_{pbmc}. Clinical applicability of the assay was demonstrated. Therefore, we believe that the developed assay is suitable for quantification of TPA_{pbmc} in clinical studies.

REFERENCES

1. Mackean M, Planting A, Twelves C, Schellens J, Allman D, Osterwalder B, et al. Phase I and pharmacologic study of intermittent twice-daily oral therapy with capecitabine in patients with advanced and/or metastatic cancer. J Clin Oncol 1998;16:2977–85.

2. Judson IR, Beale PJ, Trigo JM, Aherne W, Crompton T, Jones D, et al. A human capecitabine excretion balance and pharmacokinetic study after administration of a single oral dose of 14C-labelled drug. Invest New Drugs 1999;17:49–56.

3. Budman DR, Meropol NJ, Reigner B, Creaven PJ, Lichtman SM, Berghorn E, et al. Preliminary studies of a novel oral fluoropyrimidine carbamate: capecitabine. J Clin Oncol 1998;16:1795–802.

4. Miwa M, Ura M, Nishida M, Sawada N, Ishikawa T, Mori K, et al. Design of a novel oral fluoropyrimidine carbamate, capecitabine, which generates 5 fluorouracil selectively in tumours by enzymes concentrated in human liver and cancer tissue. Eur J Cancer 1998;34:1274–81.

5. Tabata T, Katoh M, Tokudome S, Hosakawa M, Chiba K, Nakajima M, et al. Bioactivation of capecitabine in human liver: involvement of the cytosolic enzyme on 5′-deoxy-5-fluorocytidine formation. Drug Metab Dispos 2004;32:762–7.

6. Walko CM, Lindley C. Capecitabine: a review. Clin Ther 2005;27:23–44.

7. Ishikawa T, Sekiguchi F, Fukase Y, Sawada N, Ishitsuka H. Positive correlation between the efficacy of capecitabine and doxifluridine and the ratio of thymidine phosphorylase to dihydropyrimidine dehydrogenase activities in tumors in human cancer xenografts. Cancer Res 1998;58:685–90.

8. Schüller J, Cassidy J, Dumont E, Roos B, Durston S, Banken L, et al. Preferential activation of capecitabine in tumor following oral administration to colorectal cancer patients. Cancer Chemother Pharmacol 2000;45:291–7.

9. Longley DB, Harkin DP, Johnston PG. 5-fluorouracil: mechanisms of action and clinical strategies. Nat Rev Cancer 2003;3:330–8.

10. Midgley R, Kerr DJ. Capecitabine: have we got the dose right? Nat Clin Pract Oncol 2009;6:17–24.

11. Deenen MJ, Meulendijks D, Cats A, Sechterberger MK, Severens JL, Boot H, et al. Upfront Genotyping of DPYD*2A to Individualize Fluoropyrimidine Therapy: A Safety and Cost Analysis. J Clin Oncol 2016;34:227–34.

12. Meulendijks D, Henricks LM, Sonke GS, Deenen MJ, Froehlich TK, Amstutz U, et al. Clinical relevance of DPYD variants c.1679T>G, c.1236G>A/HapB3, and c.1601G>A as predictors of severe fluoropyrimidine-associated toxicity: a systematic review and meta-analysis of individual patient data. Lancet Oncol 2015;16:1639–50.

13. Jennings BA, Loke YK, Skinner J, Keane M, Chu GS, Turner R, et al. Evaluating predictive pharmacogenetic signatures of adverse events in colorectal cancer patients treated with fluoropyrimidines. PLoS One 2013;8:e78053.

14. Milano G, Etienne-Grimaldi M-C, Mari M, Lassalle S, Formento J-L, Francoual M, et al. Candidate mechanisms for capecitabine-related hand-foot syndrome. Br J Clin Pharmacol 2008;66:88–95.

15. Evrard A, Cuq P, Ciccolini J, Vian L, Cano JP. Increased cytotoxicity and bystander effect of 5-fluorouracil and 5-deoxy-5-fluorouridine in human colorectal cancer cells transfected with thymidine phosphorylase. Br J Cancer 1999;80:1726–33.

16. Toi M, Bando H, Horiguchi S, Takada M, Kataoka A, Ueno T, et al. Modulation of thymidine phosphorylase by neoadjuvant chemotherapy in primary breast cancer. Br J Cancer 2004;90:2338–43.

17. Han J-Y, Hong EK, Lee SY, Yoon SM, Lee DH, Lee JS. Thymidine phosphorylase expression in tumour cells and tumour response to capecitabine plus docetaxel chemotherapy in non-small cell lung cancer. J Clin Pathol 2005;58:650–4.

18. Zhang J, Gu SY, Gan Y, Wang ZH, Wang BY, Guo HY, et al. Vinorelbine and capecitabine in anthracycline- and/or taxane-pretreated

3

metastatic breast cancer: Sequential or combinational? Cancer Chemother Pharmacol 2013;71:103–13.

19. Sawada N, Ishikawa T, Sekiguchi F, Tanaka Y, Ishitsuka H. X-ray irradiation induces thymidine phosphorylase and enhances the efficacy of capecitabine (Xeloda) in human cancer xenografts. Clin Cancer Res 1999;5:2948–53.

20. Zhang S-H, Zhang H, He H-W, Li L, Li X-Q, Zhang Y-P, et al. Lidamycin up-regulates the expression of thymidine phosphorylase and enhances the effects of capecitabine on the growth and pulmonary metastases of murine breast carcinoma. Cancer Chemother Pharmacol 2013;72:777–88.

21. Di Gennaro E, Piro G, Chianese MI, Franco R, Di Cintio A, Moccia T, et al. Vorinostat synergises with capecitabine through upregulation of thymidine phosphorylase. Br J Cancer 2010;103:1680–91.

22. van Kuilenburg ABP, Zoetekouw L. Determination of thymidine phosphorylase activity by a non-radiochemical assay using reversed-phase high-performance liquid chromatography. J Chromatogr B Analyt Technol Biomed Life Sci 2005;820:271–5.

23. van Kuilenburg ABP, Zoetekouw L. Determination of thymidine phosphorylase activity in human blood cells and fibroblasts by a nonradiochemical assay using reversed-phase high-performance liquid chromatography. Nucleosides Nucleotides Nucleic Acids 2006;25:1261–4.

24. Pluim D, Schilders KAA, Jacobs BAW, Vaartjes D, Beijnen JH, Schellens JHM. Pharmacodynamic assay of thymidylate synthase activity in peripheral blood mononuclear cells. Anal Bioanal Chem 2013;405:2495–503.

25. Pluim D, Jacobs BAW, Krähenbühl MD, Ruijter AEM, Beijnen JH, Schellens JHM. Correction of peripheral blood mononuclear cell cytosolic protein for hemoglobin contamination. Anal Bioanal Chem 2013;405:2391–5.

26. Pluim D, Jacobs BAW, Deenen MJ, Ruijter AEM, van Geel RMJM, Burylo AM, et al. Improved pharmacodynamic assay for dihydropyrimidine dehydrogenase activity in peripheral blood mononuclear cells. Bioanalysis 2015;7:519–29.

27. Shaw T, Smillie RH, MacPhee DG. The role of blood platelets in nucleoside metabolism: assay, cellular location and significance of thymidine phosphorylase in human blood. Mutat Res 1988;200:99–116.

28. Martí R, López LC, Hirano M. Assessment of thymidine phosphorylase function: measurement of plasma thymidine (and deoxyuridine) and thymidine phosphorylase activity. Methods Mol Biol 2012;837:121–33.

29. Van Kuilenburg AB, Van Lenthe H, Tromp A, Veltman PC, Van Gennip AH. Pitfalls in the diagnosis of patients with a partial dihydropyrimidine dehydrogenase deficiency. Clin Chem 2000;46:9–17.

P A R T   2

PHENOTYPIC VARIABILITY IN DIHYDROPYRIMIDINE
DEHYDROGENASE AND THYMIDYLATE SYNTHASE ACTIVITY

C H A P T E R   4

PRONOUNCED BETWEEN-SUBJECT AND
CIRCADIAN VARIABILITY IN THYMIDYLATE SYNTHASE AND
DIHYDROPYRIMIDINE DEHYDROGENASE ENZYME ACTIVITY
IN HUMAN VOLUNTEERS

Bart A.W. Jacobs, Maarten J. Deenen, Dick Pluim, J.G. Coen van Hasselt,
Martin D. Krähenbühl, Robin M.J.M. van Geel, Niels de Vries, Hilde Rosing,
Didier Meulendijks, Artur M. Burylo, Annemieke Cats, Jos H. Beijnen,
Alwin D.R. Huitema, Jan H.M. Schellens

ABSTRACT

Aims

Enzymatic activities of thymidylate synthase (TS) and dihydropyrimidine dehydrogenase (DPD) are important for the tolerability and efficacy of the fluoropyrimidine drugs. In this study, we explored between-subject variability (BSV) and circadian rhythmicity in DPD and TS activity in human volunteers.

4

Methods

The BSV in DPD activity (n=20) in peripheral blood mononuclear cells (PBMCs) and in plasma, by means of the dihydrouracil (DHU) and uracil (U) plasma levels and DHU:U ratio (n=40), and TS activity in PBMCs (n=19), were examined. Samples were collected every 4 hours throughout one day for assessment of circadian rhythmicity in DPD and TS activity in PBMCs (n=12) and DHU:U plasma ratios (n=23). In addition, the effects of genetic polymorphisms and gene expression on DPD and TS activity were explored.

Results

Population mean (±SD) DPD activity in PBMCs and DHU:U plasma ratio were 9.2 (±2.1) nmol/mg/h and 10.6 (±2.4), respectively. Individual TS activity in PBMCs ranged from 0.024-0.596 nmol/mg/h. Circadian rhythmicity was demonstrated for all phenotype markers. Between 00:30 – 02:00 h, DPD activity in PBMCs peaked, while the DHU:U plasma ratio and TS activity in PBMCs showed trough activity. Peak-to-trough ratios for TS and DPD activity in PBMCs were 1.62 and 1.69, respectively. For the DHU:U plasma ratio, peak-to-trough ratio was 1.43.

Conclusions

Between-subject and circadian variability in DPD and TS activity were demonstrated. Circadian rhythmicity in DPD might be tissue dependent. The results suggest influence of circadian rhythms on phenotype-guided fluoropyrimidine dosing and support implications for chronotherapy with high-dose fluoropyrimidine administration during the night.

INTRODUCTION

Anticancer drugs belonging to the group of the fluoropyrimidines are extensively used in the treatment of colorectal, breast and gastric cancer. Most frequently applied fluoropyrimidine drugs are 5-fluorouracil (5-FU) and its oral pre-prodrug capecitabine. After oral administration, capecitabine is rapidly absorbed and via a three-step enzymatic cascade converted into 5-FU. Approximately 80% of 5-FU is rapidly catabolized by the enzyme dihydropyrimidine dehydrogenase (DPD) to inactive metabolites [1–3]. About 1-3% of 5-FU is anabolized to active metabolites, of which 5-fluoro-2'-deoxyuridine-5'-monophosphate (FdUMP) possesses the highest anticancer potency [4]. This metabolite inhibits the enzyme thymidylate synthase (TS). Through inhibition of TS, synthesis of deoxythymidine triphosphate (dTTP) is reduced. Depletion of dTTP disrupts DNA synthesis and cell death ensues.

Approximately 10-30% of all patients treated with fluoropyrimidine-based chemotherapy develops severe, sometimes even lethal, toxicity [5]. Unfortunately, identification of patients at risk of severe toxicity is hampered by the unavailability of sensitive clinical biomarker tests. Genetic polymorphisms in the gene encoding for DPD, *DPYD*, may result in DPD deficiency. The polymorphisms *DPYD**2A and *DPYD* 2846A>T are proven risk alleles and are strongly associated with fluoropyrimidine-induced severe toxicity [6]. Given the combined frequency of these two mutations of 2-3% [7,8], an important, but only a small fraction of patients at risk is identified by these two polymorphisms. Polymorphisms in *TYMS*, the gene encoding TS, have also been associated with fluoropyrimidine-induced toxicity [6,9]. However, relevance of these mutations requires clinical validation.

In order to reduce the incidence of fluoropyrimidine-induced toxicity and optimize dosing, more sensitive biomarkers are required. Phenotyping methods could provide increased sensitivity for the identification of patients at risk of fluoropyrimidine-induced toxicity. In order to prevent invasive procedures, DPD activity is often determined in peripheral blood mononuclear cells (PBMCs). Clearance of 5-FU has shown to correlate well with DPD activity in PBMCs (DPDA$_{pbmc}$) [10]. Furthermore, previous studies have shown that approximately 50% of the patients suffering from severe fluoropyrimidine-induced toxicity had relatively low DPDA$_{pbmc}$ [11–13]. In addition, clearance of 5-FU and fluoropyrimidine-induced toxicity are also associated with pre-therapeutic plasma levels of the endogenous DPD substrate uracil (U) in plasma, and the ratio of the reaction product dihydrouracil (DHU) and U in plasma [14–17].

Although application of phenotyping assays seems promising for identification of patients at risk, only few medical centers use these methods in routine clinical practice [18,19]. Several factors might account for this. The development and validation of accurate and robust phenotyping assays is challenging, which is illustrated by high variability in U and DHU plasma levels among different studies [14]. Importantly, enzymatic activity of DPD and TS might possess circadian rhythms, which impedes interpretation of assay results.

4

Expression of DPD in PBMCs and the DHU:U plasma ratio have previously shown to peak at 19:00 h [20]. Others found that human $DPDA_{pbmc}$ peaked at the beginning or during the night [21,22]. However, lack of a circadian rhythm has also been suggested [23]. TS might also possess a circadian rhythm. In human oral mucosa, TS activity was found to be lowest during the night [24]. Toxicity studies in mice provided evidence that 5-FU-induced toxicity is relatively low when the drug was administered at time of trough TS activity [25,26].

In human patients, a 5-FU dosing regimen that is adapted to anticipated nocturnal peak activity of DPD showed excellent tolerability [27]. Nonetheless, fluoropyrimidine chronotherapy remains controversial because convincing pharmacological data supporting chronotherapy is lacking. In addition, implementation of chronotherapy in routine clinical practice is often impractical.

Taken together, DPD and TS phenotype assays are promising for upfront identification of patients at risk of developing fluoropyrimidine-induced toxicity. To facilitate implementation of pretreatment screening of patients, examination of circadian rhythms in DPD and TS phenotype markers is essential. Moreover, circadian rhythms in DPD and TS activity could provide a rationale for clinical evaluation of fluoropyrimidine chronotherapy in order to improve treatment safety.

The purpose of the current study was to gain insight in the between-subject and circadian variability in DPD and TS enzyme activity in human volunteers. Secondary objectives were to explore the effect of genetic polymorphisms and gene expression on DPD and TS enzyme activities. For these reasons, we performed an observational study in healthy volunteers and determined $DPDA_{pbmc}$, U and DHU plasma levels, TS activity in PBMCs (TSA_{pbmc}) using newly developed and validated bioanalytical methods [28,29]. We applied a mixed-effect modeling approach to quantify circadian rhythmicity.

MATERIALS AND METHODS
Study design and sample collection

In total, 40 healthy volunteers participated in this study. Included subjects were $\geq$ 18 years old and not known with cancer, not treated with investigational drugs in the past 30 days prior to study assessments, and had not undergone surgery within the past 6 months. Age, gender, regular sleep and wake up time were recorded. From 20 volunteers, blood was collected at 9:00 h for determination of $DPDA_{pbmc}$, TSA_{pbmc}, DHU and U plasma levels and *DPYD* and *TYMS* gene expression. Of these 20 volunteers, 12 underwent additional blood sampling at 13:00, 17:00, 21:00, 1:00, 5:00, and 9:00 h the following day to examine circadian variability in $DPDA_{pbmc}$, TSA_{pbmc}, DHU and U plasma levels. From the remaining 20 volunteers, we collected samples only for determination of DHU and U plasma levels. Of those 20 volunteers, 9 underwent blood sampling once at 9:00 h and 11 volunteers were repeatedly sampled at the previously defined time points for evaluation of circadian variability. Thus, circadian variability in $DPDA_{pbmc}$ and TSA_{pbmc} was assessed in 12 volunteers, and circadian variability in DHU and U plasma levels in 23 volunteers.

In order to take blood samples at night, volunteers were hospitalized. Intravenous cannulas were used for the volunteers participating in the overnight sampling part of this study. Hereby, disturbance of the normal day-night rhythm was limited. The study protocol was approved by the Medical Ethics Committee of the Slotervaart Hospital, Amsterdam, The Netherlands. All volunteers provided written informed consent prior to study assessments.

Determination of DPD and TS activity in PBMCs

A volume of 8 mL of peripheral heparinized blood was collected for the assessment of $DPDA_{pbmc}$ and TSA_{pbmc}. PBMCs were isolated using Ficoll-Paque density gradient centrifugation and stored at -80°C until further analysis [28,29]. $DPDA_{pbmc}$ and TSA_{pbmc} were determined by validated radioassays [28,29]. Activity of DPD was expressed by the amount of ^{3}H-dihydrothymine formed per mg PBMC protein after one hour of *ex vivo* incubation (nmol/mg/h) with the DPD substrate of ^{3}H-thymine [28]. TS activity was expressed by the amount of 5-^{3}H-2'-deoxyuridine 5'-monophosphate that was metabolized *ex vivo* per mg PBMC protein per hour of incubation (nmol/mg/h) [29]. PBMC protein levels were corrected for hemoglobin contamination using a spectrophotometric method [30].

Quantification of uracil and dihydrouracil plasma levels

A volume of 4 mL of heparinized whole blood was centrifuged at 1500 *g* for 10 minutes at 4°C. Isolated plasma was stored at -20°C until further analysis. DHU and U were quantified in plasma using mass spectrometry (Jacobs *et al.* submitted). After defrosting, a volume of 20 µL of internal standard working solution containing 1,3-U-^{15}N$_2$ and 5,6-DHU-^{13}C$_4$,^{15}N$_2$ was added to 300 µL plasma. Protein precipitation was performed using 900 µL of MeOH and acetonitrile (1:1, v/v). Samples were vortex-mixed for 10 s, shaken for 10 min at 1250 rpm (Labinco, Breda, The Netherlands) and centrifuged at 14.000 rpm for 10 min. Clear supernatants were dried under a stream of nitrogen at 40°C and reconstituted in 100 µL 0.1% formic acid in water. U and DHU plasma levels were determined using an ultra-performance liquid chromatography – tandem mass spectrometry (UPLC-MS/MS) system. Chromatographic separation was performed on an Acquity UPLC® HSS T3 (150 x 2.1 mm ID, particle size 1.8 µm; Waters, Milford, USA) column. Mobile phases consisted of 0.1% formic acid in UPLC-grade water (eluent A) and 0.1% formic acid in UPLC-grade acetonitrile (eluent B) at a flow of 0.3 mL/min. The following gradient was used: 0% B from 0-3.0 min, 0-90% B from 3.0-3.2 min, 90% B from 3.2-3.7 min, 0% B from 3.7-5 min. A Qtrap 5500 triple quadrupole mass spectrometer (AB Sciex, Framingham, USA) was operated in the negative mode for quantification of U and in the positive mode for quantification of DHU. Selected mass transitions for U and DHU were *m/z* 110.9 → *m/z* 42.0 and *m/z* 114.9 → *m/z* 55.0. Validated concentration ranges for U and DHU were 1-100 ng/mL and 10-1000 ng/mL, respectively.

4

Gene expression of *DPYD* and *TYMS*

PBMCs were isolated from 8 mL of whole blood using Vacutainer® cell preparation (CPT) tubes (Becton Dickinson, Franklin Lakes, USA). Tubes were centrifuged at 1800 *g* for 20 min at room temperature. The PBMCs were transferred into a clean 50 mL tube and washed twice with NaCl 0.9%. Then, PBMCs were lysed in RNA-Bee (TelStat, Friendswood, USA) and stored at -80 °C until total RNA extraction. Isolation of total RNA was performed according to the RNA-Bee manufacturer's instructions. A quantity of 350 ng of the isolated total mRNA, random primers (Invitrogen) and SuperScript II reverse transcriptase (Invitrogen) were used for the synthesis of cDNA using the following PCR protocol: 25°C for 10 min, 42 °C for 50 min, 70 °C for 15 min, refrigeration at 4 °C. Quantification of TYMS and DPYD gene expression was performed in triplicate using SYBR Green PCR Master Mix (Applied Biosystems, Foster City, USA) and the 7500 Fast Real-Time PCR (RT-PCR) system (Applied Biosystems, Foster City, USA). Relative gene expression was determined using the method [31]. Peptidylprolyl isomerase B (PPIB) was used as housekeeping gene and Human Reference RNA (Stratagene, La Jolla, USA) as external calibrator. RT-PCR primer sequences are available upon request.

Genetic polymorphisms in *DPYD* and *TYMS*

Genomic DNA was isolated from 3 mL of EDTA blood using the QIAamp DNA mini kit (Qiagen, Valencia, USA). The polymorphisms *DPYD**2 and 2846A>T were determined by RT-PCR using allele-specific TaqMan probes (Applied Biosystems, Bleijswijk, The Netherlands) [8]. Polymorphisms within the 5'UTR 28-bp tandem repeat (VNTR) in *TYMS* were analyzed using Sanger sequencing. Additionally, we screened for the G>C SNPs within the first tandem repeat of the 2R allele. Patients were stratified based on the 28-bp VNTR in *TYMS* to either the low *TYM*S expression group (*2/*2, *2/*3C or *3C/*3C) or high *TYMS* expression group (*2/*3G, *3C/*3G or *3G/*3G). Primer sequences are available upon request.

Mixed-effect modeling of circadian rhythms

Mixed-effect modeling was applied to describe the circadian rhythms in DPDA$_{pbmc}$, U and DHU plasma levels and TSA$_{pbmc}$ using NONMEM (version 7.3.0) [32]. Piraña (version 2.9.1) was used for model management [33]. Circadian rhythms were modeled applying cosine functions as follows:

$$Y(t) = Mesor \times \left\{ 1 + \sum_{i=1}^{n} \left[AMP_i \times \cos\left(2\pi \times i \times \frac{[t - PS_i]}{24} \right) \right] \right\} \qquad (1)$$

where *Y* represents the studied phenotype biomarker, *Mesor* is the 24-hour mean value, *AMP$_i$* is the relative amplitude and *PS$_i$* is the phase shift (time of peak) for cosine function *i*. The time of day is represented by *t*. Between-subject variability (BSV) on model

parameters was described using log-normal models. Residual unexplained variability (RUV) was estimated using additive residual error models. Circadian variability in U and DHU plasma levels was estimated using a single set of parameters for AMP_i and PS_i. Model evaluation was guided by goodness-of-fit (GOF) plots, visual predictive checks (VPC), drop in objective function value (dOFV) and precision of obtained parameter estimates. Model management and diagnostics were done using R [34], the Xpose4 package (version 4.5.3) for R and PsN (version 4.2) [33].

Statistical analysis

Statistical analyses were performed in R (version 3.1.2) [34]. Descriptive statistics were used to describe DPDA$_{pbmc}$, TSA$_{pbmc}$, U and DHU plasma levels and DHU:U plasma ratios. Assessments of normality were done using the Shapiro-Wilk test. Mann-Whitney U tests were applied for comparing continuous variables between subgroups. Pearson correlations were estimated to examine the relationship between DPDA$_{pbmc}$ and U plasma levels and the DHU:U plasma ratio. The Pearson and Filon's statistical test was applied to explore the difference between the overlapping correlations of DPDA$_{pbmc}$ and U plasma level and of DPDA$_{pbmc}$ and DHU:U ratio using the cocor package for R [35]. Associations between gene expression and DPDA$_{pbmc}$ and TSA$_{pbmc}$ were explored using the Pearson correlation test. Intra-day variability in DPDA$_{pbmc}$, TSA$_{pbmc}$, DHU:U plasma ratio and U and DHU plasma levels were assessed using repeated measures analysis of variance (rANOVA) tests with Tukey post hoc analysis, unless stated differently. P-values < 0.05 were considered statistically significant.

RESULTS

Volunteer characteristics

A total of 40 volunteers (21 females) with a mean age of 28.8 years (range: 20.3-49.7 years) were included. Of the 40 volunteers, 39 were Caucasian. Mean (range) wake and sleep times were 7:00 h (6:00–8:30 h) and 23:25 h (21:45–01:50 h). Sample collection for baseline assessment of DPDA$_{pbmc}$, TSA$_{pbmc}$, DHU and U plasma levels and *DPYD* and *TYMS* gene expression was on average at 9:25 h (range: 8:45–11:15 h).

Baseline characteristics of DPD and TS phenotype markers

Mean and BSV in TSA$_{pbmc}$, DPDA$_{pbmc}$, DHU:U plasma ratio and U and DHU plasma levels are summarized in Table 1. For one volunteer the amount of isolated PBMC protein was insufficient for TSA$_{pbmc}$ analysis. TSA$_{pbmc}$ followed a non-normal distribution ($p<0.001$), whereas for the other variables this test was not significant. Large BSV in baseline TSA$_{pbmc}$ was found as illustrated by a factor 25 difference between the maximum and minimum observed values.

Table 1. Descriptive statistics for baseline values of thymidylate synthase and dihydropyrimidine dehydrogenase activity in peripheral blood mononuclear cells and plasma levels of uracil (U) and dihydrouracil (DHU), including the DHU:U plasma ratio, in healthy volunteers. Mean time of sample collection was 9:25 h (range: 8:45–11:15 h).

Variable	n	Mean ± sd	CV (%)
TS activity in PBMCs (nmol/mg/h)	19	0.072 (0.024 – 0.596)§	-
DPD activity in PBMCs (nmol/mg/h)	20	9.2 ± 2.1	23
DHU:U plasma ratio	40	10.6 ± 2.4	22
U concentration (ng/mL)		9.8 ± 2.9	29
DHU concentration (ng/mL)		98 ± 23.8	24

Abbreviations: TS = thymidylate synthase, DPD = dihydropyrimidine dehydrogenase, PBMCs = peripheral blood mononuclear cells, DHU = dihydrouracil, U = uracil, n = number of subjects, sd = standard deviation, CV = coefficient of variation.
§ Median and range are shown for TS activity, since non-normal distribution was demonstrated.

Intra-day variability in markers for TS and DPD activity

Individual and population average TSA_{pbmc} and $DPDA_{pbmc}$ are shown in Figure 1. Trough TSA_{pbmc} and peak $DPDA_{pbmc}$ were observed at 1:00 h while peak TSA_{pbmc} and trough $DPDA_{pbmc}$ were both detected at 17:00 h and 13:00 h, respectively. Peak-to-trough ratio of $DPDA_{pbmc}$ was 1.69 and for TSA_{pbmc} 1.62. Figure 2 displays the intra-day variability in U, DHU and DHU:U in plasma. Peak and trough U plasma levels occurred at 5:00 h and 17:00 h. Throughout the day, DHU plasma levels showed significant differences with peak levels at 9:00 h and trough levels at 1:00 h. Peak-to-trough ratios for U and DHU plasma levels were 1.39 and 1.22. Intra-day variability in U and DHU plasma levels also resulted in clear intra-day variability in DHU:U plasma ratios. Peak and trough DHU:U ratio were detected at 17:00 h and 5:00 h with a peak-to-trough ratio of 1.43. All examined phenotype markers revealed significant intra-day variability (Table 2).

Mixed-effect modeling of circadian rhythms

A mixed-effect modeling approach was applied to quantify circadian variability. A combined model for circadian rhythms in U and DHU plasma levels and $DPDA_{pbmc}$ was developed. Base models included BSV terms for mesors of U (*Mesor$_u$*) and DHU (*Mesor$_{DHU}$*) plasma levels and $DPDA_{pbmc}$ (*Mesor$_{DPD}$*). One cosine function adequately described circadian rhythms in U and DHU plasma levels.

Equation 2 illustrates the function for model prediction of U and DHU plasma levels as function of the time of day (0-24 h):

$$\mathrm{Rhythm_{U\&DHU}}(t) = \mathrm{AMP_{U\&DHU}} \times \cos\left(2\,\pi\,\frac{[\mathrm{t\text{-}PS_{U\&DHU}}]}{24}\right) \qquad (2)$$

where circadian variability in U and DHU plasma levels is represented by *Rhythm$_{U\&DHU}$*, the amplitude *AMP$_{U\&DHU}$*, phase shift by *PS$_{U\&DHU}$* and time of day by *t*.
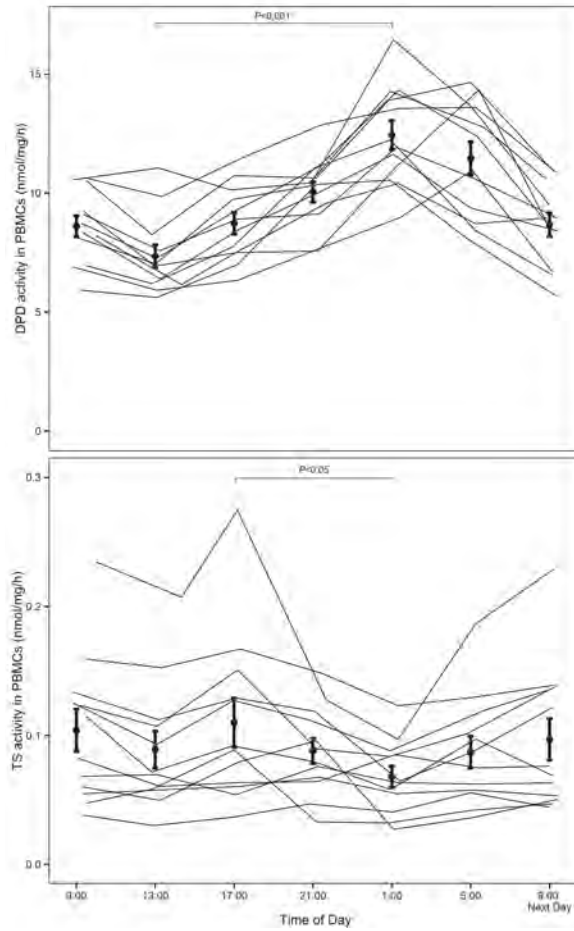
Figure 1. Intraday variability in dihydropyrimidine dehydrogenase (upper panel) and thymidylate synthase activity (lower panel) in peripheral blood mononuclear cells from volunteers (n = 12). Grey lines represent individual lines for DPD and TS activity. Mean ± standard error per timepoint are shown by black points and error bars. Differences between peak and trough activities are supported by *P*-values. Abbreviations: DPD = dihydropyrimidine dehydrogenase; PBMCs = peripheral blood mononuclear cells; TS = thymidylate synthase

Equation 2 was incorporated in the population model for circadian variability in U and DHU plasma levels, as illustrated by equations 3 and 4:

$$U(t) = Mesor_U \times (1 + Rhythm_{U\&DHU}(t)) + \varepsilon_U \tag{3}$$

$$DHU(t) = Mesor_{DHU} \times (1 - Rhythm_{U\&DHU}(t)) + \varepsilon_{DHU} \tag{4}$$

4
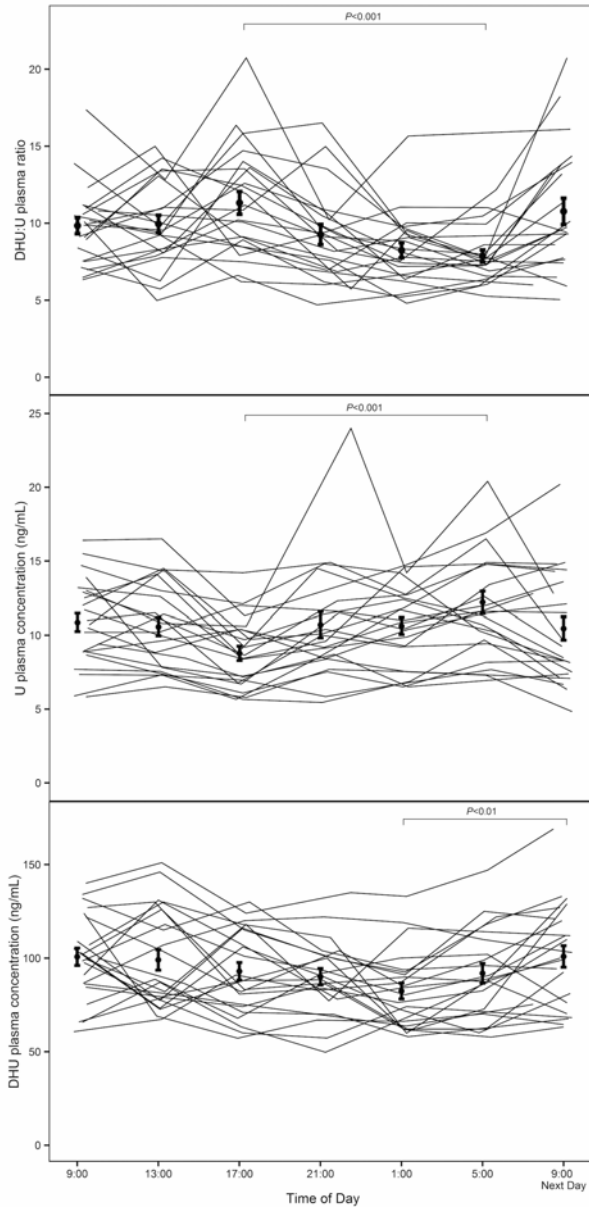
Figure 2. Intraday variability in the dihydrouracil : uracil plasma ratio (upper panel), uracil plasma levels (middle panel) and dihydrouracil plasma levels (lower panel) in 23 healthy volunteers. Grey solid lines represent individual curves. Mean ± standard error per time point is shown by black points and error bars. Differences between peak and trough levels are supported by *P*-values. Abbreviations: DHU = dihydrouracil; U = uracil.

In these equations, additive residual errors for U and DHU plasma levels are represented by ε_U and ε_{DHU}, with mean zero and variance σ^2.

Table 2. Results of the repeated measures ANOVA of thymidylate synthase and dihydropyrimidine dehydrogenase activity in peripheral blood mononuclear cells, dihydrouracil:uracil plasma ratio and uracil and dihydrouracil plasma levels in healthy volunteers.

Variable	n	Trough ± S.E.M.	Peak ± S.E.M.	Time of trough (hh:mm)	Time of peak (hh:mm)	Peak: Trough	p-value of repeated measures ANOVA
TS activity in PBMCs (nmol/mg/h)	12	0.068 ± 0.008	0.110 ± 0.019 *	01:00 h	17:00 h	1.62	0.012 §
DPD activity in PBMCs (nmol/mg/h)	12	7.35 ± 0.48	12.4 ± 0.61 ***	13:00 h	01:00 h	1.69	< 0.0001
DHU:U plasma ratio	23	7.87 ± 0.40	11.32 ± 0.74 ***	05:00 h	17:00 h	1.43	< 0.0001
U concentration ng/mL)	23	8.78 ± 0.49	12.21 ± 0.75 ***	17:00 h	5:00 h	1.39	0.0002
DHU concentration (ng/mL)	23	82.4 ± 4.2	100.9 ± 8.8 **	01:00 h	09:00 h	1.22	0.0009

Abbreviation: TS = thymidylate synthase, DPD = dihydropyrimidine dehydrogenase, PBMCs = peripheral blood mononuclear cells, DHU = dihydrouracil, U = uracil, n = number of subjects, S.E.M. = standard error of the mean, ANOVA = analysis of variance.
Differences between peak and trough levels were based on post hoc test: $p \leq 0.001$ (***); $p \leq 0.01$ (**); $p \leq 0.05$ (*); $p > 0.05$ (ns).
§ In case of TS activity in PBMCs, the nonparametric repeated measures ANOVA (Friedman test) with post hoc analysis was applied.

4

The circadian rhythm of DPDA$_{pbmc}$ was adequately described using a single cosine function. Covariance between BSV of *Mesor*$_U$ and *Mesor*$_{DHU}$ was assessed. The estimated correlation coefficient was 0.68 (dOFV=-17.2). In addition, there was a negative correlation between BSV of *Mesor*$_U$ and *Mesor*$_{DPD}$. The correlation coefficients between BSV of *Mesor*$_U$ and *Mesor*$_{DHU}$ and BSV of *Mesor*$_U$ and *Mesor*$_{DPD}$ were included in the final model. Furthermore, there was a positive correlation between RUV in U and DHU plasma levels, which was also included in the final model (dOFV=-9.9).

The optimal model for TSA$_{pbmc}$ contained two cosine functions to describe circadian variability. This model was further improved by addition of a single BSV term on both amplitudes (dOFV=-16.7).

VPCs of the final circadian models are shown in Figure 3. The parameter estimates are given in Table 3. The typical circadian rhythms of the studied phenotype

Figure 3. Visual predictive checks for final models for circadian rhythms in dihydropyrimidine dehydrogenase (A) and thymidylate synthase (B) activity in peripheral blood mononuclear cells, and uracil (C) and dihydrouracil (D) plasma levels. Lines represent the 10th percentile, median and 90th percentile of observed data. Shaded areas represent corresponding 95% confidence intervals of simulated data. Abbreviations: DPD = dihydropyrimidine dehydrogenase; PBMCs = peripheral blood mononuclear cells; TS = thymidylate synthase

Table 3. Parameter estimates of the final models of circadian rhythms in uracil and dihydrouracil plasma levels, thymidylate synthase and dihydropyrimidine dehydrogenase activity in peripheral blood mononuclear cells. The circadian rhythm in thymidylate synthase activity was described by two cosine functions, for which separate amplitudes and phase shifts were estimated.

Parameter	Estimate	RSE (%)
Structural model parameter		
$Mesor_U$ (ng/mL)	9.95	4.3
$Mesor_{DHU}$ (ng/mL)	91.4	2.9
$Amplitude_{U\&DHU}$	0.082	15.5
Phase shift$_{U\&DHU}$ (hh:mm)	01:56	21.4
$Mesor_{DPD}$ (nmol/mg/h)	9.94	4.0
$Amplitude_{DPD}$	0.245	9.3
Phase shift$_{DPD}$ (hh:mm)	01:46	18.4
$Mesor_{TS}$ (nmol/mg/h)	0.080	19.4
$Amplitude_{TS}$ 1	0.129	28.9
$Amplitude_{TS}$ 2	0.106	29.6
Phase shift$_{TS}$ 1 (hh:mm)	13:24	3.1
Phase shift$_{TS}$ 2 (hh:mm)	18:42	1.1
Between-subject variability		
$Mesor_U$ (CV%)	24.3	10.7
$Mesor_{DHU}$ (CV%)	17.8	14.3
$Mesor_{DPD}$ (CV%)	17.5	17.8
$Mesor_{TS}$ (CV%)	92.3	16.8
$Amplitude_{TS}$ 1 and 2 (CV%)	56.5	33.2
Residual unexplained variability		
$\sigma_{additive, U}$ (ng/mL)	2.05	21.5
$\sigma_{additive, DHU}$ (ng/mL)	16.2	11.8
$\sigma_{additive, DPD}$ (nmol/mg/h)	1.14	19.5
$\sigma_{additive, TS}$ (nmol/mg/h)	0.014	20.3
Correlations		
ρ (BSV Base$_U$, BSV Base$_{DHU}$)	0.68	-
ρ (BSV Base$_U$, BSV Base$_{DPD}$)	-0.16	-
ρ (σ_U, σ_{DHU})	0.26	-

Abbreviations: Mesor = rhythm-adjusted mean, Phase shift = time of peak, TS = thymidylate synthase, DPD = dihydropyrimidine dehydrogenase, DHU = dihydrouracil, U = uracil, RSE = relative standard error, CV = coefficient of variation, BSV = between-subject variability, σ = residual variability, ρ = correlation coefficient.

markers are shown in Figure 4. GOF plots are provided as supplementary material (Supplementary Figures S1-4).

Associations between DPD activity in PBMCs and in plasma
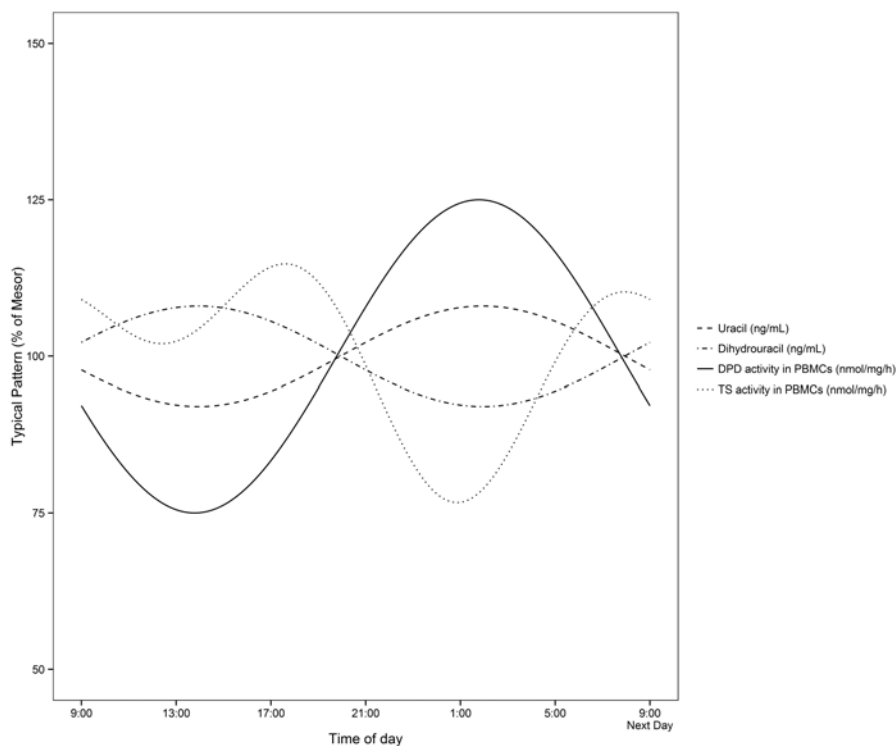
Figure 4. Typical patterns of circadian variability in dihydropyrimidine dehydrogenase and thymidylate synthase enzyme activity in peripheral blood mononuclear cells, and u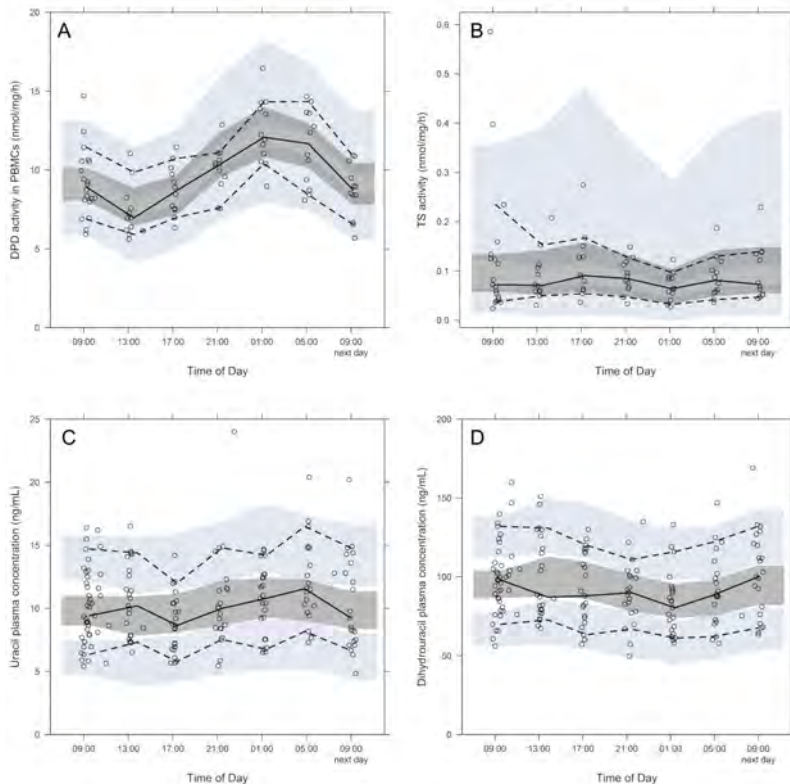racil and dihydrouracil plasma levels in healthy volunteers. Circadian variability is expressed as a percentage of the mesor (rhythm-adjusted mean). Abbreviations: DPD = dihydropyrimidine dehydrogenase; TS = thymidylate synthase; PBMCs = peripheral blood mononuclear cells

There was a modest but significant negative correlation between $DPDA_{pbmc}$ and U plasma levels ($r^2=0.26$; $p=0.02$; Supplementary Figure S5). There was a trend towards a positive association between $DPDA_{pbmc}$ and DHU:U plasma ratio ($r^2=0.17$; $p=0.07$). Difference in overlapping correlations between $DPDA_{pbmc}$ and U plasma level and of $DPDA_{pbmc}$ and DHU:U ratio was not statistically significant.

Associations between *TYMS* and *DPYD* genotypes and phenotypes

There were 10 volunteers with the *TYMS* low expression genotype and 9 volunteers with the *TYMS* high expression genotype. Although the average TSA_{pbmc} was as expected higher in volunteers with the high expression genotype, the difference was not significant ($p=0.32$; Supplementary Figure S6). Among the volunteers, we identified one volunteer with the very uncommon 2RC/3RC expression genotype. The proportion of individuals with this genotype was previously reported to be 2% [36]. TSA_{pbmc} in this volunteer was relatively low (0.036 nmol/mg/h; Supplementary Figure S6). None of the 40 volunteers was carrier of the *DPYD*2A* allele, and one volunteer was heterozygous for *DPYD* 2846A>T.

Associations between TS and DPD enzyme activity and gene expression in PBMCs

To assess whether TS and DPD enzyme activity in PBMCs are regulated on a transcriptional level, we explored associations between gene expression and TSA_{pbmc} and $DPDA_{pbmc}$ (Supplementary Figure S7). There was a strong positive correlation between TSA_{pbmc} and *TYMS* gene expression (r^2=0.84; p<0.001). In contrast, a weak, but significant negative correlation was found for $DPDA_{pbmc}$ and *DPYD* gene expression (r^2=0.22; p=0.04).

4

DISCUSSION

This study clearly identified and quantified wide BSV and circadian rhythmicity in phenotypic markers of TS and DPD activity. Intra-day variability was noticeable in the presented data. Eventually, we were able to describe circadian rhythms in $DPDA_{pbmc}$, U and DHU plasma levels using in a combined model and rhythmicity in TSA_{pbmc} by the sum of two cosine functions. Model parameters were estimated with adequate precision and model diagnostics did not suggest structural deviations. Therefore, this is the first report to successfully describe and fully quantify circadian rhythmicity of TSA_{pbmc}, $DPDA_{pbmc}$, U and DHU plasma levels using the mixed-modeling approach.

Although there was a moderate correlation between baseline $DPDA_{pbmc}$ and U plasma levels, circadian rhythmicity in $DPDA_{pbmc}$ and U and DHU plasma levels clearly suggested two different patterns in DPD activity. Time of peak $DPDA_{pbmc}$ was estimated at 01:46 h. However, at that time, we also discovered peak U and trough DHU plasma levels, suggestive for trough DPD activity at the same timepoint. Magnitude of circadian variation was more pronounced for $DPDA_{pbmc}$ than for U and DHU plasma levels, which is illustrated by relative amplitudes of 0.245 for $DPDA_{pbmc}$ and 0.082 for U and DHU plasma levels. Residual unexplained variability was relatively large in the circadian model for U and DHU in plasma. This indicates that there are unidentified variables, other than circadian rhythmicity, accounting for variability in U and DHU plasma levels.

Others have also reported circadian rhythmicity on surrogate markers for systemic DPD activity [20,21,37]. Results from these studies show large differences. Jiang et al. determined circadian rhythmicity in DHU:U plasma ratios and DPD protein expression in PBMCs in human volunteers and found peak levels for both markers at approximately 18:40 h. They found an average DHU:U plasma ratio in their study of 5.1 and found a large effect of circadian rhythmicity on this marker, considering the observed peak-to-trough ratio of 3.4 [20]. Compared to our study, they showed more pronounced circadian variability in U and DHU and earlier peak expression of DPD protein in PBMCs. Their average DHU:U plasma ratio is remarkably lower than the average DHU:U plasma that we observed. Zeng et al. reported peak DHU:U plasma ratios in patients at 2:30 h and with a relative amplitude of 0.13 [37]. Although the magnitude of circadian variability of their findings was in line with ours, time of peak is completely opposite to our results. Peak $DPDA_{pbmc}$ in patients who were treated with 5-FU was detected around midnight by Harris et al. [21]. Besides the time of peak activity also the magnitude of rhythmicity was very close to our results on $DPDA_{pbmc}$.

4

DPD activity in PBMCs and the DPD phenotype in plasma might be regulated by different mechanisms. Circadian rhythms are generally maintained by a central circadian clock located in the hypothalamus [38]. The circadian clock consists of a transcription-translation based oscillatory feedback mechanism involving a set of genes, called clock genes. Clock proteins control circadian rhythms of other genes by regulating transcriptional processes. However, circadian clocks have been found in several peripheral tissues. This allows for tissue specific regulation of rhythmicity. Surprisingly, circadian clock genes in PBMCs show expression in a circular manner which has been shown to be conserved in cultured PBMCs [39,40]. Previous experiments suggested that DPD activity is coordinated by the clock gene *PER1* [41], which is one of the genes that show circadian rhythmicity in PBMCs [39,40]. Tissue specific regulation of clock genes might cause DPD activity in PBMCs to deviate from DPD activity in other body compartments, which could lead to differences in circadian rhythms for DHU:U in plasma and $DPDA_{pbmc}$. Alternatively, other enzymatic processes might contribute to rhythmicity in U and DHU plasma levels. The enzyme uridine phosphorylase (UP), which degrades uridine to U, and the enzyme DPD show opposite circadian rhythms in mice [42]. If these two enzymes also show opposite rhythms in humans this could contribute to circadian variability in U plasma levels. Since $DPDA_{pbmc}$ and DHU:U plasma ratio show opposing circadian rhythms, patient samples for DPD phenotyping or therapeutic drug monitoring of 5-FU should preferably be collected at the intersect of both rhythms, which is at approximately 8:00 h and 20:00 h.

Correlation between $DPDA_{pbmc}$ and U plasma level and of $DPDA_{pbmc}$ and DHU:U ratio were rather weak. These weak correlations could be caused by differences in analytical methods and biological sample matrices. The method for DPD activity in PBMCs is based on *ex vivo* conversion of the radiolabeled DPD substrate ^{3}H-dihydrothymine and showed to be highly selective for the enzyme DPD [28]. Conversely, enzymes, other than DPD, might contribute to the regulation of U and DHU plasma levels. The enzyme UP is involved in the formation of U and dihydropyrimidinase catalyzes the degradation of DHU. Consequently, BSV in UP and dihydropyrimidinase activity could affect U and DHU plasma levels, which in turn, could attribute to the weak correlation with $DPDA_{pbmc}$. DPD-based adaptive dosing of fluoropyrimidines using the DHU:U plasma ratio could be biased by the involvement of other enzymes. Additional clinical research is needed to evaluate the applicability of DHU:U plasma for DPD-based adaptive dosing of fluoropyrimidines.

TSA_{pbmc} displayed circadian variability and particularly large BSV. Smaaland et al. discovered a circadian rhythm in bone marrow DNA synthesis of healthy human volunteers. They observed trough DNA synthesis at midnight, a minor peak in DNA synthesis at 8:00 h and maximum DNA synthesis at 16:00 h [43]. This is in agreement with the pattern we observed in TSA_{pbmc}. Since TS activity is required for DNA synthesis it might be anticipated that these processes are depending on each other and, therefore, show similar patterns.

Strong correlation between TSA_{pbmc} and *TYMS* gene expression in PBMCs clearly suggests that BSV in TS activity is regulated on a transcriptional level. Within cancer tissue, others have found correlations between TS protein and gene expression as well

[44,45]. One volunteer carried the G>C SNP in the 2R allele and was identified with 2RC/3RC genotype in *TYMS*. The 2RC allele has been associated with low TS expression *in vitro* [36,46]. We also found that the TSA$_{pbmc}$ for this subject was relatively low. Moreover, we recently showed that patients carrying the 2RC allele are at strongly increased risk of developing fluoropyrimidine-induced toxicity [9].

DPD$_{pbmc}$ showed a weak negative correlation with *DPYD* gene expression. A trend towards negative correlation between DPD activity and gene expression was also found in human mucosa tissue [47]. It seems plausible that DPD activity is regulated on a posttranscriptional level, which indicates that *DPYD* gene expression can not be used for the prediction of the DPD phenotype in PBMCs.

Although various pharmacological methods were used to measure the TS and DPD activity patterns, a drawback of the study might be the relatively small number of individuals. For this reason, we performed mixed-effect modeling to use all available data for full quantitative description of the time course of the markers. Larger studies are needed to assess the associations between *DPYD* and *TYMS* polymorphisms and DPD and TS phenotypes more extensively.

Taken together, multiple studies have been performed in order to assess circadian rhythms in DPDA$_{pbmc}$, U and DHU. These studies show differences concerning time of peak levels and magnitude of circadian rhythms. This might be due to limited sample size, variability among populations, and differences in bioanalytical methods. Other factors that are organized in a circadian manner, like exposure to light, intake of food, liver blood flow, body temperature, activity, other enzymes or mediators, may additionally play a role in regulation of circadian rhythmicity of U and DHU plasma levels, TSA$_{pbmc}$ and DPDA$_{pbmc}$. However, further research is warranted to identify factors that are associated with rhythmicity in DPD and TS.

By extensively validating our developed phenotyping assays we maximized our effort to obtain accurate and representative values for the phenotype markers. We discovered substantial BSV in baseline DPDA$_{pbmc}$, U and DHU plasma levels and large BSV in baseline TSA$_{pbmc}$. Circadian rhythmicity in DPDA$_{pbmc}$ was opposite and more prominent compared to rhythmicity in U and DHU plasma levels. And TSA$_{pbmc}$ showed peak activity in the afternoon and trough activity during the night. These results highly suggest possible influence of circadian rhythms on phenotype-guided fluoropyrimidine dosing. Moreover, there might be implications for fluoropyrimidine chronotherapy. Tolerability to fluoropyrimidines in mice has been shown to be largest at time of trough TS and peak DPD activity [26], which should occur during the night according to our results. Levi et al. previously showed superior 5-FU tolerability, when the drug was administered at night [27]. The pharmacological results in the current study support this clinical observation that fluoropyrimidine chronotherapy, with relatively high dose intensity during the night, might show better tolerability.

Capecitabine is usually administered twice daily at a 12-hour interval with equal morning and evening doses. Because of this dosing regimen, circadian rhythms in DPD and TS activity could in particular affect tolerability of capecitabine. We are currently

performing a pharmacological study of chronomodulated capecitabine therapy in patients to explore the role of circadian rhythms in DPD and TS activity on treatment tolerability and drug exposure. In this pharmacological study, the morning:evening ratio of the daily capecitabine dose is 3:5 in order to administer high-dose capecitabine in the late evening (http://www.trialregister.nl, study identifier: NTR4639). In addition, we are exploring the applicability of our phenotype markers with regard to phenotype adjusted fluoropyrimidine treatment in a prospective study (http://www.clinicaltrials.gov, study identifier: NCT02324452). In conclusion, markers for TS and DPD show circadian variability, which offers opportunities for improved fluoropyrimidine treatment safety.

ACKNOWLEDGEMENT

REFERENCES

1. Heggie GD, Sommadossi JP, Cross DS, Huster WJ, Diasio RB. Clinical pharmacokinetics of 5-fluorouracil and its metabolites in plasma, urine, and bile. Cancer Res 1987;47:2203–6.

2. Judson IR, Beale PJ, Trigo JM, Aherne W, Crompton T, Jones D, et al. A human capecitabine excretion balance and pharmacokinetic study after administration of a single oral dose of 14C-labelled drug. Invest New Drugs 1999;17:49–56.

3. Thorn CF, Marsh S, Carrillo MW, McLeod HL, Klein TE, Altman RB. PharmGKB summary: fluoropyrimidine pathways. Pharmacogenet Genomics 2011;21:237–42.

4. Longley DB, Harkin DP, Johnston PG. 5-fluorouracil: mechanisms of action and clinical strategies. Nat Rev Cancer 2003;3:330–8.

5. Midgley R, Kerr DJ. Capecitabine: have we got the dose right? Nat Clin Pract Oncol 2009;6:17–24.

6. Rosmarin D, Palles C, Church D, Domingo E, Jones A, Johnstone E, et al. Genetic markers of toxicity from capecitabine and other fluorouracil-based regimens: Investigation in the QUASAR2 study, systematic review, and meta-analysis. J Clin Oncol 2014;32:1031–9.

7. Loganayagam A, Arenas Hernandez M, Corrigan A, Fairbanks L, Lewis CM, Harper P, et al. Pharmacogenetic variants in the DPYD, TYMS, CDA and MTHFR genes are clinically significant predictors of fluoropyrimidine toxicity. Br J Cancer 2013;108:2505–15.

8. Deenen MJ, Tol J, Burylo AM, Doodeman VD, de Boer A, Vincent A, et al. Relationship between single nucleotide polymorphisms and haplotypes in DPYD and toxicity and efficacy of capecitabine in advanced colorectal cancer. Clin Cancer Res 2011;17:3455–68.

9. Meulendijks D, Jacobs BAW, Aliev A, Pluim D, van Werkhoven E, Deenen MJ, et al. Increased risk of severe fluoropyrimidine-associated toxicity in patients carrying a G to C substitution in the first 28-bp tandem repeat of the thymidylate synthase 2R allele. Int J Cancer 2015:2–31.

10. Fleming RA, Milano G, Thyss A, Etienne MC, Renée N, Schneider M, et al. Correlation between dihydropyrimidine dehydrogenase activity in peripheral mononuclear cells and systemic clearance of fluorouracil in cancer patients. Cancer Res 1992;52:2899–902.

11. Van Kuilenburg ABP, Meinsma R, Zoetekouw L, Van Gennip AH. Increased risk of grade IV neutropenia after administration of 5-fluorouracil due to a dihydropyrimidine dehydrogenase deficiency: High prevalence of the IVS14+1G>A mutation. Int J Cancer 2002;101:253–8.

12. Milano G, Etienne MC, Pierrefite V, Barberi-Heyob M, Deporte-Fety R, Renée N. Dihydropyrimidine dehydrogenase deficiency and fluorouracil-related toxicity. Br J Cancer 1999;79:627–30.

13. van Kuilenburg AB, Haasjes J, Richel DJ, Zoetekouw L, Van Lenthe H, De Abreu RA, et al. Clinical implications of dihydropyrimidine dehydrogenase (DPD) deficiency in patients with severe 5-fluorouracil-associated toxicity: identification of new mutations in the DPD gene. Clin Cancer Res 2000;6:4705–12.

14. Sistonen J, Büchel B, Froehlich TK, Kummer D, Fontana S, Joerger M, et al. Predicting 5-fluorouracil toxicity: DPD genotype and 5,6-dihydrouracil:uracil ratio. Pharmacogenomics 2014;15:1653–66.

15. Zhou ZW, Wang GQ, Wan D Sen, Lu ZH, Chen YB, Li S, et al. The dihydrouracil/uracil ratios in plasma and toxicities of 5-fluorouracil-based adjuvant chemotherapy in colorectal cancer patients. Chemotherapy 2007;53:127–31.

16. Gamelin M, Boisdron-Celle M, Guérin-Meyer V, Delva R, Lortholary A, Genevieve F, et al. Correlation between uracil and dihydrouracil plasma ratio, fluorouracil (5-FU) pharmacokinetic parameters, and tolerance in patients with advanced colorectal cancer: A potential interest for predicting 5-FU toxicity and determining optimal 5-FU dosage. J Clin Oncol 1999;17:1105–10.

17. Boisdron-Celle M, Remaud G, Traore S, Poirier A, Gamelin L, Morel A, et al. 5-Fluorouracil-related severe toxicity: a comparison of different methods for the pretherapeutic detection of dihydropyrimidine dehydrogenase deficiency. Cancer Lett 2007;249:271–82.

4

4

18. Thomas F, Hennebelle I, Delmas C, Lochon I, Dhelens C, Garnier Tixidre C, et al. Genotyping of a family with a novel deleterious DPYD mutation supports the pretherapeutic screening of DPD deficiency with dihydrouracil/uracil ratio. Clin Pharmacol Ther 2016;99:235–42.

19. Launay M, Dahan L, Duval M, Rodallec A, Milano G, Duluc M, et al. Beating the odds: Efficacy and toxicity of dihydropyrimidine dehydrogenase-driven adaptive dosing of 5-FU in patients with digestive cancer. Br J Clin Pharmacol 2016;81:124–30.

20. Jiang H, Lu J, Ji J. Circadian rhythm of dihydrouracil/uracil ratios in biological fluids: a potential biomarker for dihydropyrimidine dehydrogenase levels. Br J Pharmacol 2004;141:616–23.

21. Harris BE, Song R, Soong SJ, Diasio RB. Relationship between dihydropyrimidine dehydrogenase activity and plasma 5-fluorouracil levels with evidence for circadian variation of enzyme activity and plasma drug levels in cancer patients receiving 5-fluorouracil by protracted continuous infusion. Cancer Res 1990;50:197–201.

22. Petit E, Milano G, Levi F, Thyss A, Bailleul F, Schneider M. Circadian rhythm-varying plasma concentration of 5-fluorouracil during a five-day continuous venous infusion at a constant rate in cancer patients. Cancer Res 1988;48:1676–9.

23. Van Kuilenburg AB, Poorter RL, Peters GJ, Van Gennip AH, Van Lenthe H, Stroomer AE, et al. No circadian variation of dihydropyrimidine dehydrogenase, uridine phosphorylase, beta-alanine, and 5-fluorouracil during continuous infusion of 5-fluorouracil. Adv Exp Med Biol 1998;431:811–6.

24. Bjarnason GA, Jordan RC, Wood PA, Li Q, Lincoln DW, Sothern RB, et al. Circadian expression of clock genes in human oral mucosa and skin: association with specific cell-cycle phases. Am J Pathol 2001;158:1793–801.

25. Lincoln DW, Hrushesky WJM, Wood PA. Circadian organization of thymidylate synthase activity in normal tissues: A possible basis for 5-fluorouracil chronotherapeutic advantage. Int J Cancer 2000;88:479–85.

26. Wood PA, Du-Quiton J, You S, Hrushesky WJM. Circadian clock coordinates cancer cell cycle progression, thymidylate synthase, and 5-fluorouracil therapeutic index. Mol Cancer Ther 2006;5:2023–33.

27. Lévi F, Zidani R, Misset J. Randomised multicentre trial of chronotherapy with oxaliplatin, fluorouracil, and folinic acid in metastatic colorectal cancer. Lancet 1997;350:681–6.

28. Pluim D, Jacobs BAW, Deenen MJ, Ruijter AEM, van Geel RMJM, Burylo AM, et al. Improved pharmacodynamic assay for dihydropyrimidine dehydrogenase activity in peripheral blood mononuclear cells. Bioanalysis 2015;7:519–29.

29. Pluim D, Schilders KAA, Jacobs BAW, Vaartjes D, Beijnen JH, Schellens JHM. Pharmacodynamic assay of thymidylate synthase activity in peripheral blood mononuclear cells. Anal Bioanal Chem 2013;405:2495–503.

30. Pluim D, Jacobs BAW, Krähenbühl MD, Ruijter AEM, Beijnen JH, Schellens JHM. Correction of peripheral blood mononuclear cell cytosolic protein for hemoglobin contamination. Anal Bioanal Chem 2013;405:2391–5.

31. Livak KJ, Schmittgen TD. Analysis of relative gene expression data using real-time quantitative PCR and the 2(-Delta Delta C(T)) Method. Methods 2001;25:402–8.

32. Beal S, Sheiner L. NONMEM user guides. Ellicott City, Maryland, USA: Icon Development Solutions, 1989.

33. Keizer RJ, Karlsson MO, Hooker A. Modeling and Simulation Workbench for NONMEM: Tutorial on Pirana, PsN, and Xpose. CPT Pharmacometrics Syst Pharmacol 2013;2:e50.

34. R Development Core Team. R: A Language and Environment for Statistical Computing. Vienna, Austria: R Foundation for Statistical Computing, 2016.

35. Diedenhofen B, Musch J. cocor: A Comprehensive Solution for the Statistical Comparison of Correlations. PLoS One 2015;10:e0121945.

36. Gusella M, Bolzonella C, Crepaldi G, Ferrazzi E, Padrini R. A novel G/C single-nucleotide polymorphism in the double

28-bp repeat thymidylate synthase allele. Pharmacogenomics J 2006;6:421–4.

37. Zeng Z-L, Sun J, Guo L, Li S, Wu M, Qiu F, et al. Circadian rhythm in dihydropyrimidine dehydrogenase activity and reduced glutathione content in peripheral blood of nasopharyngeal carcinoma patients. Chronobiol Int 2005;22:741–54.

38. Innominato PF, Lévi FA, Bjarnason GA. Chronotherapy and the molecular clock: Clinical implications in oncology. Adv Drug Deliv Rev 2010;62:979–1001.

39. Boivin DB, James FO, Wu A, Cho-Park PF, Xiong H, Sun ZS. Circadian clock genes oscillate in human peripheral blood mononuclear cells. Blood 2003;102:4143–5.

40. Ebisawa T, Numazawa K, Shimada H, Izutsu H, Sasaki T, Kato N, et al. Self-sustained circadian rhythm in cultured human mononuclear cells isolated from peripheral blood. Neurosci Res 2010;66:223–7.

41. Krugluger W, Brandstaetter A, Kállay E, Schueller J, Krexner E, Kriwanek S, et al. Regulation of genes of the circadian clock in human colon cancer: reduced period-1 and dihydropyrimidine dehydrogenase transcription correlates in high-grade tumors. Cancer Res 2007;67:7917–22.

42. Naguib FN, Soong SJ, el Kouni MH. Circadian rhythm of orotate phosphoribosyltransferase, pyrimidine nucleoside phosphorylases and dihydrouracil dehydrogenase in mouse liver. Possible relevance to chemotherapy with 5-fluoropyrimidines. Biochem Pharmacol 1993;45:667–73.

43. Smaaland R, Laerum OD, Lote K, Sletvold O, Sothern RB, Bjerknes R. DNA synthesis in human bone marrow is circadian stage dependent. Blood 1991;77:2603–11.

44. Kristensen MH, Weidinger M, Bzorek M, Pedersen PL, Mejer J. Correlation between thymidylate synthase gene variants, RNA and protein levels in primary colorectal adenocarcinomas. J Int Med Res 2010;38:484–97.

45. Monica V, Familiari U, Chiusa L, Rossi G, Novero D, Busso S, et al. Messenger RNA and protein expression of thymidylate synthase and DNA repair genes in thymic tumors. Lung Cancer 2013;79:228–35.

46. Mandola M V, Stoehlmacher J, Muller-Weeks S, Cesarone G, Yu MC, Lenz HJ, et al. A novel single nucleotide polymorphism within the 5' tandem repeat polymorphism of the thymidylate synthase gene abolishes USF-1 binding and alters transcriptional activity. Cancer Res 2003;63:2898-904.

47. Uetake H, Ichikawa W, Takechi T, Fukushima M, Nihei Z, Sugihara K. Relationship between intratumoral dihydropyrimidine dehydrogenase activity and gene expression in human colorectal cancer. Clin Cancer Res 1999;5:2836–9.

4

SUPPLEMENTARY FIGURES
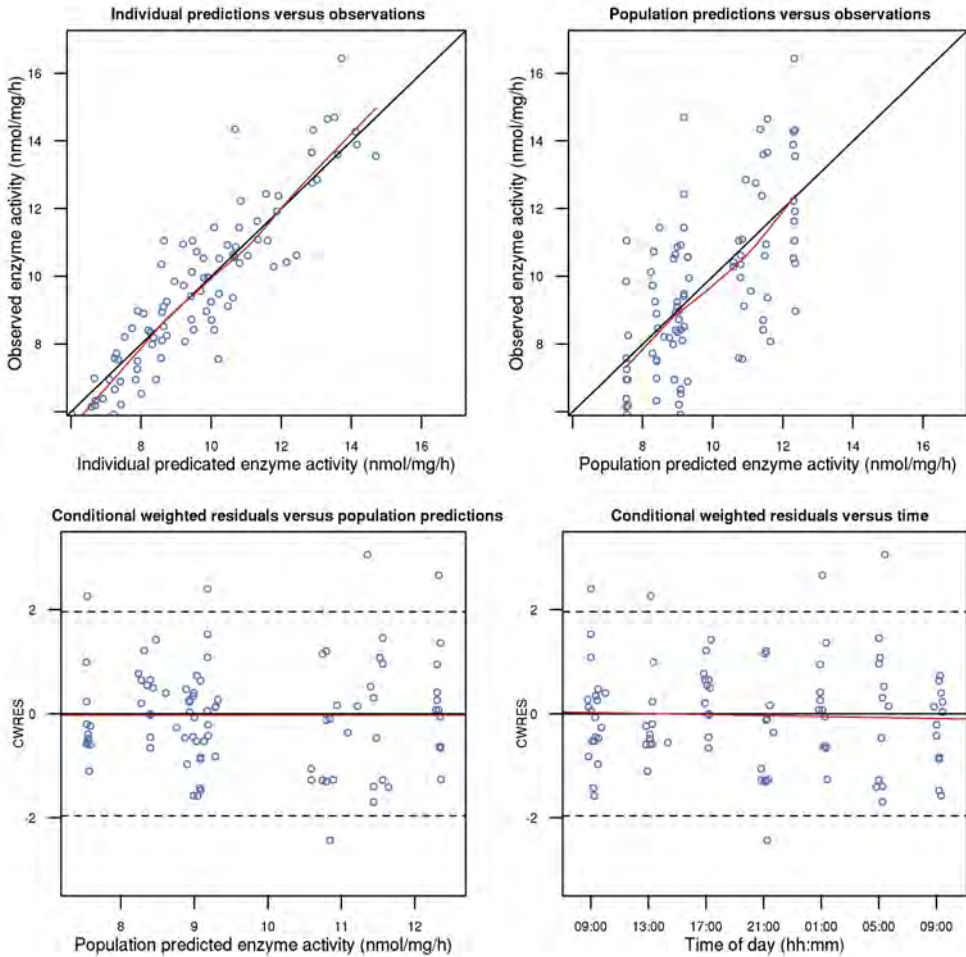
Figure S1. Goodness of fit plots for circadian model predicted dihydropyrimidine dehydrogenase activity in peripheral blood mononuclear cells. Blue dots represented observed data and red lines represent the trend of the data. Abbreviation: CWRES = conditional weighed residuals.
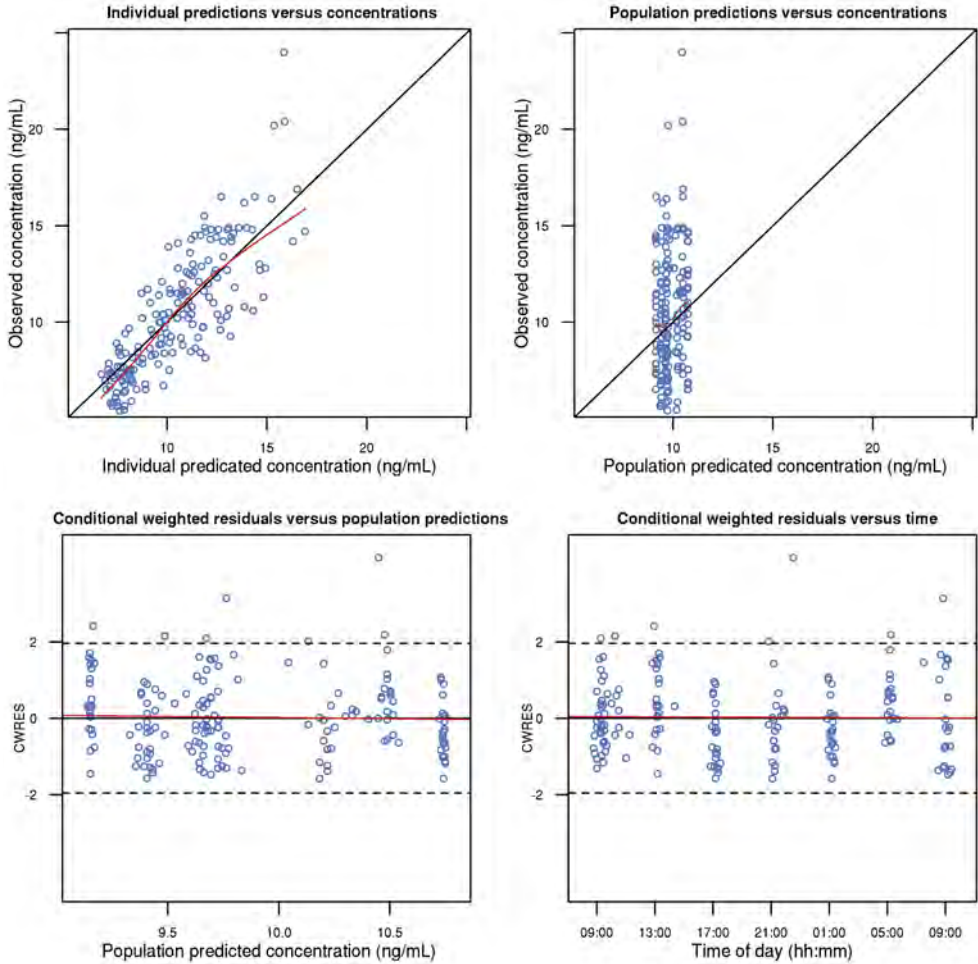
Figure S2. Goodness of fit plots for circadian model predicted uracil plasma levels. Blue dots represented observed data and red lines represent the trend of the data. Abbreviation: CWRES = conditional weighed residuals.

4
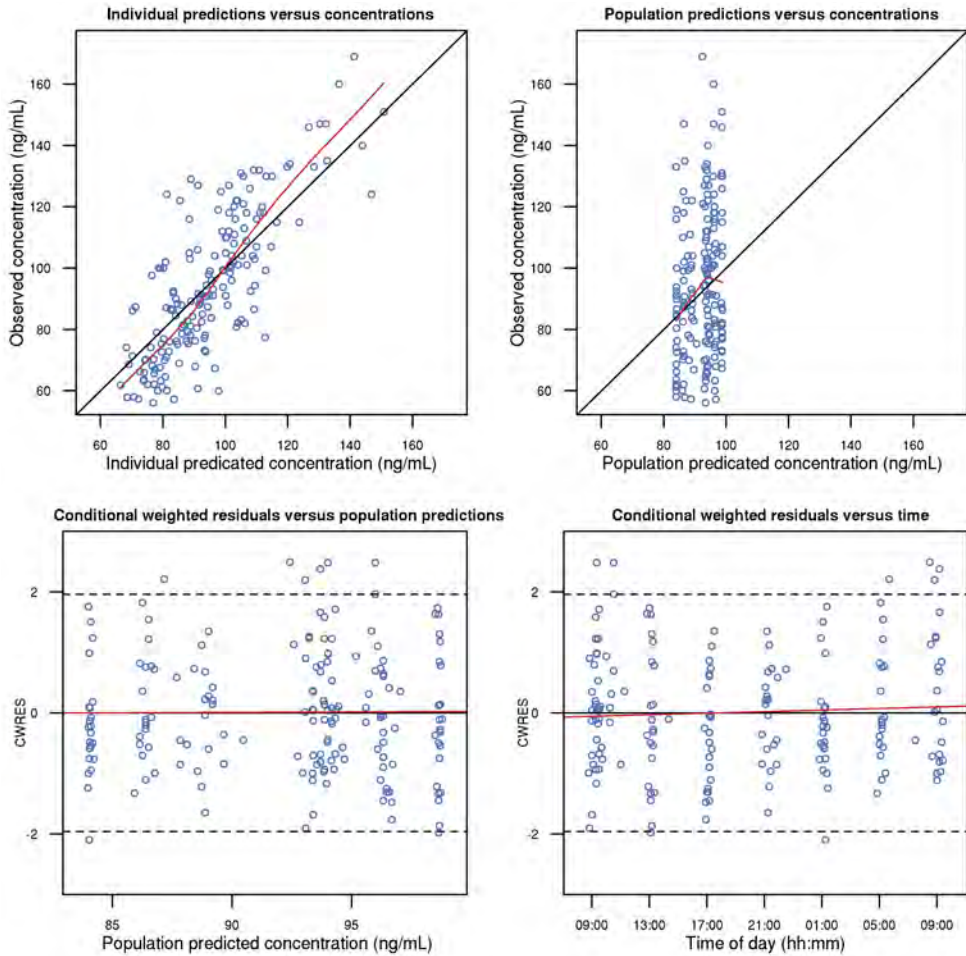
Figure S3. Goodness of fit plots for circadian model predicted dihydrouracil plasma levels. Blue dots represent observed data and red lines represent the trend of the data. Abbreviation: CWRES = conditional weighed residuals.
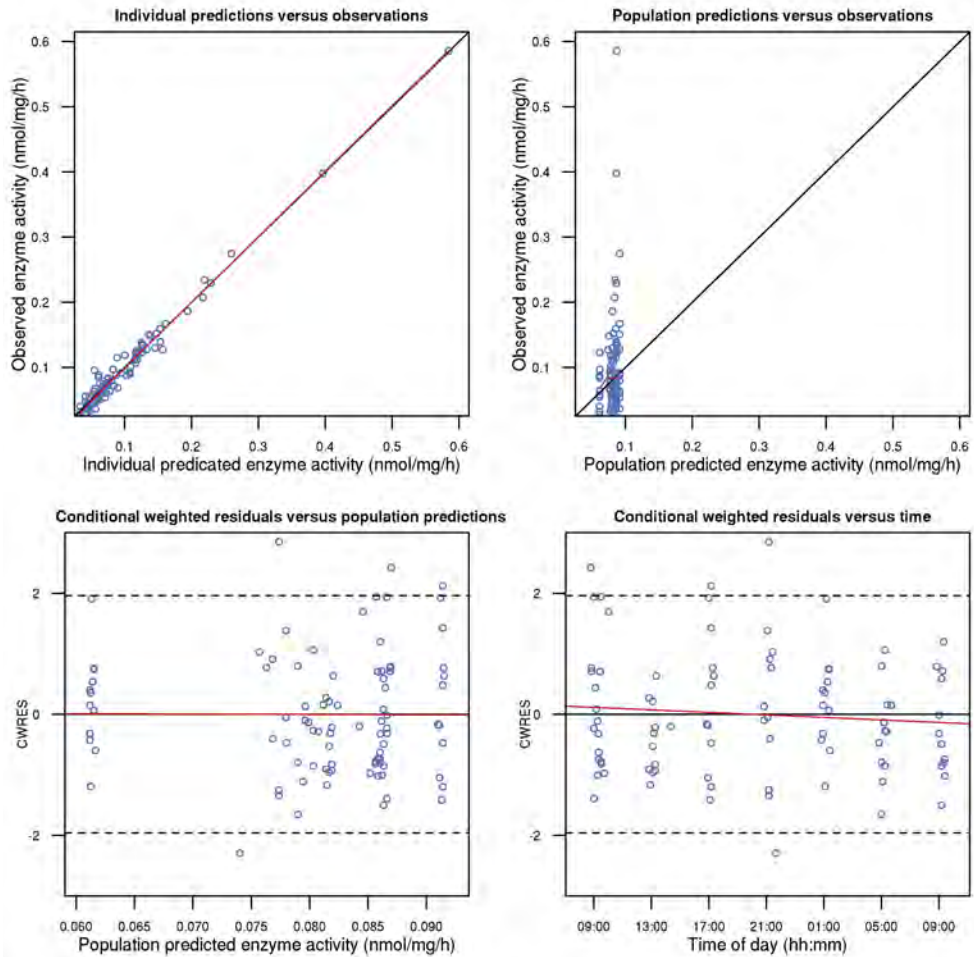
Figure S4. Goodness of fit plots for circadian model predicted thymidylate synthase activity in peripheral blood mononuclear cells. Blue dots represent observed data and red lines represent the trend of the data. Abbreviation: CWRES = conditional weighed residuals.

4
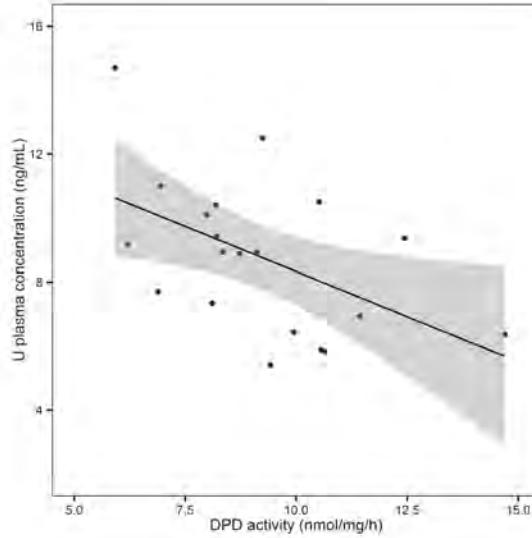
Figure S5. Correlation between baseline dihydropyrimidine dehydrogenase activity in peripheral blood mononuclear cells and uracil plasma levels ($r^2 = 0.26$, $p=0.02$) in 20 healthy volunteers. The shaded area represents the 95% confidence interval of the line. Abbreviation: DPD = dihydropyrimidine dehydrogenase, U = uracil.
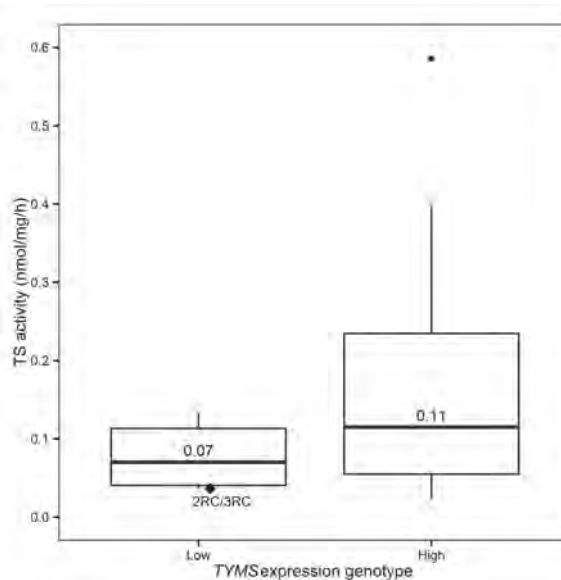
Figure S6. Baseline thymidylate synthase activity in peripheral blood mononuclear cells for low (n=10) and high (n=9) *TYMS* expression genotypes. Median TS activity per group is shown in the plot. Range in TS activity was highest for the *TYMS* high expression group. Difference in TS activity between groups was not statistically significant ($p=0.32$). TS activity of the volunteer with the 2RC/3RC genotype is separately shown (♦). Abbreviations: TS = thymidylate synthase.
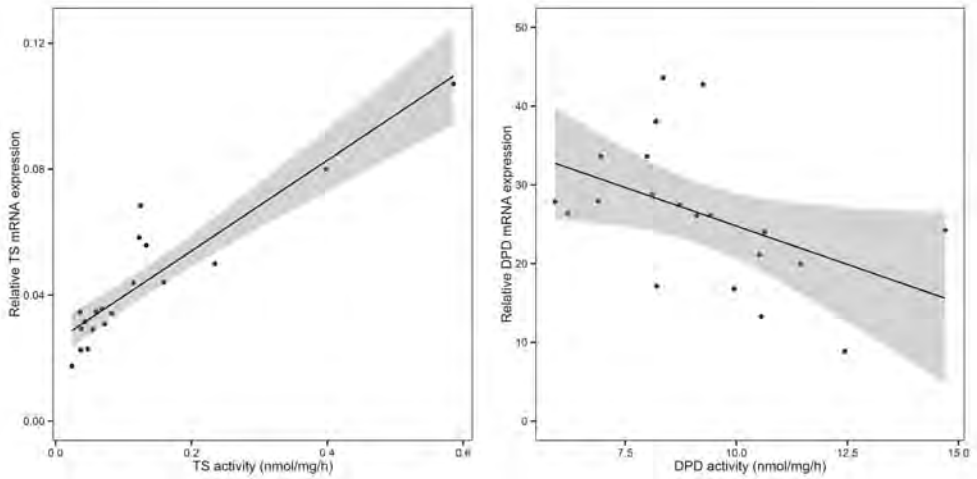
Figure S7. Strong positive correlation between thymidylate synthase activity and gene expression (r^2 =0.84; p<0.001) (left panel) and weak negative correlation between dihydropyrimidine dehydrogenase activity and gene expression (r^2=0.22; p=0.04) (right panel) in human peripheral blood mononuclear cells obtained from 20 healthy volunteers. Shaded areas represent 95% confidence intervals of the lines. Abbreviations: TS = thymidylate synthase, DPD = dihydropyrimidine dehydrogenase.

CHAPTER 5

THE IMPACT OF LIVER RESECTION ON THE DIHYDROURACIL:URACIL PLASMA RATIO IN PATIENTS WITH COLORECTAL LIVER METASTASES

Bart A.W. Jacobs, Nikol Snoeren, Morsal Samim, Hilde Rosing,
Niels de Vries, Maarten J. Deenen, Jos H. Beijnen, Jan H.M. Schellens,
Miriam Koopman, Richard van Hillegersberg

ABSTRACT

Background

The dihydrouracil (DHU) : uracil (U) plasma ratio is a promising marker for identification of dihydropyrimidine dehydrogenase (DPD) deficient patients. The objective of this study was to determine the effect of liver resection on the DHU:U plasma ratio in patients with colorectal liver metastases (CRLM).

Methods

An observational study was performed in which DHU:U plasma ratios in patients with CRLM were analysed prior to and one day after liver resection. In addition, the DHU:U plasma ratio was quantified in patients 4-8 weeks after liver resection to explore long-term effects on the DHU:U plasma ratio. Quantification of U and DHU plasma levels was performed using a validated ultra-performance liquid chromatography – tandem mass spectrometry (UPLC-MS/MS) assay.

Results

The median (range) DHU:U plasma ratio in 15 patients prior to liver resection was 10.7 (2.6-14.4) and was significantly reduced to 5.5 (<detection limit (LoD)-10.5) one day after resection (p=0.0026). This reduction was caused by a decrease in DHU plasma levels from 112.0 (79.8-153) ng/mL to 41.2 (<LoD-160) ng/mL one day after resection (p=0.0004). Recovery of the DHU:U plasma ratio occurred 4-8 weeks after liver resection, which was shown by a median (range) DHU:U plasma ratio in six patients of 9.1 (6.9-14.5).

Conclusion

Liver resection leads to very low DHU:U plasma ratios one day after liver resection, which is possibly caused by a reduction in DPD activity. Quantification of the DHU:U plasma ratios directly after liver resection could lead to false positive identification of DPD deficiency and is therefore not advised.

INTRODUCTION

Colorectal cancer remains one of the most commonly diagnosed cancer types worldwide [1]. Approximately 50% of the patients with advanced colorectal cancer develop liver metastases [2,3]. For patients with resectable colorectal liver metastases (CRLM), partial liver resection is the standard of care. In addition, some patients undergo adjuvant treatment with the 5-fluorouracil (5-FU) pro-drug capecitabine in order to improve survival.

After oral administration, capecitabine is rapidly converted to 5-FU through a three-step enzymatic cascade. Only 1-3% of the formed 5-FU is intracellularly anabolized to metabolites that possess anti-cancer properties. Approximately 80% of the formed 5-FU is catabolized by the enzyme dihydropyrimidine dehydrogenase (DPD) to the inactive metabolite dihydro-5-FU, which is further degraded and renally excreted [4,5]. The liver highly expresses DPD and plays an important role in the clearance of 5-FU [6].

Most commonly reported capecitabine side effects are hand-foot syndrome, diarrhoea, nausea and vomiting [7,8]. In particular, DPD-deficient patients are at risk for developing severe and sometimes lethal toxicity [9,10]. Upfront screening for single nucleotide polymorphisms in the gene encoding DPD, *DPYD*, could identify patients at risk of fluoropyrimidine-induced toxicity [9,11–13]. The sensitivity of *DPYD* genotyping approaches, however, remains rather low.

Phenotyping approaches for DPD activity might further improve the identification of patients at risk of developing fluoropyrimidine-induced severe toxicity. Most DPD phenotyping methods are based on *ex vivo* quantification of DPD activity in peripheral blood mononuclear cells (PBMCs) [14,15]. Although DPD activity in PBMCs is associated with fluoropyrimidine-induced severe toxicity and clearance [16–19], this approach remains laborious and is not suitable for examination of dynamic changes in systemic DPD activity. Alternatively, determination of the ratio between dihydrouracil (DHU) and the endogenous DPD substrate uracil (U) in plasma might be used for phenotyping DPD activity.

The pre-therapeutic DHU:U plasma ratio showed good correlation with clearance of 5-FU [20,21] and fluoropyrimidine-induced toxicity [22–24]. Upfront determination of the DHU:U plasma ratio is an attractive approach and less laborious than examination of DPD activity in PBMCs. Moreover, since the DHU:U plasma ratio is quantified in human plasma, it is likely that this marker is useful for detecting dynamic changes in systemic DPD activity.

There is, however, limited data on factors, such as hepatic function, which potentially play an important role in the regulation of the DHU:U plasma ratio. Identification of such factors is essential for interpretation of the DHU:U plasma ratio with respect to DPD phenotype-guided dosing. Since DPD is highly expressed in liver tissue, changes in liver tissue possibly affect the DHU:U plasma ratio. The aim of the study was to determine the effect of liver resection by quantification of the DHU:U plasma ratio in patients with CRLM prior to and one day after liver resection. Furthermore, we explored whether changes in DHU:U plasma ratio after liver resection were reversible and whether they were associated with capecitabine-induced toxicity.

METHODS

Patient population and sample collection

The primary study objective was to determine the DHU:U plasma ratio in patients with CRLM prior to and one day after partial liver resection. Patients were considered eligible in case heparinized plasma for quantification of the DHU:U ratio was obtained both at the day of liver resection, prior to the surgical operation, and one day after the resection (Group A). The included patients either participated in a multicentre randomized phase III clinical trial (www.clinicaltrials.gov, study identifier: NCT00394992), in which subjects were randomized after liver resection to receive capecitabine plus oxaliplatin (CAPOX) or CAPOX plus bevacizumab [25], or included patients underwent partial liver resection for CRLM in the University Utrecht Medical Centre as standard of care. All patients provided written informed consent. For the patients participating in the phase III trial [25], toxicities were evaluated after every cycle of chemotherapy and assessed according to the National Cancer Institute Common Toxicity Criteria for Adverse Events (CTC-AE) version 3.0.

In addition, we were interested in long-term changes in the DHU:U plasma ratio after partial liver resection. Therefore, we also explored the effects of liver resection on the DHU:U plasma ratio in samples that were collected 4-8 weeks after resection from patients, who participated in the phase III trial [25], but for whom no plasma was available prior to and one day after liver resection (Group B). The plasma samples were stored at -70°C until analysis.

Quantification of uracil and dihydrouracil plasma levels

U and DHU were quantified in plasma using an ultra-performance liquid chromatography – tandem mass spectrometry (UPLC-MS/MS) assay as described previously [26]. In short, an internal standard solution containing 1,3-U-$^{15}N_2$ and 5,6-DHU-$^{13}C_4$,$^{15}N_2$ was added to 300 µL plasma. Protein precipitation was performed using 900 µL of methanol and acetonitrile (1:1, v/v). Samples were vortex-mixed for 10 s, shaken for 10 min and centrifuged at 14.000 g for 10 min. The supernatants were dried under a stream of nitrogen at 40°C and reconstituted in 100 µL 0.1% formic acid in water. Chromatographic separation was performed on an Acquity UPLC® HSS T3 (150 x 2.1 mm ID, particle size 1.8 µm; Waters, Milford, USA) column. Mobile phases consisted of 0.1% formic acid in water (eluent A) and 0.1% formic acid in acetonitrile (eluent B) at a flow of 0.3 mL/min. The following gradient was used: 0% B from 0-3.0 min, 0-90% B from 3.0-3.2 min, 90% B from 3.2-3.7 min, 0% B from 3.7-5 min. A Qtrap 5500 triple quadrupole mass spectrometer (AB Sciex, Framingham, USA) was operated in the negative mode for quantification of U and in the positive mode for quantification of DHU. Validated concentration ranges for U and DHU were 1-100 ng/mL and 10-1000 ng/mL, respectively.

Data analysis

Differences between DHU:U plasma ratios, and the U and DHU plasma levels, prior to and one day after liver resection were assessed using the two-tailed Wilcoxon matched-pairs test. The two-tailed Mann-Whitney test was used for comparing DHU:U plasma ratios,

and U and DHU plasma levels, one day after liver resection of CRLM (Group A) and 4-8 weeks after liver resection (Group B). The statistical analyses were performed in R (version 3.3.0) [27]. P values <0.05 were considered statistically significant. Observations below the detection limit (<LoD) were considered to be zero for statistical analyses.

RESULTS

Patient characteristics

Plasma samples from 21 patients who underwent partial liver resection for CRLM were available for quantification of the DHU:U ratio. From 15 patients, plasma samples were collected prior to and one day after resection (Group A). In addition, exploratory analysis of the DHU:U plasma ratio 4-8 weeks after resection was performed in samples from six patients (Group B). Patient characteristics of both study groups are summarized in Table 1.

Table 1. Demographic and disease characteristics.

Characteristic	Group A	Group B
Number of subjects	15	6
Age (years)		
Median (range)	67 (54– 82)	60 (40– 73)
Gender		
Male	9	5
Female	6	1
Location of primary tumour		
Caecum	1	-
Colon	6	4
Rectosigmoid	-	1
Rectum	8	1
Clinical stage		
T3N0	7	2
T3N1	6	1
T3N2	2	1
T4N0	-	1
T4N2	-	1
Number of CRLM		
Median (range)	1 (1 – 6)	1 (1 – 1)
Radical resection		
R0	14	6
R1	1	-

Abbreviation: CRLM, colorectal liver metastases

Reduction in DHU:U plasma one day after liver resection

The median (range) DHU:U plasma ratio prior to liver resection was 10.7 (2.6-14.4). The DHU:U plasma ratio was significantly reduced to 5.5 (<LoD-10.5) one day after resection (p=0.0026; Figure 1A). U plasma levels prior to and one day after resection were 11.0 (8.6-36.9) ng/mL and 11.1 (3.9-17.1) ng/mL (p=0.3232; Figure 1B), respectively. In all patients except for two, the DHU plasma level was decreased one day after liver resection. The median (range) DHU plasma level prior to resection was 112.0 (79.8-153) ng/mL and was 41.2 (<LoD-160) ng/mL one day after resection (p=0.0004; Figure 1C). In four patients, the DHU plasma levels were undetectable one day after liver resection.

The DHU:U plasma ratio 4-8 weeks after liver resection

The median (range) time interval of plasma collection in Group B was 46.5 (29-55) days after liver resection. The median (range) DHU:U plasma ratio in this group was 9.1
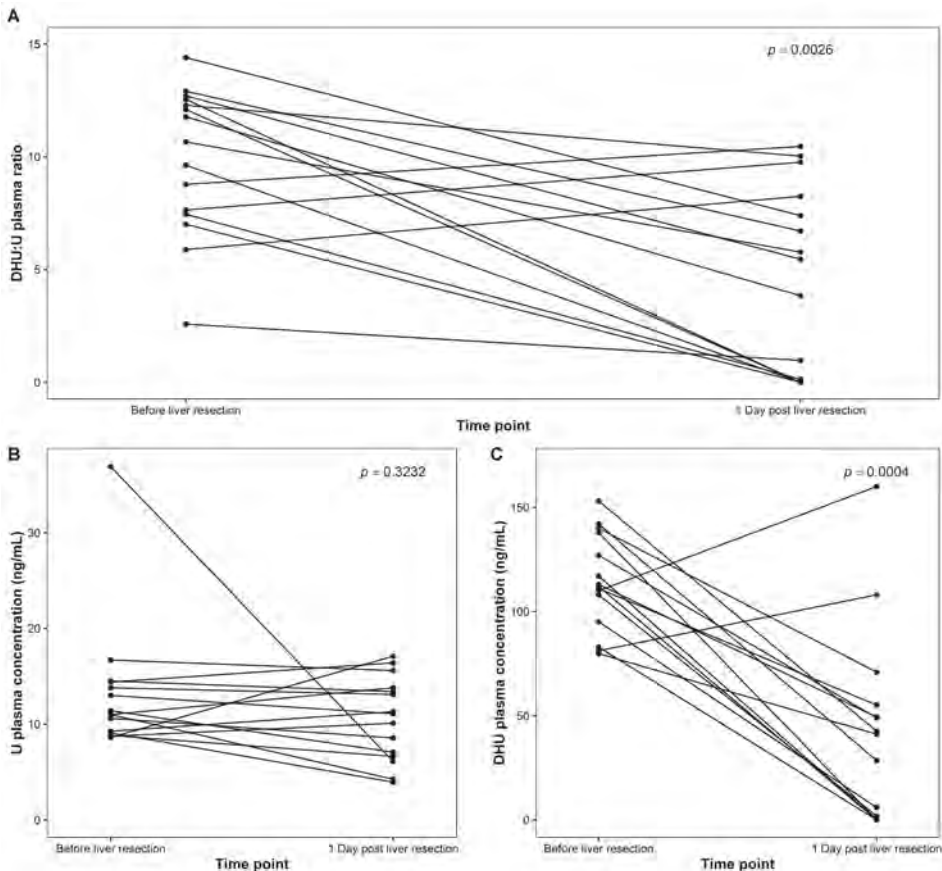
Figure 1. The dihydrouracil:uracil plasma ratio (A), uracil (B) and dihydrouracil (C) plasma levels of 15 patients prior to and one day after liver resection for colorectal liver metastases. Abbreviations: CRLM, colorectal liver metastases; DHU, dihydrouracil; U, uracil.

(6.9-14.5), which was significantly higher compared to DHU:U plasma ratios one day after resection (p=0.0135; Figure 2A). As shown in Figure 2B, U plasma levels were not statistically different in the samples that were collected one day after liver resection or 4-8 weeks after. Contrarily, the median (range) DHU plasma level was 106.5 (88.1-120.0) ng/mL 4-8 weeks after resection and was significantly higher than the DHU levels one day after resection (p=0.003; Figure 2C).

Tolerability of capecitabine

Treatment characteristics of four patients in Group A were available for exploratory analysis of treatment toxicity (Table 2). Capecitabine was administered on days 1-14 of every 21-day cycle with a dose of 1000 mg/m^2 bi-daily. Oxaliplatin 130 mg/m^2 and bevacizumab 7.5 mg/kg, for patients who underwent treatment with CAPOX-B, were
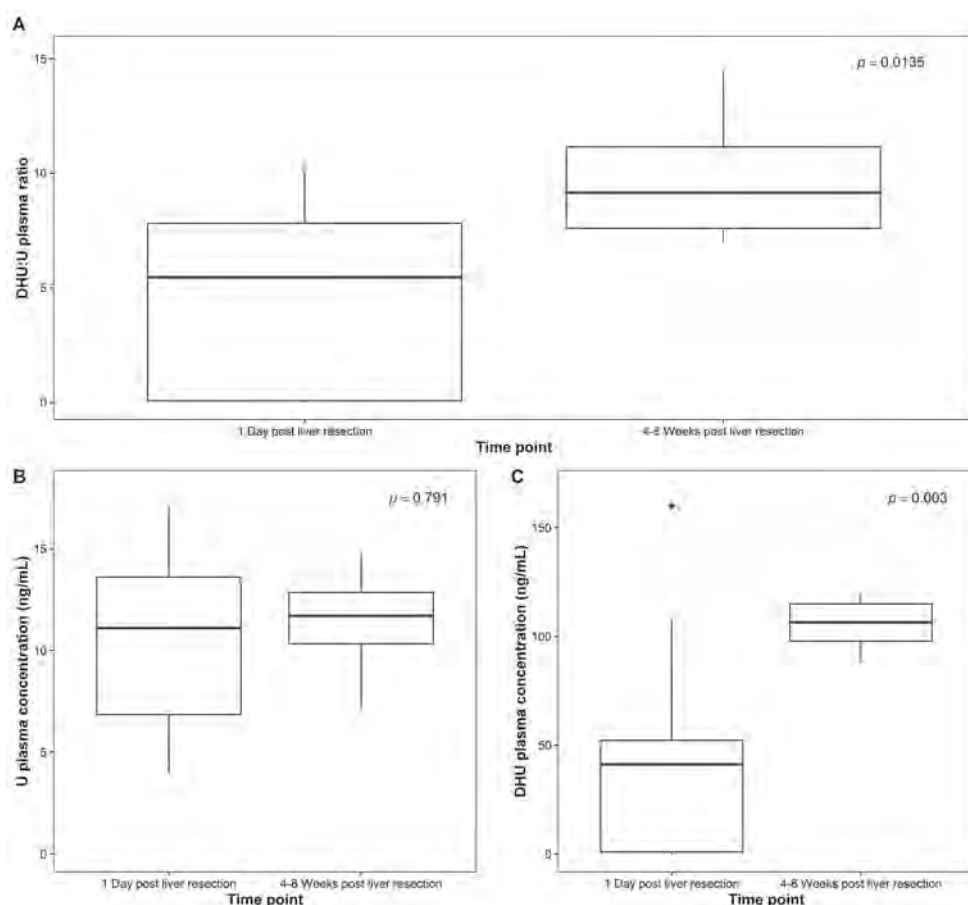
Figure 2. The dihydrouracil:uracil plasma ratio (A), uracil (B) and dihydrouracil (C) plasma levels one day (n=15 patients) and 4-8 weeks (n=6 patients) after liver resection in patients with colorectal liver metastases. Abbreviations: CRLM, colorectal liver metastases; DHU, dihydrouracil; U, uracil.

5

Table 2. Treatment characteristics of four patients who received adjuvant treatment with CAPOX(-B) after liver resection.

	Patient 1	Patient 2	Patient 3	Patient 4
Gender	Male	Male	Female	Female
Age (years)	73	72	66	61
Primary tumor	Colon	Ceacum	Rectum	Colon
Clinical stage	T3N0	T3N0	T3N0	T3N0
Number of CRLM	5	1	3	1
DHU:U plasma ratio (% of normal)[a]				
Before liver resection	5.9 (55%)	12.1 (114%)	9.6 (91%)	7.5 (70%)
1 Day after liver resection	8.2 (78%)	<LoD [b]	<LoD [b]	0.4 (3%)
Adjuvant chemotherapy	CAPOX-B	CAPOX-B	CAPOX	CAPOX / FOLFOX
Start first cycle of chemotherapy (days after liver resection)	51	57	56	53
Capecitabine starting dose	2000 mg BID	1650 mg BID	1800 mg BID	2000 mg BID
Number of cycles received	3	8	8	CAPOX: 2 FOLFOX: 9
Toxicity during treatment (maximum grade)	INF4; DIA3; FTG2; INS2; TAS2; HMR2; NEU2; HMG1; FEV1; ISR1; ABP1; WAE1; VOM1	NAU3; DIA2; HYP2; TAS2; HBR2; ANR2; FTG1; WGT1; HFS1; VOM1; CRA1; NEU1; LIB1	HGC3; DIA2; MUC2; NAU2; NEU2; ABP2; WAE2; VOM1; FLT1; HFS1; FTG1; ISR1; HBR1; ANR1; DZN1; LIB1; SMP1	*During CAPOX:* VOM3; DHT3; DIA2; NAU2; VIS2; HFS1; MUC1; PRF1 *During FOLFOX:* INF3; NEU3; DPN2; HFS2; HTF2; FTG1; DIA1; MUC1; NAU1; TAS1; WAE1
Capecitabine dose reduction	No	Yes, after C4	Yes, after C3	None
Treatment delay	Yes, after C2	Yes, after C7	Yes, after C3 and C7	None

Table 2. (continued)

	Patient 1	Patient 2	Patient 3	Patient 4
Serious adverse event(s)	Hospitalization due to capecitabine-related diarrhoea	None	None	1) Hospitalization due to dehydration (during CAPOX treatment) 2) Hospitalization due to infection (during FOLFOX treatment)

Abbreviations: INF, infection; DIA, diarrhoea; VOM, vomiting; FTG, fatigue; INS, insomnia; TAS, taste alteration; HMR, haemorrhoids; HMG, haemorrhage; FEV, fever; ISR, injection site reaction; ABP, abdominal pain; WAE, watery eye; HYP, hypersensitivity; WGT, weight loss; HFS, hand-foot syndrome; NAU, nausea; HBR, heartburn/dyspepsia; ANR, anorexia; NEU, neuropathy; LIB, libido; MUC, mucositis/stomatitis; FLT, flatulence; DZN, dizziness; CRA, arm cramps; HGC, hyperglycaemia; SMP, steroid myopathy; DHT, dehydration; VIS, vision − blurred vision; PRF, pain right flank; DPN, dyspnoea; HTF, hot flushes; CAPOX, capecitabine plus oxaliplatin, FOLFOX, 5-fluorouracil plus folinic acid and oxaliplatin; C, cycle; BID, bi-daily; CRLM, colorectal liver metastases; LoD, detection limit.
[a] Mean (s.d.) DHU:U plasma ratio in 40 healthy volunteers [28]: 10.6 ± 2.4.
[b] The DHU plasma concentration was below the detection limit. As a consequence, the DHU:U plasma ratio was undetectable.

5

administered on day 1 of each cycle. In case of the four patients, adjuvant chemotherapy was started 51-57 days after liver resection.

The DHU:U plasma ratio of patient 1, a 73-year old male, was increased from 5.9 to 8.2 one day after liver resection. He received 3 cycles of CAPOX-B and poorly tolerated the chemotherapy. The patient was admitted to the hospital for capecitabine-induced diarrhoea (grade 3). He also experienced a severe infection (grade 4) and multiple grade 1-2 toxicities. Furthermore, the patient required treatment delay after 2 cycles.

Patient 2, a 72-year old male, and patient 3, a 66-year old female, both had undetectable DHU plasma levels one day after liver resection. Both patients received 8 cycles of adjuvant chemotherapy. Nonetheless, both patients required a capecitabine dose reduction after cycle 4 and cycle 3, respectively, and a treatment delay. Patient 2 suffered from severe diarrhoea (grade 3) and multiple grade 1-2 toxicities. Patient 3 experienced severe hyperglycaemia (grade 3) and several grade 1-2 toxicities.

Patient 4, a 61-year old female, was treated with 2 cycles of CAPOX. The DHU:U plasma ratio was relatively low one day after liver resection. She experienced severe vomiting (grade 3) and dehydration (grade 3), for which she was hospitalized. In addition, she suffered from multiple grade 1-2 toxicities. After 2 cycles, it was decided to switch from CAPOX to FOLFOX. During FOLFOX treatment, she also experienced grade 1-3 toxicities.

DISCUSSION

The results of this study clearly show that the DHU:U plasma ratio is decreased one day after liver resection. The reduction in the DHU:U plasma ratio is the result of ~50% decrease in the DHU plasma level. Our results also show that the decrease in DHU:U plasma ratio is reversible, since the DHU:U plasma ratios 4-8 weeks after liver resection were in line with values prior to liver resection and comparable to DHU:U ratios in healthy volunteers [28]. This is, to our knowledge, the first study to report dynamic changes in the DHU:U plasma ratio after liver resection in humans.

The effect of unresected CRLM on a DPD phenotype marker was recently studied by Van Staveren et al. [29]. In their study, the DPD phenotype was assessed by uracil pharmacokinetics after administration of an oral dose of uracil. They found unaltered uracil pharmacokinetics in patients with CRLM [29]. In our study, patients with CRLM showed DHU:U plasma ratios prior to liver resection that were comparable to DHU:U plasma ratios of healthy volunteers (reference mean (±s.d.) DHU:U plasma ratio: 10.6±2.4) [28]. Based on these findings, it seems that the DPD phenotype markers are unaltered in patients with unresected CRLM.

The recovery of the DHU:U plasma ratio after 4-8 weeks could be related to liver regeneration. Liver regeneration is a complex physiological process that immediately starts after liver resection and discontinues when the liver reaches its original volume. A study with human patients demonstrated that liver function recovers within 30 days after partial liver resection [30]. Preclinical experiments in rats showed that it only takes 5-7 days until the liver reaches its original volume [31]. More specific, a study of liver resection in rats demonstrated that DPD activity recovers four days after liver resection

[32]. One day after liver resection, however, DPD activity in rat liver was reduced by 45% [32]. *In vitro* experiments further illustrated that uracil metabolism in regenerating rat liver was only 25% compared to normal rat liver [33]. So it seems, that during the first phase after liver resection, hepatic DPD activity can be reduced, but rapidly recovers thereafter. Results of our study demonstrate that DPD activity is reduced directly after liver resection and that DPD activity recovers within 4-8 weeks after resection, which is in line with the data on human liver regeneration and DPD activity in rat liver. The exact mechanism behind the recovery in DPD activity remains unclear and warrants further research.

Based on our cases series of four patients, it seems unlikely that the DHU:U plasma ratio one day after liver resection gives an appropriate representation of the DPD phenotype during adjuvant chemotherapy. The DHU:U plasma ratio in patient 1 was increased one day after liver resection, while it was highly reduced in patients 2, 3 and 4. Adjuvant chemotherapy was started 51-57 days after liver resection. All four patients poorly tolerated CAPOX-(B) and mainly suffered from severe diarrhoea, nausea and vomiting. These toxicities can be related to capecitabine, but could also be caused or provoked by oxaliplatin and bevacizumab. Larger studies are needed to examine the relationship between DHU:U plasma ratio after liver resection and capecitabine-induced toxicity.

The primary aim of our study was to quantify changes in DHU:U plasma ratio after liver resection. Although the number of patients was relatively small, the results of the study clearly demonstrated a reduction in DHU:U plasma ratio after liver resection. A limitation of the study is that we cannot rule out that the reduction in DHU:U plasma ratio is the effect of reduced systemic DPD activity. Dynamic changes in other enzymes, such as dihydropyriminidase, which is important for the degradation of DHU and which is also expressed in liver tissue, might also affect DHU levels. However, the question remains whether this would be of clinical relevance since dihydropyriminidase deficiency has thus far not been associated with capecitabine-induced toxicity. Furthermore, other studies are warranted to determine whether changes in DHU:U plasma ratio are caused specifically by liver resection or by non-specific surgical effect(s), such as the use of anaesthesia.

Besides liver resection, we previously also found that circadian rhythmicity is a factor that influences the DHU:U plasma ratio [28]. More research is needed to study the role of other factors, such as exposure to light, intake of food and physical activity that contribute to the DHU:U plasma ratio. This research is warranted for validation of the DHU:U plasma ratio in order to allow clinical implementation of this DPD phenotype marker.

In conclusion, liver resection leads to very low DHU:U plasma ratios one day after liver resection. Quantification of the DHU:U plasma ratios directly after liver resection might lead to false positive identification of DPD deficiency. Therefore, DPD-phenotype guided fluoropyrimidine dosing should not be based on DHU:U plasma ratios in samples that are collected directly after liver resection.

ACKNOWLEDGEMENTS

REFERENCES

1. Torre LA, Bray F, Siegel RL, Ferlay J, Lortet-Tieulent J, Jemal A. Global Cancer Statistics, 2012. Ca Cancer J Clin 2015;65:87–108.

2. Haddad AJ, Bani Hani M, Pawlik TM, Cunningham SC. Colorectal liver metastases. Int J Surg Oncol 2011;2011:285840.

3. Borner MM. Neoadjuvant chemotherapy for unresectable liver metastases of colorectal cancer--too good to be true? Ann Oncol 1999;10:623–6.

4. Heggie GD, Sommadossi JP, Cross DS, Huster WJ, Diasio RB. Clinical pharmacokinetics of 5-fluorouracil and its metabolites in plasma, urine, and bile. Cancer Res 1987;47:2203–6.

5. Judson IR, Beale PJ, Trigo JM, Aherne W, Crompton T, Jones D, et al. A human capecitabine excretion balance and pharmacokinetic study after administration of a single oral dose of 14C-labelled drug. Invest New Drugs 1999;17:49–56.

6. Naguib FN, el Kouni MH, Cha S. Enzymes of uracil catabolism in normal and neoplastic human tissues. Cancer Res 1985;45:5405–12.

7. Mikhail SE, Sun JF, Marshall JL. Safety of capecitabine: a review. Expert Opin Drug Saf 2010;9:831–41.

8. Twelves C, Wong A, Nowacki MP, Abt M, Burris H, Carrato A, et al. Capecitabine as adjuvant treatment for stage III colon cancer. N Engl J Med 2005;352:2696–704.

9. Deenen MJ, Meulendijks D, Cats A, Sechterberger MK, Severens JL, Boot H, et al. Upfront Genotyping of DPYD*2A to Individualize Fluoropyrimidine Therapy: A Safety and Cost Analysis. J Clin Oncol 2016;34:227–34.

10. Meulendijks D, Henricks LM, Sonke GS, Deenen MJ, Froehlich TK, Amstutz U, et al. Clinical relevance of DPYD variants c.1679T>G, c.1236G>A/HapB3, and c.1601G>A as predictors of severe fluoropyrimidine-associated toxicity: a systematic review and meta-analysis of individual patient data. Lancet Oncol 2015;16:1639–50.

11. Jennings BA, Loke YK, Skinner J, Keane M, Chu GS, Turner R, et al. Evaluating predictive pharmacogenetic signatures of adverse events in colorectal cancer patients treated with fluoropyrimidines. PLoS One 2013;8:e78053.

12. Loganayagam A, Arenas Hernandez M, Corrigan A, Fairbanks L, Lewis CM, Harper P, et al. Pharmacogenetic variants in the DPYD, TYMS, CDA and MTHFR genes are clinically significant predictors of fluoropyrimidine toxicity. Br J Cancer 2013;108:2505–15.

13. Lee AM, Shi Q, Pavey E, Alberts SR, Sargent DJ, Sinicrope FA, et al. DPYD Variants as Predictors of 5-fluorouracil Toxicity in Adjuvant Colon Cancer Treatment (NCCTG N0147). J Natl Cancer Inst 2014;106:1–12.

14. Van Kuilenburg AB, Van Lenthe H, Tromp A, Veltman PC, Van Gennip AH. Pitfalls in the diagnosis of patients with a partial dihydropyrimidine dehydrogenase deficiency. Clin Chem 2000;46:9–17.

15. Pluim D, Jacobs BAW, Deenen MJ, Ruijter AEM, van Geel RMJM, Burylo AM, et al. Improved pharmacodynamic assay for dihydropyrimidine dehydrogenase activity in peripheral blood mononuclear cells. Bioanalysis 2015;7:519–29.

16. Van Kuilenburg ABP, Meinsma R, Zoetekouw L, Van Gennip AH. Increased risk of grade IV neutropenia after administration of 5-fluorouracil due to a dihydropyrimidine dehydrogenase deficiency: High prevalence of the IVS14+1G>A mutation. Int J Cancer 2002;101:253–8.

17. Milano G, Etienne MC, Pierrefite V, Barberi-Heyob M, Deporte-Fety R, Renée N. Dihydropyrimidine dehydrogenase deficiency and fluorouracil-related toxicity. Br J Cancer 1999;79:627–30.

18. van Kuilenburg AB, Haasjes J, Richel DJ, Zoetekouw L, Van Lenthe H, De Abreu RA, et al. Clinical implications of dihydropyrimidine dehydrogenase (DPD) deficiency in patients with severe 5-fluorouracil-associated toxicity: identification of new mutations in the DPD gene. Clin Cancer Res 2000;6:4705–12.

19. Fleming RA, Milano G, Thyss A, Etienne MC, Renée N, Schneider M, et al. Correlation between dihydropyrimidine dehydrogenase activity in peripheral mononuclear cells and

5

systemic clearance of fluorouracil in cancer patients. Cancer Res 1992;52:2899–902.

20. Gamelin M, Boisdron-Celle M, Guérin-Meyer V, Delva R, Lortholary A, Genevieve F, et al. Correlation between uracil and dihydrouracil plasma ratio, fluorouracil (5-FU) pharmacokinetic parameters, and tolerance in patients with advanced colorectal cancer: A potential interest for predicting 5-FU toxicity and determining optimal 5-FU dosage. J Clin Oncol 1999;17:1105–10.

21. Jiang H, Lu J, Jiang J, Hu P. Important role of the dihydrouracil/uracil ratio in marked interpatient variations of fluoropyrimidine pharmacokinetics and pharmacodynamics. J Clin Pharmacol 2004;44:1260–72.

22. Sistonen J, Büchel B, Froehlich TK, Kummer D, Fontana S, Joerger M, et al. Predicting 5-fluorouracil toxicity: DPD genotype and 5,6-dihydrouracil:uracil ratio. Pharmacogenomics 2014;15:1653–66.

23. Zhou ZW, Wang GQ, Wan D Sen, Lu ZH, Chen YB, Li S, et al. The dihydrouracil/uracil ratios in plasma and toxicities of 5-fluorouracil-based adjuvant chemotherapy in colorectal cancer patients. Chemotherapy 2007;53:127–31.

24. Boisdron-Celle M, Remaud G, Traore S, Poirier A, Gamelin L, Morel A, et al. 5-Fluorouracil-related severe toxicity: a comparison of different methods for the pretherapeutic detection of dihydropyrimidine dehydrogenase deficiency. Cancer Lett 2007;249:271–82.

25. Snoeren N, Voest EE, Bergman AM, Dalesio O, Verheul HM, Tollenaar RAEM, et al. A randomized two arm phase III study in patients post radical resection of liver metastases of colorectal cancer to investigate bevacizumab in combination with capecitabine plus oxaliplatin (CAPOX) vs CAPOX alone as adjuvant treatment. BMC Cancer 2010;10:545.

26. Jacobs BAW, Rosing H, de Vries N, Meulendijks D, Henricks LM, Schellens JHM, et al. Development and validation of a rapid and sensitive UPLC–MS/MS method for determination of uracil and dihydrouracil in human plasma. J Pharm Biomed Anal 2016;126:75–82.

27. R Development Core Team. R: A Language and Environment for Statistical Computing. Vienna, Austria: R Foundation for Statistical Computing 2016.

28. Jacobs BAW, Deenen MJ, Pluim D, van Hasselt JGC, Krähenbühl MD, van Geel RMJM, et al. Pronounced between-subject and circadian variability in thymidylate synthase and dihydropyrimidine dehydrogenase enzyme activity in human volunteers. Br J Clin Pharmacol 2016;82:706–16.

29. van Staveren MC, Opdam F, Guchelaar H-J, van Kuilenburg ABP, Maring JG, Gelderblom H. Influence of metastatic disease on the usefulness of uracil pharmacokinetics as a screening tool for DPD activity in colorectal cancer patients. Cancer Chemother Pharmacol 2015:1–6.

30. Yoshida M, Shiraishi S, Sakamoto F, Beppu T, Utsunomiya D, Okabe H, et al. Assessment of hepatic functional regeneration after hepatectomy using (99m)Tc-GSA SPECT/CT fused imaging. Ann Nucl Med 2014;28:780–8.

31. Michalopoulos GK, DeFrances MC. Liver regeneration. Science 1997;276:60–6.

32. Fritzon P. The relation between uracil-catabolizing enzymes and rate of rat liver regeneration. J Biol Chem 1962;237:150–6.

33. Canellkakis ES. Pyrimidine metabolism. III. The interaction of the catabolic and anabolic pathways of uracil metabolism. J Biol Chem 1957;227:701–9.

C H A P T E R   6

INCREASED RISK OF SEVERE FLUOROPYRIMIDINE-
ASSOCIATED TOXICITY IN PATIENTS CARRYING A G>C
SUBSTITUTION IN THE FIRST 28-BP TANDEM REPEAT OF
THE THYMIDYLATE SYNTHASE 2R ALLELE

Didier Meulendijks, Bart A.W. Jacobs, Abidin Aliev, Dick Pluim, Erik van Werkhoven,
Maarten J. Deenen, Jos H. Beijnen, Annemieke Cats, Jan H.M. Schellens

ABSTRACT

The fluoropyrimidines act by inhibiting thymidylate synthase (TS). Recent studies have shown that patients' risk of severe fluoropyrimidine-associated toxicity is affected by polymorphisms in the 5'-untranslated region of *TYMS*, the gene encoding TS. A G>C substitution in the promoter enhancer region of *TYMS*, rs183205964 (known as the 2RC allele), markedly reduces TS activity *in vitro*, but its clinical relevance is unknown. We determined rs183205964 in 1605 patients previously enrolled in a prospective multicenter study. Associations between putative low TS expression genotypes (3RC/2RC, 2RG/2RC, and 2RC/2RC) and severe toxicity were investigated using univariable and multivariable logistic regression. Activity of TS and *TYMS* gene expression were determined in peripheral blood mononuclear cells (PBMCs) of a patient carrying genotype 2RC/2RC and of a control group of healthy individuals. Among 1605 patients, 28 patients (1.7%) carried the 2RC allele. Twenty patients (1.2%) carried a risk-associated genotype (2RG/2RC, n=13; 3RC/2RC, n=6; and 2RC/2RC, n=1), the eight remaining patients had genotype 3RG/2RC. Early severe toxicity and toxicity-related hospitalization were significantly more frequent in risk-associated genotype carriers (OR 3.0, 95%CI 1.04-8.93, *p*=0.043 and OR 3.8, 95%CI 1.19-11.9, *p*=0.024, respectively, in multivariable analysis). The patient with genotype 2RC/2RC was hospitalized twice and had severe febrile neutropenia, diarrhea, and hand-foot syndrome. Baseline TS activity and gene expression in PBMCs of this patient, and a healthy individual with the 2RC allele, were found to be within the normal range. This study suggests that patients carrying rs183205964 are at strongly increased risk of severe, potentially life-threatening, toxicity when treated with fluoropyrimidines.

INTRODUCTION

The fluoropyrimidines 5-fluorouracil (5-FU), capecitabine, and tegafur are the backbone of chemotherapeutic treatment of gastrointestinal, breast, and head & neck cancers. Fluoropyrimidines act by inhibiting thymidylate synthase (TS), an enzyme which is crucial for DNA replication and repair, by providing the only *de novo* source of deoxythymidine monophosphate. While most patients tolerate treatment well, around 20% experiences severe, potentially lethal, treatment-related toxicity. The best recognized cause of intolerance to fluoropyrimidines is deficiency of the main 5-FU metabolizing enzyme, dihydropyrimidine dehydrogenase (DPD). Single nucleotide polymorphisms (SNPs) in *DPYD*, the gene encoding DPD, are now established predictors of fluoropyrimidine-associated toxicity, and upfront screening for these variants can improve patient safety [1,2]. The expression of TS is influenced by polymorphisms in *TYMS*, the gene encoding TS [3–5]. However, in contrast to *DPYD* variants, the clinical relevance of these polymorphisms as predictors of treatment-related toxicity is far from established.

TYMS is located on chromosome 18p11.32, consists of seven exons, and is ~16,000 bp long. The 5′-untranslated region (5'-UTR) of *TYMS* contains a variable number of 28-bp tandem repeats (VNTR) which acts as an enhancer to the promoter and stimulates transcriptional activity [3,4,6]. The vast majority of individuals carry *TYMS* alleles that contain 2 or 3 repeats in this promoter enhancer region, designated 2R and 3R, with allele frequencies of ~0.47 and 0.53, respectively [7]. The VNTR affects expression of TS, and *in vitro* studies have shown that a 2R enhancer region produces 3.6 times less mRNA compared with 3R [3]. Similarly, tumor tissue with a 2R/3R genotype produced significantly less cellular TS protein compared with 3R/3R [4]. Kawakami showed that in addition to stimulating gene transcription, a higher number of repeats also confers a greater translational efficiency [5]. In line with these non-clinical observations, a recent meta-analysis has shown that, upon treatment with capecitabine, patients carrying the 2R allele are at increased risk of severe fluoropyrimidine-associated toxicity [7].

Transcription of *TYMS* is regulated by 2R and 3R due to 6 bp enhancer box (E-box) sequences, of CACTTG, that occur within the tandem repeats [8]. To these sequences, upstream stimulating factor 1 (USF-1) can bind, thereby stimulating transcription of *TYMS*. The 2R allele contains one functionally relevant E-box element, in the first repeat, while the 3R allele contains up to two binding sites, occurring in the first and the second repeat. Whether or not a second binding site is present in the second repeat of the 3R allele, depends on a G>C SNP that occurs at the 12th nucleotide of the second repeat in the CACTTG sequence. If present, the USF-1 binding site in the second repeat is abolished, and the transcriptional activity of the 3R allele containing the G>C SNP is reduced to approximately that of the 2R allele in *in vitro* studies [8]. The 3R allele containing the G>C SNP is commonly referred to as 3RC to distinguish it from the wild type 3RG allele.

In 2006, a novel G>C SNP was described for the first time in patients, occurring in the first repeat of the 2R allele. This variant, rs183205964, disrupts the last functional E-box sequence present in the 2R allele (Supplementary Figure 1). It was described to have an estimated allele frequency of 0.015-0.042, and is referred to as 2RC, to distinguish it

from the wild type allele 2RG [9,10]. Independent studies have shown that this mutation markedly reduces TS expression *in vitro*, to a level lower than that of the 2RG allele [8,11]. Whether rs183205964 is associated with reduced TS activity in patients, and whether this results in greater sensitivity to fluoropyrimidines, has not been investigated. We hypothesized that patients carrying the putative low TS expression 2RC risk allele are at higher risk of fluoropyrimidine-associated toxicity upon treatment with fluoropyrimidines, and conducted a pharmacogenetic study to determine the clinical relevance of this variant.

MATERIAL AND METHODS
Patients and Study Design

Sixteen-hundred thirty-one patients who were previously enrolled in a prospective multicenter study of *DPYD**2A genotype-guided dosing of fluoropyrimidines (NCT00838370) were considered for genotyping of *TYMS* in the context of this pharmacogenetic study (Figure 1). The study population consisted of patients with cancer intended to undergo treatment with fluoropyrimidine-based anticancer therapy, either as single agent or in combination with other chemotherapy or radiotherapy, according to existing standard of care. Prior chemotherapy and radiotherapy were allowed. The primary endpoint of NCT00838370 was toxicity, which was recorded during each treatment cycle according to CTC-AE v3.0. Hematology (including neutrophils, leukocytes, and platelets) was monitored according to local protocol (prior to each cycle in most cases). Information on hospitalizations for toxicity and reasons for ending treatment were also collected for the purpose of the study. In study NCT00838370, patients were genotyped for *DPYD**2A prior to treatment using germline DNA. Heterozygous and homozygous *DPYD**2A variant allele carriers were treated with an initially reduced dose of the fluoropyrimidine during the first two cycles of treatment, followed by further dose individualization based on tolerability. Eighteen patients carrying the *DPYD**2A variant were excluded from the current analysis. No intervention was applied in the remaining 1613 patients who proved to be wild type for *DPYD**2A; they were treated according to standard of care treatment regimens (Supplementary Table 1). These 1613 patients were considered eligible for inclusion in this analysis. All patients provided written informed consent prior to study procedures.

The association between rs183205964 and severe fluoropyrimidine-induced toxicity was investigated by comparing the risk of severe treatment-related toxicity between patients carrying 2RC risk-associated genotypes and patients not carrying risk-associated genotypes. Based on the available *in vitro* data on the relationship between *TYMS* alleles and putative low TS expression phenotypes, the following genotypes were considered risk-associated genotypes: 3RC/2RC, 2RG/2RC, and 2RC/2RC. Patients carrying the 3RG/2RC genotype were not included in the risk group, as they were expected to have higher TS activity in view of the 3RG allele [12,13]. The risk of severe treatment-related toxicity in the group of patients with risk-associated genotypes was compared with that of the rest of the population in univariable and multivariable analysis. In a separate, exploratory, analysis the association between the 3RG/2RC genotype and risk of severe toxicity was investigated.
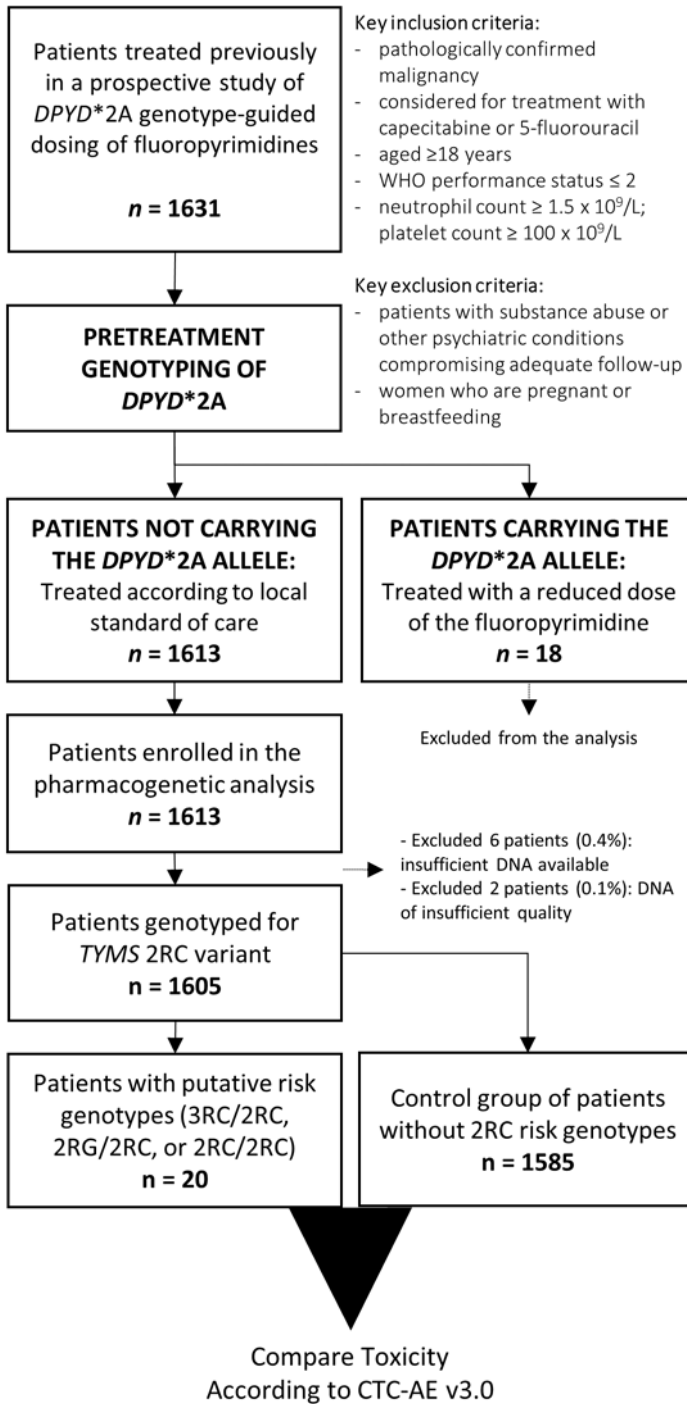
Figure 1. Flow chart of the study. Abbreviations: *TYMS* = thymidylate synthase; CTC-AE = Common Toxicity Criteria for Adverse Events (version 3.0)

Genotyping of *TYMS* and *DPYD*, thymidylate synthase activity assays, and *TYMS* gene expression

A synopsis is provided here (details in Appendix). All patients were screened for the variable number of 28-bp tandem repeats (VNTR) in the 5'-UTR of *TYMS* (rs34743033), the G>C SNP in the second repeat of the 3R allele (rs2853542), and the G>C SNP in the first repeat of the 2R allele (rs183205964) using PCR. To investigate the effect of the 2RC risk-associated allele on TS enzyme activity, we determined TS activity in peripheral blood mononuclear cells (PBMCs) of a patient with a homozygous 2RC/2RC genotype, a healthy control with a heterozygous (3RC/2RC) genotype, and 18 healthy controls with non-2RC genotypes, using a fully validated radioassay [14]. In addition to TS activity, relative *TYMS* mRNA expression was determined in PBMCs of the patient with the homozygous 2RC/2RC genotype, a healthy control with a 3RC/2RC genotype, and 19 healthy controls (Jacobs *et al.*, *submitted*).

The prevalence of four *DPYD* variants known to be associated with fluoropyrimidine-induced toxicity – 2846A>T, 1679T>G, 1236G>A, and 1601G>A – was compared between groups of patients with risk-associated genotypes and controls in order to exclude DPD deficiency as a possible confounding factor.

Determination of PBMC dihydropyrimidine dehydrogenase enzyme activity and the *CYP3A4*22* allele

To exclude other possible causes of intolerance to fluoropyrimidines in the single patient carrying the 2RC/2RC genotype, DPD activity in PBMCs of this patient was determined, as described previously [15]. In addition, since the patient was treated with the combination of capecitabine and docetaxel, we investigated potential CYP3A4 deficiency – which could lead to increased exposure to docetaxel – in the same patient, by determining the most clinically relevant dysfunctional *CYP3A4* allele, *CYP3A4*22*, using a commercial RT-PCR assay (Applied Biosystems).

Statistical considerations and data analysis

Demographic and clinical characteristics of patients with risk-associated genotypes and the control group were described and differences were tested using the Student's *t*-test, the Mann-Whitney U test, Fisher's exact test, or the Chi-square test, where appropriate. The 2RC risk allele was tested for deviation from Hardy-Weinberg equilibrium using the exact test [16]. To test associations with toxicity, we considered the maximum grade toxicity experienced during the first cycle. An analysis of the entire treatment duration was regarded not informative in view of the fact that there was a wide variety of treatment durations in this heterogeneous daily-care patient population. Global (any) toxicity and individual types of toxicity – gastrointestinal, hematological, and hand-foot syndrome (HFS) – were dichotomized as absent to moderate (grade 0, 1, or 2) versus severe (grade 3, 4, or 5). Associations between risk-associated genotypes and toxicity or toxicity-related outcomes, which included treatment-related hospitalization and treatment

discontinuation due to adverse events, were tested in univariable and multivariable logistic regression models, adjusting for factors known to be associated with risk of toxicity in patients treated with fluoropyrimidines: age (continuous), gender (female or male), and treatment regimen (5-FU-based, capecitabine monotherapy, capecitabine plus platinum, capecitabine plus taxane, capecitabine-based triplet combination, capecitabine plus other drug, or capecitabine plus radiotherapy). The planned starting dose of capecitabine was highly collinear with type of regimen and was not predictive of toxicity after adjustment for treatment regimen; it was therefore not included in the models. Also tumor type, disease stage, or previous treatment were not predictive of toxicity and not included as covariates.

In view of the low frequency of the homozygous variant genotype, we tested for an association between the 2RC risk allele and severe toxicity using a dominant model (wild type vs. heterozygous or homozygous). A log-additive model was explored as well. Because the 2RC allele occurs within the VNTR, the effect of the VNTR polymorphism on risk of toxicity was also investigated, assuming a log-additive model for the VNTR, with correction for clinical covariates.

Associations between risk-associated genotypes and severe toxicity or toxicity-related outcomes were reported as an odds ratio (OR) and a 95% confidence interval (CI), with corresponding *p* values. For all statistical tests the threshold for significance was set at $p < 0.05$. All statistical analyses were performed in R v3.1.0.

RESULTS

Patients and *TYMS* genotyping

As shown in Figure 1, 1605 out of 1613 patients (99.5%) were genotyped for rs183205964. Among 1605 patients, 28 patients had the 2RC variant allele (1.7%). Genotypes with the 2RC allele containing in total ≤1 intact USF binding sites were considered risk-associated genotypes, as a reduced activity of *TYMS* is expected for these genotypes compared to genotypes with ≥2 USF binding sites [8]. There were 20 patients carrying a putative risk-associated genotype (2RG/2RC, *n* = 13; 3RC/2RC, *n* = 6; 2RC/2RC, *n* = 1). Eight patients carried the presumed non-risk 2RC genotype 3RG/2RC (containing 2 USF binding sites). The allele frequency of the 2RC allele in the studied population was 0.009, and there was no statistically significant deviation from Hardy-Weinberg equilibrium (*p* = 0.120). The characteristics of the patients with risk-associated genotypes as well as the rest of the population are summarized in Table 1, the treatment regimens that patients received are summarized in Supplementary Table 1. There were no significant differences between groups with regard to patient characteristics.

Association of the 2RC allele with fluoropyrimidine-associated toxicity

The frequencies of toxicity and toxicity-related outcomes occurring during the first cycle are summarized in Table 2 (frequencies by treatment regimen are available in

6

Table 1. Patient characteristics according to *TYMS* 2RC genotype.

Characteristic	Control (n = 1585)	Risk-associated genotypes combined (n = 20)	Individual risk-associated genotypes[a]			p value[b]
			3RC/2RC (n = 6)	2RG/2RC (n = 13)	2RC/2RC (n = 1)	
Age, median (range)	61 (21-89)	63 (49-78)	68 (51-78)	63 (49-78)	50	0.398
Sex						0.258
Male	712 (55%)	6 (30%)	0 (0%)	6 (46%)	0 (0%)	
Female	873 (45%)	14 (70%)	6 (100%)	7 (54%)	1 (100%)	
Tumor type						0.115
Colorectal cancer (locally adv.)	524 (33%)	11 (55%)	4 (67%)	7 (54%)	0 (0%)	
Colorectal cancer (metastatic)	319 (20%)	0 (0%)	0 (0%)	0 (0%)	0 (0%)	
Gastric cancer (locally adv.)	112 (7%)	1 (5%)	0 (0%)	1 (8%)	0 (0%)	
Gastric cancer (metastatic)	114 (7%)	0 (0%)	0 (0%)	0 (0%)	0 (0%)	
Breast cancer (locally adv.)	117 (7%)	2 (10%)	0 (0%)	1 (8%)	1 (100%)	
Breast cancer (metastatic)	245 (15%)	5 (25%)	2 (33%)	3 (23%)	0 (0%)	
Other (e.g. HNSCC, SCCAC)	154 (10%)	1 (5%)	0 (0%)	1 (8%)	0 (0%)	
Treatment						0.125
Capecitabine monotherapy	417 (26%)	7 (35%)	2 (33%)	5 (38%)	0 (0%)	
Capecitabine plus radiotherapy	426 (27%)	10 (50%)	3 (50%)	7 (54%)	0 (0%)	
Capecitabine plus taxane	63 (4%)	1 (5%)	0 (0%)	0 (0%)	1 (100%)	
Capecitabine plus platinum	377 (24%)	1 (5%)	1 (17%)	0 (0%)	0 (0%)	
Capecitabine triplet	112 (7%)	1 (5%)	0 (0%)	1 (8%)	0 (0%)	
Capecitabine plus other	22 (1%)	0 (0%)	0 (0%)	0 (0%)	0 (0%)	
5-FU-based	168 (11%)	0 (0%)	0 (0%)	0 (0%)	0 (0%)	
Daily dose of capecitabine in mg/m², median (range)	2000 (500-2500)	1650 (1650-2500)	2000 (1500-2500)	1650 (1600-2500)	1650	0.102

6

Table 1. (continued)

Characteristic	Control (n = 1585)	Risk-associated genotypes combined (n = 20)	Individual risk-associated genotypes [a]			p value [b]
			3RC/2RC (n = 6)	2RG/2RC (n = 13)	2RC/2RC (n = 1)	
Origin						
Caucasian	1519 (96%)	20 (100%)	6 (100%)	13 (100%)	1 (100%)	0.972
Other	86 (4%)	0 (0%)	0 (0%)	0 (0%)	0 (0%)	
Previous chemotherapy						
No	1230 (78%)	16 (80%)	6 (100%)	9 (69%)	1 (100%)	0.936
Yes	355 (22%)	4 (20%)	0 (0%)	4 (31%)	0 (0%)	
DPYD SNPs [c]						
No	1418 (90%)	19 (90%)	5 (83%)	12 (92%)	1 (100%)	1.000
Yes	163 (10%)	2 (10%)	1 (17%)	1 (8%)	0 (0%)	

Abbreviations: *TYMS* = thymidylate synthase (gene); HNSCC = head & neck squamous cell carcinoma; SCCAC = squamous cell carcinoma of the anal canal; 5-FU = 5-fluorouracil; *DPYD* = dihydropyrimidine dehydrogenase (gene); SNPs = single nucleotide polymorphisms

[a] The number of intact upstream stimulating factor (USF) binding sites for the different risk-associated genotypes was 1 for 3RC/2RC, 1 for 2RG/2RC, and 0 for 2RC/2RC.

[b] Student's t-test (age), Mann-Whitney U test (dose of capecitabine), Fisher's exact test (sex, origin, previous chemotherapy, *DPYD* SNPs), or Chi-square test (tumor type, treatment)

[c] Two patients in the risk group had a mutation in *DPYD*: one had 1601G>A (2RG/2RC) and one had 1236G>A (3RC/2RC). Of these patients, the former had no toxicity (grade 0) and the latter had grade 3 toxicity as maximum toxicity.

Supplementary Table 2). The association between risk-associated genotypes and severe fluoropyrimidine-induced toxicity during the first cycle was investigated in univariable and in multivariable logistic regression analyses, assuming a dominant model, the results of which are shown in Table 3. In univariable analysis, risk of global severe toxicity was significantly higher in patients with risk-associated genotypes than in the control group (OR 3.0, 95%CI 1.06-8.22, p = 0.039). There was a trend towards increased incidence of early gastrointestinal toxicity (OR 3.4, 95%CI 0.98-11.9, p = 0.054). Also hematological toxicity appeared to be more frequent, but not significantly (OR 3.4, p = 0.259). Of the patients with 2RC risk-associated genotypes, none had early severe HFS, compared to 1% of the patients in the control group. Treatment-related hospitalization and treatment discontinuation due to adverse events were both significantly more frequent in patients with risk-associated genotypes in univariable analysis. Also after adjustment for age, gender, and treatment regimen, risk of global severe toxicity and treatment-related hospitalization remained significantly increased in patients with risk-associated genotypes.

Table 2. Maximum toxicity grade during the first cycle of treatment according to *TYMS* 2RC genotype.

Toxicity	Control (n = 1585)	Risk-associated genotypes combined (n = 20)	Individual risk-associated genotypes		
			3RC/2RC (n = 6)	2RG/2RC (n = 13)	2RC/2RC (n = 1)
Global toxicity					
Grade 0-2	1424 (90%)	15 (75%)	5 (83%)	10 (77%)	0 (0%)
Grade 3-5	161 (10%)	5 (25%)	1 (17%)	3 (23%)	1 (100%)
Gastrointestinal toxicity					
Grade 0-2	1507 (95%)	17 (85%)	5 (83%)	11 (85%)	1 (100%)
Grade 3-5	78 (5%)	3 (15%)	1 (17%)	2 (15%)	0 (0%)
Hematological toxicity					
Grade 0-2	1521 (96%)	18 (90%)	6 (100%)	12 (92%)	0 (0%)
Grade 3-5	64 (4%)	2 (10%)	0 (0%)	1 (8%)	1 (100%)
Hand-foot syndrome					
Grade 0-2	1564 (99%)	20 (100%)	6 (100%)	13 (100%)	1 (100%)
Grade 3-5	21 (1%)	0 (0%)	0 (0%)	0 (0%)	0 (0%)
Hospitalization for toxicity					
No	1488 (94%)	16 (80%)	5 (83%)	11 (85%)	0 (0%)
Yes	97 (6%)	4 (20%)	1 (17%)	2 (15%)	1 (100%)
Treatment discontinuation due to toxicity					
No	1488 (94%)	16 (80%)	4 (67%)	11 (85%)	1 (100%)
Yes	97 (6%)	4 (20%)	2 (33%)	2 (15%)	0 (0%)

Table 3. Univariable and multivariable analysis of risk for severe toxicity for patients carrying *TYMS* 2RC risk-associated genotypes versus non-2RC genotypes.

Outcome	OR	95% CI	p value
Univariable			
Global severe toxicity	3.0	1.06 to 8.22	0.039
Gastrointestinal severe toxicity	3.4	0.98 to 11.9	0.054
Hematological severe toxicity	3.4	0.41 to 27.8	0.259
Hospitalization for toxicity	3.8	1.26 to 11.7	0.018
Treatment discontinuation	3.6	1.17 to 10.8	0.025
Multivariable [a]			
Global severe toxicity	3.0	1.04 to 8.93	0.043
Gastrointestinal severe toxicity	2.7	0.73 to 10.0	0.136
Hematological severe toxicity	4.3	0.81 to 23.2	0.088
Hospitalization for toxicity	3.8	1.19 to 11.9	0.024
Treatment discontinuation	2.9	0.92 to 9.21	0.070

Abbreviations: OR = odds ratio; CI = confidence interval.
[a] The following covariates were included in multivariable analysis: age, gender, and treatment with concomitant chemotherapy or radiotherapy (effect estimates of the covariates are listed in Supplementary Table 3).

6

When the association between the 2RC allele and treatment-related toxicity was evaluated in multivariable analysis using a log-additive model, similar results were obtained for the association with global toxicity (OR 3.0, 95%CI 1.07-8.42, *p* = 0.037), gastrointestinal toxicity (OR 2.2, 95%CI 0.65-7.16, *p* = 0.208), hematological toxicity (OR 4.0, 95%CI 0.90-18.0, *p* = 0.068), treatment-related hospitalization (OR 3.7, 95%CI 1.29-10.8, *p* = 0.015), and treatment discontinuation due to adverse events (OR 2.2, 95%CI 0.73-6.52, *p* = 0.165).

We also investigated associations between 2RC and severe toxicity when considering the entire treatment duration. This analysis showed that risk of severe toxicity during the overall treatment duration was increased in patients with 2RC risk-associated genotypes, but not significantly (OR 1.5, 95%CI 0.56-4.09, *p* = 0.408), possibly as a result of the wide range of treatment durations.

As the 2RC allele occurs within the *TYMS* VNTR, we also investigated the effect of the VNTR on risk of toxicity. This analysis showed that there was no association between the VNTR and treatment-related toxicity (OR 1.1 for each additional 2R allele, 95%CI 0.85-1.36, *p* = 0.545).

The incidence of early severe toxicity in patients with the 3RG/2RC genotype was not significantly increased compared to the rest of the population, as the OR for global severe toxicity was 1.2 (95% CI 0.10-10.1, *p* = 0.841) in univariable analysis and 0.8 (95% CI 0.17-13.9, *p* = 0.871) in multivariable analysis. There were also no differences in risk of experiencing the individual types of toxicity (not shown).

Clinical course of treatment of the patient with the 2RC/2RC genotype

Since only one patient with a homozygous variant genotype was identified, this patient will be described in detail. She was a female patient, aged 54, with a triple negative $T_1N_0M_0$ ductal carcinoma, who received surgery, followed by radiotherapy up to 64.4 Gy, and was subsequently planned for adjuvant chemotherapy with capecitabine 825 mg/m^2 b.i.d. on days 1-14, combined with 75 mg/m^2 infusional docetaxel (day 1) for six cycles every three weeks (in the context of a clinical study [17]).

Nine days after starting treatment, she was hospitalized with high fever (40.5°C), severe neutropenia (0.4 x 10^9/L; grade IV) and leukocytopenia (1.9 x 10^9/L; grade III). Capecitabine was interrupted. The focus of the fever was thought to be an infection of the breast, and she was released on oral antibiotics two days later. Capecitabine was withheld for five weeks until wound healing had completed, and treatment was then restarted, at the same dose of capecitabine and docetaxel. On day 14 of cycle 2, she developed severe HFS (grade III); no neutropenia was noted. The dose of capecitabine was reduced to 75% in cycle 3, which was started one week later when HFS had subsided. The dose of docetaxel was left unchanged. On day 4 of cycle 3, she again developed HFS, grade III, and capecitabine was again interrupted. On day 8 of cycle 3, despite interruption of capecitabine, the patient was hospitalized with febrile neutropenia (<0.1 x 10^9/L), HFS grade III, and diarrhea grade III. The patient was hospitalized for three days, and then continued to have HFS, which persisted as grade II until fourteen days later, and then gradually faded away in one week. In view of the intolerable side-effects, it was decided to permanently discontinue treatment with capecitabine and docetaxel. An alternative treatment of six cycles of adriamycin (60 mg/m^2) and cyclophosphamide (600 mg/m^2) was initiated, which was well-tolerated. The patient is currently alive and disease-free, but continues to suffer from cognitive problems (related to information processing and working memory) ever since receiving chemotherapy with capecitabine and docetaxel.

Since only one patient was homozygous for 2RC, we could not perform multivariable analysis to evaluate risk of severe toxicity. However, the patient experienced grade IV toxicity, which was very rare in the overall population (2.2%). The fact that the single patient with a homozygous 2RC genotype had grade IV toxicity, therefore, resulted in a statistically significant higher incidence of global grade ≥IV toxicity for the 2RC/2RC genotype compared to patients without this genotype (p = 0.022, Fisher's exact test).

DPD activity was found to be normal to high in this patient: 12.4 nmol/mg*h (reference range: 6-14 nmol/mg/h). Genotyping of *CYP3A4*22* showed that the mutation was not present.

Association of the 2RC allele with thymidylate synthase activity and *TYMS* gene expression in PBMCs

TS activity in the patient with the 2RC/2RC genotype was 0.066 nmol/mg/hour, which is close to the median activity of 0.072 nmol/mg/hour observed in controls (range: 0.031-

0.134 nmol/mg/hour) and therefore not reduced (Supplementary Figure 2A). TS activity in PBMCs of the subject carrying the 3RC/2RC genotype was low but within the normal range (0.036 nmol/mg/hour). Likewise, *TYMS* mRNA expression levels in the 2RC variant allele carriers were very close to the median observed in controls with non-2RC genotypes (Supplementary Figure 2B).

DISCUSSION

This is the first analysis investigating the clinical relevance of the G>C SNP at the 12th nucleotide of the first 28-bp tandem repeat of the 2R allele of in the 5'-UTR *TYMS*, which has been reported to result in significant reductions in *TYMS* gene expression *in vitro*, as a result of abolishing a USF-1 binding site [8,11]. In total 28/1605 patients carried the risk allele, and therefore the observed allele frequency of 0.009 was lower than previously reported in Caucasians in smaller studies (0.015-0.042) [9,10]. The higher frequency compared to other studies could be explained by sample-to-sample variation, and also publication bias may have contributed to the higher allele frequencies described in initial reports. True differences in the frequency of 2RC depending on ethnicity are also possible, as has been demonstrated for the *TYMS* VNTR polymorphism [18]. Our analysis showed that early severe fluoropyrimidine-associated toxicity and toxicity-related hospitalizations were more frequent among patients carrying 2RC risk-associated genotypes – 3RC/2RC, 2RG/2RC, or 2RC/2RC – indicating that these genotypes are likely to be associated with a higher risk of severe toxicity.

We identified one patient with a homozygous 2RC/2RC variant genotype. This patient experienced severe, recurrent, fluoropyrimidine-associated toxicity while being treated with a relatively low dose of capecitabine in combination with docetaxel. We were able to largely exclude other possible causes of intolerance to treatment in this patient. DPD enzyme activity was normal to high, and the disruptive *CYP3A4*22* allele was not found, making it less likely that either DPD deficiency or CYP3A4 deficiency (which could increase exposure to docetaxel) played a role in the observed toxicities. Considering the spectrum of toxicities observed (neutropenia, diarrhea, and HFS), it is not likely that they were related to docetaxel, and no other toxicities that raised suspicion towards docetaxel were present (*e.g.* peripheral neuropathy, nail toxicity, or dysgeusia).

In contrast to what we expected based on *in vitro* studies, both PBMC TS activity and *TYMS* expression in the patient with the 2RC/2RC genotype and the control subject with the 3RC/2RC genotype were not found to be reduced. This was rather surprising in view of the observed course of treatment, and the statistical association between 2RC and severe toxicity. There are several possible explanations as to why PBMC TS activity was not reduced. Mandola *et al.*, who first studied the effect of USF-1 binding sites in *TYMS* on gene transcription, noticed that in the absence of USF-1 there was almost no difference in gene expression between 2RG and 2RC [8]. Only upon stimulation with USF-1 differences in gene expression became apparent. It could be speculated that under normal conditions in mature PBMCs, the expression of TS is not so much dependent on

6

stimulation by USF-1 (although PBMCs, as do almost all tissues, express USF-1 [19]). It could be that only under conditions where increased TS expression is required, such as during cell growth or upon challenge with a dose of fluoropyrimidines, the contribution of USF-1 becomes important. There are no data to support this hypothesis, but it has been shown that the relative contribution of USF-1 in modulating gene transcription is cell type specific and is highly context-dependent [20,21]. For USF-2, a transcription factor similar to USF-1, it has been shown that its expression is repressed in quiescent mast cells, and only becomes active during cell growth [22].

Our results, combined with what is known from *in vitro* studies, support the hypothesis that rs183205964 induces a clinically relevant change in the cell's sensitivity to the effects of fluoropyrimidines. Risk of early severe toxicity was increased in the overall group of patients with risk-associated genotypes, which consisted of 19 patients who carried the 2RC allele in heterozygous form, and one patient with the 2RC/2RC genotype, suggesting that both patients with a heterozygous or a homozygous 2RC genotype are at increased risk of toxicity. The group consisted, however, of patients with different heterozygous genotypes, 3RC/2RC and 2RG/2RC. It is hypothetically possible that the extent by which expression of TS is affected by these genotypes is not equal, but we did not have sufficient statistical power to investigate these potential differences. Also based on the available *in vitro* data we cannot draw a firm conclusion as to whether there would be a difference in risk between these groups.

We defined, *a priori*, the patients with the 3RG/2RC genotype as not at risk, in view of the presence of the 3RG allele [12,13]. We identified eight such patients, and indeed found no indications for an increased risk of toxicity in these patients (OR 1.2 compared to the control group). We can, however, not exclude the possibility that we missed a potential association due to the small number of patients that could be studied.

If reduced compensatory TS expression is indeed a consequence of the 2RC variant, then patients carrying 2RC risk-associated genotypes should not be treated with full-dose fluoropyrimidines but should receive either an alternative treatment or treatment with a reduced dose of fluoropyrimidines. It remains to be established what degree of dose reduction would be safe in these patients. Dose-adaptation in patients with DPD deficiency is relatively straightforward, since reductions in DPD activity are associated with predictable changes in 5-FU clearance. For TS, however, predicting the safe and efficacious dose in case of reduced TS activity is less straightforward. First of all, it is unknown to what degree compensatory TS expression is reduced. Even if this could be measured accurately, then we do not know what the relationship is between TS expression and pharmacodynamic effect. The safe dose would have to be determined by careful dose-escalation and pharmacodynamic measurements during exposure to 5-FU. A second important issue is whether reduced-dose treatment in patients with reduced TS activity results in sufficient antitumor effect, as tumor TS activity might be higher than in normal tissue and less dependent on the germ line genotype, as shown for instance in colorectal cancer [23]. Considering these facts, and if our findings are confirmed in future studies, it would be logical to consider the presence of the 2RC allele an indication

for treatment with a reduced dose or, if possible, with a non-fluoropyrimidine-based treatment regimen.

Several potential limitations of our study need to be highlighted. Although we analyzed a cohort of patients treated in a prospective study, our study was retrospective in nature, which potentially introduced bias. However, the fact that toxicity data were collected systematically for all patients and the fact that DNA was collected from nearly all participating patients (>99.5%), reduces the chances of information and selection bias being introduced. Secondly, patients were treated with a variety of treatment regimens and were of different ages and sex. It could be that these factors interact with the risk-associated genotypes, and it is possible that only subsets of patients are at increased risk (*e.g.* patients treated with a certain regimen). This might have limited our ability to accurately measure the risk associated with the 2RC allele. However, the fact that this cohort represents a daily-care cancer population is also a potential strength of the study, as it shows that even in a heterogeneous population an effect of the variant allele could be detected. Risk of severe toxicity was not found to be increased when considering the entire treatment duration, which was expected in view of strong heterogeneity in duration of treatment. Future studies investigating more homogeneous populations should focus on longer treatment durations to further establish the clinical relevance of the 2RC allele as a predictor of fluoropyrimidine-associated toxicity. Lastly, a crucial aspect in determining the clinical validity of pharmacogenetic variants is that findings be replicated. Therefore, our findings need to be replicated in a second, independent population of patients treated with fluoropyrimidines, in order to confirm the clinical validity of rs183205964.

The role of *TYMS* genotypes as predictors of treatment-related toxicity in patients treated with fluoropyrimidines has only recently started to be recognized. Recently, Rosmarin *et al.* showed that rs2612091 in *ENOSF1* (enolase superfamily member 1), a gene adjacent to *TYMS* and known to regulate TS activity [24,25], might explain previously observed associations between the *TYMS* VNTR polymorphism and fluoropyrimidine-associated toxicity [26]. *ENOSF1* rs2612091 genotyping should therefore be considered in future studies, as it might be an independent predictor in addition to the 2RC allele and *TYMS* VNTR, and may further improve the predictive value to identify patients at risk of toxicity.

We showed that patients carrying 2RC risk-associated genotypes were at increased risk of early fluoropyrimidine-associated toxicity. A patient with the not previously described 2RC/2RC genotype suffered recurrent severe fluoropyrimidine-associated toxicity while being treated with capecitabine 825 mg/m^2 twice daily. In contrast to what has been shown in *in vitro* studies, TS activity and *TYMS* expression were not found to be reduced in this patient. More research on the functional consequences of rs183205964 is now needed. While the associations found in this study require confirmation in an independent cohort, caution should be taken in administering fluoropyrimidines to patients who are known to carry the rs183205964 variant allele, particularly if present in homozygous form.

ACKNOWLEDGEMENTS

6

REFERENCES

1. Caudle KE, Thorn CF, Klein TE, Swen JJ, McLeod HL, Diasio RB, et al. Clinical Pharmacogenetics Implementation Consortium guidelines for dihydropyrimidine dehydrogenase genotype and fluoropyrimidine dosing. Clin Pharmacol Ther 2013;94:640–5.

2. Deenen MJ, Meulendijks D, Cats A, Sechterberger MK, Severens JL, Boot H, et al. Upfront genotyping of DPYD*2A to individualize fluoropyrimidine therapy: a safety and cost analysis. J Clin Oncol 2016;34:227–34.

3. Horie N, Aiba H, Oguro K, Hojo H, Takeishi K. Functional analysis and DNA polymorphism of the tandemly repeated sequences in the 5'-terminal regulatory region of the human gene for thymidylate synthase. Cell Struct Funct 1995;20:191–7.

4. Kawakami K, Omura K, Kanehira E, Watanabe Y. Polymorphic tandem repeats in the thymidylate synthase gene is associated with its protein expression in human gastrointestinal cancers. Anticancer Res 1999;19:3249–52.

5. Kawakami K, Salonga D, Park JM, Danenberg KD, Uetake H, Brabender J, et al. Different lengths of a polymorphic repeat sequence in the thymidylate synthase gene affect translational efficiency but not its gene expression. Clin Cancer Res 2001;7:4096–101.

6. Pullarkat ST, Stoehlmacher J, Ghaderi V, Xiong YP, Ingles SA, Sherrod A, et al. Thymidylate synthase gene polymorphism determines response and toxicity of 5-FU chemotherapy. Pharmacogenomics J 2001;1:65–70.

7. Rosmarin D, Palles C, Church D, Domingo E, Jones A, Johnstone E, et al. Genetic markers of toxicity from capecitabine and other fluorouracil-based regimens: Investigation in the QUASAR2 study, systematic review, and meta-analysis. J Clin Oncol 2014;32:1031–9.

8. Mandola M V, Stoehlmacher J, Muller-Weeks S, Cesarone G, Yu MC, Lenz HJ, et al. A novel single nucleotide polymorphism within the 5' tandem repeat polymorphism of the thymidylate synthase gene abolishes USF-1 binding and alters transcriptional activity. Cancer Res 2003;63:2898-904.

9. Lincz LF, Scorgie FE, Garg MB, Ackland SP. Identification of a novel single nucleotide polymorphism in the first tandem repeat sequence of the thymidylate synthase 2R allele. Int J Cancer 2007;120:1930–4.

10. Gusella M, Bolzonella C, Crepaldi G, Ferrazzi E, Padrini R. A novel G/C single-nucleotide polymorphism in the double 28-bp repeat thymidylate synthase allele. Pharmacogenomics J 2006;6:421–4.

11. de Bock CE, Garg MB, Scott N, Sakoff JA, Scorgie FE, Ackland SP, et al. Association of thymidylate synthase enhancer region polymorphisms with thymidylate synthase activity in vivo. Pharmacogenomics J 2011;11:307–14.

12. Marcuello E, Altés A, del Rio E, César A, Menoyo A, Baiget M. Single nucleotide polymorphism in the 5' tandem repeat sequences ofthymidylate synthase gene predicts for response to fluorouracil-based chemotherapy in advanced colorectal cancer patients. Int J Cancer 2004;112:733–7.

13. Morganti M, Ciantelli M, Giglioni B, Putignano AL, Nobili S, Papi L, et al. Relationships between promoter polymorphisms in the thymidylate synthase gene and mRNA levels in colorectal cancers. Eur J Cancer 2005;41:2176–83.

14. Pluim D, Schilders KAA, Jacobs BAW, Vaartjes D, Beijnen JH, Schellens JHM. Pharmacodynamic assay of thymidylate synthase activity in peripheral blood mononuclear cells. Anal Bioanal Chem 2013;405:2495–503.

15. Pluim D, Jacobs BAW, Deenen MJ, Ruijter AE, Van Geel RMJM, Burylo AM, et al. Improved pharmacodynamic assay for dihydropyrimidine dehydrogenase activity in peripheral blood mononuclear cells. Bioanalysis 2015;7:519–29.

16. Wigginton JE, Cutler DJ, Abecasis GR. A note on exact tests of Hardy-Weinberg equilibrium. Am J Hum Genet 2005;76:887–93.

17. Rutgers E, Piccart-Gebhart MJ, Bogaerts J, Delaloge S, 't Veer LV, Rubio IT, et al. The EORTC 10041/BIG 03-04 MINDACT trial is feasible: results of the pilot phase. Eur J Cancer 2011;47:2742–9.

6

18. Marsh S, Ameyaw MM, Githang'a J, Indalo A, Ofori-Adjei D, McLeod HL. Novel thymidylate synthase enhancer region alleles in African populations. Hum Mutat 2000;16:528.

19. The Protein Atlas, accessed at 12-21-2014. http://www.proteinatlas.org/.

20. Corre S, Galibert M-D. Upstream stimulating factors: highly versatile stress-responsive transcription factors. Pigment Cell Res 2005;18:337–48.

21. Sirito M, Lin Q, Maity T, Sawadogo M. Ubiquitous expression of the 43- and 44-kDa forms of transcription factor USF in mammalian cells. Nucleic Acids Res 1994;22:427–33.

22. Zhang ZC, Nechushtan H, Jacob-Hirsch J, Avni D, Meyuhas O, Razin E. Growth-dependent and PKC-mediated translational regulation of the upstream stimulating factor-2 (USF2) mRNA in hematopoietic cells. Oncogene 1998;16:763–9.

23. Mauritz R, Giovannetti E, Beumer IJ, Smid K, Van Groeningen CJ, Pinedo HM, et al. Polymorphisms in the enhancer region of the thymidylate synthase gene are associated with thymidylate synthase levels in normal tissues but not in malignant tissues of patients with colorectal cancer. Clin Colorectal Cancer 2009;8:146–54.

24. Dolnick BJ. The rTS signaling pathway as a target for drug development. Clin Colorectal Cancer 2005;5:57–60.

25. Chu E, Koeller DM, Casey JL, Drake JC, Chabner BA, Elwood PC, et al. Autoregulation of human thymidylate synthase messenger RNA translation by thymidylate synthase. Proc Natl Acad Sci U S A 1991;88:8977–81.

26. Rosmarin D, Palles C, Pagnamenta A, Kaur K, Pita G, Martin M, et al. A candidate gene study of capecitabine-related toxicity in colorectal cancer identifies new toxicity variants at DPYD and a putative role for ENOSF1 rather than TYMS. Gut 2014:1–10.

6

APPENDIX

Supplementary Methods

Genotyping of *TYMS* variants

Genomic DNA was isolated from peripheral blood cells using MagNA Pure LC (Roche Diagnostics, Almere, the Netherlands). All patients were screened for the variable number of 28-bp tandem repeats (VNTR) in the 5'-UTR of *TYMS* (rs34743033), the G>C SNP in the second repeat of the 3R allele (rs2853542), and the G>C SNP in the first repeat of the 2R allele (rs183205964) using PCR (primer sequences and PCR conditions are available upon request). After PCR, the VNTR was visualized on a 3% agarose gel with TAE buffer and ethidium bromide. In addition, a separate sample of the same PCR product was incubated overnight with HaeIII (Fisher Scientific, Landsmeer, the Netherlands), and subsequently visualized on 3% agarose gel with TAE buffer and ethidium bromide to determine the presence of the G>C SNP. Samples with a pattern representative of the G>C SNP in the first repeat of 2R were Sanger sequenced to confirm the presence of rs183205964. In each run two sequenced positive controls and two negative controls were included.

Determination of thymidylate synthase enzyme activity in peripheral blood mononuclear cells

To investigate the effect of the 2RC risk-associated allele on TS enzyme activity, we determined TS activity in peripheral blood mononuclear cells (PBMCs) of a patient with a homozygous 2RC/2RC genotype, a healthy control with a heterozygous (3RC/2RC) genotype, and 18 healthy controls with non-2RC genotypes, using a fully validated radioassay [1]. The healthy controls participated in a study investigating the circadian rhythm of TS (Jacobs *et al.*, *submitted*). Blood was sampled from the patient with the 2RC/2RC genotype several years after last treatment with chemotherapy. Peripheral blood was drawn into two 10 mL heparinized blood collection tubes. PBMCs were then isolated using Ficoll gradient centrifugation, and stored as dry cell pellets at -80°C until further processing. TS activity was measured as described previously [1]. The corrected protein concentration in the PBMC lysates was calculated by subtracting the contaminating hemoglobin concentration from the total protein concentration [2]. TS reactions were performed in triplicate using 290 µg of PBMC lysate protein as input. TS activity was expressed relative to the protein concentration. A quality control sample, containing PBMC lysate from a tumor cell line, was included in each analytical run to monitor assay performance.

Determination of *TYMS* mRNA expression

In addition to TS activity, relative *TYMS* mRNA expression was determined in PBMCs of the patient with the homozygous 2RC/2RC genotype, a healthy control with a 3RC/2RC genotype, and 19 healthy controls (Jacobs *et al.*, *submitted*). PBMCs were isolated from 8 mL of whole blood, lysed in RNA-Bee (Bio-Connect, Huissen, the Netherlands),

and stored at -80°C until total RNA extraction. The procedure for RNA isolation was performed according to the RNA-Bee manufacturer's instructions. cDNA was synthesized in 20 μL using 350 ng of isolated total mRNA, 3 μg random primers (Invitrogen, Leek, the Netherlands) and 200U SuperScript II Reverse Transcriptase (Invitrogen), using the following PCR protocol: 25°C for 10 min, 42°C for 50 min, and 70°C for 15 min. Quantitation of cDNA was performed using SYBR® Green PCR Master Mix (Applied Biosystems, Foster City, CA, USA) on a 7500 Fast Real-Time PCR system (Applied Biosystems). Gene expression of *TYMS* relative to peptidylprolyl isomerase B (*PPIB*) as the reference gene was determined using the 2-ΔΔCt method. Human Reference RNA (Stratagene, La Jolla, CA, USA) was used as external calibrator. Processing of Human Reference RNA was identical to the mRNA obtained from the samples of patients and healthy controls. Relative *TYMS* gene expression in the PBMC sample of the patient was compared with relative expression of *TYMS* in the controls.

Determination of *DPYD* genotypes

The prevalence of four *DPYD* variants known to be associated with fluoropyrimidine-induced toxicity – 2846A>T, 1679T>G, 1236G>A, and 1601G>A – was compared between groups of patients with risk-associated genotypes and controls in order to exclude DPD deficiency as a possible confounding factor. The *DPYD* variants had been determined in the context of another study investigating their clinical relevance, which will be reported elsewhere. *DPYD* variants were determined according to previously described methods [3].

Determination of PBMC dihydropyrimidine dehydrogenase enzyme activity and the *CYP3A4*22* allele

To exclude other possible causes of intolerance to fluoropyrimidines in the single patient carrying the 2RC/2RC genotype, DPD activity in PBMCs of this patient was determined, as described previously [4]. In addition, since the patient was treated with the combination of capecitabine and docetaxel, we investigated potential CYP3A4 deficiency – which could lead to increased exposure to docetaxel – in the same patient, by determining the most clinically relevant dysfunctional *CYP3A4* allele, *CYP3A4*22*, using a commercial RT-PCR assay (Applied Biosystems).

Supplementary figures and tables

Figure S1. Single nucleotide polymorphisms in the *TYMS* VNTR

Figure S2. Thymidylate synthase enzyme activity (A) and *TYMS* gene expression (B) in peripheral blood mononuclear cells according to 2RC genotype

Table S1. Treatment regimens administered.

Treatment regimen	N	schedule	total daily starting dose (mg/m2) [a]
Capecitabine monotherapy	424		
capecitabine		d1-14 (Q3W)	2000
Capecitabine plus radiotherapy	436		
capecitabine	404	continuous	1650
radiotherapy		-	-
Capecitabine, mitomycin C, radiotherapy	32		
capecitabine		continuous	1650
mitomycin C		day 1	10
radiotherapy		-	-
Capecitabine-based triplet combinations	113		
Docetaxel, oxaliplatin, capecitabine	24		
docetaxel		d1 (Q3W)	50
oxaliplatin		d1 (Q3W)	100
capecitabine		d1-14 (Q3W)	1700
Epirubicin, cisplatin, capecitabine	84		
epirubicin		d1 (Q3W)	50
cisplatin		d1 (Q3W)	60
capecitabine		d1-14 (Q3W)	2000
Epirubicin, oxaliplatin, capecitabine	5		
epirubicin		d1 (Q3W)	50
oxaliplatin		d1 (Q3W)	130
capecitabine		d1-14 (Q3W)	2000
Capecitabine plus platinum	378		
Capecitabine plus oxaliplatin	368		
oxaliplatin		d1 (Q3W)	130
capecitabine		d1-14 (Q3W)	2000
Capecitabine plus carboplatin	6		
carboplatin		d1 (Q3W)	AUC3 [b]
capecitabine		d1-14 (Q3W)	2000
Capecitabine plus cisplatin	4		
cisplatin		d1 (Q3W)	60
capecitabine		d1-14 (Q3W)	2000
Capecitabine plus taxane	64		
Capecitabine plus docetaxel	60		
docetaxel		d1 (Q3W)	75
capecitabine		d1-14 (Q3W)	2000
Capecitabine plus paclitaxel	4		
paclitaxel		d1, d8 (Q3W)	90
capecitabine		d1-14 (Q3W)	1650
Capecitabine plus other	22		
Capecitabine plus irinotecan	5		
irinotecan		d1 (Q3W)	240
capecitabine		d1-14 (Q3W)	2000

Table S1. (continued)

Treatment regimen	N	schedule	total daily starting dose (mg/m2) [a]
Capecitabine plus other drug	17		
other drug (vinorelbin, lapatinib, everolimus)		-	-
capecitabine		d1-14 (Q3W)	2000
5-FU-based	168		
5-FU (+ LV)			
5-FU Q4W	10	d1-5 (Q4W)	425
5-FU QW	9	d1 (QW)	400
5-FU/LV plus cisplatin	3		
5-FU + LV		d1-5 (Q3W)	1000
cisplatin		d1 (Q3W)	75
5-FU/LV plus oxaliplatin (FOLFOX)	75		
5-FU + LV		d1-2 (Q2W)	1000
oxaliplatin		d1 (Q2W)	85
5-FU/LV plus irinotecan (FOLFIRI)	10		
5-FU + LV		d1-2 (Q2W)	1000
irinotecan		d1 (Q2W)	180
5-FU, docetaxel, cisplatin	7		
5-FU		d1-5 (Q3W)	750
docetaxel		d1 (Q3W)	75
cisplatin		d1 (Q3W)	75
5-FU, epirubicin, cisplatin	4		
5-FU		d1-21 (Q3W)	200
epirubicin		d1 (Q3W)	50
cisplatin		d1 (Q3W)	60
5-FU plus radiotherapy	32		
5-FU		d1-4/d1-5 (Q4W)	800
radiotherapy		-	-
5-FU, epirubicin, cyclophosphamide	18		
5-FU		d1 (Q3W)	500
epirubicin		d1 (Q3W)	100
cyclophosphamide		d1 (Q3W)	500

Abbreviations: IQR = interquartile range; 5-FU = 5-fluorouracil; LV = leucovorin/folinic acid
[a] capecitabine was applied b.i.d. according to standard of care
[b] AUC3 = dosed at a target area under the curve (AUC) of 3 mg/ml·min, according to the formula of Calvert (Calvert *et al.* J Clin Oncol. 1989;7:1748-1756)

Table S2. Frequencies of global early severe toxicity by treatment regimen.

Treatments	Grade 0-2 toxicity N (%)	Grade ≥3 toxicity N (%)
Capecitabine monotherapy	404 (95%)	20 (5%)
Capecitabine plus radiotherapy	389 (89%)	47 (11%)
Capecitabine plus taxane	40 (63%)	24 (38%)
Capecitabine plus platinum	351 (93%)	27 (7%)
Capecitabine triplet combination	89 (79%)	24 (21%)
Capecitabine plus other	17 (77%)	5 (23%)
5-FU based	149 (89%)	19 (11%)

6

Table S3. Effect of clinical covariates on risk of global early severe toxicity in multivariable analysis.

	OR	95% CI	p value
Patient characteristics			
Age (per year)	1.02	1.01 to 1.04	0.003
Gender (female *vs.* male gender)	1.43	0.99 to 2.07	0.054
Treatments			
Capecitabine monotherapy	1.0	(reference)	-
Capecitabine plus radiotherapy	2.6	1.51 to 4.60	0.011
Capecitabine plus taxane	14.8	7.29 to 30.1	<0.001
Capecitabine plus platinum	1.8	0.98 to 3.33	0.057
Capecitabine triplet combination	6.6	3.41 to 12.8	<0.001
Capecitabine plus other	7.6	2.50 to 23.1	<0.001
5-FU based	3.1	1.57 to 5.98	0.001

Abbreviations: OR = odds ratio; CI = confidence interval

REFERENCES

1. Pluim D, Schilders KAA, Jacobs BAW, Vaartjes D, Beijnen JH, Schellens JHM. Pharmacodynamic assay of thymidylate synthase activity in peripheral blood mononuclear cells. Anal Bioanal Chem 2013;405:2495–503.

2. Pluim D, Jacobs BAW, Krähenbühl MD, Ruijter AEM, Beijnen JH, Schellens JHM. Correction of peripheral blood mononuclear cell cytosolic protein for hemoglobin contamination. Anal Bioanal Chem 2013;405:2391–5.

3. Deenen MJ, Tol J, Burylo AM, Doodeman VD, de Boer A, Vincent A, et al. Relationship between single nucleotide polymorphisms and haplotypes in DPYD and toxicity and efficacy of capecitabine in advanced colorectal cancer. Clin Cancer Res 2011;17:3455–68.

4. Pluim D, Jacobs BAW, Deenen MJ, Ruijter AE, Van Geel RMJM, Burylo AM, et al. Improved pharmacodynamic assay for dihydropyrimidine dehydrogenase activity in peripheral blood mononuclear cells. Bioanalysis 2015;7:519–29.

6

P A R T 3

PHARMACOKINETICS OF CAPECITABINE AND METABOLITES

C H A P T E R   7

COMPREHENSIVE POPULATION PHARMACOKINETIC ANALYSIS OF CAPECITABINE AND FOUR METABOLITES IN CANCER PATIENTS

Bart A.W. Jacobs, Maarten J. Deenen, Markus Joerger, Hilde Rosing, Niels de Vries, Didier Meulendijks, Jos H. Beijnen, Jan H.M. Schellens, Alwin D.R. Huitema

ABSTRACT

Capecitabine is an oral pro-drug of the anti-cancer drug 5-fluorouracil (5-FU) and is extensively metabolized into active and inactive metabolites. The aim of the current study was to develop a comprehensive population pharmacokinetic model using the data from seven clinical studies (n=237 patients). Nonlinear mixed-effects modeling was applied to describe the pharmacokinetics of capecitabine and its metabolites 5′-deoxy-5-fluorocytidine (dFCR), 5′-deoxy-5-fluorouridine (dFUR), 5-FU and fluoro-β-alanine (FBAL) in plasma. A four-transit model adequately described capecitabine absorption. Capecitabine, dFCR and FBAL pharmacokinetics were well described by two-compartment models and dFUR and 5-FU were subject to flip-flop pharmacokinetics. Partial and total gastrectomy resulted in a factor 1.46 (relative standard error (RSE) 16%) and 3.14 (RSE 25.3%) increase in capecitabine absorption rate. 5-FU elimination was decreased by 21.5% in patients carrying the *DPYD**2A allele. This comprehensive population gives an extensive overview of capecitabine and metabolite pharmacokinetics in a large and heterogeneous population of cancer patients.

INTRODUCTION

Capecitabine is an oral pro-drug of 5-fluorouracil (5-FU) and is frequently used for the treatment of breast, colorectal and gastric cancer. After oral administration, capecitabine is rapidly and completely absorbed. Thereafter, it is metabolized to subsequently 5'-deoxy-5-fluorocytidine (dFCR), 5'-deoxy-5-fluorouridine (dFUR) and 5-FU via a three-step enzymatic cascade involving the enzymes carboxylesterase (CES), cytidine deaminase (CDA) and thymidine phosphorylase (TP), respectively (Figure 1) [1,2]. Approximately 80% of 5-FU is rapidly catabolized to inactive metabolites and a small proportion of 5-FU is intracellularly anabolized to cytotoxic metabolites [3,4]. The enzyme dihydropyrimidine dehydrogenase (DPD) catalyzes the initial step of 5-FU catabolism that leads to the formation of 5,6-dihydro-5-fluorouracil (FUH$_2$) [5]. FUH$_2$ is eventually metabolized to fluoro-β-alanine (FBAL), which is cleared renally [2].

7
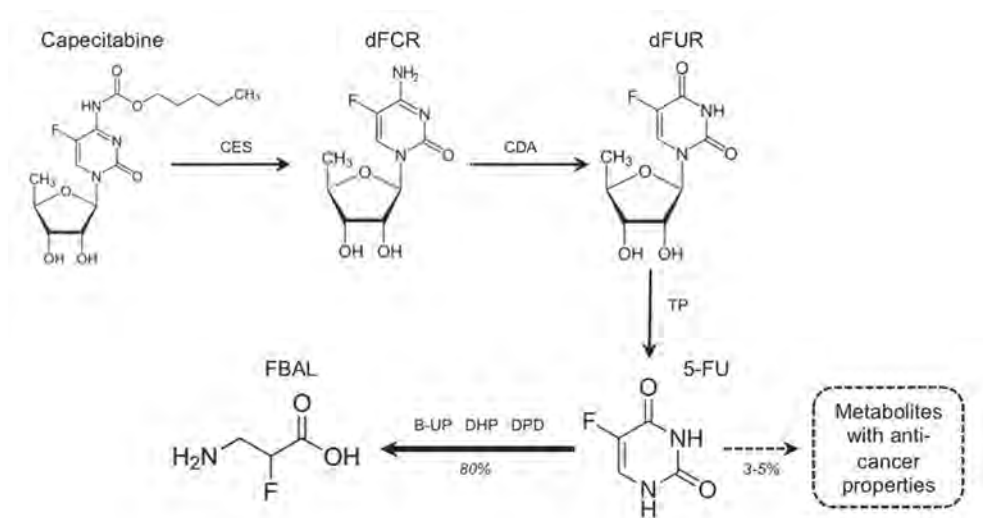
Figure 1. Chemical structures and metabolic pathway of capecitabine, dFCR, dFUR, 5-FU and FBAL. Abbreviations: dFCR, 5'-deoxy-5-fluorocytidine; dFUR, 5'-deoxy-5-fluorouridine; 5-FU, 5-fluorouracil; FBAL, fluoro-β-alanine; CES, carboxylesterase; CDA, cytidine deaminase; TP, thymidine phosphorylase; DPD, dihydropyrimidine dehydrogenase; DHP, dihydropyriminidase; B-UP, β-ureidopropionase.

Several studies have been conducted to investigate the pharmacokinetics (PK) of capecitabine and its metabolites [2]. Most capecitabine PK studies have employed non-compartmental PK analysis, which does not allow for simultaneous analysis of parent and metabolite PK [2]. Moreover, this approach does not allow for appropriate quantification of between-subject and between-occasion variabilities in parent and metabolite PK parameters.

A few population PK studies of capecitabine have been performed. Two previously developed population PK models only incorporated PK data of the metabolites dFUR, 5-FU and FBAL [6,7]. Another study only described a relatively small population and did not include the final metabolite FBAL [8]. We have collected PK data of capecitabine and metabolites in several studies of various patient populations and treatment regimens. One of the studies exclusively included patients carrying the *DPYD**2A allele: an allele encoding non-functional DPD enzyme that is strongly associated with severe fluoropyrimidine-induced toxicity [9–13]. The aim of this study was to develop a comprehensive population PK model by integration of all available PK data.

METHODS

Study population

Pooled data of seven clinical studies of capecitabine were used for the current analysis [14–19]. An overview of the studies is given in Table 1. In all studies, capecitabine was preferably administered within 30 minutes after food intake. Rich PK sampling designs were applied. Study 1 included patients who were heterozygous for the *DPYD**2A risk allele [9]. The other studies included patients with gastric, esophageal, colorectal and anal cancer who were treated with capecitabine-based chemotherapy with or without radiotherapy. All studies were approved by the Medical Ethics Committee of the Netherlands Cancer Institute and were performed in compliance with the WHO declaration of Helsinki. Individual PK data were included for the current analysis if at least one observation for capecitabine, dFCR, dFUR, 5-FU and FBAL was available, the individual *DPYD**2A status was known, and information on the time of sampling was available. Actual times of capecitabine administration and sample collection were used for the population PK analysis.

Bioanalytical analysis and data handling

Capecitabine, dFCR, dFUR, 5-FU and FBAL plasma concentrations were quantified using three validated liquid chromatography – tandem mass spectrometry (LC–MS/MS) assays [20,21]. Assay 1 was used for quantification of capecitabine, dFCR and dFUR plasma concentrations in study 7 and for the first 27 patients who participated in study 3 [20]. The remaining plasma concentrations of capecitabine, dFCR and dFUR were quantified using assay 2 [21]. The lower limit of quantification (LLoQ) for capecitabine, dFCR and dFUR in assay 1 were 27.8, 40.8 and 40.6 nmol/L [20]. For assay 2, the LLoQ values were 139, 204 and 203 nmol/L [21]. Assay 1 and 2 were both validated in accordance with the FDA guideline on bioanalytical method validation [20,21], which assured comparable assay performance. The third LC-MS/MS assay was used to quantify all 5-FU and FBAL plasma concentrations [21]. The LLoQ for 5-FU and FBAL were 384 and 467 nmol/L [21]. Plasma concentrations below the LLoQ were not reported. For the absorption phase, the last observation below LLoQ that was obtained prior to the first observation above LLoQ was included in the dataset as LLoQ/2. Including these observations as LLoQ/2

Table 1. Summary of the clinical studies.

Study number	Number of subjects	Median (range) capecitabine dose (mg)	Study description	Co-treatment	Sampling design	Sampling schedule (h after intake)	Reference
1	19	800 (300 – 1000)	Study of cancer patients carrying the DPYD*2A risk allele who received ~50% of the registered capecitabine dose	Variable	Rich sampling on treatment day one	0.25, 0.5, 1, 2, 3, 4, 5, 6, 8	[9]
2	30	1650 (1150 – 1700)	Phase I study in patients with cancer of the stomach or gastroesophageal junction	Docetaxel and oxaliplatin	Rich sampling on treatment day one	0, 0.5, 1, 2, 3, 4, 6, 8	[14]
3	31	1500 (1000 – 2000)	Phase I-II study in patients with gastric and esophageal cancer; capecitabine treatment was started after tumor resection	Radiotherapy	Rich sampling on day 22 and 43 of treatment	0, 0.25, 0.5, 0.75, 1, 1.5, 2, 3, 4	[15]
4	41	1150 (300 – 1500)	Phase I-II study in patients with gastric and esophageal cancer; capecitabine treatment was started after tumor resection	Radiotherapy and cisplatin	Rich sampling on day 22 and 43 of treatment	0, 0.25, 0.5, 0.75, 1, 1.5, 2, 3, 4	[16,17]
5	48	1925 (1000 – 2600)	Study to determine proteomic profile and capecitabine pharmacokinetics in patients with advanced colorectal cancer	Oxaliplatin	Rich sampling on treatment day one	0, 0.5, 1, 1.5, 2, 3, 4, 5, 6	[18]
6	50	2000 (1300 – 2000)	Study to determine proteomic profile and pharmacokinetics in patients with advanced gastric cancer	Cisplatin and epirubicin	Rich sampling on treatment day one	0, 0.5, 1, 1.5, 2, 3, 4, 5, 6, 8	[18]
7	18	1475 (900 – 1650)	Phase I study in patients with advanced anal cancer	Radiotherapy and mitomycin-c	Rich sampling on treatment day one	0, 0.25, 0.5, 1, 2, 3, 4, 6, 8	[19]

7

increased the amount of informative data that was needed for adequate modeling of the capecitabine absorption process [22].

Population PK modeling

Nonlinear mixed-effects modeling, using the software package NONMEM (version 7.3) [23], was applied for model development. Parameter estimation was achieved using the first-order conditional estimation method with interaction. R (version 3.3.0) was applied for data formatting and visualization [24]. Piraña (version 2.9.2) was used for model management [25]. The R-package Xpose4 (version 4.5.3) and Perl speaks NONMEM (PsN, version 4.4.8) were used for model diagnostics [25].

Structural model development

Sequential population PK modeling was applied during the initial stage of model development. In the first step, a model of capecitabine PK was established. Estimated population PK parameters were then fixed and the base model was extended with the data of the first metabolite, dFCR. After optimization of the PK model for dFCR, the parameter estimates were fixed as well. The procedure of including PK data of the subsequent metabolite, model optimization and fixing the population PK parameters was repeated until capecitabine and all four metabolites were included in the population PK model. After sequential optimization, all parameters were re-estimated simultaneously using the structural model and parameter estimates of sequential analysis as initial values.

For capecitabine, several absorption models were examined during the first stage of model development: first-order absorption with lag time, combined zero-order and first-order absorption, mixture models of first-order absorption, and first-order transit absorption with a chain of transit compartments [26]. One- and two-compartmental models with first-order elimination were considered for the parent compound and the metabolites.

The phenomenon of flip-flop PK was evaluated by visual inspection. In case of flip-flop PK, only the elimination rate constant could be estimated for the specific metabolite. As the bioavailability of capecitabine and the fractions converted to the consecutive metabolites were unknown, all parameters were estimated relative to these values.

Statistical model

Between-subject variability (BSV) and between-occasion variability (BOV) were estimated using an exponential model (Eq. 1):

$$\theta_{i,k} = \theta_{pop} \times \exp(\eta_i + \kappa_k) \tag{1}$$

where $\theta_{i,k}$ represents the parameter estimate for individual i on occasion k, θ_{pop} the typical value for the population parameter, η_i being the individual-specific random effect from

a normal distribution with mean zero and variance ω^2, and κ_k the occasion-specific random effect from a normal distribution with mean zero and variance π^2.

Residual unexplained variability (RUV) was modeled using a combined additive and proportional model including a proportion and additive model (Eq. 2):

$$C_{o,ij} = C_{p,ij} \times \left(1 + \varepsilon_{prop}\right) + \varepsilon_{add} \tag{2}$$

where $C_{o,ij}$ represents the observed and $C_{p,ij}$ the model-predicted plasma concentration for individual i at timepoint j, and ε_{prop} and ε_{add} represent the proportional and additional residual error, respectively, which were assumed to be normally distributed with a mean of zero and variance σ^2. The variance of ε_{add} was fixed to the square of the LLoQ/2, taken the specific LLoQ for each assay into account.

Covariate model

Covariate-parameter associations were exclusively examined in case they were considered physiologically plausible. An overview of the explored covariates is given in Table 2. In order to accelerate the covariate analyses, fixed-effect and random-effect parameters upstream of the studied covariate-parameter associations were fixed.

The effect of age on model-predicted parameters was estimated as follows (Eq. 3):

$$\theta_i = \theta_{pop} \times \left(\frac{age_i}{age_{pop}}\right)^{\theta_{cov}} \tag{3}$$

where age_i represents age of individual i, age_{pop} is the average age within the study population and θ_{cov} represents the covariate effect.

The effect of the categorical covariates gender, gastrectomy and genetic polymorphisms were explored. Besides the effect of the *DPYD**2A mutation, the effect of the *DPYD* c.2846A>T and c.1236G>A mutations on 5-FU elimination were studied. The consequence of the *CDA* c.79A>C mutation on the apparent clearance of dFCR was also explored. Genetic polymorphisms were determined as described previously [9,14,18,19].

The effect of the categorical covariates were modeled as follows (Eq. 4):

$$\theta_i = \theta_{pop} \times \theta_{cov}^{R_i} \tag{4}$$

where R_i represents the covariate of interest with a value of 1 in presence of a specific covariate and with a value of 0 in absence of the covariate.

Table 2. Characteristics of the study population and potential covariates study population.

Characteristic	Unit	Value
Total number of subjects	*n*	237
Gender		
Male	*n* (%)	159 (67.1)
Female	*n* (%)	78 (32.9)
Age (mean (range))	years	57.5 (27.8 – 77.8)
Gastric surgery		
No gastrectomy	*n* (%)	154 (65.0)
Total gastrectomy	*n* (%)	24 (10.1)
Partial gastrectomy	*n* (%)	44 (18.6)
Esophagogastrectomy	*n* (%)	15 (6.3)
DPYD*2A		
Wild-type	*n* (%)	216 (91.1)
Heterozygous mutant	*n* (%)	21 (8.9)
DPYD c.2846A>T		
Wild-type	*n* (%)	207 (87.3)
Heterozygous mutant	*n* (%)	11 (4.6)
Unknown	*n* (%)	19 (8.0)
DPYD c.1236G>A		
Wild-type	*n* (%)	159 (67.1)
Heterozygous mutant	*n* (%)	11 (4.6)
Unknown	*n* (%)	67 (28.3)
CDA c.79A>C		
Wild-type	*n* (%)	79 (33.3)
Heterozygous mutant	*n* (%)	62 (26.2)
Homozygous mutant	*n* (%)	22 (9.3)
Unknown	*n* (%)	74 (31.2)

Abbreviations: *DPYD*, dihydropyrimidine dehydrogenase; *CDA*, cytidine deaminase

In case of missing categorical covariates a separate parameter for the missing group was estimated [27], as follows (Eq. 5):

$$\theta_i = \theta_{pop} \times \theta_{missing} \qquad (5)$$

where $\theta_{missing}$ represents the covariate effect for the subjects with missing covariate data.

Model evaluation

Model evaluation was guided by standard goodness-of-fit (GOF) plots [28], prediction-corrected visual predictive checks (pcVPC) [29], successful minimization, drop in objective function value (dOFV) and precision of obtained parameter estimates. Parameter precision was estimated using the COVARIANCE step in NONMEM. A drop in dOFV of >3.84, corresponding to a p <0.05, was considered statistically significant for hierarchical models. The pcVPC of the final model was generated from 1000 simulations. The 5th, 50th and 95th percentiles of the prediction-corrected observations and simulations were visually compared. The combined error model allowed for simulation of negative plasma concentrations, which were replaced by LLoQ/2.

RESULTS

Pharmacokinetic data of 237 patients were included for the population PK analysis. This resulted in the availability of a total of 8988 observations for capecitabine, dFCR, dFUR, 5-FU and FBAL. The patients received a median (range) capecitabine dose of 1650 (300–2600) mg. For 63 out of 237 patients, PK data of two occasions were available. For one patient, participating in study 1, PK data were collected on three occasions. For all other patients, PK data were available from a single occasion. The number of patients and the median (range) capecitabine dose per study are summarized in Table 1. Patient characteristics are shown in Table 2.

The PK database included 560 observations below the LLoQ that were imputed as LLoQ/2. A graphical overview of the PK data is shown in Figure 2. Capecitabine demonstrated rapid absorption and elimination. The average capecitabine peak concentration was observed approximately 0.5 h after dosing. For dFCR, dFUR and 5-FU, the average peak level was found around 1 hour after dosing. The peak concentration of FBAL appeared relatively late: approximately 2.5 h after dose administration. The plasma concentration-time profiles of dFCR, dFUR and 5-FU demonstrated similar patterns. FBAL was less rapidly eliminated from plasma than the other compounds.

Population PK model

The structure of the final model is depicted in Figure 3 and the final parameter estimates are summarized in Table 3. A detailed description of model development is provided in the following two paragraphs.

Capecitabine pharmacokinetics

The capecitabine absorption rate was highly variable between subjects and occasions. In 95 of the 301 occasions (31.6%), capecitabine peak concentrations were observed at the first observation after drug administration. For these curves, adequate estimation of the absorption phase was not possible. With the different absorption models tested, these curves caused run failure and/or estimation problems. Therefore, a zero-order absorption process in which the dose was fully absorbed between time of capecitabine
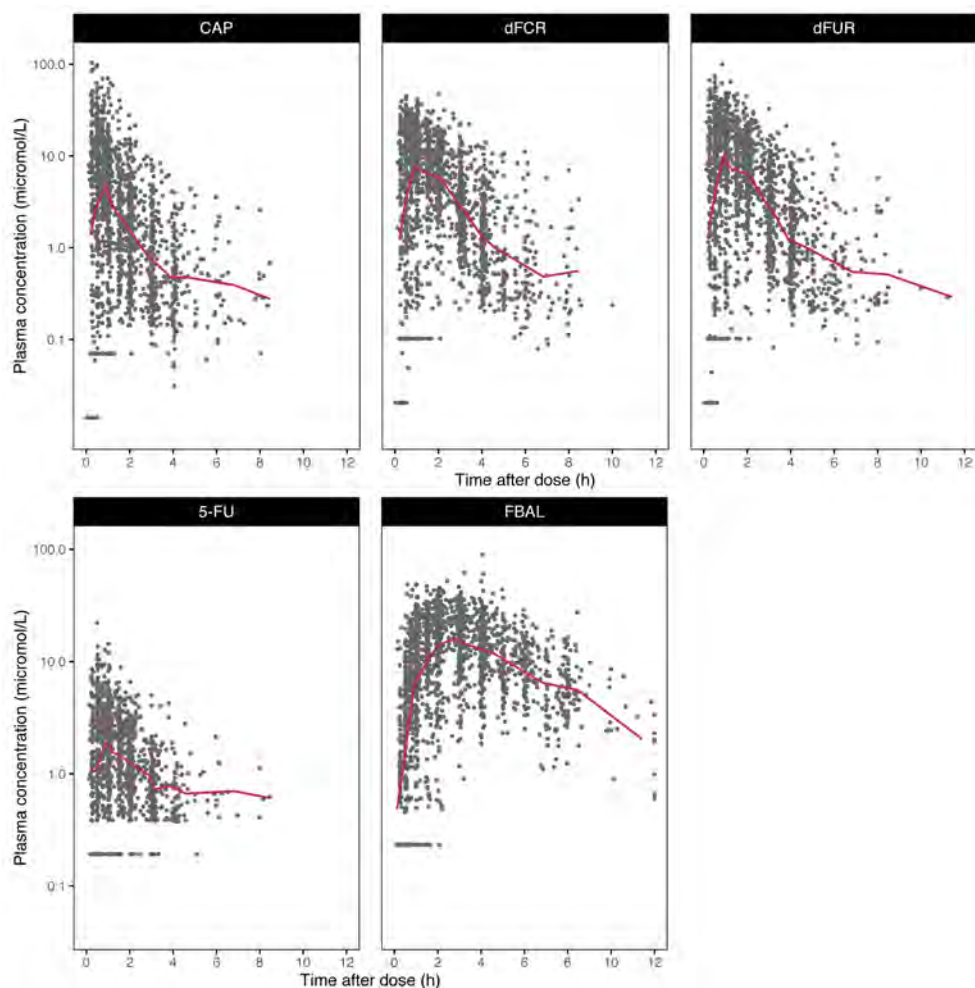
Figure 2. Log plasma concentration – time profiles of capecitabine, dFCR, dFUR, 5-FU and FBAL. The *red lines* illustrate average plasma concentration – time profiles. Abbreviations: CAP, capecitabine; dFCR, 5′-deoxy-5-fluorocytidine; dFUR, 5′-deoxy-5-fluorouridine; 5-FU, 5-fluorouracil; FBAL, fluoro-β-alanine.

intake and the time of the first observation was assumed for these curves. Interestingly, this was necessary in 21 of the 42 occasions from the patients who underwent total gastrectomy. For the remaining 206 occasions (68.4%), a first-order transit absorption model including four transit compartments resulted in adequate description of capecitabine absorption. Visual inspection of the random-effect distribution on the transit rate constant (k_{tr}) suggested that capecitabine absorption occurred relatively fast for the patients who previously underwent gastrectomy for advanced gastric cancer. Therefore, partial gastrectomy and total gastrectomy were included as categorical covariates on the transit rate constant, which resulted in a significantly improved model fit (Supplementary Table 1).
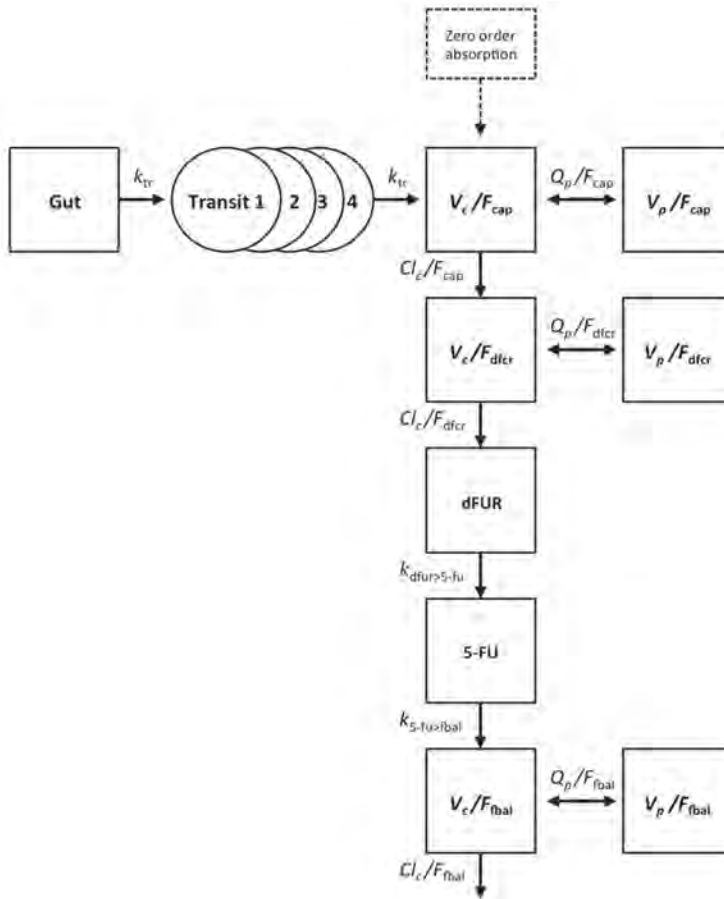
Figure 3. Schematic representation of the population pharmacokinetic model of capecitabine, dFCR, dFUR, 5-FU and FBAL. Abbreviations: k_{tr}, transit rate constant; CL_c/F, apparent clearance of central compartment; V_c/F, apparent central volume of distribution; Q_p/F, apparent intercompartmental clearance; V_p/F, apparent peripheral volume of distribution; k, rate constant; CAP, capecitabine; dFCR, 5'-deoxy-5-fluorocytidine; dFUR, 5'-deoxy-5-fluorouridine; 5-FU, 5-fluorouracil; FBAL, fluoro-β-alanine.

The mean transit time (MTT), which was calculated by (the number of transit compartments + 1) / k_{tr}, was 0.67 h and 0.31 h for patient who underwent partial and total gastrectomy, respectively. For the other patients, the estimated MTT was 0.98 h. BSV and BOV on the k_{tr} were successfully estimated and were found to be relatively large.

Capecitabine distribution and elimination was best described by a two-compartmental model with linear inter-compartmental clearance. BSV terms for the apparent central clearance (CL_c/F_{cap}) and volume of distribution (V_c/F_{cap}) were included. In particular, BSV on V_c/F_{cap} was estimated to be large (132.1%). There was a significant correlation between BSV on CL_c/F_{cap} and BSV on V_c/F_{cap}.

Table 3. Parameter estimates of the population pharmacokinetic model of capecitabine, dFCR, dFUR, 5-FU and FBAL.

Parameter	Estimate (RSE %)
k_{tr} (h^{-1})	5.08 (8.7)
Effect of partial gastrectomy	1.46 (16.0)
Effect of total gastrectomy	3.14 (25.3)
CL_c/F_{cap} (L/h)	337 (5.3)
V_c/F_{cap} (L)	207 (11.0)
Q_p/F_{cap} (L/h)	15.8 (8.2)
V_p/F_{cap} (L)	31.4 (8.3)
CL_c/F_{dfcr} (L/h)	148 (4.3)
V_c/F_{dfcr} (L)	20.5 (3.6)
Q_p/F_{dfcr} (L/h)	94.1 (6.4)
V_p/F_{dfcr} (L)	39 (3.6)
$k_{dfur>5\text{-}fu}$ (h^{-1})	129 (2.9)
$k_{5\text{-}fu>fbal}$ (h^{-1})	777 (3.6)
Effect of *DPYD**2A heterozygous mutation	0.785 (11.2)
CL_c/F_{fbal} (L/h)	36.7 (5.2)
Effect of age	-0.97 (19.1)
Effect of gender female	0.757 (6.5)
V_c/F_{fbal} (L)	84.7 (4.8)
Q_p/F_{fbal} (L/h)	11.7 (11.7)
V_p/F_{fbal} (L)	39 (33.3)
BSV	**%CV (RSE %), Shrinkage [%]**
k_{tr} (h^{-1})	60.7 (17.0) [38.6]
CL_c/F_{cap} (L/h)	57.5 (6.4) [6.6]
V_c/F_{cap} (L)	132.1 (7.8) [12.6]
CL_c/F_{dfcr} (L/h)	47.1 (4.4) [4.1]
$k_{dfur>5\text{-}fu}$ (h^{-1})	33.6 (6.0) [9.0]
$k_{5\text{-}fu>fbal}$ (h^{-1})	41.5 (6.0) [9.4]
CL_c/F_{fbal} (L/h)	32.3 (7.9) [15.6]
V_p/F_{fbal} (L)	46.7 (4.7) [10.3]

Metabolite population PK modeling

The population PK model of capecitabine was extended with the four metabolites. As shown in Figure 2, the mean plasma concentration-time curve for the first metabolite, dFCR, followed a bi-exponential decay. A two-compartmental model with linear clearance, which included a BSV term on dFCR clearance from the central compartment (CL_c/F_{dfcr}), adequately described dFCR distribution and elimination.

Decay in the plasma concentrations of the following two metabolites, dFUR and 5-FU, illustrated great similarity to that of dFCR (Figure 2). These findings clearly indicated flip-flop PK for dFUR and 5-FU. The elimination rate constants for dFUR ($k_{dfur>5\text{-}fu}$) and 5-FU

Table 3. (continued)

Parameter	
BOV	**%CV (RSE %), Shrinkage [%]**
k_{tr} (h^{-1})	57.4% (12.5) [44.6]
Correlations	**Coefficient**
ρ (BSV CL_c/F_{cap}, V_c/F_{cap})	0.53
ρ (BSV $k_{dfur>5-fu}$, $k_{5fu>fbal}$)	0.63
Proportional RUV	**%CV (RSE %), Shrinkage [%]**
Capecitabine	57.6 (3.3) [4.3]
dFCR	40.5 (2.7) [6.1]
dFUR	42.7 (3.0) [6.3]
5-FU	37.7 (2.5) [3.9]
FBAL	30.4 (1.3) [7.7]

Abbreviations: BSV, between-subject variability; BOV, between-occasion variability; RUV, residual unexplained variability; RSE, relative standard error; CV, coefficient of variation; k_{tr}, transit rate constant; CL_c/F, apparent clearance of central compartment; V_c/F, apparent central volume of distribution; Q_p/F, apparent intercompartmental clearance; V_p/F, apparent peripheral volume of distribution; k, rate constant; ρ, correlation coefficient; DPYD, dihydropyrimidine dehydrogenase; CAP, capecitabine; dFCR, 5'-deoxy-5-fluorocytidine; dFUR, 5'-deoxy-5-fluorouridine; 5-FU, 5-fluorouracil; FBAL, fluoro-β-alanine.

7

($k_{5-fu>fbal}$) were estimated. BSV terms on these rate constants were successfully included. There was significant covariance between BSV in $k_{dfur>5-fu}$ and $k_{5fu>fbal}$.

The decay in plasma levels of the final metabolite FBAL occurred less rapid than for capecitabine and the previous metabolites. Distribution and elimination of FBAL were best described with a two-compartment model. BSV on the apparent clearance (CL_c/F_{fbal}) and distribution volume (V_c/F_{fbal}) were successfully estimated.

Covariate model

An overview of the explored covariate-parameter associations is shown in Supplementary Table 1. The estimated $k_{5-fu>fbal}$ was 21.5% lower in patients who were heterozygous for the DPYD*2A mutation (dOFV -7.12). Patients carrying the DPYD c.1236G>A and c.2846A>T variants did not demonstrate altered 5-FU elimination. The estimated CL_c/F_{dfcr} was not affected by the heterozygous or homozygous CDA c.79A>C mutation. There was an effect of age (dOFV -40.71) and gender (dOFV -25.89) on the CL_c/F_{fbal}. Both the effect of age and gender were included in the final model. The effects of partial and total

gastrectomy on the transit absorption rate were already incorporated in the first phase of model development.

Model evaluation

The fixed and random-effect parameters were estimated with adequate precision, as illustrated by relative standard errors of ≤33.3% and ≤17.0%, respectively (Table 3). Shrinkage was ≤15.6% for random-effect parameters accounting for BSV, although relatively high for random-effect parameters of BSV (38.6%) and BOV (44.6%) on k_{tr}. There was substantial unexplained variability on capecitabine plasma levels, as illustrated by the estimated proportional RUV of 57.6%. For the four metabolites, the proportional RUV was moderate with CV values ranging between 30.4–42.7%. Shrinkage on the proportional RUV parameters was low (≤7.7%). Overall, the population PK parameters were estimated with adequate precision. GOF plots for the final model (Figure 4) and the pcVPC (Figure 5) did not indicate model misspecification.

DISCUSSION

We successfully developed a population PK model that adequately described the PK of capecitabine and its metabolites dFCR, dFUR, 5-FU and FBAL in a large and heterogeneous population of cancer patients. This study is unique with respect to the number of included metabolites, variability among study populations, treatment schedules and with regard to the large total number of observations.

The absorption process was successfully described using a transit absorption model. In general, a transit model approaches the physiological absorption conditions better than change-point (lag-time) models that have incorporated in the previously developed population PK models [7,8,30].

Capecitabine was rapidly absorbed, especially in patients who underwent partial or total gastrectomy. The physicochemical properties of the drug might be essential for this finding. Capecitabine is highly water-soluble and shows good permeability [31]. Current data suggest that availability of gastric fluid is not required for the dissolution of capecitabine. The passage rate of capecitabine through the upper part of the gastro-intestinal tract is most likely increased after gastrectomy, which resulted in quick intestinal availability of capecitabine.

Intake of food was previously found to delay capecitabine absorption [31]. Although capecitabine was preferably administered within 30 minutes after a meal in all seven studies, the amount and the type of food were not specified. It could be that the intake of food was reduced in patients who previously underwent gastrectomy, which in turn, could have resulted in rapid capecitabine uptake. In general, the food effect could have been an important factor attributing to BOV and BSV in capecitabine absorption.

A first-pass effect seems to play a major role in the bioavailability of capecitabine and metabolites. The enzymes CES, CDA, TP and DPD are highly active in liver tissue [32,33]. Between-subject variability in enzymatic phenotypes, liver perfusion and liver function likely contribute to variability in parameter estimates regarding capecitabine, dFCR, dFUR and 5-FU PK.
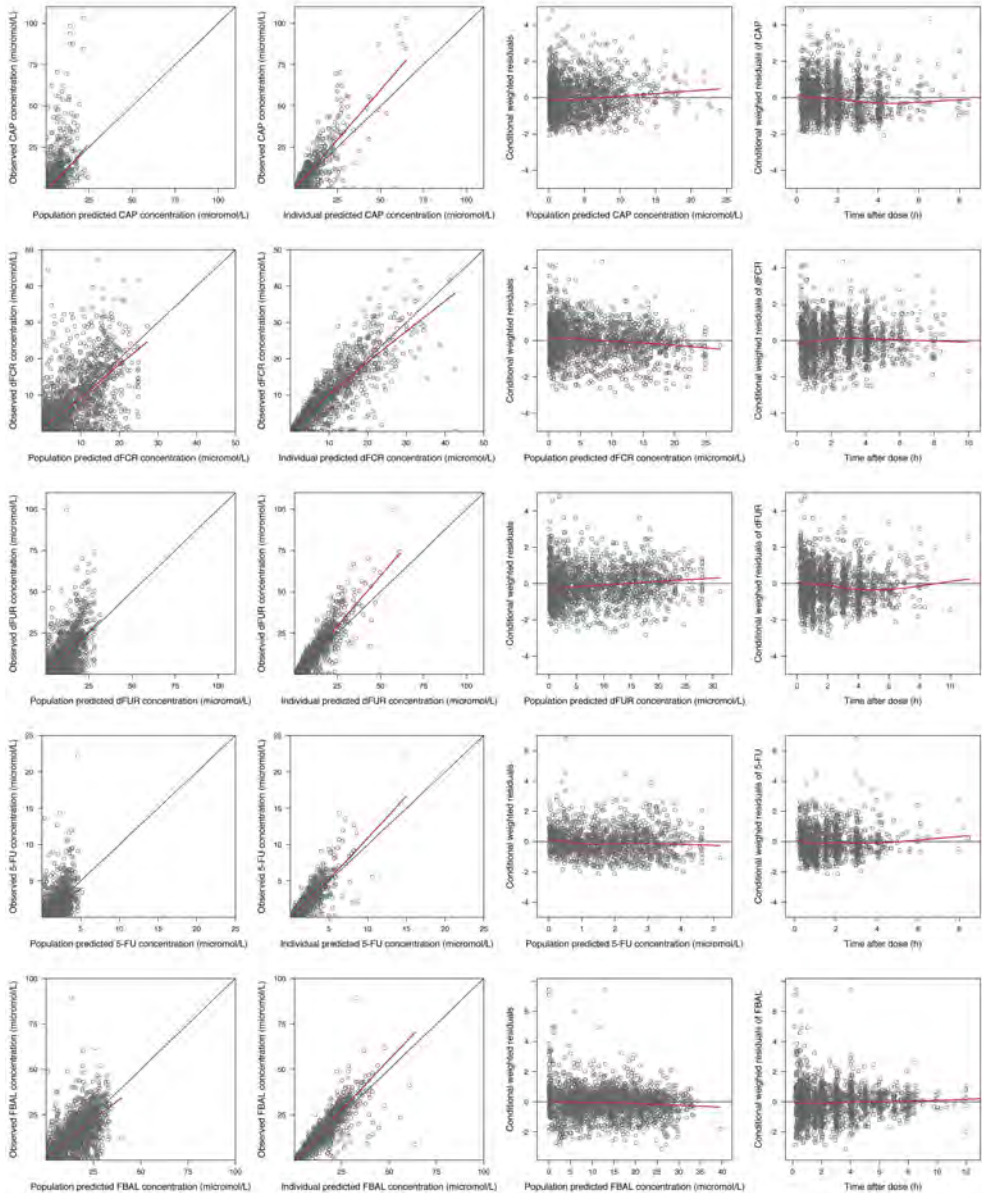
Figure 4. Goodness-of-fit plots for model-predicted capecitabine, dFCR, dFUR, 5-FU and FBAL plasma concentrations. *Black lines* represent the lines of identity and the *red lines* indicate the trend in observations. Abbreviations: CAP, capecitabine; dFCR, 5'-deoxy-5-fluorocytidine; dFUR, 5'-deoxy-5-fluorouridine; 5-FU, 5-fluorouracil; FBAL, fluoro-β-alanine.

The genetic polymorphism *CDA* c.79A>C, which has been associated with moderately decreased CDA activity [34], did not show to significantly affect the CL_c/F_{dfcr}. Although the allele frequency of the *DPYD**2A allele in the general population is low (~1%) [9,13,35], data of a total of 21 variant allele carriers were available. For patients carrying the *DPYD**2A allele, the $k_{5\text{-fu>fbal}}$ was estimated to be reduced by 21.5%. Not all *DPYD**2A
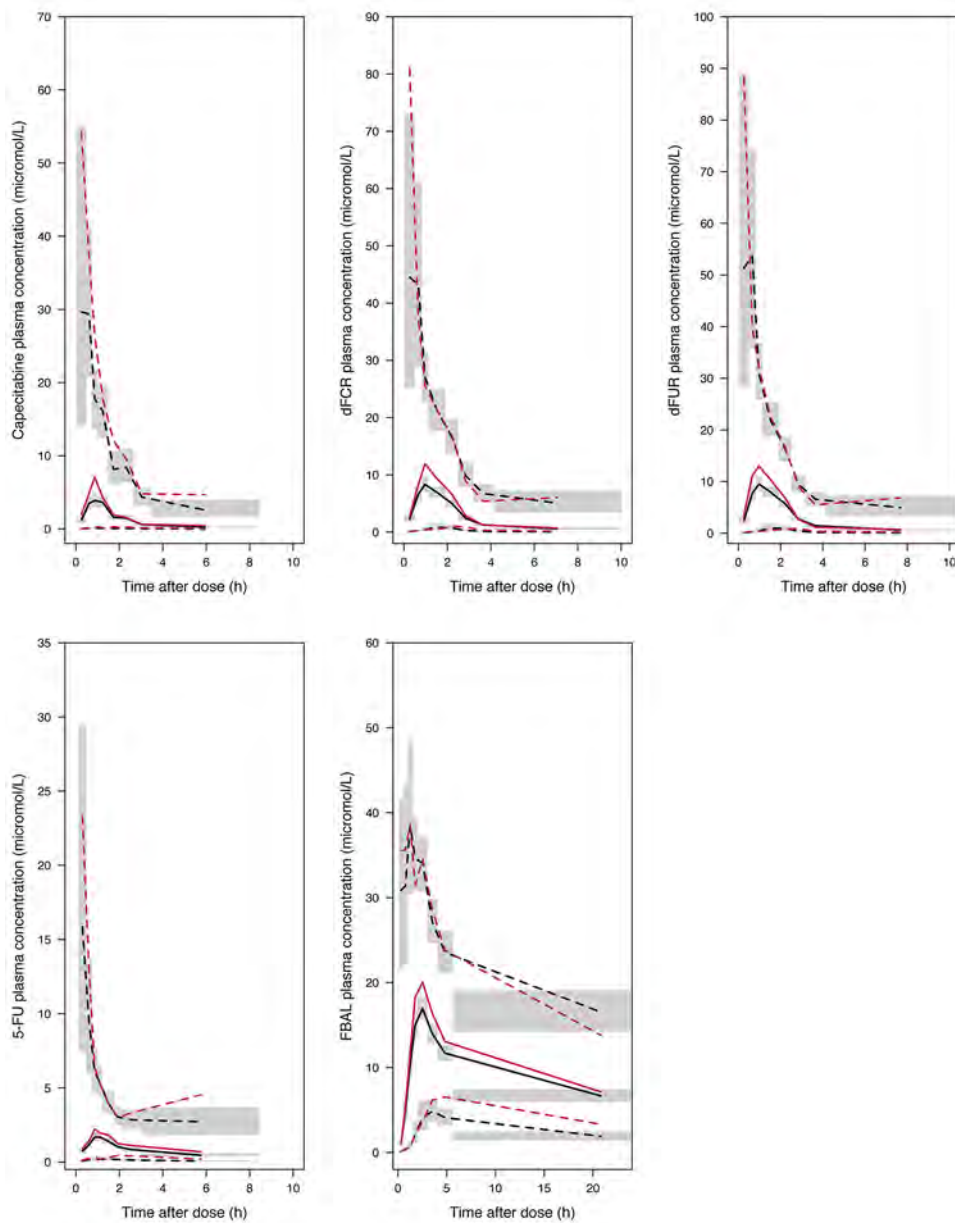
Figure 5. Prediction-corrected visual predictive checks of capecitabine, dFCR, dFUR, 5-FU and FBAL. *Red solid* and *black solid* lines represent the median prediction-corrected observed and predicted data. *Red dashed* and *black dashed* lines illustrate the 5th and 95th percentile of the prediction-corrected observed and predicted data. The grey shades illustrate the 95% confidence intervals of the simulated data. Abbreviations: dFCR, 5'-deoxy-5-fluorocytidine; dFUR, 5'-deoxy-5-fluorouridine; 5-FU, 5-fluorouracil; FBAL, fluoro-β-alanine.

allele carriers, however, demonstrated a reduced DPD phenotype [9]. This could explain why the reduction in $k_{5\text{-fu>fbal}}$ did not exceed 21.5% for patients carrying the *DPYD**2A allele. Previously, the *DPYD**2A allele has been associated with a 1.3-1.5 fold increase in 5-FU exposure after intravenous administration [36]. Current results support the clinical findings of increased fluoropyrimidine-induced toxicity due to the *DPYD**2A mutation [13,37].

Effects of the *DPYD* c.2846A>T and c.1236G>A variants on $k_{5\text{-fu>fbal}}$ were explored, but were not statistically significant. Additional population PK analyses including larger numbers of *DPYD* c.2846A>T and c.1236G>A allele carriers are warranted for improved analyses of possible covariate effects.

Two-compartmental distribution models were used for adequate description of capecitabine, dFCR and FBAL distribution. None of the previously described population PK models by Gieschke et al. and Urien et al. included peripheral compartments [6–8]. Furthermore, we demonstrated that there is large BSV in the PK of capecitabine and dFCR. These two analytes were not included in the population PK models that were previously described by Gieschke et al [6,7]. By neglecting variability in capecitabine and dFCR PK, the previously developed models did not accurately reflect the source of variability in dFUR and 5-FU plasma exposure. Population PK studies described by Gieschke et al. mainly included PK data of colorectal cancer patients who were treated with capecitabine monotherapy [6,7]. The currently described model was based on a more heterogeneous population of cancer patients who were treated with different capecitabine-based treatment regimens. This enabled us to identify the effect of gastrectomy on capecitabine absorption and the effect of the *DPYD**2A mutation on 5-FU elimination after capecitabine intake, which have not been described previously.

A limitation in the current study is that capecitabine absorption was not adequately estimated for all PK curves. Although rich sampling was applied in all studies, the capecitabine peak concentration was often detected in the first sample after dose. This could have been avoided by increasing the PK sampling intensity within the 0.5 h after capecitabine intake. For these curves, zero-order absorption was assumed, which enabled us to include the PK data for the current analysis.

Overall, the population PK parameters were estimated with adequate precision. GOF plots and pcVPC did not indicate any structural model misspecification. In conclusion, a comprehensive population PK model of capecitabine and the metabolites dFCR, dFUR, 5-FU and FBAL has been successfully developed and validated. This model adequately describes the complexity of capecitabine and metabolites PK in a large and variable population of cancer patients.

7

REFERENCES

1. Judson IR, Beale PJ, Trigo JM, Aherne W, Crompton T, Jones D, et al. A human capecitabine excretion balance and pharmacokinetic study after administration of a single oral dose of 14C-labelled drug. Invest New Drugs 1999;17:49–56.

2. Reigner B, Blesch K, Weidekamm E. Clinical pharmacokinetics of capecitabine. Clin Pharmacokinet 2001;40:85–104.

3. Diasio RB, Harris BE. Clinical pharmacology of 5-fluorouracil. Clin Pharmacokinet 1989;16:215–37.

4. Longley DB, Harkin DP, Johnston PG. 5-fluorouracil: mechanisms of action and clinical strategies. Nat Rev Cancer 2003;3:330–8.

5. Heggie GD, Sommadossi JP, Cross DS, Huster WJ, Diasio RB. Clinical pharmacokinetics of 5-fluorouracil and its metabolites in plasma, urine, and bile. Cancer Res 1987;47:2203–6.

6. Gieschke R, Burger H-U, Reigner B, Blesch KS, Steimer J-L. Population pharmacokinetics and concentration-effect relationships of capecitabine metabolites in colorectal cancer patients. Br J Clin Pharmacol 2003;55:252–63.

7. Gieschke R, Reigner B, Blesch KS, Steimer JL. Population pharmacokinetic analysis of the major metabolites of capecitabine. J Pharmacokinet Pharmacodyn 2002;29:25–47.

8. Urien S, Rezaí K, Lokiec F. Pharmacokinetic modelling of 5-FU production from capecitabine--a population study in 40 adult patients with metastatic cancer. J Pharmacokinet Pharmacodyn 2005;32:817–33.

9. Deenen MJ, Meulendijks D, Cats A, Sechterberger MK, Severens JL, Boot H, et al. Upfront Genotyping of DPYD*2A to Individualize Fluoropyrimidine Therapy: A Safety and Cost Analysis. J Clin Oncol 2016;34:227–34.

10. Meulendijks D, Henricks LM, Sonke GS, Deenen MJ, Froehlich TK, Amstutz U, et al. Clinical relevance of DPYD variants c.1679T>G, c.1236G>A/HapB3, and c.1601G>A as predictors of severe fluoropyrimidine-associated toxicity: a systematic review and meta-analysis of individual patient data. Lancet Oncol 2015;16:1639–50.

11. Jennings BA, Loke YK, Skinner J, Keane M, Chu GS, Turner R, et al. Evaluating predictive pharmacogenetic signatures of adverse events in colorectal cancer patients treated with fluoropyrimidines. PLoS One 2013;8:e78053.

12. Loganayagam A, Arenas Hernandez M, Corrigan A, Fairbanks L, Lewis CM, Harper P, et al. Pharmacogenetic variants in the DPYD, TYMS, CDA and MTHFR genes are clinically significant predictors of fluoropyrimidine toxicity. Br J Cancer 2013;108:2505–15.

13. Lee AM, Shi Q, Pavey E, Alberts SR, Sargent DJ, Sinicrope FA, et al. DPYD Variants as Predictors of 5-fluorouracil Toxicity in Adjuvant Colon Cancer Treatment (NCCTG N0147). J Natl Cancer Inst 2014;106:1–12.

14. Deenen MJ, Meulendijks D, Boot H, Legdeur M-CJC, Beijnen JH, Schellens JHM, et al. Phase 1a/1b and pharmacogenetic study of docetaxel, oxaliplatin and capecitabine in patients with advanced cancer of the stomach or the gastroesophageal junction. Cancer Chemother Pharmacol 2015;76:1285–95.

15. Jansen EPM, Boot H, Saunders MP, Crosby TDL, Dubbelman R, Bartelink H, et al. A phase I-II study of postoperative capecitabine-based chemoradiotherapy in gastric cancer. Int J Radiat Oncol Biol Phys 2007;69:1424–8.

16. Jansen EPM, Boot H, Dubbelman R, Bartelink H, Cats A, Verheij M. Postoperative chemoradiotherapy in gastric cancer -- a Phase I/II dose-finding study of radiotherapy with dose escalation of cisplatin and capecitabine chemotherapy. Br J Cancer 2007;97:712–6.

17. Jansen EPM, Boot H, Dubbelman R, Verheij M, Cats A. Postoperative chemoradiotherapy in gastric cancer--a phase I-II study of radiotherapy with dose escalation of weekly cisplatin and daily capecitabine chemotherapy. Ann Oncol 2010;21:530–4.

18. Joerger M, Huitema ADR, Boot H, Cats A, Doodeman VD, Smits PHM, et al. Germline TYMS genotype is highly predictive in patients with metastatic gastrointestinal malignancies receiving capecitabine-based chemotherapy. Cancer Chemother Pharmacol 2015;75:763–72.

19. Deenen MJ, Dewit L, Boot H, Beijnen JH, Schellens JHM, Cats A. Simultaneous integrated boost-intensity modulated radiation therapy with concomitant capecitabine and mitomycin C for locally advanced anal carcinoma: a phase 1 study. Int J Radiat Oncol Biol Phys 2013;85:e201–7.

20. Vainchtein LD, Rosing H, Schellens JHM, Beijnen JH. A new, validated HPLC-MS/MS method for the simultaneous determination of the anti-cancer agent capecitabine and its metabolites: 5′-deoxy-5-fluorocytidine, 5′-deoxy-5-fluorouridine, 5-fluorouracil and 5-fluorodihydrouracil, in human plasma. Biomed Chromatogr 2010;24:374–86.

21. Deenen MJ, Rosing H, Hillebrand MJ, Schellens JHM, Beijnen JH. Quantitative determination of capecitabine and its six metabolites in human plasma using liquid chromatography coupled to electrospray tandem mass spectrometry. J Chromatogr B Analyt Technol Biomed Life Sci 2013;913-914:30–40.

22. Keizer RJ, Jansen RS, Rosing H, Thijssen B, Beijnen JH, Schellens JHM, et al. Incorporation of concentration data below the limit of quantification in population pharmacokinetic analyses. Pharmacol Res Perspect 2015;3:e00131.

23. Beal S, Sheiner L. NONMEM user guides. Ellicott City, Maryland, USA: Icon Development Solutions, 1989.

24. R Development Core Team. R: A Language and Environment for Statistical Computing. Vienna, Austria: R Foundation for Statistical Computing, 2016.

25. Keizer RJ, Karlsson MO, Hooker A. Modeling and Simulation Workbench for NONMEM: Tutorial on Pirana, PsN, and Xpose. CPT Pharmacometrics Syst Pharmacol 2013;2:e50.

26. Rousseau A, Léger F, Le Meur Y, Saint-Marcoux F, Paintaud G, Buchler M, et al. Population pharmacokinetic modeling of oral cyclosporin using NONMEM: comparison of absorption pharmacokinetic models and design of a Bayesian estimator. Ther Drug Monit 2004;26:23–30.

27. Keizer RJ, Zandvliet AS, Beijnen JH, Schellens JHM, Huitema ADR. Performance of Methods for Handling Missing Categorical Covariate Data in Population Pharmacokinetic Analyses. AAPS J 2012;14:601–11.

28. Hooker AC, Staatz CE, Karlsson MO. Conditional weighted residuals (CWRES): a model diagnostic for the FOCE method. Pharm Res 2007;24:2187–97.

29. Bergstrand M, Hooker AC, Wallin JE, Karlsson MO. Prediction-corrected visual predictive checks for diagnosing nonlinear mixed-effects models. AAPS J 2011;13:143–51.

30. Blesch KS, Gieschke R, Tsukamoto Y, Reigner BG, Burger HU, Steimer J-L. Clinical pharmacokinetic/pharmacodynamic and physiologically based pharmacokinetic modeling in new drug development: the capecitabine experience. Invest New Drugs 2003;21:195–223.

31. Reigner B, Verweij J, Dirix L, Cassidy J, Twelves C, Allman D, et al. Effect of food on the pharmacokinetics of capecitabine and its metabolites following oral administration in cancer patients. Clin Cancer Res 1998;4:941–8.

32. Tabata T, Katoh M, Tokudome S, Hosakawa M, Chiba K, Nakajima M, et al. Bioactivation of capecitabine in human liver: involvement of the cytosolic enzyme on 5′-deoxy-5-fluorocytidine formation. Drug Metab Dispos 2004;32:762–7.

33. Naguib FN, el Kouni MH, Cha S. Enzymes of uracil catabolism in normal and neoplastic human tissues. Cancer Res 1985;45:5405–12.

34. Gilbert JA, Salavaggione OE, Ji Y, Pelleymounter LL, Eckloff BW, Wieben ED, et al. Gemcitabine pharmacogenomics: cytidine deaminase and deoxycytidylate deaminase gene resequencing and functional genomics. Clin Cancer Res 2006;12:1794–803.

35. Rosmarin D, Palles C, Church D, Domingo E, Jones A, Johnstone E, et al. Genetic markers of toxicity from capecitabine and other fluorouracil-based regimens: Investigation in the QUASAR2 study, systematic review, and meta-analysis. J Clin Oncol 2014;32:1031–9.

36. van Kuilenburg ABP, Häusler P, Schalhorn A, Tanck MWT, Proost JH, Terborg C, et al. Evaluation of 5-fluorouracil pharmacokinetics in cancer patients with

7

a c.1905+1G>A mutation in DPYD by means of a Bayesian limited sampling strategy. Clin Pharmacokinet 2012;51:163–74.

37. Deenen MJ, Tol J, Burylo AM, Doodeman VD, de Boer A, Vincent A, et al. Relationship between single nucleotide polymorphisms and haplotypes in DPYD and toxicity and efficacy of capecitabine in advanced colorectal cancer. Clin Cancer Res 2011;17:3455–68.

7

SUPPLEMENTARY TABLE

Table S1. Overview of evaluated covariate-parameter effects.

Included covariate effects	Value	dOFV
Partial gastrectomy on k_{tr} *	1.48	-9.47
Total gastrectomy on k_{tr} *	3.18	-29.84
DPYD*2A on $k_{5-fu>fbal}$	0.785	-7.12
Effect of age on CL_c/F_{fbal}	-0.97	-40.71
Effect of gender on CL_c/F_{fbal}	0.757	-25.89

Evaluated covariate effects that were not included in the model

Esophagogastrectomy on k_{tr}
CDA c.79A>C on CL_c/F_{dfcr}
DPYD c.2846A>T on $k_{5-fu>fbal}$
DPYD c.1236G>A on $k_{5-fu>fbal}$
Effect of age on k_{tr}, CL_c/F_{cap}, CL_c/F_{dfcr}, $k_{dfur>5-fu}$, $k_{5-fu>fbal}$
Effect of gender on k_{tr}, CL_c/F_{cap}, CL_c/F_{dfcr}, $k_{dfur>5-fu}$, $k_{5-fu>fbal}$

* These covariate effects were included in the first phase of model development. Estimates of the covariate effects were slightly different compared to the final run estimates of the final run.
Abbreviations: dOFV, delta objective function value; k_{tr}, transit rate constant; CL_c/F, apparent clearance of central compartment; k rate constant; *DPYD*, dihydropyrimidine dehydrogenase; *CDA*, cytidine deaminase; CAP, capecitabine; dFCR, 5'-deoxy-5-fluorocytidine; dFUR, 5'-deoxy-5-fluorouridine; 5-FU, 5-fluorouracil; FBAL, fluoro-β-alanine.

7

C H A P T E R   8

A PHASE 0 CLINICAL TRIAL OF NOVEL CANDIDATE EXTENDED-RELEASE FORMULATIONS OF CAPECITABINE

Bart A.W. Jacobs, Jelte Meulenaar, Hilde Rosing, Dick Pluim, Matthijs M. Tibben,
Niels de Vries, Bastiaan Nuijen, Alwin D.R. Huitema, Jos H. Beijnen,
Jan H.M. Schellens, Serena Marchetti

ABSTRACT

Purpose

To examine the pharmacokinetic (PK) profile of several candidate extended-release (ER) formulations of capecitabine in patients.

Methods

In a phase 0 clinical study PK profiles of several oral candidate ER formulations of capecitabine were compared to the PK profile of capecitabine after administration of the commercially available immediate release (IR) tablet. A single dose of 1000 mg IR formulation (two 500 mg tablets) was administered on day 1 and a single dose of a 1000 mg candidate ER formulation of capecitabine (two 500 mg tablets) was administered on day 2. Candidate ER formulations of capecitabine differed with regard to the amount of the ER excipient (Kollidon® SR) in tablet matrix (0-5% w/w) and coating (0-12 mg/cm^2).

Results

PK profiles of 9 different candidate ER formulations were examined. The tablet coating seemed the main determinant for ER of capecitabine and tablet integrity. Average (± standard deviation) AUC_{0-2h}, relative to AUC_{0-2h} after oral administration of the IR tablet, were 43.3% (±34.9%) and 1.2% (±1.2%) for candidate ER formulations coated with 3 and 6 mg/cm^2, respectively. Corresponding AUC_{0-last} were 93.6% (±40.2%) and 44.0% (±5.4%).

Conclusion

Modulation of capecitabine release in patients can be accomplished by varying tablet coating content. Proof of principle was demonstrated for candidate ER formulations with coating content of 3 mg/cm^2.

INTRODUCTION

Capecitabine is an orally available pre-prodrug of 5-fluorouracil (5-FU) that is used for treatment of colorectal, gastric and breast cancer. The recommended dosing schedule of capecitabine is 1250 mg/m^2 twice daily on day 1-14 of a 21-day cycle [1,2]. Currently commercially available capecitabine formulations are immediate-release (IR) tablets. After oral administration of these tablets, capecitabine is rapidly and almost completely absorbed. Capecitabine is subsequently converted to 5-FU through a three-step enzymatic cascade. Time to maximum plasma concentration (t_{max}) of capecitabine and 5-FU is approximately 1-1.5 h with high and variable peak concentrations [3,4]. Average elimination half-life of both compounds is less than 1 h [3–5]. Approximately 80% percent of formed 5-FU is catabolized to inactive metabolites by the enzyme dihydropyrimidine dehydrogenase (DPD) [5], while only a small fraction of 5-FU is anabolized to active metabolites that inhibit cell proliferation through inhibition of thymidylate synthase (TS) and misincorporation in DNA and RNA [6,7]. Capecitabine and 5-FU are undetectable in plasma approximately 6 hours after oral intake [3,4]. As a consequence, a gap in exposure to capecitabine and 5-FU of approximately 6 hours is expected within every dosing interval according to the twice daily administration schedule of the currently available IR capecitabine.

Approximately 10-30% of patients who are treated with capecitabine will develop severe ($\geq$ National Cancer Institute Common Toxicity Criteria grade 3) toxicity and treatment-related death is observed in approximately 0.5-1% of patients [8–10]. The treatment-induced toxicity is poorly predictable and seriously limits the clinical application of capecitabine.

Previously, tolerability, but also efficacy, of 5-FU continuous infusion was shown to be superior to 5-FU bolus administration [11]. Currently available IR formulations of capecitabine lead to short lasting 5-FU exposure, which resembles the PK profile of 5-FU after intravenous bolus infusion. In view of this, a more continuous exposure to capecitabine might reduce toxicity and improve efficacy and thus improve the clinical applicability of capecitabine.

Extended-release (ER) formulations may overcome the exposure gap of IR capecitabine formulations. Previously, we reported slow dissolution behavior of amorphous capecitabine compared to crystalline capecitabine [12]. A prototype ER tablet formulation was developed with amorphous capecitabine [13]. This prototype ER tablet contained a co-spray dried (CoSD) mixture of capecitabine and the ER excipient Kollidon® SR (98% capecitabine / 2% Kollidon® SR, w/w). Based on *in vitro – in vivo* correlation modeling, it was estimated that this prototype formulation would lead to 12 hours of continuous exposure to capecitabine after oral administration in patients [13]. In addition, several other candidate ER formulations of capecitabine were developed that contained 500 mg amorphous capecitabine, but differed with respect to the content of Kollidon® SR in the CoSD mixture. To further modulate capecitabine dissolution, candidate ER tablets were also coated with Kollidon® SR with variable coating thicknesses. These candidate ER formulations of capecitabine were all available for clinical testing.

8

A phase 0 clinical study design is attractive for early evaluation of pharmacokinetics (PK) of novel drugs or formulations [14]. The current phase 0 study was performed to investigate the candidate ER formulations of capecitabine to allow rapid selection of the most promising formulation for further clinical development. The primary objective of this study was to examine the PK of these candidate ER formulations of capecitabine in comparison with the original IR formulation of capecitabine.

MATERIALS AND METHODS

Patient selection

Patients aged $\geq$ 18 years with advanced solid tumors, World Health Organization (WHO) performance status of $\leq$2, a life expectancy of at least 3 months, and adequate bone marrow, hepatic and renal function were eligible for enrollment. Relevant exclusion criteria were known DPD deficiency, as demonstrated by a *DPYD*2A* genetic mutation, bowel obstructions or motility disorder that might influence the absorption of capecitabine. Patients provided written informed consent before study enrollment. The study was approved by the independent Medical Ethics Committee of The Netherlands Cancer Institute and was conducted in accordance with Good Clinical Practice guidelines and the Declaration of Helsinki, and registered in the Dutch Trial Registry (http://www.trialregister.nl, study identifier: NTR3647).

Candidate ER formulations of capecitabine

Capecitabine was CoSD with Kollidon® SR as previously described [13]. The content of Kollidon® SR in the CoSD mixture was variable: 0, 1, 2, 3, 4, or 5% (w/w). All candidate ER formulations contained 500 mg of capecitabine. Magnesium stearate and silica colloidalis anhydrica were added to the CoSD powder of capecitabine and Kollidon® SR before tableting. Tableting of candidate ER formulations of capecitabine was previously described [13].

Candidate ER tablets were coated with Kollidon® SR that was dissolved in a mixture of acetone: isopropanol (1:1, v/v) at ambient temperature. Talcum was dispersed in this mixture for manufacturing purposes. Using a pan-coating procedure, the mixture of Kollidon® SR and talcum (2:1, w/w) was applied on the tablet surfaces with variable amounts, leading to final coating contents of 0, 3, 6, 9 and 12 mg/cm^2.

In total, 30 different candidate ER formulations containing 500 mg of capecitabine with 0-5% (w/w) Kollidon® SR within tablet matrix and coating contents of 0-12 mg/cm^2 were available for clinical testing in this phase 0 study. In addition, a capecitabine formulation with 500 mg of crystalline capecitabine was produced with a coating content of 6 mg/cm^2. Production of the candidate ER formulations of capecitabine was performed under Good Manufacturing Practice (GMP) conditions.

Study design

This was a single center, open-label, pharmacological cross-over study in which the PK profile of different oral ER formulations of capecitabine were compared to the PK profile

of IR capecitabine (Xeloda®). Patients were hospitalized during three consecutive days. On the first day, patients received a single dose of 1000 mg IR capecitabine (two tablets of 500 mg) at approximately 9:00 h. On the second day, patients received a single dose of 1000 mg of one candidate ER formulation of capecitabine (two tablets of 500 mg) at approximately 9:00 h. Patients fasted overnight before intake of the study medication and were not allowed to eat and drink (except a small amount of water < 50 mL) up to 1 hour after drug intake to prevent interference of food on capecitabine absorption. Blood samples for PK analysis were collected just before and after oral administration of IR capecitabine and of a candidate ER formulation of capecitabine. A follow-up visit was planned on day 9 of the study for examination of preliminary safety. Toxicity was scored according to the Common Terminology Criteria for Adverse Events version 4.03. Only one candidate ER formulation was tested in each patient. The study design is illustrated in Figure 1.

Based on obtained PK data from previously tested ER formulations and before enrollment of a subsequent patient, a decision was made which candidate ER formulation to apply next for in clinical examination.

Predefined criteria for adequate ER of capecitabine were a) mean area under the capecitabine plasma-concentration time curve (AUC) to the last quantifiable observation (AUC_{0-last}) was $\geq$ 50% of the mean AUC_{0-last} of capecitabine after intake of the same dose of IR capecitabine and, b) mean AUC of capecitabine up to 2 hours (AUC_{0-2h}) that was <50% of that of IR capecitabine. The number of candidate ER formulations to be examined was limited to 12. Each tested formulation was administered to a minimum of 1 and up to a maximum of 3 patients, except for one candidate ER formulation. Extension of administration up to a maximum of 6 patients was allowed for one formulation.

PHARMACOKINETIC ANALYSES

Peripheral blood was collected at baseline and after oral administration of 1000 mg IR capecitabine and after 1000 mg of a candidate capecitabine ER formulation (Figure 1). Samples were collected at baseline and at 0.5, 1, 1.5, 2, 3, 4, 6, 12 and 24 h after drug administration. After intake of a candidate capecitabine ER formulation, an additional blood sample was collected 33 h postdose.
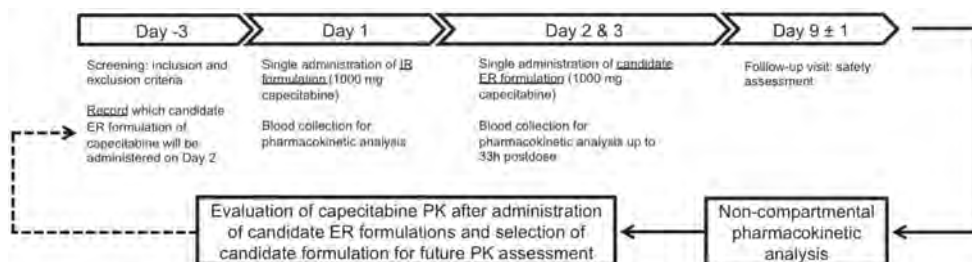
Figure 1. Phase 0 clinical study design. Abbreviations: IR = immediate-release, ER = extended-release, PK = pharmacokinetic

Blood samples were collected in lithium-heparinized tubes, gently mixed and directly placed on ice, followed by centrifugation at 1500 g for 10 min at 4°C. Plasma was isolated and stored at -70°C until analysis. Capecitabine and its metabolites 5'-deoxy-5-fluorocytidine (dFCR), 5'-deoxy-5-fluorouridine (dFUR), 5-fluorouracil (5-FU) and fluoro-β-alanine (FBAL) were quantified using liquid chromatography with tandem mass spectrometric detection (LC–MS/MS) [15].

Non-compartmental PK analyses and descriptive statistics were performed with R version 3.1.2 [16]. A previously validated R script was used for non-compartmental PK analyses. Primary endpoints were relative AUC_{0-last} and AUC_{0-2h} of capecitabine, which were expressed by individual estimates of AUC_{0-last} and AUC_{0-2h} after intake of a candidate ER formulation as a percentage of the values after intake of IR capecitabine. Maximum plasma concentrations (C_{max}) and t_{max} were also extracted from the data.

RESULTS

A total of 15 patients were enrolled into this phase 0 study, of which 13 patients were evaluable for PK analyses (Supplementary table 1). Two patients withdrew from the study due to decline in clinical status.

Pharmacokinetic results

Characteristics of candidate ER formulations of capecitabine that were examined are reported in Table 1. Coating content of the candidate ER formulations showed to be rate limiting for extended release of capecitabine in patients (Figure 2). The results did not suggest that the content of Kollidon® SR in the CoSD powder significantly contributed to ER of capecitabine in patients. Therefore, it was decided to pool the PK data of the candidate ER formulations of capecitabine based on tablet coating content. The corresponding PK data of the different tested formulations are given in Table 2.

Formulation A (5% Kollidon® SR within the tablet matrix without coating) was the first tested candidate ER formulation of capecitabine. The observed PK profile of formulation A (upper left panel of Figure 2B) was similar to the pattern observed after intake of IR capecitabine (Figure 2A). Formulation I, containing the highest tested tablet coating content (12 mg/cm²) was selected next for PK examination. Administration of this formulation, however, did not lead to any detectable levels of capecitabine in plasma.

The relative AUC_{0-2h} and AUC_{0-last} for candidate ER formulations of capecitabine with coating contents of 3 mg/cm² were on average (± sd) 43.3% (±34.9%) and 93.6% (±40.2%), respectively.

The relative AUC_{0-2h} for formulations with a coating content of 6 mg/cm² was on average (± sd) 1.2% (±1.2%). Of the examined candidate ER formulations coated with 6 mg/cm², the tablet matrices contained 5% Kollidon® SR (formulation E), 0% Kollidon® SR (formulation F) or consisted of crystalline capecitabine (formulation G). As shown, these candidate ER formulations lead to exposure of capecitabine up to 33 hours (lower left panel Figure 2B). Differences with respect to the content of Kollidon® SR in the tablet matrix or the use of crystalline instead of amorphous capecitabine did not influence

Table 1. Characteristics of the tested candidate extended-release formulations of capecitabine. All formulations contained 500 mg of capecitabine and differed with respect to tablet coating content and proportion of Kollidon® SR in co-spray dried powder that was used for tableting.

Formulation	Coating content (mg/cm²)	Kollidon® SR in tablet matrix (%, w/w)[b]	Number of patients
A	0	5	3
B	3	5	2
C	3	4	2
D	3	0	1
E	6	5	1
F	6	0	1
G[a]	6	0	1
H	9	5	1
I	12	5	1

[a] Contains crystalline instead of amorphous capecitabine
[b] Percent of Kollidon® SR in co-spray dried powder with capecitabine

8
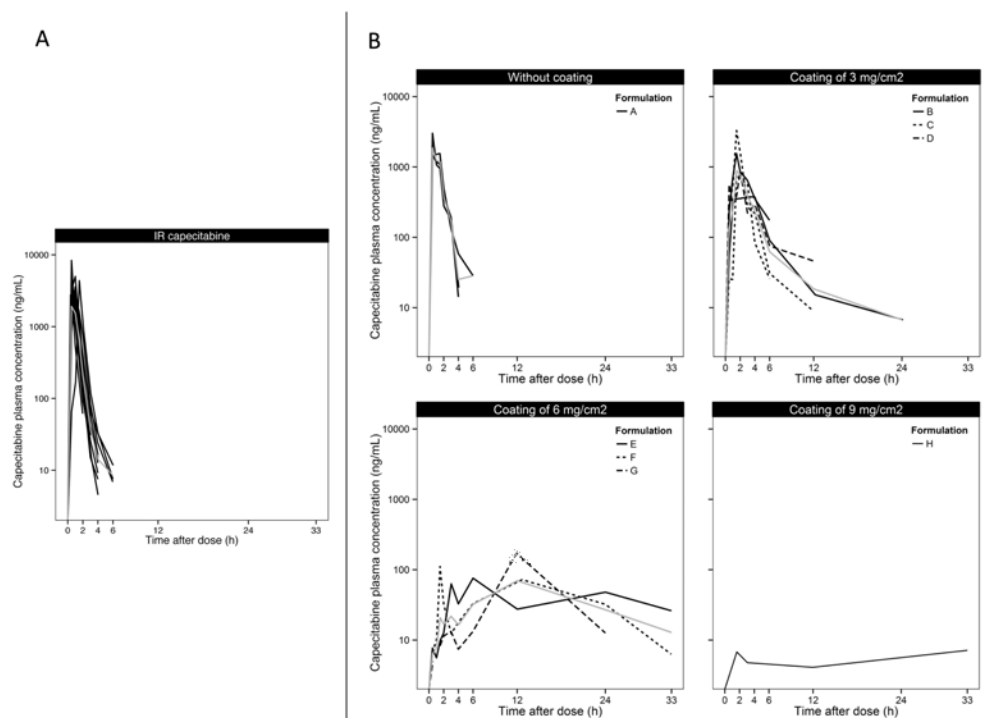
Figure 2. Log plasma concentration of capecitabine vs. time after administration of 1000 mg IR capecitabine (A) and 1000 mg candidate ER formulation of capecitabine (B). Pharmacokinetic profiles of candidate ER formulations were grouped by coating content and formulation code. A total of 13 patients were evaluable for pharmacokinetic analyses. Pharmacokinetic profiles of individual patients are shown in black. Grey lines represent average capecitabine plasma exposure. Abbreviations: IR = immediate-release, ER = extended-release.

Table 2. Pharmacokinetic parameters for capecitabine after oral administration of IR capecitabine and candidate ER formulations. Pharmacokinetic results for candidate ER formulations are grouped according on tablet coating content. Capecitabine could not be detected in plasma after administration of the candidate ER formulation with coating content of 12 mg/cm² (Formulation I).

Parameter	IR capecitabine	Candidate ER formulations of capecitabine			
		Tablet coating 0 mg/cm²	Tablet coating 3 mg/cm²	Tablet coating 6 mg/cm²	Tablet coating 9 mg/cm²
	Mean ± SD (N=13)	Mean ± SD (N=3)	Mean ± SD (N=5)	Mean ± SD (N=3)	Estimate (N=1)
AUC_{0-last} (μg*h/mL)	3.20 ± 0.96	2.73 ± 0.32	2.67 ± 0.94	1.43 ± 0.25	0.17
Relative AUC_{0-last} (%) [a]	N/A	107 ± 20.0	93.6 ± 40.2	44.0 ± 5.4	3.4
AUC_{0-2h} (μg*h/mL)	3.00 ± 0.93	2.33 ± 0.32	1.17 ± 0.83	0.03 ± 0.03	0.01
Relative AUC_{0-2h} (%) [a]	N/A	95.8 ± 16.6	43.3 ± 34.9	1.2 ± 1.2	0.1
C_{max} (μg/mL)	3.80 ± 1.64	2.00 ± 0.87	1.38 ± 1.16	0.12 ± 0.05	0.01
t_{max} (h)	0.72 ± 0.35	0.82 ± 0.57	1.92 ± 0.69	6.50 ± 5.22	33

[a] Relative AUC_{0-last} and AUC_{0-2h} were normalized to corresponding estimates for IR capecitabine
Abbreviations: AUC_{0-last} = area under the plasma concentration-time curve up to last observation, AUC_{0-2h} = area under the plasma concentration-time curve up to 2h post dose C_{max} = maximum plasma concentration, t_{max} = time to reach maximum plasma concentration, SD = standard deviation, IR = immediate-release, ER = extended-release, N/A = not applicable, N = number of patients

8

the PK profile of capecitabine. The average relative AUC_{0-last} for formulations with coating content of 6 mg/cm^2 was below 50%.

The candidate ER formulation with coating content of 9 mg/cm^2 resulted in relatively low capecitabine exposure.

The PK results of capecitabine metabolites were in agreement with the findings from the PK profiles of capecitabine (Supplementary table 2). Based on the available PK results, it was found that coating content was crucial for ER release of capecitabine in patients. Examination of other candidate ER formulations would most probably not lead to other insights and was therefore considered unnecessary.

Average AUC_{0-2h} and AUC_{0-last} of tablet formulations with 3 mg/cm^2 met predefined criteria for ER of capecitabine. However, these results were influenced by a single observation of 104% for AUC_{0-2h} of one out of two patients exposed to formulation C, which indicated immediate release of capecitabine. Altogether, proof of concept was demonstrated for candidate ER formulations for capecitabine with coating content of 3 mg/cm^2.

Preliminary tolerability

Adverse events that were possibly, probably or definitely related to study treatment were grade 1 diarrhea in one patient, grade 2 diarrhea in one patient and grade 3 fatigue in one patient.

DISCUSSION

This is, to our knowledge, the first report that describes the applicability of a phase 0 trial design for development and optimization of an oral extended-release formulation in oncology. Within one year, this trial design enabled rapid examination of pharmacokinetics of nine candidate ER formulations of capecitabine in patients.

The availability of multiple candidate ER formulations of capecitabine allowed for a PK-driven study approach. The candidate ER formulation to apply in the next included patient was chosen based on PK results obtained by the patient previously treated in the study. A major advantage of this approach is that candidate ER formulations can be selected based on actual clinical data. This was especially important since the first tested candidate ER formulation, which was selected based on *in vitro* dissolution data, did not show any ER properties in humans. This implies poor predictability of the *in vitro* dissolution test for *in vivo* absorption behavior.

Results of this study suggest that prolonged exposure to capecitabine in patients can be achieved with candidate ER formulations of capecitabine. Particularly, coating content of the candidate ER formulations seems to be essential for slow release of capecitabine. Results do not suggest that the content of Kollidon® SR in the CoSD powder significantly contributed to *in vivo* ER of capecitabine. Therefore, release of capecitabine from candidate ER formulations seems to be rate-limited by the tablet coating thickness. The uncoated candidate formulation with 5% Kollidon® SR in the CoSD powder resulted in immediate release of capecitabine. However, *in vitro* examination of a prototype

8

with only 2% Kollidon® SR in the CoSD powder showed capecitabine release for up to 12 hours [13].

Application of tablet coating seems to be crucial to prevent disintegration of the tested candidate formulations and to maintain ER characteristics. It appears that candidate ER formulations with coating content of 3, 6, 9 and 12 mg/cm^2 have unique PK profiles. On average, formulations with coating content of 3 mg/cm^2 seem to fulfill predefined criteria of adequate ER of capecitabine. However, immediate release of capecitabine was observed in one patient after oral administration of formulation C, which might be explained by an incomplete coverage of the whole tablet with this relative thin coating, resulting in rapid disintegration of the tablet. Tablet coating content of 12 mg/cm^2 prevents the candidate ER formulation from disintegration at all. Although a coating of 12 mg/cm^2, but also 9 mg/cm^2, provides formulation robustness, coating thickness seems too high for significant release of capecitabine.

Candidate ER formulations with coating content of 6 mg/cm^2 provide continuous capecitabine exposure for over 24 hours, with acceptable relative AUC_{0-2h} but with rather low relative AUC_{0-last}. The findings also suggest that amorphous capecitabine, which showed slow dissolution *in vitro* compared to crystalline capecitabine [12], is not important for slow dissolution of capecitabine in patients. Results from the study point out that ER of capecitabine can be achieved by modulation of tablet coating content and that subtle deviations in coating content highly affect capecitabine release and plasma exposure.

The use of amorphous capecitabine requires that tablets are stored in the refrigerator or freezer to ensure physical stability [12, 13]. For this reason, the use of crystalline capecitabine, which is physically stable at ambient temperatures and therefore more convenient, is considered for the future ER formulation of capecitabine. Kollidon® SR will be omitted from the tablet matrix, since the presence of this excipient in the tablet matrix did not attribute to ER of capecitabine in patients.

A reproducible coating process is crucial for the manufacturing of the subsequent ER formulation of capecitabine. Optimization of critical tablet coating parameters, such as pan speed, coating time and temperature during the coating process, is required to improve tablet coating reproducibility and robustness.

Others have also described development of extended-release formulations of capecitabine. Agnihotri et al. developed capecitabine-loaded hydrogel microsphere that showed slow release of capecitabine *in vitro* [17]. Singh et al. developed a prototype mucoadhesive cum floating gastroretentive system containing amorphous capecitabine that showed extended release of capecitabine in rats [18]. However, no data are available describing the translation of their concepts to the clinical situation.

Diarrhea and fatigue are common side effects after administration of capecitabine [8]. Preliminary observed toxicity after a single oral dose of study drug administered was mild and did not require intervention or special attention. A clinical phase I dose-escalation study is needed to further evaluate the safety of ER capecitabine treatment and to determine the maximum tolerated dose and preliminary efficacy.

In conclusion, a unique and innovative study was performed with the goal to accelerate the development of an ER formulation of capecitabine. The PK profiles of nine different candidate formulations for ER of capecitabine were examined in patients within a short period of time. Modulation of capecitabine release can be accomplished by varying tablet coating content and proof of principle was demonstrated for candidate ER formulations with coating content of 3 mg/cm^2.

ACKNOWLEDGMENTS

8

REFERENCES

1. Schellens JHM. Capecitabine. Oncologist 2007;12:152–5.

2. Midgley R, Kerr DJ. Capecitabine: have we got the dose right? Nat Clin Pract Oncol 2009;6:17–24.

3. Budman DR, Meropol NJ, Reigner B, Creaven PJ, Lichtman SM, Berghorn E, et al. Preliminary studies of a novel oral fluoropyrimidine carbamate: capecitabine. J Clin Oncol 1998;16:1795–802.

4. Mackean M, Planting A, Twelves C, Schellens J, Allman D, Osterwalder B, et al. Phase I and pharmacologic study of intermittent twice-daily oral therapy with capecitabine in patients with advanced and/or metastatic cancer. J Clin Oncol 1998;16:2977–85.

5. Reigner B, Blesch K, Weidekamm E. Clinical pharmacokinetics of capecitabine. Clin Pharmacokinet 2001;40:85–104.

6. de Bono JS, Twelves CJ. The oral fluorinated pyrimidines. Invest New Drugs 2001;19:41–59.

7. Wilson PM, Danenberg PV, Johnston PG, Lenz H-J, Ladner RD. Standing the test of time: targeting thymidylate biosynthesis in cancer therapy. Nat Rev Clin Oncol 2014;11:282–98.

8. Twelves C, Wong A, Nowacki MP, Abt M, Burris H, Carrato A, et al. Capecitabine as adjuvant treatment for stage III colon cancer. N Engl J Med 2005;352:2696–704.

9. Scheithauer W, McKendrick J, Begbie S, Borner M, Burns WI, Burris HA, et al. Oral capecitabine as an alternative to i.v. 5-fluorouracil-based adjuvant therapy for colon cancer: Safety results of a randomized, phase III trial. Ann Oncol 2003;14:1735–43.

10. Mikhail SE, Sun JF, Marshall JL. Safety of capecitabine: a review. Expert Opin Drug Saf 2010;9:831–41.

11. Meta-analysis Group In Cancer. Efficacy of intravenous continuous infusion of fluorouracil compared with bolus administration in advanced colorectal cancer. J Clin Oncol 1998;16:301–8.

12. Meulenaar J, Beijnen JH, Schellens JHM, Nuijen B. Slow dissolution behaviour of amorphous capecitabine. Int J Pharm 2013;441:213–7.

13. Meulenaar J, Keizer RJ, Beijnen JH, Schellens JHM, Huitema ADR, Nuijen B. Development of an extended-release formulation of capecitabine making use of in vitro-in vivo correlation modelling. J Pharm Sci 2013:478–84.

14. Marchetti S, Schellens JHM. The impact of FDA and EMEA guidelines on drug development in relation to Phase 0 trials. Br J Cancer 2007;97:577–81.

15. Deenen MJ, Rosing H, Hillebrand MJ, Schellens JHM, Beijnen JH. Quantitative determination of capecitabine and its six metabolites in human plasma using liquid chromatography coupled to electrospray tandem mass spectrometry. J Chromatogr B Analyt Technol Biomed Life Sci 2013;913-914:30–40.

16. R Development Core Team. R: A Language and Environment for Statistical Computing. Vienna, Austria: R Foundation for Statistical Computing, 2016.

17. Agnihotri SA, Aminabhavi TM. Novel interpenetrating network chitosan-poly(ethylene oxide-g-acrylamide) hydrogel microspheres for the controlled release of capecitabine. Int J Pharm 2006;324:103–15.

18. Singh Y, Singh M, Meher JG, Pawar VK, Chourasia MK. Trichotomous gastric retention of amorphous capecitabine: An attempt to overcome pharmacokinetic gap. Int J Pharm 2014;478:811–21.

SUPPLEMENTARY TABLES

Table S1. Demographics of evaluable participants.

Characteristic	Number of patients	%
Total number of patients	13	
Sex		
Male	6	46
Female	7	54
Age		
Median (range), years	65 (48 – 75)	
WHO performance status		
0	5	38
1	7	54
2	1	8
Primary tumor type		
Colorectal	4	31
NSCLC	4	31
SCLC	1	8
Head and neck	1	8
Carcinoid	1	8
Bladder	1	8
Unknown	1	8
Stage of cancer		
Metastatic	13	100
Prior treatment		
Chemotherapy	13	100
Radiotherapy	4	31
Surgery	7	54

Abbreviations: WHO = World Health Organization, NSCLC = non-small cell lung cancer, SCLC = small cell lung cancer

8

8

Table S2. Summary of pharmacokinetic parameters for 5′-deoxy-5-fluorocytidine (dFCR), 5′-deoxy-5-fluorouridine (dFUR), 5-fluorouracil (5-FU) and fluoro-β-alanine (FBAL) after oral administration of IR capecitabine and candidate ER formulations. Pharmacokinetic results for candidate ER formulations are grouped according on tablet coating content.

| | Parameter | IR capecitabine | | Candidate ER formulations of capecitabine | | | | | | | |
| | | | | Tablet coating 0 mg/cm² | | Tablet coating 3 mg/cm² | | Tablet coating 6 mg/cm² | | Tablet coating 9 mg/cm² | |
		Mean ± SD	N	Mean ± SD	N	Mean ± SD	N	Mean ± SD	N	Estimate	N
dFCR	AUC$_{0\text{-last}}$ (µg*h/mL)	6.76 ± 3.32	13	4.71 ± 0.40	3	5.27 ± 1.97	5	4.69 ± 3.47	3	N/A	1
	Relative AUC$_{0\text{-last}}$ (%) [a]	N/A	N/A	98.0 ± 6.8	3	85.7 ± 17.7	5	66.8 ± 41.6	3	N/A	1
	AUC$_{0\text{-2h}}$ (µg*h/mL)	6.76 ± 3.32	13	3.40 ± 0.58	3	1.46 ± 0.79	5	0.05 ± 0.05	3	N/A	1
	Relative AUC$_{0\text{-2h}}$ (%) [a]	N/A	N/A	85.9 ± 7.3	3	31.1 ± 19.2	5	1.4 ± 1.6	3	N/A	1
	C$_{max}$ (µg/mL)	4.67 ± 1.93	13	2.58 ± 1.65	3	1.71 ± 0.91	5	0.44 ± 0.41	3	N/A	1
	t$_{max}$ (h)	0.88 ± 0.30	13	1.15 ± 0.58	3	2.40 ± 1.08	5	6.63 ± 4.98	3	N/A	1
dFUR	AUC$_{0\text{-last}}$ (µg*h/mL)	4.02 ± 1.20	13	3.37 ± 0.62	3	3.48 ± 1.38	5	2.31 ± 1.42	3	N/A	1
	Relative AUC$_{0\text{-last}}$ (%) [a]	N/A	N/A	90.0 ± 16.8	3	113 ± 47.9	5	49.2 ± 24.9	3	N/A	1
	AUC$_{0\text{-2h}}$ (µg*h/mL)	3.20 ± 1.07	13	2.45 ± 0.73	3	0.95 ± 0.31	5	0.03 ± 0.03	3	N/A	1
	Relative AUC$_{0\text{-2h}}$ (%) [a]	N/A	N/A	78.9 ± 10.1	3	42.9 ± 27.6	5	1.0 ± 1.1	3	N/A	1
	C$_{max}$ (µg/mL)	3.07 ± 1.53	13	1.88 ± 0.59	3	1.20 ± 0.57	5	0.22 ± 0.18	3	N/A	1
	t$_{max}$ (h)	0.96 ± 0.25	13	1.15 ± 0.58	3	2.40 ± 1.08	5	6.47 ± 5.22	3	N/A	1
5-FU	AUC$_{0\text{-t}}$ (µg*h/mL)	0.41 ± 0.17	13	0.25 ± 0.07	3	0.26 ± 0.13	5	N/A	3	N/A	1
	Relative AUC$_{0\text{-last}}$ (%) [a]	N/A	N/A	93.5 ± 21.9	3	79.3 ± 41.9	5	N/A	3	N/A	1
	AUC$_{0\text{-2h}}$ (µg*h/mL)	0.36 ± 0.15	13	0.21 ± 0.07	3	0.10 ± 0.03	5	N/A	3	N/A	1
	Relative AUC$_{0\text{-2h}}$ (%) [a]	N/A	N/A	80.7 ± 12.5	3	40.5 ± 32.3	5	N/A	3	N/A	1
	C$_{max}$ (µg/mL)	0.34 ± 0.20	13	0.16 ± 0.06	3	0.11 ± 0.05	5	N/A	3	N/A	1
	t$_{max}$ (h)	0.88 ± 0.30	13	1.15 ± 0.58	3	2.00 ± 0.61	5	N/A	3	N/A	1

Table S2. (continued)

| | | IR capecitabine | | Candidate ER formulations of capecitabine | | | | | | | |
| | Parameter | Mean ± SD | N | Tablet coating 0 mg/cm² | | Tablet coating 3 mg/cm² | | Tablet coating 6 mg/cm² | | Tablet coating 9 mg/cm² | |
				Mean ± SD	N	Mean ± SD	N	Mean ± SD	N	Estimate	N
	AUC_{0-t} (µg*h/mL)	13.8 ± 5.40	13	13.2 ± 10.4	3	14.8 ± 3.29	5	1.18 ± 3.75	3	0.69	1
	Relative AUC_{0-last} (%) [a]	N/A	N/A	107 ± 6.4	3	113 ± 14.4	5	62.2 ± 6.8	3	5.3	1
FBAL	AUC_{0-2h} (µg*h/mL)	3.05 ± 1.27	13	2.31 ± 1.49	3	0.83 ± 0.32	5	0.18 ± 0.10	3	0.59	1
	Relative AUC_{0-2h} (%) [a]	N/A	N/A	82.6 ± 16.1	3	28.4 ± 13.2	5	9.7 ± 10.0	3	1.3	1
	C_{max} (µg/mL)	2.87 ± 0.85	13	2.15 ± 0.91	3	1.90 ± 0.64	5	0.78 ± 0.23	3	0.04	1
	t_{max} (h)	1.86 ± 0.48	13	1.85 ± 0.30	3	3.61 ± 0.55	5	13.4 ± 9.2	3	2.12	1

[a] Relative AUC_{0-last} and AUC_{0-2h} were normalized to corresponding estimates for IR capecitabine.
N/A: not applicable, inadequate data for parameter estimation. Abbreviations: AUC_{0-last} = area under the plasma concentration-time curve up to last observation, AUC_{0-2h} = area under the plasma concentration-time curve up to 2h post dose C_{max} = maximum plasma concentration, t_{max} = time to reach maximum plasma concentration, SD = standard deviation, ER = extended-release, N/A = not applicable, N = number of patients, dFCR = 5'-deoxy-5-fluorocytidine, dFUR = 5'deoxy-5-fluorouridine, 5-FU = 5-fluorouracil, FBAL = fluoro-beta-alanine, IR = immediate-release

8

CHAPTER 9

EXPLORING THE INTRACELLULAR PHARMACOKINETICS
OF THE 5-FLUOROURACIL NUCLEOTIDES DURING
CAPECITABINE TREATMENT

Ellen J.B. Derissen, Bart A.W. Jacobs, Alwin D.R. Huitema, Hilde Rosing,
Jan H.M. Schellens, Jos H. Beijnen

ABSTRACT

Aim

Three intracellularly formed metabolites are responsible for the antineoplastic effect of capecitabine: 5-fluorouridine 5'-triphosphate (FUTP), 5-fluoro-2'-deoxyuridine 5'-triphosphate (FdUTP), and 5-fluoro-2'-deoxyuridine 5'-monophosphate (FdUMP). The objective of this study was to explore the pharmacokinetics of these intracellular metabolites during capecitabine treatment.

Methods

Serial plasma and peripheral blood mononuclear cell (PBMC) samples were collected from 13 patients treated with capecitabine 1000 mg QD (group A) and eight patients receiving capecitabine 850 mg m^{-2} BID for fourteen days, every three weeks (group B). Samples were collected on day 1 and, for four patients of group B, also on day 14. The capecitabine and 5-fluorouracil (5-FU) plasma concentrations and intracellular metabolite concentrations were determined using LC–MS/MS. Pharmacokinetic parameters were estimated using non-compartmental analysis.

Results

Only FUTP could be measured in the PBMC samples. The FdUTP and FdUMP concentrations were below the detection limits (LOD). No significant correlation was found between the plasma 5-FU and intracellular FUTP exposure. The FUTP concentration–time profiles demonstrated considerable inter-individual variation and accumulation of the metabolite in PBMCs. FUTP levels ranged between <LOD and 1.0 µM on day 1, and from 0.64 to 14 µM on day 14. The area under the FUTP concentration–time curve was significantly increased on day 14 of the treatment compared to day 1 (mean ± SD: 28 ± 19 µM h vs. 2.0 ± 1.9 µM h).

Conclusions

To our knowledge, this is the first time that intracellular FUTP concentrations were measured in patients treated with capecitabine. During 14 days of treatment with capecitabine twice daily, intracellular accumulation of FUTP occurs.

INTRODUCTION

Capecitabine is a widely used chemotherapeutic agent, which has an important place in the treatment of several malignancies, including colorectal, gastric, pancreatic, breast and head and neck cancer. It was developed as a tumour-selective prodrug of 5-fluorouracil (5-FU). After oral administration, capecitabine is extensively absorbed from the gastrointestinal tract, and then converted into 5-FU by an enzymatic cascade involving three steps (Figure 1). First, capecitabine is converted to 5'-deoxy-5-fluorocytidine (5'-dFCR) by carboxylesterase, an enzyme located primarily in the liver. 5'-dFCR is then converted to 5'-deoxy-5-fluorouridine (5'-dFUR) by cytidine deaminase, which is principally located in the liver and in tumour tissue. The third step, the conversion of 5'-dFUR to 5-FU is catalysed by thymidine phosphorylase. This enzyme is present at higher concentrations in solid tumour tissue than in normal tissues [1]. Therefore, the third activation step preferentially takes place in tumour tissue rather than normal tissue [2].

5-FU is further activated intracellularly by ribosylation and sequential phosphorylation. Ultimately, three intracellularly formed metabolites (nucleotides) are held responsible for the antineoplastic effect of capecitabine. These are 5-fluorouridine 5'-triphosphate (FUTP), 5-fluoro-2'-deoxyuridine 5'-triphosphate (FdUTP), and 5-fluoro-2'-deoxyuridine 5'-monophosphate (FdUMP). In brief, FUTP is incorporated into RNA and interferes with normal RNA processing and function. FdUTP is incorporated into DNA, leading to DNA damage and ultimately cell death. FdUMP inhibits thymidylate synthase, the enzyme that catalyses the transformation of deoxyuridine monophosphate (dUMP) to deoxythymidine monophosphate (dTMP). Inhibition of thymidylate synthase by FdUMP leads to accumulation of deoxyuridine triphosphate (dUTP) and depletion of deoxythymidine triphosphate (dTTP). This imbalance has deleterious consequences for DNA synthesis and repair, ultimately leading to cell death (Figure 1) [3,4].

As the anticancer activity of capecitabine depends on these three 5-FU nucleotides, it would be interesting and clinically relevant to monitor their intracellular concentrations during capecitabine treatment. This would provide insight into the amounts of activated drug reaching the site of action. This information could ultimately be very useful to optimize current treatment regimens.

Until now, information about the intracellular metabolism of the 5-FU nucleotides originated mainly from *in vitro* experiments and animal studies [5-8]. Little is known about the formation of 5-FU nucleotides in patients who are treated with 5-FU due to the long lack of a suitable bioanalytical assay.

Several studies were conducted that examined the FdUMP concentrations in tumour tissues of patients who were treated with an intravenous 5-FU bolus injection (500 mg m^{-2}) [9-11]. These studies used a competitive-binding assay with thymidylate synthase, isolated from Lactobacillus casei, as a binding protein. The quantification of FdUMP was based on the displacement of a known amount of radiolabelled [3H]-FdUMP, measured by scintillation counting [12].

However, for the quantification of FUTP and FdUTP in cells of patients who were treated with 5-FU, a sufficiently sensitive assay was missing. Therefore, we recently developed an
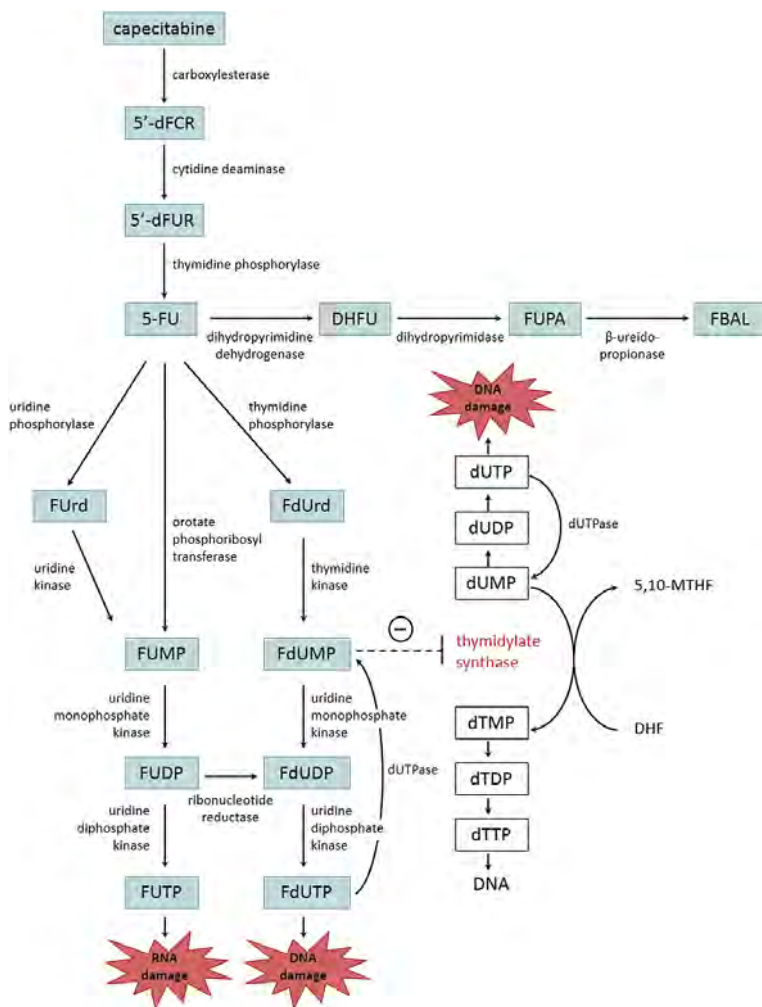
Figure 1. Capecitabine metabolism and mechanisms of action. Abbreviations: 5'-dFCR, 5'-deoxy-5-fluorocytidine; 5'-dFUR, 5'-deoxy-5-fluorouridine; DHFU, dihydrofluorouracil; FUPA, α-fluoro-β-ureidopropionic acid; FBAL, α-fluoro-β-alanine; 5-FU, 5-fluorouracil; FUrd, 5-fluorouridine; FdUrd, 5-fluoro-2'-*deoxy*uridine; FUMP, 5-fluorouridine 5'-monophosphate; FUDP, 5-fluorouridine 5'-diphosphate; FUTP, 5-fluorouridine 5'-triphosphate; FdUMP, 5-fluoro-2'-*deoxy*uridine 5'-monophosphate; FdUDP, 5-fluoro-2'-*deoxy*uridine 5'-diphosphate; FdUTP, 5-fluoro-2'-*deoxy*uridine 5'-triphosphate; dUMP, 2'-*deoxy*urdine 5'-monophosphate; dUDP, 2'-*deoxy*urdine 5'-diphosphate; dUTP, 2'-*deoxy*urdine 5'-triphosphate; dTMP, 2'-*deoxy*thymidine 5'-monophosphate; dTDP, 2'-*deoxy*thymidine 5'-diphosphate; dTTP, 2'-*deoxy*thymidine 5'-triphosphate; DHF, dihydrofolate; 5,10-MTHF, 5,10-methylene-tetrahydrofolate.

ultrasensitive liquid chromatography–tandem mass spectrometry (LC–MS/MS) assay for the quantification of the active 5-FU nucleotides in peripheral blood mononuclear cells (PBMCs) [13]. PBMCs were selected as a cell model for the intracellular activation, because they are easy to collect at various time points after drug administration. With the advent

of this assay, it has become possible to get insight into the intracellular 5-FU nucleotide concentrations in samples of patients who are treated with 5-FU or capecitabine.

The aim of the current study was to explore the intracellular pharmacokinetics (PK) of the three pharmacologically active 5-FU nucleotides during capecitabine treatment. Except for a small pilot in our previous publication on the development of a bioanalytical assay [13], this is, to our knowledge, the first time that intracellular 5-FU nucleotides were quantified during capecitabine treatment.

METHODS

Study design and treatment schedule

The intracellular PK of the active 5-FU nucleotides was assessed in two groups of patients. For group A, the intracellular PK of the 5-FU nucleotides was studied only on day 1 of the treatment. Based on the results in this group, we wondered if intracellular accumulation would occur during a treatment cycle, in which capecitabine is administered twice daily for 14 consecutive days. Therefore group B was added to the study. For this group the intracellular PK was examined on day 1 and also on day 14 of the treatment with capecitabine.

Group A included 13 patients treated with capecitabine for one of its approved therapeutic indications (e.g. colon, breast, pancreatic and gastric cancer). All patients received a one-time capecitabine dose of 1000 mg QD to study the PK, and were then treated with a standard dose. Patients were instructed not to eat or drink (except a small amount of water <50 ml) from 11 h before the drug intake until 1 h after drug intake. PBMC samples were collected on day 1 of the first treatment cycle, just before oral administration of capecitabine (pre-dose) and 1, 2, 4, 6 and 24 h after capecitabine administration. To monitor the capecitabine and 5-FU plasma concentrations, plasma samples were collected pre-dose and 0.5, 1, 1.5, 2, 3, 4, 6, 12 and 24 h after capecitabine intake.

Group B consisted of eight patients who participated in a phase I/II study in advanced gastro-oesophageal cancer. The primary objective of this study was to explore the safety and preliminary activity of the combination of docetaxel, oxaliplatin and capecitabine. Patients received capecitabine 850 mg m^{-2} twice daily for 14 days, every three weeks. Capecitabine tablets were taken with water within 30 min after a meal. PBMC samples were collected at day 1 of the first treatment cycle (for five patients) and at day 14 of this cycle (for four patients). PBMC samples were collected pre-dose and 2, 4, 6 and 8 h after oral capecitabine administration. For one patient an additional sample was taken 10 h after capecitabine administration. Plasma samples, to monitor the capecitabine and 5-FU plasma concentrations, were collected pre-dose and 0.5, 1, 2, 3, 4, 6 and 8 h after capecitabine intake. Sample collection at day 14 of the treatment was included in the protocol to examine whether intracellular accumulation of 5-FU nucleotides occurs during a treatment cycle.

The study was approved by the Medical Ethics Committee of our Institute and was conducted in accordance with the Declaration of Helsinki. All patients provided written informed consent before enrolment.

Quantification of capecitabine and 5-FU in plasma

Capecitabine and 5-FU were quantified in plasma by the two validated LC–MS/MS assays described by Deenen *et al.* [14]. In brief, stable labelled isotopes of the analytes were used as internal standards and added to 100 µl of plasma, followed by a protein precipitation step. The capecitabine assay was based on reversed-phase chromatography using an XBridge C18 column (50 mm × 2.1 mm ID, particle size 5 µm; Waters Corporation, Milford, MA, USA) and a mobile phase gradient, in which mobile phase A consisted of 0.05% formic acid in water and mobile phase B was 0.05% formic acid in methanol. For the quantification of 5-FU, the chromatography was performed on a Luna HILIC column (150 mm × 2.1 mm ID, particle size 3 µm; Phenomenex, Torrance, CA, USA) using isocratic elution with 10 mM formic acid in water (pH 4.0) mixed with acetonitrile (20:80, v/v). Detection of the analytes was performed on an API4000 triple quadrupole mass spectrometer equipped with an electrospray ionization probe (AB Sciex, Framingham, MA, USA). Capecitabine was detected in the positive ion mode and 5-FU in the negative ion mode. The lower limits of quantification (LLQs) of the assays were 139 nM for capecitabine and 384 nM for 5-FU [14].

Quantification of the 5-FU nucleotides in PBMCs

PBMCs were isolated and FUTP, FdUTP and FdUMP concentrations were determined as previously described using our validated LC–MS/MS assay [13]. In brief, 16 ml of blood was collected and PBMCs were isolated immediately using cold Ficoll-Paque PLUS density gradient (GE Healthcare, Pittsburgh, PA, USA). The collected PBMCs were resuspended in 70 µl PBS resulting in a homogeneous cell suspension with a total volume of approximately 100 µl. A 30 µl aliquot of this cell suspension was used to perform a cell count using a haematology analyser (Cell-Dyn Sapphire; Abbott Diagnostics). A 60 µl aliquot of the cell suspension was used for determination of the 5-FU nucleotide concentrations. To this end, cells were lysed by the addition of 100 µl methanol and extensive vortex mixing. After centrifugation, the supernatant (PBMC lysate) was collected and stored at −70 °C until analysis. Directly prior to LC–MS/MS analysis, the PBMC lysates were spiked with internal standard. Chromatographic separations were performed by weak anion exchange chromatography using a Biobasic AX column (50 mm × 2.1 mm ID, particle size 5 µm, Thermo Scientific). A stepwise gradient was used, in which the eluent pH was increased and the NH_4Ac concentration decreased. Detection was performed using a QTrap 5500 mass spectrometer equipped with an electrospray ionization probe operating in the negative ion mode (AB Sciex). The LLQs *in PBMC lysate* were 0.488 nM for FUTP, 1.66 nM for FdUTP and 0.748 nM for FdUMP. Accuracies were between −2.2 and 7.0% deviation for all analytes, and the coefficient of variation values were ≤4.9% [13].

The analytical results, expressed as nM in PBMC lysate, were multiplied with the lysate sample volume to obtain the absolute 5-FU nucleotide amounts in a sample. These amounts were then divided by the number of cells present in the sample to obtain the 5-FU nucleotide amounts *per 10^6 PBMCs*. Intracellular concentrations are generally expressed as the amount of drug per 10^6 cells. However, in order to compare the intracellular concentrations with the plasma concentrations, the intracellular concentrations were also converted to the amount of drug *per volume unit (µM)*. To this end, we measured the number of lymphocytes, monocytes and (residual) granulocytes in each individual sample and used the mean cell volumes of lymphocytes (174 fL), monocytes (339 fL) and granulocytes (302 fL) as determined by Sharma *et al.* [15] and later confirmed by Simiele *et al.* [16].

Pharmacokinetic and statistical analysis

The individual non-compartmental PK parameters in plasma and in PBMCs were determined using validated scripts in the software package R (version 3.1.2). The mean and coefficient of variation (CV) of the following PK parameters were reported: the maximum observed concentration (C_{max}), the time to reach C_{max} (t_{max}) and the area under the concentration–time curve between $t = 0$ and the time point of the last quantifiable data point (AUC_{0-t}).

For the plasma samples, also the terminal elimination half-life ($t_{1/2}$) was calculated, using the terminal elimination rate constant (k_e) based on the last three data points. For the calculation of the mean $t_{1/2}$, only curves that contained sufficient data points to assess this parameter were included. This meant that curves lacking a clear elimination phase were excluded from the calculation of this specific PK parameter. For the PBMC samples, the $t_{1/2}$ could not be calculated due to the limited number of data points in the descending part of the FUTP curves. The intracellular FUTP concentrations after 24 h were reported as a percentage of the C_{max}.

The relationship between the plasma 5-FU exposure and intracellular FUTP exposure was explored. Pearson's correlation was used to assess whether there was a linear relationship between the AUC_{0-t} of 5-FU in plasma and the AUC_{0-t} of FUTP measured in PBMCs. The correlation was considered statistically significant if the *P* value was less than 0.05.

To assess whether intracellular accumulation occurred during 14 days of capecitabine treatment twice daily, the AUC_{0-8h} values for FUTP determined on day 1 and on day 14 of the treatment were compared. A one-sided Mann–Whitney U test was performed to assess (for group B) whether there was a significant increase of the AUC_{0-8h} values for intracellular FUTP at day 14 compared to day 1. The result was considered statistically significant if the *P* value was less than 0.025. Statistical analyses were performed using SPSS Statistics version 23 (IBM Corp.).

9

RESULTS

Plasma pharmacokinetics

The mean plasma concentration–time curves for capecitabine and 5-FU are shown in Figure 2. The different shapes of the curves for group A and group B are probably related to whether or not the patients took food around the time of drug intake [17]. The results of the non-compartmental PK analysis are shown in Table 1. On average, the C_{max} for capecitabine was reached after 0.7 h in patient group A and after 3.3 h in group B. This difference is probably also related to the effect of food. The mean terminal elimination half-lives of capecitabine and 5-FU were 0.4 and 0.6 h for group A and 0.7 and 0.8 h for group B, respectively. These PK data are in line with previously published data in the literature [18]. The plasma concentration–time curves determined on day 14 demonstrate (despite the limited number of sampling times and missing the C_{max}) that there was no accumulation of 5-FU or capecitabine in plasma (Figure 2B).

Intracellular pharmacokinetics

In the PBMC samples, only the intracellular FUTP concentrations could be quantified. The FdUTP and FdUMP concentrations in the collected PBMC lysates were all below the detection limits of the assay. The LLQs of the LC–MS/MS assay (in PBMC lysate), mentioned in the methods section, are not directly translatable to the lowest measurable intracellular FdUTP and FdUMP concentrations in PBMCs, because the latter also depends on the number of collected lymphocytes, monocytes and granulocytes in the sample. Clinical samples derived from 16 ml whole blood using the described isolation method were found to contain $0.5–20 \times 10^6$ PBMCs.

   The intracellular concentration–time curves for FUTP are shown in Figure 3 and demonstrate considerable inter-individual variation. The results of the non-compartmental PK analysis are given in Table 1. Intracellular FUTP circulates much longer than the corresponding plasma levels of capecitabine and 5-FU. On day 1 of the treatment, the C_{max} for FUTP was reached on average after 3.5 h in patient group A. As for the plasma concentrations, also for the intracellular levels, C_{max} was achieved much later in group B, after 7.2 h. Remarkable is the long presence of FUTP in the cell. Twenty-four hours after the intake of capecitabine, the intracellular FUTP concentration was on average still 41% of the C_{max} (range: 21–89%).

Relationship between plasma 5-FU and intracellular FUTP exposure

No significant linear correlation was found between the AUC_{0-t} of 5-FU in plasma and the AUC_{0-24h} of intracellular FUTP determined on the first treatment day (Figure 4). The Pearson correlation coefficient (*r*) was 0.107 (*P* = 0.727, *n* = 13) for group A. The sample size of group B was too small to make a reliable statement about possible linear correlation.
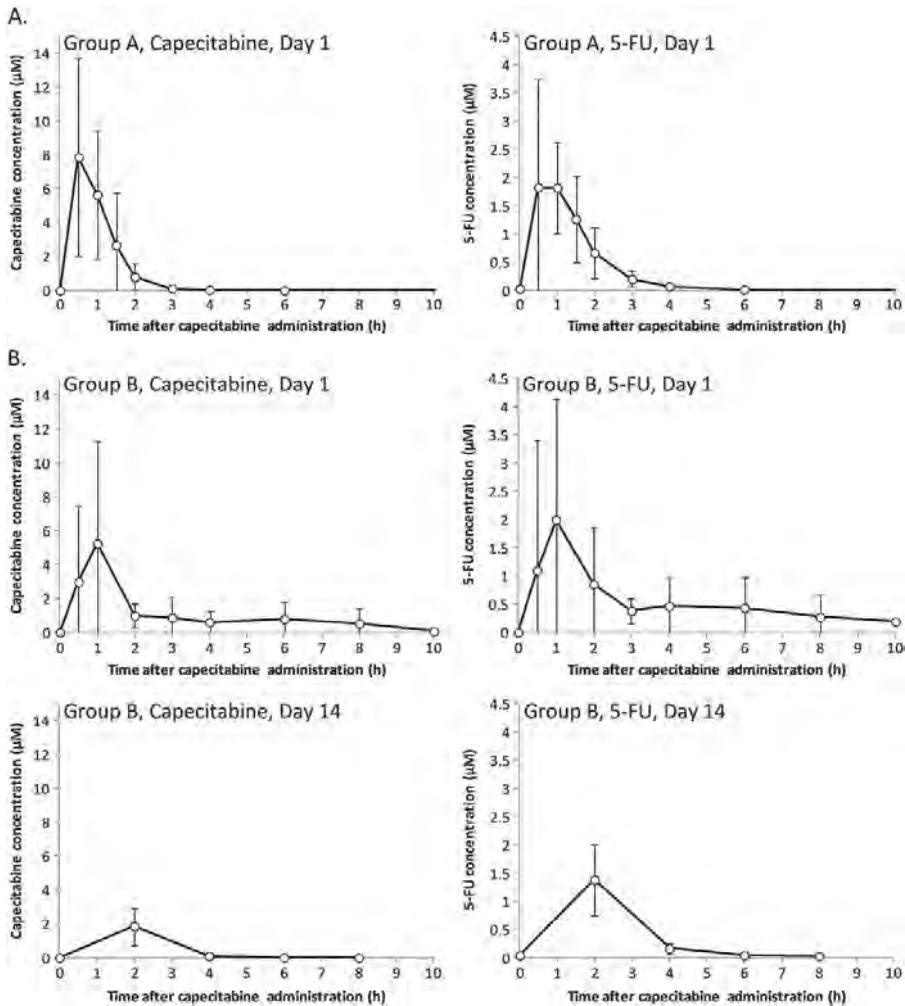
Figure 2. Plasma concentration–time curves of capecitabine and 5-FU for patient group A (receiving capecitabine 1000 mg QD) measured at day 1 of the first treatment cycle (A), and for patient group B (receiving capecitabine 850 mg m^{-2} BID) measured at day 1 and at day 14 of the first treatment cycle (B). Despite the limited number of sampling times on day 14 and the missing C_{max}, the plasma concentration–time curves determined on day 14 demonstrate that there was no accumulation of capecitabine or 5-FU in plasma. Curves were depicted up to 10 h after capecitabine intake, although more samples were collected for group A. The data are shown as mean values (symbols) with standard deviations (error bars).

Intracellular FUTP accumulation

After 14 days of capecitabine treatment (twice daily), intracellular FUTP concentrations are clearly higher than after the first capecitabine administration on day 1 (Figure 3B). The AUC$_{0-8h}$ for intracellular FUTP was significantly increased on day 14 of the treatment compared to day 1 (Mann–Whitney U = 20, P = 0.008, one-sided, Figure 5). The mean

Table 1. Summary statistics for pharmacokinetic parameters of capecitabine and 5-FU in plasma and FUTP in PBMCs, on day 1, after a single capecitabine dose. The data are shown as mean values (and coefficients of variation %).

	Patient group A (receiving capecitabine 1000 mg QD)			Patient group B (receiving capecitabine 850 mg m^{-2} BID)		
	Capecitabine	5-FU	FUTP	Capecitabine	5-FU	FUTP
n	13	13	13	8	8	5
C_{max}	11 µM (43%)	2.6 µM (58%)	0.38 µM (62%) 0.086 pmol/10^6 PBMCs (57%)	7.3 µM (71%)	3.0 µM (69%)	0.54 µM (69%) 0.13 pmol/10^6 PBMCs (69%)
t_{max}	0.7 h (45%)	0.9 h (34%)	3.5 h (61%)	3.3 h (89%)	3.4 h (86%)	7.2 h (25%)
$t_{1/2}$ [a]	0.4 h (19%)	0.6 h (24%)	-	0.7 h (70%) $n=7$	0.8 h (48%) $n=7$	-
AUC_{0-t}	8.8 µM h (31%)	3.0 µM h (45%)	5.3 µM h (68%) 1.2 pmol h/10^6 PBMCs (64%)	11 µM h (46%) $n=7$	5.3 µM h (30%)	2.1 µM h (84%) 0.51 pmol h/10^6 PBMCs (83%)

Abbreviations: 5-FU, 5-fluorouracil; AUC_{0-t}, the area under the concentration–time curve from time zero to the time point of the last quantifiable data point; BID, twice a day; C_{max}, the maximum observed concentration; FUTP, 5-fluorouridine 5'-triphosphate; PBMCs, peripheral blood mononuclear cells; QD, one a day; $t_{1/2}$, terminal elimination half-life; t_{max}, the time to reach the maximum observed concentration.
[a] For the calculation of the mean $t_{1/2}$, only curves of patients containing sufficient data points to assess this parameter were included. Where not all patients were included, the number of evaluable patients (n) is indicated.

9
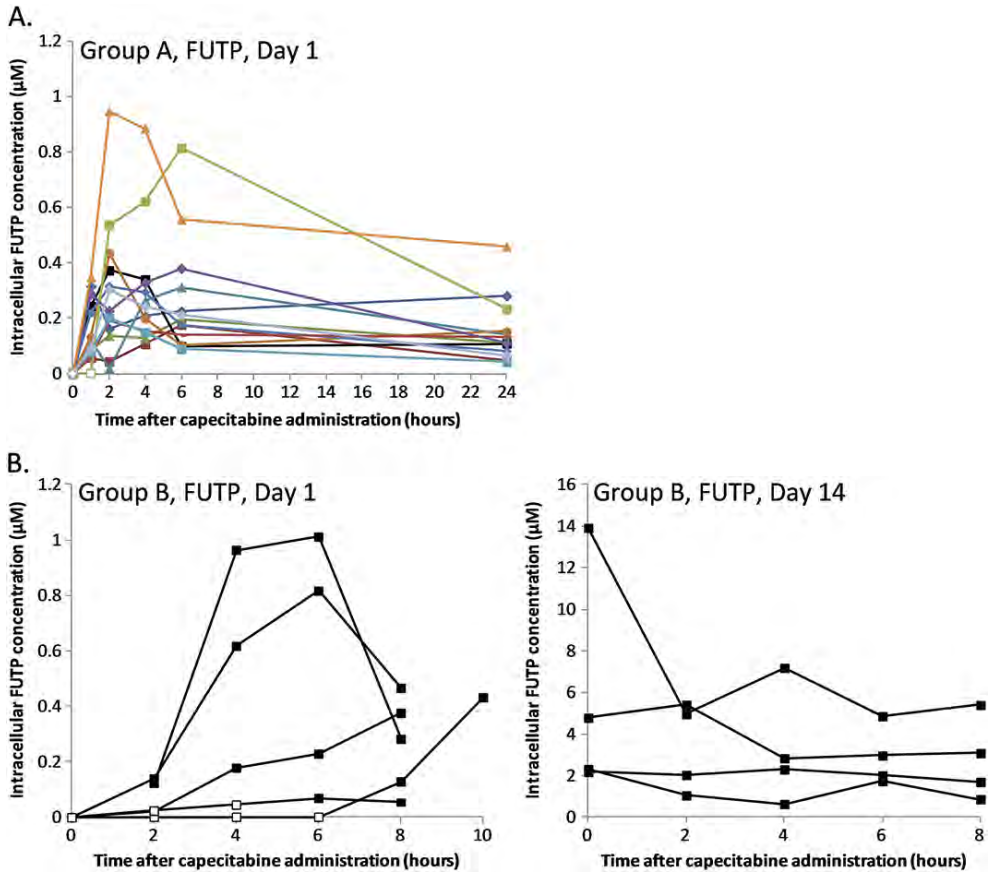
Figure 3. Intracellular concentration–time curves of 5-fluorouridine 5'-triphosphate (FUTP) for patient group A (receiving capecitabine 1000 mg QD) measured at day 1 of the first treatment cycle (A), and for patient group B (receiving capecitabine 850 mg m^{-2} BID) measured at day 1 and at day 14 of the first treatment cycle (B). Concentrations within the range of the assay are indicated by solid markers and concentrations below the LLQ by open markers.

AUC_{0-8h} (± SD) on day 1 was 2.0 ± 1.9 µM h *vs.* 28 ± 19 µM h on day 14. Apparently, during these 14 days of consecutive treatment, intracellular accumulation of FUTP occurs.

DISCUSSION

To our knowledge, this is the first time that intracellular FUTP concentrations were measured in patients who were treated with capecitabine. Our measurements show that FUTP is present in higher concentrations than FdUTP and FdUMP (which were both below the detection limits of the assay). Apparently, capecitabine is mainly converted into FUTP and to a lesser extent into FdUTP and FdUMP. However, this does not necessarily mean that the RNA pathway has a more prominent role in the mechanism of action than the DNA pathway. It is known that the *deoxy*ribonucleotides are naturally present within
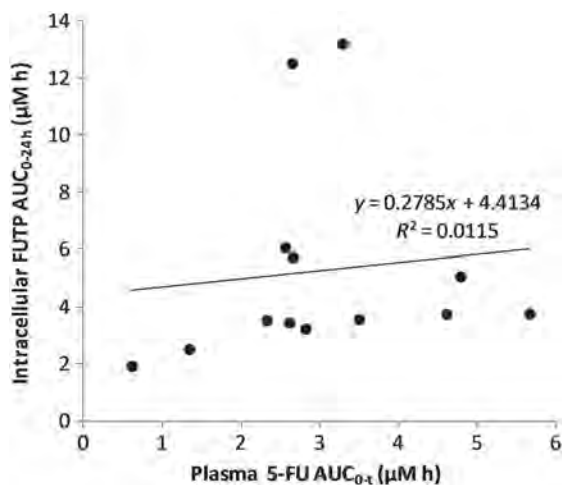
Figure 4. Relationship between the $AUC_0.t$ of 5-FU in plasma and the AUC_{0-24h} of intracellular FUTP in PBMCs determined for group A on day 1 of the treatment.

9
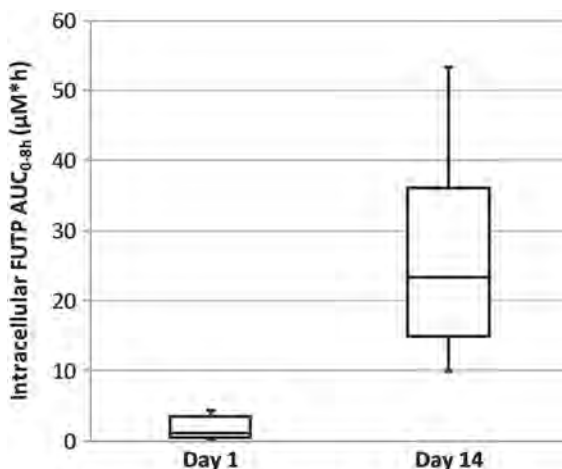
Figure 5. Box plot for the AUC_{0-8h} of FUTP on day 1 and on day 14 of capecitabine treatment (twice daily). The box represents the median and the 25th and 75th percentiles of the data. The whiskers represent the range. The AUC_{0-8h} for intracellular FUTP was significantly increased on day 14 of the treatment compared to day 1 (Mann–Whitney U = 20, P = 0.008, one-sided).

cells in much lower concentrations than the ribonucleotides [19, 20]. This means that the low FdUTP and FdUMP concentrations may still have a very important role.

A second important finding of this exploratory intracellular PK study is the long intracellular residence of FUTP, and its consequent intracellular accumulation after dosing capecitabine twice daily for 14 days. The prolonged intracellular retention of FUTP is an important finding, especially in view of the rapid plasma kinetics of capecitabine and 5-FU.

It was already known that 5-FU plasma levels do not reflect the 5-FU concentrations in tumour tissue. Peters *et al*. found that 5-FU was retained for a much longer period of time in tissues than in plasma, and that 4–48 h after an IV 5-FU bolus of 500 mg m^{-2}, the 5-FU tissue concentrations were at least 10 times higher than the plasma concentrations [11].

On the basis of this exploratory study, we now know that FUTP retains in cells for at least 24 h after a single capecitabine dose. The prolonged retention of FUTP in (tumour) tissue must be taken into consideration when designing new dose regimens.

It would be interesting to know whether also intracellular accumulation of FdUTP and FdUMP occurs during 14 days of treatment with capecitabine, especially given that the effects of these nucleotides are more cell cycle dependent than the effect of FUTP [21]. Prolonged intracellular exposure to FdUMP and FdUTP will affect more cells during their S-phases. Unfortunately, a more sensitive assay is required to measure the intracellular FdUTP and FdUMP levels.

Capecitabine was developed as an oral alternative to continuous intravenous 5-FU infusion [22]. It is known that prolonged exposure to 5-FU has a beneficial effect compared to brief exposure. In advanced colorectal cancer, continuous intravenous infusion resulted in significantly higher response rates and less toxicity compared with intravenous bolus injections [23]. Prolonged 5-FU exposure will probably lead to a *prolonged* intracellular exposure to 5-FU nucleotides, which is beneficial, especially as the effects of the 5-FU nucleotides are cell cycle dependent. We wondered if prolonged 5-FU plasma levels also lead to *higher* intracellular nucleotide concentrations than brief exposure to an equal amount of 5-FU. This would be the case if the transporters involved in the cellular uptake or the enzymes involved in the intracellular ribosylation or phosphorylation would become saturated above a certain 5-FU concentration. Remarkably, the FUTP concentrations which we reported in our analytical paper, measured 30 min after an intravenous 5-FU bolus (400 mg m^{-2} in 30 min) were in the same range as the FUTP concentrations measured after 14 days of capecitabine treatment twice daily (4.7–11 µM *vs.* 0.64–14 µM) [13]. This indicates that also brief, high 5-FU exposure can rapidly lead to high intracellular FUTP concentrations and the capacities of the cell membrane transporters and intracellular enzymes are probably not the limiting factors.

When interpreting the results of this intracellular PK study, we should keep in mind that the capecitabine dose that patients received during the study, 1000 mg QD for group A and 850 mg m^{-2} BID for group B, is lower than the typical dose that is used when capecitabine is given as a single agent: 1250 mg m^{-2} twice daily for 14 days followed by a 7-day rest period.

Furthermore, it should be realized that the FdUMP fraction which is bound to thymidylate synthase is not measured by the employed assay, because this fraction is precipitated during the extraction step with methanol [24, 25].

In addition, we have to keep in mind that the nucleotide concentrations measured in PBMCs may be different than the concentrations that would be found in tumour cells. PBMCs were used as a cell model for the intracellular activation, because these cells can be obtained more easily than tumour biopsies. This was particularly relevant as we wanted to follow the intracellular FUTP concentrations over time. Therefore samples had

to be collected at multiple time points after capecitabine intake, which was not possible for tumour tissue.

However, by measuring the 5-FU nucleotide concentrations in PBMCs, no account is taken of the tumour-specific activation of capecitabine. The third activation step, the conversion of 5'-dFUR to 5-FU preferentially takes place within the tumour, because the responsible enzyme, thymidine phosphorylase, is more present in tumour tissue [1]. This means that the FUTP concentrations in tumour cells could be higher than those measured in PBMCs. On the other hand, it could be argued that PBMCs will probably be exposed to higher 5'-dFUR concentrations than solid tumour tissues, which in turn could lead to higher FUTP concentrations in PBMCs than in tumour cells.

Nevertheless, we believe that measurement of the active metabolites in PBMCs will provide useful information. By measuring in cells, the intracellular 'activation machinery' is at least to some extent represented. Therefore we hypothesize that these measurements in PBMCs will better reflect the active metabolite concentrations in other tissues (including tumour tissue) than the capecitabine and 5-FU plasma concentrations.

Further research is needed to determine whether there is indeed a correlation between the intracellular 5-FU nucleotide levels measured in PBMCs and clinical response or the occurrence of adverse reactions. Depending on the outcome of this study, PBMCs could serve as a surrogate matrix to give an impression of the cytotoxic metabolite concentrations in other tissues.

These intracellular measurements would be primarily useful to optimize dosing regimens for the total population. How long are the active metabolites present within the cell? What would be a suitable dose regimen (i.e. dose and dose interval) based on these results?

The use of intracellular measurements to optimize the capecitabine dose for individual patients (i.e. intracellular therapeutic drug monitoring; TDM) seems further away. The question is, first of all, whether there is a need for individual dose optimization. Our findings indicate that the intracellular FUTP concentrations show considerable interpatient variation, but is this variation associated with a different clinical outcome, and what about the other two active metabolites? If there is a need for individual dose optimization, a second question is whether intracellular TDM would be feasible. At present the isolation of PBMCs and measurement of the nucleotides is quite laborious, which makes deployment for TDM less practical.

Finally, intracellular measurement of the active metabolite levels might be useful as a predictive marker for treatment response, at least for early stage recognition of nonresponders as a result of a deficient intracellular metabolism.

REFERENCES

1. Miwa M, Ura M, Nishida M, Sawada N, Ishikawa T, Mori K, et al. Design of a novel oral fluoropyrimidine carbamate, capecitabine, which generates 5-fluorouracil selectively in tumours by enzymes concentrated in human liver and cancer tissue. Eur J Cancer 1998;34:1274–81.

2. Schüller J, Cassidy J, Dumont E, Roos B, Durston S, Banken L, et al. Preferential activation of capecitabine in tumor following oral administration to colorectal cancer patients. Cancer Chemother Pharmacol 2000;45:291–7.

3. Grem J. Mechanisms of action and modulation of fluorouracil. Semin Radiat Oncol 1997; 7: 249–59.

4. Álvarez P, Marchal JA, Boulaiz H, Carrillo E, Vélez C, Rodríguez-Serrano F, et al. 5-Fluorouracil derivatives: a patent review. Expert Opin Ther Pat 2012;22:107–23.

5. Peters GJ, Laurensse E, Leyva A, Lankelma J, Pinedo HM. Sensitivity of human, murine, and rat cells to 5-fluorouracil and 5′-deoxy-5-fluorouridine in relation to drug-metabolizing enzymes. Cancer Res 1986;46:20–8.

6. Ciccolini J, Peillard L, Evrard A, Cuq P, Aubert C, Pelegrin A, et al. Enhanced antitumor activity of 5-fluorouracil in combination with 2′-deoxyinosine in human colorectal cell lines and human colon tumor xenografts. Clin Cancer Res 2000;6:1529–35.

7. Ciccolini J, Peillard L, Aubert C, Formento P, Milano G, Catalin J. Monitoring of the intracellular activation of 5-fluorouracil to deoxyribonucleotides in HT29 human colon cell line: application to modulation of metabolism and cytotoxicity study. Fundam Clin Pharmacol 2000;14:147–54.

8. Kamm YJL, Peters GJ, Hull WE, Punt CJA, Heerschap A. Correlation between 5-fluorouracil metabolism and treatment response in two variants of C26 murine colon carcinoma. Br J Cancer 2003;89:754–62.

9. Spears CP, Gustavsson BG, Mitchell MS, Spicer D, Berne M, Bernstein L, Danenberg PV. Thymidylate synthetase inhibition in malignant tumors and normal liver of patients given intravenous 5-fluorouracil. Cancer Res 1984;44:4144–50.

10. Spears CP, Gustavsson BG, Berne M, Frosing R, Bernstein L, Hayes AA. Mechanisms of innate resistance to thymidylate synthase inhibition after 5-fluorouracil. Cancer Res 1988;48:5894–900.

11. Peters GJ, Lankelma J, Kok RM, Noordhuis P, van Groeningen CJ, van der Wilt CL, et al. Prolonged retention of high concentrations of 5-fluorouracil in human and murine tumors as compared with plasma. Cancer Chemother Pharmacol 1993;31:269–76.

12. Moran RG, Spears CP, Heidelberger C. Biochemical determinants of tumor sensitivity to 5-fluorouracil: ultrasensitive methods for the determination of 5-fluoro-2′-deoxyuridylate, 2′-deoxyuridylate, and thymidylate synthetase. Proc Natl Acad Sci 1979;76:1456–60.

13. Derissen EJB, Hillebrand MJX, Rosing H, Schellens JHM, Beijnen JH. Development of an LC–MS/MS assay for the quantitative determination of the intracellular 5-fluorouracil nucleotides responsible for the anticancer effect of 5-fluorouracil. J Pharm Biomed Anal 2015;110:58–66.

14. Deenen MJ, Rosing H, Hillebrand MJX, Schellens JHM, Beijnen JH. Quantitative determination of capecitabine and its six metabolites in human plasma using liquid chromatography coupled to electrospray tandem mass spectrometry. J Chromatogr B Analyt Technol Biomed Life Sci 2013;913–914:30–40.

15. Sharma S, Cabana R, Shariatmadar S, Krishan A. Cellular volume and marker expression in human peripheral blood apheresis stem cells. Cytometry A 2008;73:160–7.

16. Simiele M, D'Avolio A, Baietto L, Siccardi M, Sciandra M, Agati S, et al. Evaluation of the mean corpuscular volume of peripheral blood mononuclear cells of HIV patients by a Coulter counter to determine intracellular drug concentrations. Antimicrob Agents Chemother 2011;55:2976–8.

17. Reigner B, Verweij J, Dirix L, Cassidy J, Twelves C, Allman D, et al. Effect of food on the pharmacokinetics of capecitabine and its

9

metabolites following oral administration in cancer patients. Clin Cancer Res 1998;4:941–8.

18. Reigner B, Blesch K, Weidekamm E. Clinical pharmacokinetics of capecitabine. Clin Pharmacokinet 2001;40:85–104.

19. Chen P, Liu Z, Liu S, Xie Z, Aimiuwu J, Pang J, et al. A LC–MS/MS method for the analysis of intracellular nucleoside triphosphate levels. Pharm Res 2009;26:1504–15.

20. Cohen S, Megherbi M, Jordheim LP, Lefebvre I, Perigaud C, Dumontet C, Guitton J. Simultaneous analysis of eight nucleoside triphosphates in cell lines by liquid chromatography coupled with tandem mass spectrometry. J Chromatogr B Analyt Technol Biomed Life Sci 2009;877:3831–40.

21. Sobrero AF, Aschele C, Bertino JR. Fluorouracil in colorectal cancer – a tale of two drugs: implications for biochemical modulation. J Clin Oncol 1997;15:368–81.

22. Hoff PM, Cassidy J, Schmoll HJ. The evolution of fluoropyrimidine therapy: from intravenous to oral. Oncologist 2001;6:3–11.

23. Piedbois P. Efficacy of intravenous continuous infusion of fluorouracil compared with bolus administration in advanced colorectal cancer. J Clin Oncol 1998;16:301–8.

24. Pogolotti A, Nolan P, Santi D. Methods for the complete analysis of 5-fluorouracil metabolites in cell extracts. Anal Biochem 1981;117:178–86.

25. Washtien WL, Santi DV. Assay of intracellular free and macromolecular-bound metabolites of 5-fluorodeoxyuridine and 5-fluorouracil. Cancer Res 1979;39:3397–404.

9

PART 4

CAPECITABINE CHRONOTHERAPY

C H A P T E R   1 0

PHASE I PHARMACOLOGICAL STUDY OF CONTINUOUS CHRONOMODULATED CAPECITABINE TREATMENT

Bart A.W. Jacobs, Dick Pluim, Hilde Rosing, Bastiaan Nuijen, Jos H. Beijnen, Alwin D.R. Huitema, Jan H.M. Schellens, Serena Marchetti

Interim analysis

ABSTRACT

Background

Capecitabine is an oral pro-drug of the anti-cancer drug 5-fluorouracil (5-FU). The 5-FU degrading enzyme, dihydropyrimidine dehydrogenase (DPD), and the target enzyme thymidylate synthase, are subject to circadian rhythmicity. The aim of this study was to determine the maximum tolerated dose (MTD), dose-limiting toxicity (DLT), safety, pharmacokinetics (PK) and pharmacodynamics (PD) of capecitabine therapy adapted to this circadian rhythm (chronomodulated therapy).

Methods

Patients aged ≥18 years, with WHO performance status of ≤2, advanced solid tumours potentially benefitting from capecitabine therapy were enrolled. *DPYD**2A or 2846A>T mutation carriers were excluded. A classical dose escalation 3+3 design was applied. Capecitabine was administered daily without interruptions. The daily dose was divided in morning and evening doses that were administered at 9:00 h and 24:00 h, respectively. The ratio of the morning to the evening dose was 3:5 (morning : evening). PK and PD were examined on treatment days 7 and 8.

Results

At the time of interim analysis, a total of 12 patients were enrolled. The median (range) number of administered treatment cycles was 2 (1-8). The daily capecitabine dose was escalated from 1000 mg/m^2 up to 2000 mg/m^2 in dose level 4. There were no DLTs observed and further escalation is ongoing. Continuous chronomodulated capecitabine therapy was well tolerated until the currently explored dose of 2000 mg/m^2 with main adverse events being grade 1-2 nausea and fatigue. PK analysis did not demonstrate significant circadian rhythmicity in capecitabine and metabolites exposure. DPD activity was found to be highest at 1:30 h and lowest at 10:30 h.

Conclusion

At the time of this interim analysis, the MTD has not been reached yet. The cumulative dose in dose level 4 was 20% higher than the cumulative dose of the approved regimen (1250 mg/m^2 bi-daily on day 1-14 of every 21-day cycle). Chronomodulation is promising and could lead to improved tolerability and efficacy of capecitabine.

INTRODUCTION

Capecitabine is an oral pre-pro-drug of 5-fluorouracil (5-FU) and is frequently used for the treatment of colorectal, breast and gastric cancer. After administration, capecitabine is rapidly and completely absorbed and converted to subsequently 5'-deoxy-5-fluorocytidine (dFCR), 5'-deoxy-5-fluorouridine (dFUR) and 5-FU via a three-step enzymatic pathway involving carboxyl esterase, cytidine deaminase and thymidine phosphorylase (TP), respectively [1]. Approximately 80% of 5-FU is catabolized to inactive metabolites. A small proportion of 5-FU is intracellularly anabolized to cytotoxic metabolites [2,3]. The main mechanism of action is inhibition of the enzyme thymidylate synthase (TS), which is essential for DNA synthesis [4,5]. Dihydropyrimidine dehydrogenase (DPD) is the enzyme that catalyzes 5-FU degradation into dihydro-5-FU. Dihydro-5-FU is eventually converted to fluoro-β-alanine (FBAL), which is cleared renally [1,6].

The recommended dose (RD) of capecitabine is 1250 mg/m^2 twice daily (BID) on day 1–14 of a 21-day cycle [7]. In early clinical phase I studies, however, both continuous and intermittent dosing regimens were examined [8,9]. For continuous capecitabine treatment, the RD was 666 mg/m^2 BID [9], which is ~50% lower than for intermittent treatment [8]. Intermittent and continuous treatment schedules were compared in a phase II clinical trial [10]. Both schedules showed similar efficacy [10]. However, diarrhoea, hand-foot syndrome, vomiting, nausea and stomatitis were more frequently reported with the intermittent than the continuous capecitabine treatment [10].

The time of dose administration could also influence tolerability of capecitabine. In previous studies, 5-FU degradation demonstrated circadian rhythmicity [11–13]. Chronomodulated and constant-rate infusion with intravenous 5-FU have been compared in a randomized trial [14]. Chronomodulation was achieved by nocturnal administration of 5-FU, since peak activity of DPD and trough TS activity were expected during the night. The 5-FU chronomodulated schedule was more effective and less toxic than constant-rate infusion of 5-FU [14]. Recently, we examined the circadian rhythmicity in DPD and TS activity in healthy volunteers [15]. In this study, DPD activity peaked at approximately 02:00 h, and was about 50% higher compared with afternoon activity. TS activity also demonstrated circadian rhythmicity with trough activity around 02:00 h [15]. Based on these data, we hypothesized that chronomodulated capecitabine therapy improves treatment tolerability. Since continuous BID capecitabine treatment was better tolerated than intermittent therapy (two weeks on followed by one week off) [10], chronomodulation was expected to result in even better tolerability, which potentially could lead to increased dose intensity.

The aim of this current phase I study was to determine the maximum tolerated dose (MTD), dose-limiting toxicity (DLT), pharmacokinetics (PK) and pharmacodynamics (PD) of continuous chronomodulated BID capecitabine therapy. The capecitabine evening dose was relatively high and administered at 24:00 h in order to attain capecitabine and 5-FU peak exposure around the time of the expected maximum DPD activity.

10

METHODS

Patient selection

Patients aged ≥18 years with advanced solid tumours potentially benefiting capecitabine treatment were eligible for enrolment in case the following criteria were met: World Health Organization (WHO) performance status of ≤2, a life expectancy of at least 3 months and adequate bone marrow, hepatic and renal function. Patients had to be able and willing to undergo blood sampling during daytime and during the night for PK and PD analysis. Relevant exclusion criteria were known DPD deficiency caused by mutations in genetic polymorphisms in *DPYD* (*DPYD**2A or c.2846A>T).

Study design

This study was a phase I, single centre, safety, pharmacological, open label, dose-escalation study. Patients received capecitabine tablets (150 mg and 500 mg) on day 1-21 of a 21-day cycle until disease progression, unacceptable toxicity despite dose modification and supportive measures, or patient refusal. Capecitabine was administered with water within 30 minutes after a small meal, both in the morning and late evening. A classical 3+3 dose escalation design was applied. The capecitabine was escalated according to five predefined dose levels (1000, 1275 1600, 2000 and 2550 mg/m^2). The daily dose was divided in morning and evening doses that were administered at 9:00 h and 24:00 h, respectively. The ratio of the morning to the evening dose was maintained at 3:5 (morning : evening) for all dose levels. This ratio was selected based on the 3:5 ratio in trough to peak DPD activity observed in healthy volunteers [15]. At least three patients per dose level were recruited. If one out of three patients experienced a DLT, the number of patients was expanded to maximally six. Dose escalation was permitted if no DLT occurred in any of the three patients or in not more than one out of six patients of an expanded dose level. In case of DLT in more than one out of three or two or more out of maximally six patients were observed, the dose level was declared intolerable and three additional patients were recruited at the previous dose level. The procedure continued until the dose level at which DLT occurred in maximally one of six patients was found. The capecitabine dose of this final dose level was declared the maximal tolerated dose (MTD). DLT was defined by any of the following toxicities occurring during the first three treatment weeks and considered to be possibly, probably, or definitely related to capecitabine therapy: ≥grade 3 non-haematological toxicity (except alopecia or inadequately treated diarrhoea, nausea and vomiting), grade 4 thrombocytopenia, grade 3 thrombocytopenia associated with bleeding events, ≥grade 3 anaemia, grade 4 neutropenia, grade 3 febrile neutropenia. A dosing-interruption >7 days that was possibly, probably, or definitely related to capecitabine was considered a DLT too. Toxicity was assessed each week during the first treatment cycle and at the end of each subsequent cycle according to the Common Terminology Criteria for Adverse Events (CTC-AE) version 4.03. Tumour response was evaluated every two treatment cycles according to the Response Evaluation Criteria in Solid Tumors (RECIST) version 1.1 [16]. The study protocol was approved by the Medical Ethics Committee of The Netherlands Cancer Institute and was performed in

compliance with Good Clinical Practice guidelines and the WHO Declaration of Helsinki. The study was registered in the Dutch Trial Registry (http://www.trialregister.nl, study identifier: NTR4639).

Pharmacokinetic analyses

In order to examine circadian variability, the PK of capecitabine, dFCR, dFUR, 5-FU and FBAL were examined during day- and nighttime. Peripheral blood was collected at pre-dose and 0.5, 1, 1.5, 2, 3, 5, 11, 15 (which is also pre-dose for the evening dose) hours after capecitabine intake at 9:00 h on day 7 of treatment and during the following night (day 8), 0.5, 1, 1.5, 2, 3, 5 and 9 hours after capecitabine intake at 24:00 h. Blood samples were collected in lithium-heparinized tubes, which were centrifuged for 10 min at 1500g and 4 °C after collection. Isolated plasma was stored at -70 °C until further analysis. Capecitabine and metabolite concentrations were quantified using liquid chromatography with tandem mass spectrometric detection (LC-MS/MS), as described previously [17].

Non-compartmental PK analyses (NCA) were performed using a validated script in R version 3.3.0 [18]. The following individual PK parameters were extracted: the maximum plasma concentrations (C_{max}), the time to reach maximum plasma concentration (t_{max}), the area under the plasma concentration-time curve up to five hours post-dose (AUC_{0-5h}) for capecitabine, dFCR, dFUR and 5-FU, and the AUC extrapolated to infinity (AUC_{0-inf}) for FBAL. Paired t-tests were performed for statistical comparison of the AUC_{0-5h} and AUC_{0-inf} after morning and evening administration of capecitabine.

Pharmacodynamic analyses

Circadian variability in DPD and TS activity were examined. DPD and TS activity in peripheral blood mononuclear cells (PBMCs) were determined at several time points during the day: at pre-dose, 1.5, 11 and 15 hours after capecitabine intake at 9:00 h on day 7 and 1.5 hours after capecitabine intake at 24:00 h (day 8). In addition, DPD activity in PBMCs (DPDA$_{pbmc}$) and TS activity in PBMCs (TSA$_{pbmc}$) were determined at screening (within 3 days before treatment). The PBMCs were isolated from peripheral heparinized blood using Ficoll-Paque density gradient centrifugation and stored at -80 °C until further analysis. DPDA$_{pbmc}$ and TSA$_{pbmc}$ were determined using validated radioassays [19–21]. DPDA$_{pbmc}$ was examined by *ex vivo* conversion of ^{3}H-thymine to ^{3}H-dihydrothymine and expressed as the amount of ^{3}H-dihydrothymine formed per mg PBMC protein per hour (nmol/mg/h) [19]. TSA$_{pbmc}$ activity was expressed by the amount 5-^{3}H-2'-deoxyuridine 5'-monophosphate that was metabolized *ex vivo* per mg PBMC protein per hour of incubation (nmol/mg/h) [20].

To explore the treatment effect of capecitabine on the TP phenotype, TP activity in PBMCs (TPA$_{pbmc}$) was determined at screening and on day 7 at pre-dose (9:00 h) using a previously developed assay (Jacobs et al., submitted). In brief, the PBMC protein was incubated with the TP substrate thymidine (2mM) in a reaction buffer (35 mM potassium phosphate, 1 mM DTT; pH 7.4) for 1 h at 37 °C. The reaction was terminated by placing

the samples at 100 °C for 4 minutes. The reaction product, thymine, was quantified using high-performance liquid chromatography coupled with ultraviolet detection (HPLC-UV) at 265 nm. TPA_{pbmc} was expressed by the amount of thymine formed per mg PBMC protein per hour of incubation (nmol/mg/h).

Variability in $DPDA_{pbmc}$ and TSA_{pbmc} was examined using repeated measures analysis of variance (rANOVA) and the nonparametric Friedman test, respectively. The difference between TPA_{pbmc} at screening and day 7 was examined by the paired t-test. Statistical difference was considered significant for p-values <0.05.

RESULTS

At the time of interim analysis, a total of 12 patients were enrolled in the study between July 2014 and March 2016. Patient characteristics are summarized in Table 1. The median (range) number of administered treatment cycles was 2 (1-8). Two other patients required treatment delay for toxicity. One patient went off-study due to progression of disease after one treatment cycle.

Dose-limiting toxicity and treatment tolerability

All 12 patients were evaluable for DLT and treatment safety. Table 2 gives an overview of the examined dose levels. The capecitabine dose was increased from 375 mg/m^2 at 9:00 h and 625 mg/m^2 at 24:00 h in dose level 1 up to 750 mg/m^2 at 9:00 h and 1250 mg/m^2 at 24:00 h in dose level 4. No other DLTs have been observed thus far.

Overall, continuous chronomodulated capecitabine therapy was well tolerated. An overview of the observed grade 1-2 and grade 3-4 toxicities that were possibly, probably or definitely related to the study treatment is summarized per dose level in Table 3. As shown, the most frequently observed adverse events were nausea (42%), fatigue (42%), palmar-plantar erythrodysesthesia (25%), diarrhoea (25%) and anorexia (25%). The adverse events were always mild (grade 1-2), with the exception of one patient in dose level 4 who suffered from grade 3 anaemia.

During the study, one patient experienced a serious adverse event (SAE). This patient was hospitalized for grade 3 ileus that was unrelated to study treatment. Due to a decline in clinical status, the patient went off-study and deceased within one month after initiation of the SAE.

Pharmacokinetics

PK data from 12 subjects were available for the interim analysis. The mean plasma concentration-time profiles for capecitabine, dFCR, dFUR, 5-FU and FBAL are shown per dose level and time of day in Figure 1. Results of the NCA are summarized in Table 4. Capecitabine was rapidly absorbed with mean t_{max} values between 0.83-1.83 h. The PK profiles of dFCR, dFUR and 5-FU showed the same concentration-time pattern, except for FBAL, for which mean t_{max} values were between 2-3.33 h after dose. For all compounds, the mean C_{max}, AUC_{0-5h} or AUC_{0-inf} were higher during night-time than at daytime.

Table 1. Demographic and disease characteristics.

Characteristic	Number of patients	%
Total number of patients	12	100
Sex		
Male	8	67
Female	4	33
Ethnic origin		
Caucasian	11	92
Creole	1	8
Age		
Median (range), years	64 (43-79)	
WHO performance status		
0	5	42
1	7	58
Primary tumor type		
Colorectal	7	58
Cervix	1	8
SCLC	1	8
Anal	1	8
Head and neck	1	8
Pancreas	1	8
Stage of cancer		
Metastatic	12	100
Prior treatment		
Chemotherapy	12	100
Radiotherapy	5	42
Surgery	7	58

Abbreviations: WHO, world health organisation; SCLC, small cell lung cancer

Table 2. Overview of the dose levels and dose-limiting toxicities.

Dose level	Capecitabine (mg/m²) at 9:00 h / 24:00 h	Number of patients	Dose-limiting toxicities
1	375 / 625	3	None
2	475 / 800	3	None
3	600 / 1000	3	None
4	750 / 1250	3	None

10

Table 3. Treatment-related adverse events.

Number of patients	Dose level 1 n = 3		Dose level 2 n = 3		Dose level 3 n = 3		Dose level 4 n = 3		Total (%) n = 12	
CTCAE grade toxicity	Gr. 1-2	Gr. 3-4	Gr. 1-2	Gr. 3-4	Gr. 1-2	Gr. 3-4	Gr. 1-2	Gr. 3-4	Gr. 1-2	Gr. 3-4
Toxicity										
Anaemia	-	-	-	-	-	-	-	1	-	1 (8)
Anorexia	-	-	1	-	1	-	1	-	3 (25)	-
ASAT increase	-	-	1	-	-	-	-	-	1 (8)	-
Blood bilirubin increase	-	-	-	-	1	-	-	-	1 (8)	-
Diarrhoea	2	-	-	-	1	-	-	-	3 (25)	-
Dry skin	-	-	-	-	-	-	1	-	1 (8)	-
Dysgeusia	-	-	-	-	1	-	1	-	2 (17)	-
Edema limbs	-	-	-	-	1	-	-	-	1 (8)	-
Fatigue	1	-	2	-	3	-	-	-	5 (42)	-
Fever	-	-	1	-	-	-	1	-	1 (8)	-
Itchy palms	-	-	-	-	-	-	1	-	1 (8)	-
Malaise	-	-	-	-	-	-	1	-	1 (8)	-
Mucositis	-	-	-	-	-	-	1	-	1 (8)	-
Nail ridging	-	-	-	-	1	-	-	-	1 (8)	-
Nausea	1	-	1	-	3	-	1	-	5 (42)	-
Neutropenia	-	-	-	-	-	-	1	-	1 (8)	-
Oral pain	-	-	1	-	-	-	-	-	1 (8)	-
Pain in extremity	1	-	-	-	-	-	-	-	1 (8)	-
Palmar-plantar erythrodysesthesia	-	-	1	-	1	-	1	-	3 (25)	-
Peripheral sensory neuropathy	-	-	1	-	-	-	-	-	1 (8)	-
Postnasal drip	-	-	-	-	1	-	-	-	1 (8)	-
Pruritus	-	-	-	-	-	-	1	-	1 (8)	-
Rash acneiform	-	-	-	-	1	-	-	-	1 (8)	-
Stomach pain	-	-	1	-	-	-	-	-	1 (8)	-

Table 3. (continued)

CTCAE grade toxicity	Dose level 1 $n = 3$		Dose level 2 $n = 3$		Dose level 3 $n = 3$		Dose level 4 $n = 3$		Total (%) $n = 12$	
Number of patients	Gr. 1-2	Gr. 3-4	Gr. 1-2	Gr. 3-4	Gr. 1-2	Gr. 3-4	Gr. 1-2	Gr. 3-4	Gr. 1-2	Gr. 3-4
Toxicity										
Trombocytopenia	-	-	-	-	-	-	1	-	1 (8)	-
Vomiting	-	-	-	-	2	-	-	-	2 (17)	-
Watering eyes	-	-	-	-	1	-	-	-	1 (8)	-
Weight loss	1	-	-	-	-	-	-	-	1 (8)	-

Abbreviation: CTCAE, Common Terminology Criteria for Adverse Events; Gr., grade; n, number of subjects.

10
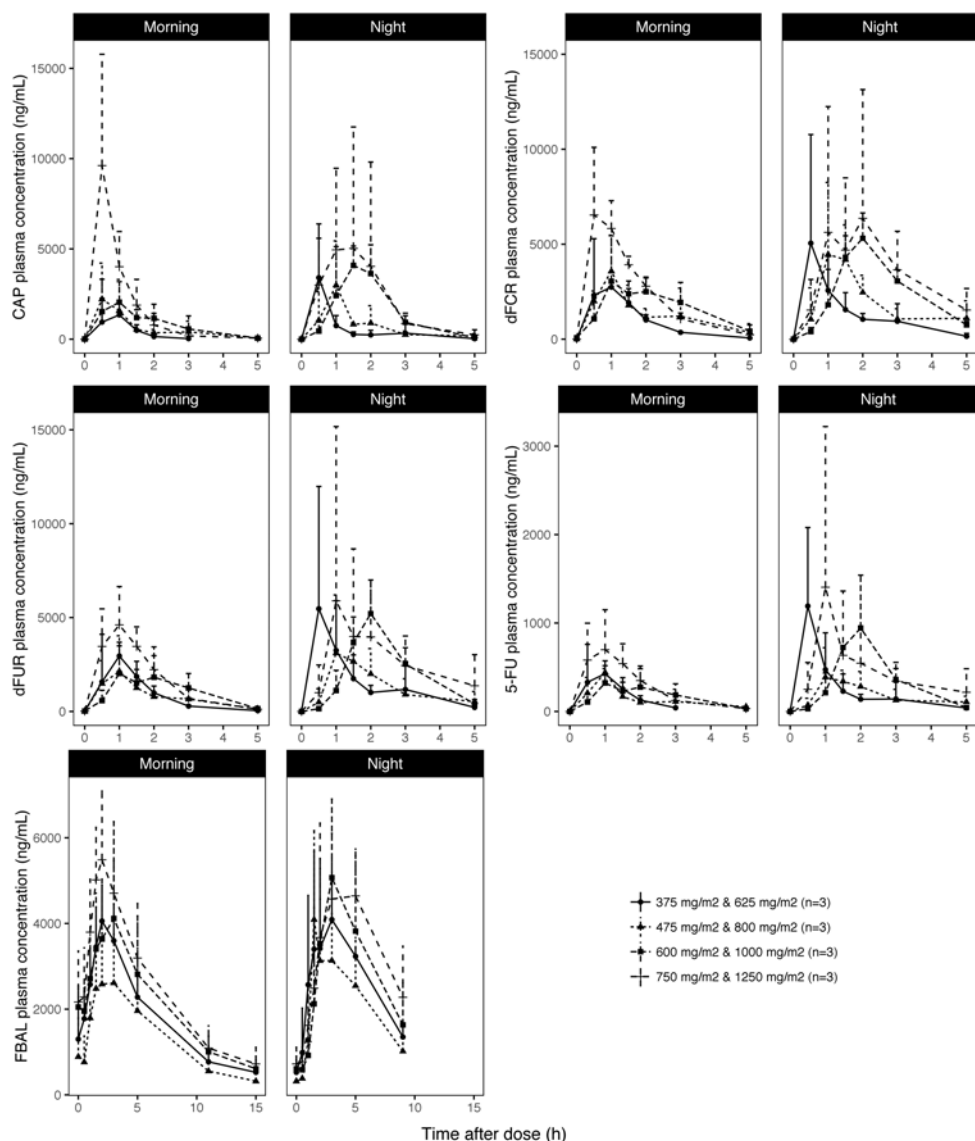
Figure 1. Mean (± SD) plasma concentration-time profiles of capecitabine (CAP), 5'-deoxy-5-fluorocytidine (dFCR), 5'-deoxy-5-fluorouridine (dFUR), 5-fluorouracil (5-FU) and fluoro-β-alanine (FBAL) at various dose levels after dose administration in the morning (at 9:00 h) and at night (24:00 h) on treatment day 7 and 8.

The dose-normalized AUC_{0-5h} and AUC_{0-inf} are shown in Figure 2. As shown in this figure, dose-normalized exposure to capecitabine, dFCR, dFUR and 5-FU were not statistically different between daytime and nighttime. For FBAL, daytime exposure was significantly higher than at night (p=0.0002).

Table 4. Pharmacokinetic parameters for capecitabine (CAP), 5'-deoxy-5-fluorocytidine (dFCR), 5'-deoxy-5-fluorouridine (dFUR), 5-fluorouracil (5-FU) and fluoro-β-alanine (FBAL), grouped per dose level and time of capecitabine administration.

		Dose level 1		Dose level 2		Dose level 3		Dose level 4	
Number of subjects		n=3		n=3		n=3		n=3	
Time of dose administration		9:00 h	24:00 h	9:00 h	24:00 h	9:00 h	24:00 h	9:00 h	24:00 h
Capecitabine dose (mg/m²)		375	625	475	800	600	1000	750	1250
		Mean (%CV)	Mean (%CV)	Mean (%CV)	Mean (%CV)	Mean (%CV)	Mean (%CV)	Mean (%CV)	Mean (%CV)
CAP	AUC_{0-5h} (µg*h/mL)	1.41 (13.5)	2.49 (25.3)	2.74 (29.6)	3.31 (31.7)	3.82 (18.6)	7.04 (5.8)	8.14 (62.8)	10.15 (83.2)
	C_{max} (µg/mL)	1.98 (22.7)	3.69 (68)	2.82 (53.5)	3.37 (59.3)	2.57 (34.6)	5.1 (9.2)	9.61 (64.2)	7.7 (75.6)
	t_{max} (h)	0.83 (34.9)	1.33 (108.3)	1.5 (88)	1.33 (43.6)	1.17 (65)	1.5 (33.3)	0.5 (0)	1.83 (56.8)
dFCR	AUC_{0-5h} (µg*h/mL)	4.26 (10.3)	6.5 (38.3)	5.47 (32)	8 (26.5)	8.01 (13.6)	11.92 (13.9)	11.64 (18.2)	16.93 (47.7)
	C_{max} (µg/mL)	3.41 (26.4)	5.76 (85.1)	3.4 (39.4)	5.22 (54.6)	4.06 (36.9)	5.31 (25)	7.12 (36.4)	10.09 (57.9)
	t_{max} (h)	0.83 (34.9)	1.5 (88)	1.5 (88)	1.33 (43.6)	2 (50)	2 (0)	0.83 (69.9)	2 (50)
dFUR	AUC_{0-5h} (µg*h/mL)	4.11 (12.2)	7.2 (27.1)	3.65 (19.5)	5.84 (27.2)	5 (29.8)	9.72 (22.6)	8.24 (26.5)	12.88 (48.2)
	C_{max} (µg/mL)	3.66 (20.8)	7.15 (70.3)	2.61 (43.3)	4.01 (59.6)	3.09 (41.1)	5.88 (13.3)	4.85 (38.1)	8.68 (80.4)
	t_{max} (h)	0.83 (34.9)	1.5 (88)	1.67 (68.9)	1.33 (43.6)	2 (50)	1.83 (15.8)	1 (50)	2 (50)
5-FU	AUC_{0-5h} (µg*h/mL)	0.58 (6.9)	0.97 (32)	0.52 (5.8)	0.8 (11.2)	0.76 (31.6)	1.43 (32.2)	1.25 (44)	1.94 (50.5)
	C_{max} (µg/mL)	0.54 (18.5)	1.03 (71.8)	0.38 (26.3)	0.51 (45.1)	0.45 (37.8)	1.04 (46.2)	0.78 (48.7)	1.35 (86.7)
	t_{max} (h)	0.83 (34.9)	1.5 (88)	1.67 (68.9)	1.33 (43.6)	2 (50)	1.83 (15.8)	1 (50)	2.67 (77.9)
FBAL	AUC_{0-inh} (µg*h/mL)	29.14 (33.7)	36.22 (6.5)	20.7 (56.7)	27.59 (61)	33.67 (39.1)	35.37 (51.3)	40.34 (38.8)	46 (34)
	C_{max} (µg/mL)	4.06 (20.7)	4.34 (18.7)	3.25 (28)	3.92 (39)	4.58 (46.3)	5.07 (36.1)	5.51 (28.7)	6.02 (7.6)
	t_{max} (h)	2 (0)	2.83 (66.8)	2.83 (66.8)	3.33 (45.9)	2.5 (34.8)	3 (0)	1.83 (15.8)	3.33 (45.9)

Abbreviations: CV, coefficient of variation; AUC_{0-5h}, area under the plasma-time curve up to five hours; AUC_{0-inf}, area under the plasma-time curve extrapolated to infinity; C_{max}, maximum plasma concentration; t_{max}, time to reach maximum plasma concentration; n, number of subjects

10
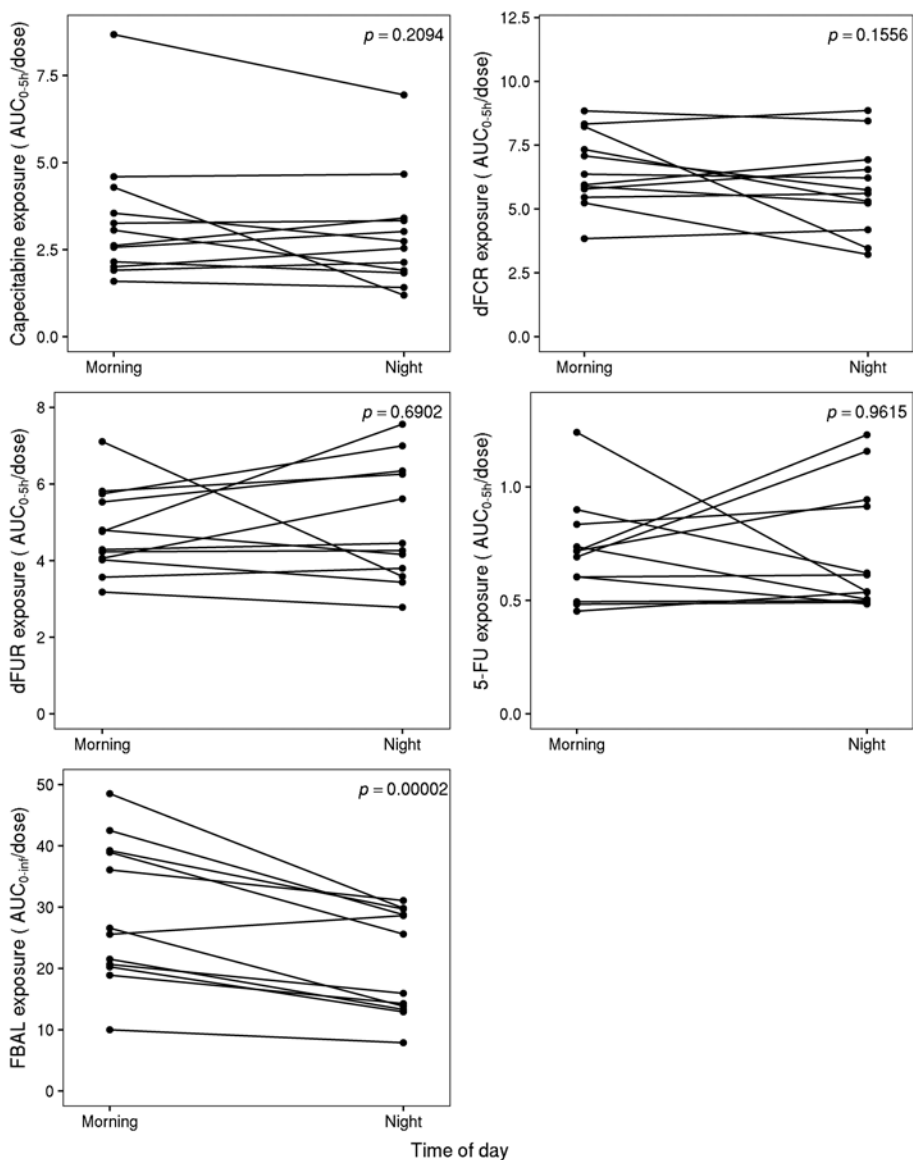
Figure 2. Dose-normalized area under the plasma concentration-time curve up to 5 hours (AUC_{0-5h}) for capecitabine (CAP), 5'-deoxy-5-fluorocytidine (dFCR), 5'-deoxy-5-fluorouridine (dFUR), 5-fluorouracil (5-FU) and extrapolated from zero to infinity (AUC_{0-inf}) for fluoro-β-alanine (FBAL) after dose administration in the morning (at 9:00 h) and in night (24:00 h) on treatment day 7 and 8, respectively.

Pharmacodynamics

TSA_{pbmc}, $DPDA_{pbmc}$ and TPA_{pbmc} were determined in all 12 subjects. Individual values of TSA_{pbmc} are shown in Figure 3 (upper panel). The median (range) TSA_{pbmc} at screening
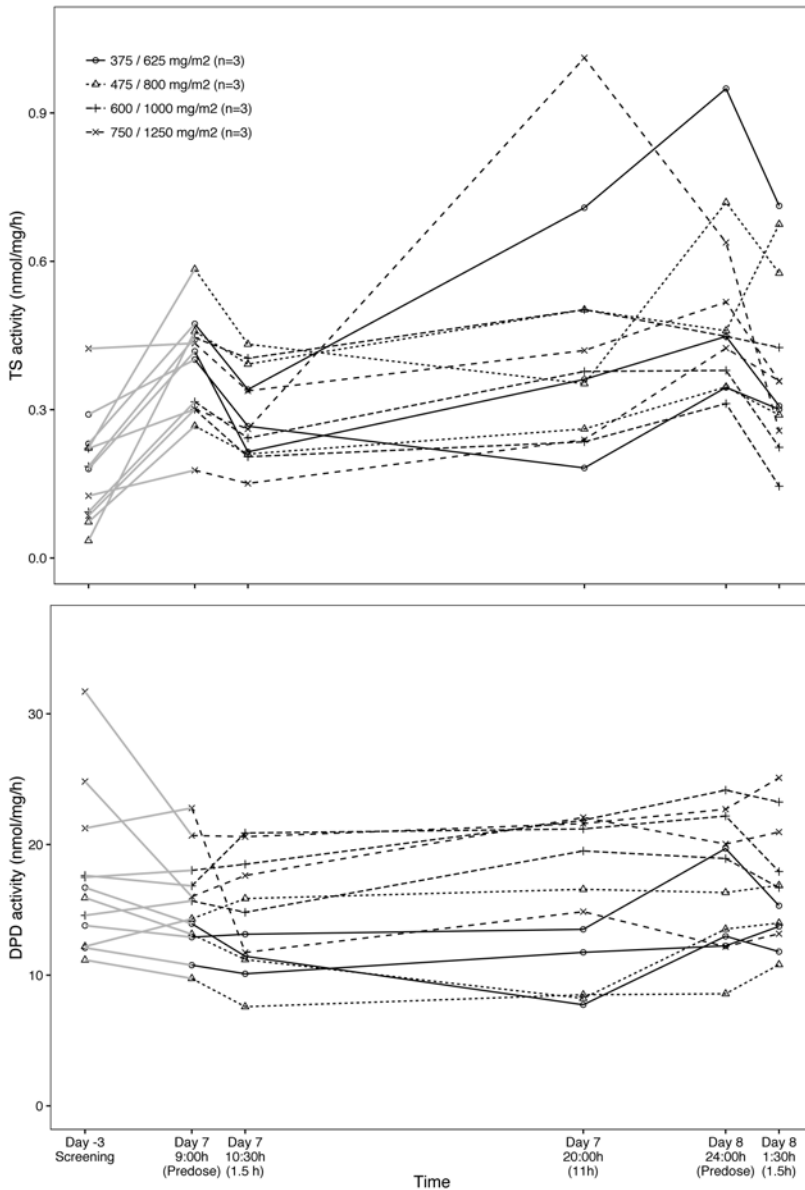
Figure 3. Thymidylate synthase (TS; upper panel) and dihydropyrimidine dehydrogenase (DPD; lower panel) activity in peripheral blood mononuclear cells versus time in 12 subjects. *Grey lines* connect values of screening (within 3 days prior to treatment) and pre-dose day 7. Absolute times (time after dose) are shown on the x-axis. The figure legend describes the dose levels.

was 0.183 (0.035-0.424) nmol/mg/h and was significantly induced to 0.410 (0.178-0.584) nmol/mg/h on day 7 at 9:00 h ($p<0.01$). TSA_{pbmc} declined again 1.5 h after the dose administration on day 7 ($p<0.01$). Maximum TSA_{pbmc} was measured at 15 hours
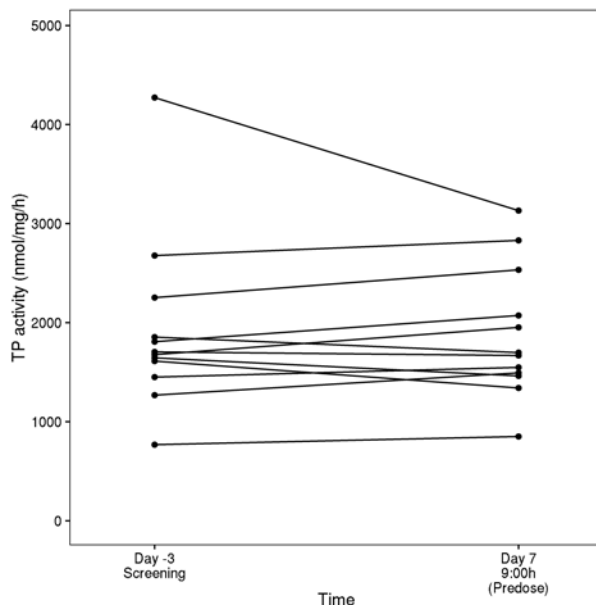
Figure 4. Thymidine phosphorylase (TP) activity in in peripheral blood mononuclear cells at screening (within 3 days prior to treatment) and pre-dose at treatment day 7 in 12 subjects.

10

post-dose (24:00 h) with median (range) activity of 0.448 (0.312-0.949) nmol/mg/h, which was significantly higher than the observed TSA_{pbmc} 1.5 h after dose administration at 9:00 h ($p<0.0001$).

The individual plots for $DPDA_{pbmc}$ are shown in Figure 3 (lower panel). The mean (±SD) $DPDA_{pbmc}$ at screening was 17.6 (± 6.0) nmol/mg/h, which was not statistically different from the values obtained on day 7 and 8. There was, however, significant intra-day variability in $DPDA_{pbmc}$: trough and peak activity were observed at 10:30 h and 01:30 h ($p<0.001$), and were 14.1 (±3.9) and 17.0 (±4.8) nmol/mg/h, respectively.

TPA_{pbmc} values were available from 12 subjects at the time of interim analysis. There was moderate between-subject variability in TPA_{pbmc} at screening with a mean (±SD) value of 1916 (±878) nmol/mg/h. There was no significant change in TPA_{pbmc} observed after 7 days of treatment

Tumour response evaluation

Five patients (42%) had stable disease as best response and received a median (range) of 5 (4-8) cycles before disease progression was observed. No partial remissions have been observed to date. Seven patients (58%) had progressive disease after the first response evaluation.

DISCUSSION

This manuscript describes the results of an interim analysis of a first phase I, safety and pharmacological study with continuous chronomodulated capecitabine therapy. Thus far, 4 dose levels have been opened. The total capecitabine dose was stepwise increased from 1000 mg/m^2/day in the first dose level up to 2000 mg/m^2/day in the dose level 4. No DLTs have been observed to date and dose escalation is still ongoing. Therefore, MTD and recommended dose for further clinical investigation have not been determined yet.

The patients who were included in the first four dose levels tolerated the chronomodulated capecitabine therapy very well. The most frequently observed adverse events were, nausea, fatigue and palmar-plantar erythrodysesthesia, diarrhoea, and anorexia. These adverse events were mild. Severe toxicity (≥grade 3) was observed in only one patient who was included in dose level 4. The adverse events were also observed in the previous phase I-III studies of continuous and intermittent capecitabine therapy [8,9,22].

Several chronomodulated treatment strategies for capecitabine have been evaluated in phase II studies [23–27]. In these studies, the total daily capecitabine dose was divided in two or three dosing moments with highest capecitabine dose administered between 18:00-20:00 h [24,25], at 23:00 h [23,26] or at 24:00h [27]. In these studies, chronomodulated capecitabine was combined with oxaliplatin [23–27], and radiotherapy [27]. The examined chronomodulated capecitabine regimens were well tolerated, except in the study performed by Qvortrup et al. [24]. They did not find improved treatment tolerability of chronomodulated capecitabine in combination with oxaliplatin compared to standard capecitabine plus oxaliplatin [24]. The reason for this could be that 80% of the capecitabine daily dose was administered between 18:00 and 20:00 h. According to our finding [15], high-dose capecitabine administration between 18:00-20:00 h could be too early to achieve adequate chronomodulation. Indeed, at that time of day, DPD activity is around the baseline value. Due to rapid elimination, most of 5-FU is probably degraded before DPD peak activity is encountered. A phase I study of intermittent capecitabine chronotherapy, in which 25% of daily dose was administered at 8:00 h, 25% at 18:00 h and 50% at 23:00 h, on day 1-14 of each 21-day cycle, demonstrated good treatment tolerability [28]. At the declared MTD level of 2750 mg capecitabine per day, only one out of nine patients experienced DLT. Our current findings are in line with previously reported results on chronomodulated capecitabine therapy.

Analysis of the first 12 patients in the current study did not demonstrate circadian rhythmicity in the dose-normalized plasma exposure to capecitabine, dFCR, dFUR and 5-FU. FBAL exposure was significantly higher during daytime. This may be due to relatively high FBAL concentrations already at pre-dose (9:00 h). Most likely, this finding does not have any clinical implications, since FBAL is an inactive metabolite. The current PK analysis does not demonstrate circadian PK of capecitabine and 5-FU. In healthy volunteers, we previously found that DPD activity in PBMCs demonstrated pronounced circadian rhythmicity, while in plasma, this effect was only minor [15]. Circadian rhythmicity might be regulated in a tissue-specific manner [29]. It could be that DPD activity in liver

10

tissue is not subject to noticeable circadian rhythmicity. This might explain the absence of circadian rhythmicity in 5-FU plasma exposure. On the other hand, peripheral 5-FU metabolism could be regulated in a circadian manner, which could contribute to improved treatment tolerability.

As demonstrated on day 7, TSA_{pbmc} was partly inhibited 1.5 hours after capecitabine. At the same time, maximum plasma concentrations of capecitabine and metabolites were found. The reduction in TSA_{pbmc} is most likely a direct consequence of target inhibition by the intracellularly activated metabolite 5-fluoro-2'-deoxyuridine-5'-monophosphate (FdUMP). At a later time point, 15 hours after dose, when capecitabine and metabolites have already been undetectable in plasma for approximately 10 hours, TSA_{pbmc} demonstrated peak activity. Previous research demonstrated that TS protein expression is subject to auto-regulation. Induction of TS protein levels resulted in reduced transcription of the TS mRNA [30]. It is likely that TS mRNA transcription was induced at the time of TSA_{pbmc} inhibition, 1.5 hours after dose. As a consequence, TSA_{pbmc} could be upregulated 15 hours after capecitabine administration. Although TSA_{pbmc} seems a potential PD marker for capecitabine therapy, current analysis did not demonstrate circadian rhythmicity in TSA_{pbmc}.

There was significant intra-day variability in $DPDA_{pbmc}$ with peak activity observed at 01:30 h and trough activity around 10:30 h. In healthy volunteers, we also found a similar pattern with trough activity in the morning and peak activity during in the early night [15]. This finding highly supports our rationale for capecitabine chronotherapy and could explain why treatment tolerability was very good in the first 4 dose levels.

Continuous chronomodulated capecitabine seems to be well tolerated. Although the MTD has not been determined yet, the currently examined total daily dose of 2000 mg/m^2 in dose level 4 also exceeds the previously determined recommended daily dose for regular treatment with continuous BID capecitabine of 1331 mg/m^2. Interestingly, the cumulative dose in dose level 4 was 20% higher than to the cumulative dose of the approved regimen (1250 mg/m^2 bi-daily on day 1-14 of every 21-day cycle). Chronomodulation is promising and could lead to improved tolerability and efficacy of capecitabine.

REFERENCES

1. Reigner B, Blesch K, Weidekamm E. Clinical pharmacokinetics of capecitabine. Clin Pharmacokinet 2001;40:85–104.

2. Diasio RB, Harris BE. Clinical pharmacology of 5-fluorouracil. Clin Pharmacokinet 1989;16:215–37.

3. Longley DB, Harkin DP, Johnston PG. 5-fluorouracil: mechanisms of action and clinical strategies. Nat Rev Cancer 2003;3:330–8.

4. Wilson PM, Danenberg P V, Johnston PG, Lenz H-J, Ladner RD. Standing the test of time: targeting thymidylate biosynthesis in cancer therapy. Nat Rev Clin Oncol 2014;11:282–98.

5. de Bono JS, Twelves CJ. The oral fluorinated pyrimidines. Invest New Drugs 2001;19:41–59.

6. Judson IR, Beale PJ, Trigo JM, Aherne W, Crompton T, Jones D, et al. A human capecitabine excretion balance and pharmacokinetic study after administration of a single oral dose of 14C-labelled drug. Invest New Drugs 1999;17:49–56.

7. Midgley R, Kerr DJ. Capecitabine: have we got the dose right? Nat Clin Pract Oncol 2009;6:17–24.

8. Mackean M, Planting A, Twelves C, Schellens J, Allman D, Osterwalder B, et al. Phase I and pharmacologic study of intermittent twice-daily oral therapy with capecitabine in patients with advanced and/or metastatic cancer. J Clin Oncol 1998;16:2977–85.

9. Budman DR, Meropol NJ, Reigner B, Creaven PJ, Lichtman SM, Berghorn E, et al. Preliminary studies of a novel oral fluoropyrimidine carbamate: capecitabine. J Clin Oncol 1998;16:1795–802.

10. Van Cutsem E, Findlay M, Osterwalder B, Kocha W, Dalley D, Pazdur R, et al. Capecitabine, an oral fluoropyrimidine carbamate with substantial activity in advanced colorectal cancer: results of a randomized phase II study. J Clin Oncol 2000;18:1337–45.

11. Harris BE, Song R, Soong SJ, Diasio RB. Relationship between dihydropyrimidine dehydrogenase activity and plasma 5-fluorouracil levels with evidence for circadian variation of enzyme activity and plasma drug levels in cancer patients receiving 5-fluorouracil by protracted continuous infusion. Cancer Res 1990;50:197–201.

12. Petit E, Milano G, Levi F, Thyss A, Bailleul F, Schneider M. Circadian rhythm-varying plasma concentration of 5-fluorouracil during a five-day continuous venous infusion at a constant rate in cancer patients. Cancer Res 1988;48:1676–9.

13. Fleming GF, Schumm P, Friberg G, Ratain MJ, Njiaju UO, Schilsky RL. Circadian variation in plasma 5-fluorouracil concentrations during a 24 hour constant-rate infusion. BMC Cancer 2015;15:1075.

14. Lévi F, Zidani R, Misset J, et al. Randomised multicentre trial of chronotherapy with oxaliplatin, fluorouracil, and folinic acid in metastatic colorectal cancer. Lancet 1997;350:681–6.

15. Jacobs BAW, Deenen MJ, Pluim D, van Hasselt JGC, Krähenbühl MD, van Geel RMJM, et al. Pronounced between-subject and circadian variability in thymidylate synthase and dihydropyrimidine dehydrogenase enzyme activity in human volunteers. Br J Clin Pharmacol 2016.

16. Eisenhauer EA, Therasse P, Bogaerts J, Schwartz LH, Sargent D, Ford R, et al. New response evaluation criteria in solid tumours: revised RECIST guideline (version 1.1). Eur J Cancer 2009;45:228–47.

17. Deenen MJ, Rosing H, Hillebrand MJ, Schellens JHM, Beijnen JH. Quantitative determination of capecitabine and its six metabolites in human plasma using liquid chromatography coupled to electrospray tandem mass spectrometry. J Chromatogr B Analyt Technol Biomed Life Sci 2013;913-914:30–40.

18. R Development Core Team. R: A Language and Environment for Statistical Computing. Vienna, Austria: R Foundation for Statistical Computing, 2016.

19. Pluim D, Jacobs BA, Deenen MJ, Ruijter AE, Van Geel RM, Burylo AM, et al. Improved pharmacodynamic assay for dihydropyrimidine dehydrogenase activity in peripheral blood mononuclear cells. Bioanalysis 2015;7:519–29.

10

20. Pluim D, Schilders KAA, Jacobs BAW, Vaartjes D, Beijnen JH, Schellens JHM. Pharmacodynamic assay of thymidylate synthase activity in peripheral blood mononuclear cells. Anal Bioanal Chem 2013;405:2495–503.

21. Pluim D, Jacobs BAW, Krähenbühl MD, Ruijter AEM, Beijnen JH, Schellens JHM. Correction of peripheral blood mononuclear cell cytosolic protein for hemoglobin contamination. Anal Bioanal Chem 2013;405:2391–5.

22. Twelves C, Wong A, Nowacki MP, Abt M, Burris H, Carrato A, et al. Capecitabine as adjuvant treatment for stage III colon cancer. N Engl J Med 2005;352:2696–704.

23. Santini D, Vincenzi B, Schiavon G, Di Seri M, Virzí V, Spalletta B, et al. Chronomodulated administration of oxaliplatin plus capecitabine (XELOX) as first line chemotherapy in advanced colorectal cancer patients: phase II study. Cancer Chemother Pharmacol 2007;59:613–20.

24. Qvortrup C, Jensen BV, Fokstuen T, Nielsen SE, Keldsen N, Glimelius B, et al. A randomized study comparing short-time infusion of oxaliplatin in combination with capecitabine XELOX(30) and chronomodulated XELOX(30) as first-line therapy in patients with advanced colorectal cancer. Ann Oncol 2010;21:87–91.

25. Qvortrup C, Yilmaz M, Ogreid D, Berglund A, Balteskard L, Ploen J, et al. Chronomodulated capecitabine in combination with short-time oxaliplatin: a Nordic phase II study of second-line therapy in patients with metastatic colorectal cancer after failure to irinotecan and 5-flourouracil. Ann Oncol 2008;19:1154–9.

26. Santini D, Vincenzi B, La Cesa A, Caricato M, Schiavon G, Spalletta B, et al. Continuous infusion of oxaliplatin plus chronomodulated capecitabine in 5-fluorouracil- and irinotecan-resistant advanced colorectal cancer patients. Oncology 2005;69:27–34.

27. Bajetta E, Pietrantonio F, Buzzoni R, Ferrario E, Valvo F, Mariani L, et al. Chronomodulated Capecitabine and Adjuvant Radiation in Intermediate-risk to High-risk Rectal Cancer: A Phase II Study. Am J Clin Oncol 2013;00:1–5.

28. Santini D, Vincenzi B, Schiavon G, La Cesa A, Gasparro S, Vincenzi A, et al. Phase I study of intermittent and chronomodulated oral therapy with capecitabine in patients with advanced and/or metastatic cancer. BMC Cancer 2006;6:42.

29. Innominato PF, Lévi FA, Bjarnason GA. Chronotherapy and the molecular clock: Clinical implications in oncology. Adv Drug Deliv Rev 2010;62:979–1001.

30. Chu E, Koeller DM, Casey JL, Drake JC, Chabner BA, Elwood PC, et al. Autoregulation of human thymidylate synthase messenger RNA translation by thymidylate synthase. Proc Natl Acad Sci U S A 1991;88:8977–81.

10

CONCLUSIONS AND PERSPECTIVES

CONCLUSIONS AND PERSPECTIVES

The fluoropyrimidine capecitabine is an oral pre-pro-drug of 5-fluorouracil (5-FU). Capecitabine is used for over 10 years for the treatment of gastro-intestinal and breast cancers. After oral intake, capecitabine is rapidly absorbed and extensively metabolized to subsequently 5'-deoxy-5-fluorocytidine (dFCR), 5'-deoxy-5-fluorouridine (dFUR) and 5-FU. These metabolic steps are catalysed by the enzymes carboxylesterase, cytidine deaminase and thymidine phosphorylase (TP), respectively [1]. Approximately 80% of 5-FU is degraded to inactive metabolites by the enzyme dihydropyrimidine dehydrogenase (DPD). Only a small proportion of 5-FU is intracellularly anabolized to cytotoxic metabolites [2,3]. The main mechanism of action is considered to be inhibition of the enzyme thymidylate synthase (TS), which is essential for DNA synthesis.

About 25% of patients experience severe treatment-induced toxicities. The most common severe side effects are diarrhoea, stomatitis, vomiting and hand-foot syndrome [4–8]. The aim of this thesis was to obtain better insight into the pharmacology of capecitabine and to explore opportunities for improved capecitabine safety.

Development and validation of phenotyping methods

Several genetic mutations in *DPYD*, the gene encoding DPD, have been associated with DPD deficiency and an increased risk of fluoropyrimidine-induced toxicity. Most convincing evidence for an increased risk of fluoropyrimidine toxicity has been demonstrated for the *DPYD**2A, c.1236G>A, c.1679T>G and c.2846A>T allele variants [9,10]. However, more than 45 other mutations in *DPYD* have been described [11]. For many mutations, the effect on the DPD phenotype is unknown. In addition, epigenetic factors and expression of microRNAs could also affect DPD activity [12,13].

Phenotyping DPD enzyme activity, in which all relevant genetic and epigenetic variations are reflected, could lead to more sensitive identification of DPD deficiency. Assessing the clinical applicability of DPD phenotyping approaches requires the availability of sensitive and accurate methods. **Chapter 1** describes the development and validation of an assay for quantification of the endogenous DPD substrate uracil (U) and the reaction product dihydrouracil (UH$_2$) in human plasma. The UH$_2$:U plasma ratio is often used as a marker for DPD activity. Previously described bioanalytical methods required extensive sample pretreatment and sometimes long analytical run times for quantification of U and UH$_2$. Our method employed protein precipitation for sample pretreatment, which together with ultra-performance liquid chromatography – tandem mass spectrometry enabled rapid, accurate, precise and sensitive quantification of U and UH$_2$ plasma levels. The use of stable isotopes of U and UH$_2$ as internal standards resulted in adequate correction of matrix effects.

While the DPD phenotype can be determined in plasma, alternative matrices can be considered. **Chapter 2** describes the development and validation of a radioassay for quantification of DPD activity in peripheral blood mononuclear cells (PBMCs). Quantification of DPD activity was achieved by determining *ex vivo* conversion of the DPD substrate ^{3}H-thymine to ^{3}H-dihydrothymine using the enzyme-rich PBMC lysate

to catalyse this reaction. Assay accuracy was improved by using the cumulative area of all chromatographic peaks as an internal standard. In addition, we found that PBMC lysate was often contaminated with hemoglobin, which resulted in inaccurate assessment of DPD activity with a mean bias of 20.3% (range: 1%-59%) [14]. We developed a simple spectrophotometric assay to quantify the amount of hemoglobin contamination in PBMCs lysate [14], which enabled more accurate quantification of DPD activity in PBMCs.

Besides DPD activity, several other enzymes play a crucial role in the metabolic pathway of capecitabine. The enzyme TP has a dual role in the activation of capecitabine: 1) it catalyses the conversion of dFUR to 5-FU and 2) it is required for intracellular activation of 5-FU. High TP activity might lead to increased formation of cytotoxic metabolites and could contribute to improved identification of patients at risk of toxicity. In **chapter 3**, the development and validation of an assay for TP activity in PBMCs was described. The TP substrate thymidine was co-incubated with PBMC lysate. The reaction product thymine was quantified by high-performance liquid chromatography coupled with UV detection. Validation experiments showed that the developed assay was accurate, precise and sensitive. Analysis of the PBMC subpopulations demonstrated that TP activity was three times higher in monocytes than in lymphocytes.

Phenotypic variability in dihydropyrimidine dehydrogenase and thymidylate synthase activity

The developed phenotyping methods were applied in translational research. **Chapter 4** describes an observational study of DPD and TS variability in healthy volunteers. Pronounced between-subject and circadian rhythmicity in DPD and TS activity was demonstrated. DPD activity in PBMCs was highly subject to circadian rhythmicity and showed peak activity during the night. The UH_2:U plasma ratio displayed modest circadian rhythmicity with peak activity during the afternoon. TS activity in PBMCs was found to be lowest during the night at the time of peak DPD activity. These results support further research for fluoropyrimidine therapy that is adapted to circadian rhythmicity.

The use of PBMCs for phenotyping analysis does not allow for detection of dynamic changes in systemic DPD activity. DPD is highly expressed in liver tissue and changes in hepatic function could hypothetically lead to altered systemic DPD activity. As demonstrated in **chapter 5**, the UH_2:U plasma ratio was significantly decreased in patients who underwent liver resection for the treatment of colorectal liver metastases one day earlier. The UH_2:U plasma ratio recovered 4-8 weeks after liver resection. Dynamic changes in UH_2:U plasma ratio can be observed after liver resection and could represent dynamic changes in systemic DPD activity.

In **Chapter 6**, Meulendijks et al. described the clinical relevance of genetic variability in the gene encoding TS, *TYMS*, with respect to fluoropyrimidine-induced toxicity. The genetic variant of interest, the 2RC allele (rs183205964), was associated with fluoropyrimidine-induced toxicity. It was expected that the 2RC allele also resulted in relatively low TS activity. One patient carrying the very rare 2RC/2RC genotype, did, however, not demonstrate reduced TS activity in PBMCs.

Capecitabine pharmacokinetics

Pharmacokinetic data of capecitabine and the metabolites dFCR, dFUR, 5-FU and FBAL were collected in seven clinical studies. The studies included patients with gastric, esophageal, colorectal and anal cancer who were treated with different capecitabine-based treatment regimens. **Chapter 7** describes the population pharmacokinetic analysis of capecitabine and metabolites in this large and heterogeneous population. Nonlinear mixed-effects modeling was applied to fully characterize the pharmacokinetics of the parent compound and its metabolites. Capecitabine absorption was well described using a four-transit model. There was wide between-subject and between-occasion variability in the absorption rate. Rapid absorption was revealed for patients who previously underwent partial of total gastrectomy. Two-compartment models adequately described capecitabine, dFCR and FBAL pharmacokinetics and flip-flop pharmacokinetics was demonstrated for dFUR and 5-FU. Patient carrying the *DPYD**2A risk allele demonstrated a 21.5% reduction in 5-FU elimination. The developed model adequately described the complexity of capecitabine and metabolite pharmacokinetics in a large and variable population of cancer patients.

It was previously shown that continuous 5-FU infusion was better tolerable and more effective than bolus infusion [15]. Currently available capecitabine tablet formulations lead to rapid absorption and degradation of capecitabine. 5-FU follows the same pattern in plasma concentration-time profile as capecitabine. More gradual and continuous exposure to capecitabine could lead to improved treatment safety and efficacy. **Chapter 8** describes a phase 0 clinical study of novel candidate extended-release formulations of capecitabine. Pharmacokinetic characteristics of these extended-release tablet formulations, which differed with respect to the amount of extended-release excipient in tablet matrix and in tablet coating, were tested in patients. Proof of principle was achieved, since extended-release of capecitabine was obtained by modulation of the tablet coating thickness.

Although the majority of 5-FU is catabolized by DPD to inactive metabolites, a small fraction is intracellularly converted to active metabolites. Results of the exploratory study described in **chapter 9** demonstrated that the cytotoxic metabolite 5-fluorouridine 5′-triphosphate (FUTP) accumulates in PBMCs after intake of capecitabine. This metabolite FUTP causes RNA damage, which attributes to capecitabine-induced cell death. Intracellular exposure to FUTP was highly prolonged compared to capecitabine and 5-FU plasma levels.

Capecitabine chronotherapy

Based on the observed circadian rhythm of DPD and TS activity in healthy volunteers, we hypothesized that capecitabine tolerability could be affected by the time of dosing. A chronomodulated treatment regimen, in which drug administration is adapted to circadian pharmacology, could improve capecitabine tolerability. Levi et al. previously demonstrated that chronomodulated 5-FU treatment leads to improved treatment safety and efficacy compared to constant-rate infusion [16].

Chapter 10 describes an interim analysis of a phase I pharmacological study of continuous chronomodulated capecitabine treatment. Chronotherapeutic treatment was

achieved by dividing the total daily dose in two unequal doses that were administered in the morning (9:00 h) and in the late evening (24:00 h). A relatively high capecitabine dose was administered at 24:00 h, since DPD activity was expected to peak during the early night. The cumulative capecitabine dose in dose level 4 was 20% higher than what is achieved using the approved dosing regimen (1250 mg/m^2 bi-daily on days 1-14 of each 21-day cycle). The maximum tolerated dose (MTD) has not been determined yet. Capecitabine and 5-FU pharmacokinetics did not demonstrate circadian rhythmicity. DPD activity in PBMCs, however, demonstrated intra-day variability with peak activity during the night. No dose-limiting toxicity has been observed thus far. Continuous chronomodulated capecitabine was well tolerated and demonstrated a promising safety profile.

PERSPECTIVES

We demonstrated that partial liver resection leads to a temporary decrease in the UH$_2$:U plasma ratio and that DPD and TS phenotype markers display circadian variability. However, little is known about the effect of physiological conditions, such as physical activity, the intake of food and exposure to light on phenotypic variability. Studies are required to identify relevant biological confounders and to determine under which circumstances sample collection leads to the most accurate determination of an individual phenotype.

As described in this thesis, the PBMC subpopulation of monocytes demonstrated higher TP activity than the PBMC subpopulation of lymphocytes. This finding highly suggests that an assay result could be affected by the composition of the isolated PBMC fraction. During isolation, the PBMC fraction could be contaminated with other blood cells, such as granulocytes and blood platelets. Additional research is recommended to determine whether the relative abundances of specific cell types in the isolated PBMC fraction lead to significantly biased assessment of DPD, TS and TP phenotypes, and whether the assay results should be corrected for the abundances of specific cell populations.

In the studies described in this thesis, DPD activity was determined in plasma and in PBMCs. Alternative DPD phenotyping methods, by means of the 2-^{13}C-uracil breath test and the uracil test dose, are also promising. Currently, a multicenter clinical study is performed in which the performance of these four different DPD phenotyping methods are compared with regard to successful identification of patients at risk of fluoropyrimidine-induced toxicity (www.clinicaltrials.gov, trial identifier: NCT02324452). Since we observed circadian rhythmicity in DPD activity in PBMCs and plasma, it is recommended to examine whether the time of day affects the DPD phenotyping results, and whether the time of day should be taken into account when fluoropyrimidines dosing is guided by the DPD phenotype.

Large between-subject variability in capecitabine and metabolites pharmacokinetics has been demonstrated. Future clinical studies of capecitabine therapy should incorporate pharmacokinetic analysis of capecitabine and metabolites in plasma and in PBMCs. It would be interesting to examine association between metabolite pharmacokinetics and pretherapeutic DPD and TP enzyme activities. Analysis of such associations could support

the implementation of phenotype-based dosing of fluoropyrimidines. Furthermore, it is encouraged to examine the association between intracellular pharmacokinetics and fluoropyrimidine-induced toxicity and efficacy. If exposure to the intracellular fluoropyrimidine metabolites is associated with treatment response, there could be an opportunity for treatment optimization by means of therapeutic drug monitoring.

Translational research of circadian rhythmicity in DPD and TS activity in healthy volunteers supported the rationale for capecitabine chronotherapy. Preliminary results of the phase I study of chronomodulated capecitabine therapy are promising. When the MTD for continuous chronomodulated capecitabine has been reached, the MTD of intermittent chronomodulated capecitabine will be determined. For the intermittent chronomodulated regimen, capecitabine will be administered bi-daily on days 1-14 of each 21-day cycle. After finishing the phase I studies, additional clinical research is needed to compare the safety and efficacy profiles of chronomodulated and conventional capecitabine therapy.

A disadvantage of the applied chronotherapeutic dosing schedule is the time of capecitabine administration. In the current phase I study, capecitabine needs to be administered in the late evening in order to attain capecitabine and 5-FU peak levels around 1:30 h. The currently used capecitabine formulation is an immediate-release tablet that leads to short-term exposure to capecitabine. The availability of an extended-release formulation of capecitabine would allow for capecitabine administration earlier in the evening. Pharmaceutical research with the aim to improve the extended-release formulation of capecitabine is therefore highly encouraged.

Concluding, the pharmacology of capecitabine and metabolites has shown to be complex. The availability of novel phenotypic assays and treatment regimens could lead to improved treatment safety and possibly also better efficacy. Since fluoropyrimidines remain the mainstay in for the treatment of several solid tumours, opportunities for treatment optimization are highly relevant and warrant further examination.

REFERENCES

1. Reigner B, Blesch K, Weidekamm E. Clinical pharmacokinetics of capecitabine. Clin Pharmacokinet 2001;40:85–104.

2. Diasio RB, Harris BE. Clinical pharmacology of 5-fluorouracil. Clin Pharmacokinet 1989;16:215–37.

3. Longley DB, Harkin DP, Johnston PG. 5-fluorouracil: mechanisms of action and clinical strategies. Nat Rev Cancer 2003;3:330–8.

4. Twelves C, Wong A, Nowacki MP, Abt M, Burris H, Carrato A, et al. Capecitabine as adjuvant treatment for stage III colon cancer. N Engl J Med 2005;352:2696–704.

5. Van Cutsem E, Twelves C, Cassidy J, Allman D, Bajetta E, Boyer M, et al. Oral capecitabine compared with intravenous fluorouracil plus leucovorin in patients with metastatic colorectal cancer: results of a large phase III study. J Clin Oncol 2001;19:4097–106.

6. Cassidy J, Twelves C, Van Cutsem E, Hoff P, Bajetta E, Boyer M, et al. First-line oral capecitabine therapy in metastatic colorectal cancer: a favorable safety profile compared with intravenous 5-fluorouracil/leucovorin. Ann Oncol 2002;13:566–75.

7. Hoff PM, Ansari R, Batist G, Cox J, Kocha W, Kuperminc M, et al. Comparison of oral capecitabine versus intravenous fluorouracil plus leucovorin as first-line treatment in 605 patients with metastatic colorectal cancer: results of a randomized phase III study. J Clin Oncol 2001;19:2282–92.

8. Kang Y-K, Kang W-K, Shin D-B, Chen J, Xiong J, Wang J, et al. Capecitabine/cisplatin versus 5-fluorouracil/cisplatin as first-line therapy in patients with advanced gastric cancer: a randomised phase III noninferiority trial. Ann Oncol 2009;20:666–73.

9. Deenen MJ, Meulendijks D, Cats A, Sechterberger MK, Severens JL, Boot H, et al. Upfront genotyping of DPYD*2A to individualize fluoropyrimidine therapy: a safety and cost analysis. J Clin Oncol 2016;34:227–34.

10. Meulendijks D, Henricks LM, Sonke GS, Deenen MJ, Froehlich TK, Amstutz U, et al. Clinical relevance of DPYD variants c.1679T>G, c.1236G>A/HapB3, and c.1601G>A as predictors of severe fluoropyrimidine-associated toxicity: a systematic review and meta-analysis of individual patient data. Lancet Oncol 2015;16:1639–50.

11. Ciccolini J, Gross E, Dahan L, Lacarelle B, Mercier C. Routine dihydropyrimidine dehydrogenase testing for anticipating 5-fluorouracil-related severe toxicities: hype or hope? Clin Colorectal Cancer 2010;9:224–8.

12. Ezzeldin HH, Lee AM, Mattison LK, Diasio RB. Methylation of the DPYD promoter: an alternative mechanism for dihydropyrimidine dehydrogenase deficiency in cancer patients. Clin Cancer Res 2005;11:8699–705.

13. Amstutz U, Offer SM, Sistonen J, Joerger M, Diasio RB, Largiadèr CR. Polymorphisms in MIR27A Associated with Early-Onset Toxicity in Fluoropyrimidine-Based Chemotherapy. Clin Cancer Res 2015;21:2038–44.

14. Pluim D, Jacobs BAW, Krähenbühl MD, Ruijter AEM, Beijnen JH, Schellens JHM. Correction of peripheral blood mononuclear cell cytosolic protein for hemoglobin contamination. Anal Bioanal Chem 2013;405:2391–5.

15. Meta-analysis Group In Cancer. Efficacy of intravenous continuous infusion of fluorouracil compared with bolus administration in advanced colorectal cancer. J Clin Oncol 1998;16:301–8.

16. Lévi F, Zidani R, Misset J. Randomised multicentre trial of chronotherapy with oxaliplatin, fluorouracil, and folinic acid in metastatic colorectal cancer. Lancet 1997;350:681–6.

A P P E N D I X

SUMMARY

Fluoropyrimidine anticancer drugs are the mainstay of treatment for advanced gastro-intestinal en breast cancers. Although the fluoropyrimidine anticancer drug 5-fluorouracil (5-FU) has been available for several decades, it remains one of the most effective drugs in the treatment of these types of cancer. The success of this intravenously available drug led to the development of more patient-friendly fluoropyrimidine drugs. About 15 years ago, an orally available pre-prodrug of 5-FU, capecitabine, became available as tablets. A major advantage of capecitabine over intravenously available 5-FU is that it can be taken at home. After oral intake, capecitabine is rapidly absorbed from the gut and metabolized into 5-FU via a three-step enzymatic pathway.

As for many chemotherapeutic drugs, capecitabine and 5-FU are dosed at their maximum tolerated doses, which are the doses that did not lead to unacceptable toxicity in the early clinical trials. There are, however, patients who do not tolerate the standard dosing regimens. Some patients even develop severe, life-threatening, side effects, such as diarrhoea and mucositis, when treated at a standard dose. It remains challenging to identify the patients who are at risk of developing these severe side effects. The studies described in this thesis are aimed at improving fluoropyrimidine treatment safety.

Methods for optimizing fluoropyrimidine treatment

Part I of this thesis includes three chapters in which the development and validation of three laboratory methods are presented. These methods are developed in order to measure the activity of two enzymes that are important for capecitabine activation and degradation. The enzyme of interest in **chapter 1** and **chapter 2** is dihydropyrimidine dehydrogenase (DPD). This enzyme is essential for detoxification of 5-FU. Patients with a deficiency in DPD demonstrate decreased clearance of 5-FU and are at risk of severe fluoropyrimidine-induced toxicity. Therefore, it is important to individualize fluoropyrimidine treatment based on the DPD phenotype. Implementation of DPD phenotype-guided dosing requires the availability of bioanalytical methods for assessing the DPD phenotype.

A method for measuring DPD activity is based on quantification of the endogenous DPD substrate uracil (U) and the reaction product dihydrouracil (UH_2) in patient plasma. **Chapter 1** describes the development and validation of an assay for the quantification of U and UH_2 in human plasma. This method is based on ultra-performance liquid chromatography coupled with tandem mass spectrometry. Protein precipitation was employed for extraction of U and UH_2 from plasma. The use of protein precipitation, together with a chromatographic run time of only 5 minutes, enables rapid measurement of U and UH_2 plasma levels. Results of the validation experiments demonstrated that the method facilitates sensitive, accurate and precise quantification of U and UH_2.

Chapter 2 focuses on the development and validation of another method for the quantification of DPD activity. The DPD phenotype was determined by the amount of 5,6-dihydrothymine formed after *ex vivo* incubation of the DPD substrate thymine with the cytosolic lysate of human peripheral blood mononuclear cells (PBMCs), which contain

the enzyme DPD. Radiolabeled thymine was used to achieve selective quantification of 5,6-dihydrothymine and thymine using radioisotope detection. PBMCs were isolated from whole blood using density gradient centrifugation. We discovered that isolated PBMCs were often contaminated with hemoglobin, which resulted in biased estimation of DPD activity. Using a simple spectrophotometrical method to quantify the amount of hemoglobin in the cytosolic lysate of PBMCs we were able to correct for this contamination. Assay accuracy was further improved by using the cumulative area of all chromatographic peaks as internal standard. Validation experiments demonstrated that DPD activity could be determined with adequate specificity, sensitivity, accuracy and precision.

While DPD is important for the detoxification of 5-FU, the enzyme thymidine phosphorylase (TP) is important for activation of 5-FU into cytotoxic metabolites. Relatively high TP activity might induce the conversion of capecitabine and 5-FU to cytotoxic metabolites. Assessment of TP activity might therefore be important for fluoropyrimidine-induced toxicity. The development and validation of a phenotypic method to determine TP activity in human PBMCs is described in **chapter 3**. TP activity was determined by the amount of thymine formed after incubation of the TP substrate thymidine with the cytosolic lysate of human PBMCs. High-performance liquid chromatography coupled with ultraviolet detection was employed to determine the amount of thymine formed after the incubation step. The assay was validated and found to be precise and sensitive. Clinical applicability was demonstrated by measuring the TP activity in PBMCs that were isolated from blood of five patients.

Phenotypic variability in healthy volunteers and patients

The second part of this thesis includes translational and clinical studies in which the developed phenotypic assays are applied. In **chapter 4**, we investigated circadian rhythmicity in phenotypic markers for DPD and thymidylate synthase (TS) in healthy volunteers. The latter enzyme is essential for DNA synthesis and is considered the main target of fluoropyrimidines. The activity of TS was also determined in isolated PBMCs. Circadian rhythmicity was demonstrated for both enzymes. During the early night, DPD activity in PBMCs showed peak activity and TS activity demonstrated trough levels. On the contrary, the UH_2:U plasma ratio in plasma was lowest during the early night. Circadian rhythmicity for DPD activity in PBMCs was found to relatively strong with an observed peak:trough ratio of 1.69. Rhythmicity in the UH_2:U ratio was less pronounced. Differences in circadian rhythmicity between DPD activity in PBMCs and plasma could be caused by tissue-specific regulation of DPD activity. Based on the large circadian rhythmicity in DPD activity in PBMCs, we initiated a clinical phase I trial to examine the role of circadian variability on tolerability to capecitabine (**chapter 10**).

The enzyme DPD is highly expressed within liver tissue. In **chapter 5**, we described dynamic changes in the plasma marker of DPD activity, the UH_2:U plasma ratio, in patients who underwent liver resection for the treatment of colorectal liver metastases. The median UH_2:U plasma ratio was significantly reduced from 10.7 before resection to 5.5 one day after resection. The drop in the UH_2:U ratio might be the result of

a reduction in hepatic DPD activity. Although there was an immediate reduction in UH_2:U ratio, the ratio recovered within 4-8 weeks after liver resection. This study demonstrated that there are dynamic changes in the UH_2:U plasma ratio after liver resection. Based on the results, we concluded that assessment of the UH_2:U plasma ratios one day after liver resection might lead to underestimation of DPD activity. Therefore, DPD phenotype-guided fluoropyrimidine dosing based on the UH_2:U plasma ratio in samples that are collected shortly after liver resection is not recommended.

Besides DPD deficiency, there is growing evidence that polymorphisms in the gene encoding the fluoropyrimidine target enzyme TS, *TYMS*, are associated with treatment-induced toxicity. The study described in **chapter 6** focuses on the association between a genetic polymorphism, a G>C substitution (rs183205964), which is also known as the 2RC allele, in the 5'-untranslated region of *TYMS* and fluoropyrimidine-induced toxicity. The 2RC has previously been associated with reduced TS activity. In a cohort of 1605 patients, it was found that patients carrying this 2RC allele are at increased risk of developing early severe toxicity and treatment-related hospitalization after treatment with intravenous and oral fluoropyrimidines. One out of the 1605 patients carried the 2RC/2RC genotype. During treatment, this patient required hospitalization for severe fluoropyrimidine-induced toxicity. We determined the TS phenotype of this patient by assessing the TS activity in PBMCs, which was within the range of TS activity in the control population of healthy volunteers. Additional research is required to examine the association genetic variability in *TYMS* and the TS phenotype in patients treated with fluoropyrimidines.

Capecitabine pharmacokinetics

The third part of this thesis focuses on the pharmacokinetic properties of the registered and experimental tablet formulations of capecitabine. In **chapter 7**, we present a population pharmacokinetic model of capecitabine, its intermediate metabolites 5'-deoxy-5-fluorocytidine (dFCR), 5'-deoxy-5-fluorouridine (dFUR) and 5-FU, and the final metabolite fluoro-β-alanine (FBAL). This population model was developed using pharmacokinetic data from a large and heterogeneous group of patients (n=237) who were treated with the commercially available tablet formulations. In general, it was found that capecitabine absorption was rapid, but highly variable between patients and occasions. In patients who underwent partial and total gastrectomy for the treatment of cancer, the capecitabine absorption rate was increased by a factor 1.46 and 3.14, respectively. We also found that 5-FU elimination was reduced by 21.5% in patients who were heterozygous for the *DPYD**2A risk allele. This *DPYD**2A allele leads to the formation of non-functional DPD enzyme. The developed model adequately described the complexity of capecitabine and metabolite pharmacokinetics.

Currently available capecitabine formulations are immediate-release tablets of which the pharmacokinetic profile can be characterized by rapid absorption and elimination. Within each 12-hour dosing interval, there is a period of approximately 6 hours with no significant plasma exposure to capecitabine and its metabolite 5-FU. An extended-release

formulation of capecitabine could provide more gradual exposure, which might lead to better treatment efficacy and safety. In **chapter 8**, we describe the results of a phase 0 pharmacokinetic study in which the pharmacokinetic properties of several candidate extended-release (ER) tablet formulations of capecitabine were explored. The examined ER formulations varied with respect to the amount of extended release excipients in the tablet matrix and tablet coating. Increasing the amount of ER excipient in the tablet matrix did not lead to sustained capecitabine exposure in plasma. Prolongation of capecitabine exposure was, however, possible by increasing the amount of ER excipient in the tablet coating. Modulation of the capecitabine pharmacokinetics was feasible by adapting the thickness of the ER tablet coating. Additional pharmaceutical and clinical research needed for optimization of the ER formulation and to examine the clinical applicability of ER capecitabine.

Cytotoxic fluoropyrimidine metabolites that possess anticancer properties are formed after intracellular activation of 5-FU. There is limited data available on the intracellular pharmacokinetics of the cytotoxic metabolites. To gain more insight, an exploratory study of intracellular pharmacokinetics of cytotoxic fluoropyrimidine metabolites was performed (**chapter 9**). The concentrations of cytotoxic metabolites were measured in PBMCs that were collected from a total of 18 patients who were treated with capecitabine. The only active metabolite that could be quantified in PBMCs was 5-fluorouridine 5'-triphosphate (FUTP). This metabolite inhibits cell proliferation by interfering with RNA synthesis. Opposite to the capecitabine and 5-FU concentrations in plasma, intracellular concentrations of FUTP accumulated after 14 days of treatment with capecitabine. Additional research is warranted to examine the clinical significance of intracellular FUTP pharmacokinetics.

Capecitabine chronotherapy

The final part of this thesis describes an interim analysis of a phase I study of chronomodulated capecitabine therapy (**chapter 10**). In this study, capecitabine was given twice daily, on 9:00 and 24:00 h, in a continuous dosing regimen. The daily capecitabine dose was divided in a morning and evening dose with a ratio of 3:5. The evening dose was administered at 24:00 h in order to obtain capecitabine and 5-FU peak exposure at the time of the anticipated peak in DPD activity. At the time of interim analysis, four dose levels were examined. The capecitabine dose in dose level four was 2000 mg/m^2/day. Dose-limiting toxicity has not been observed yet. The dose intensity in dose level four is approximately 20% higher than for the registered dosing regimen of 1250 mg/m^2 twice daily on day 1-14 of each 21-day cycle. Capecitabine chronotherapy is promising and might lead to better treatment safety and efficacy.

In conclusion, safe and effective treatment with fluoropyrimidines remains challenging. The studies presented in this thesis lead to a better understanding of fluoropyrimidine pharmacology and provide new methods that might lead to improved treatment safety.

NEDERLANDSE SAMENVATTING

Fluoropyrimidines zijn antikanker geneesmiddelen die veelvuldig worden toegepast bij de behandeling van gastro-intestinale kankers en bij borstkanker. Het fluoropyrimidine 5-fluorouracil (5-FU) is sinds tientallen jaren beschikbaar en is nog steeds een van de meest effectieve behandeling bij deze verschillende vormen van kanker. Voor de behandeling van deze tumoren wordt 5-FU toegediend via een intraveneus infuus. Het succes van dit geneesmiddel heeft er toe geleid dat er patiëntvriendelijkere fluoropyrimidines zijn ontwikkeld. Capecitabine, een prodrug van 5-FU, kwam ongeveer 15 jaar geleden beschikbaar in tabletformuleringen. Een groot voordeel van capecitabine is dat het door patiënten zelf, in de thuissituatie, kan worden ingenomen. Na inname van de capecitabine tabletten wordt het geneesmiddel snel geabsorbeerd en wordt het via drie enzymatische reacties omgezet in 5-FU.

Zoals voor veel andere chemotherapeutica worden capecitabine en 5-FU gedoseerd op de maximale toelaatbare dosering. Dit is de hoogste dosering die door de patiënten in de vroege klinische studies nog net werd verdragen. In de dagelijkse praktijk zijn er echter ook patiënten die deze dosering niet kunnen verdragen. Sommige patiënten krijgen te maken met zeer ernstige, soms zelfs levensbedreigende, bijwerkingen, zoals diarree en mucositis, bij behandeling met een standaard dosering. Het blijft een uitdaging om de patiënten die een groot risico lopen op ernstige bijwerkingen van een fluoropyrimidine bij aanvang van de behandeling te identificeren. Het algemene doel van de studies die beschreven zijn in dit proefschrift is om de veiligheid van behandeling met fluoropyrimidines te verbeteren.

Methodes om behandeling met fluoropyrimidines te optimaliseren

Deel I van dit proefschrift bestaat uit drie hoofdstukken waarin de ontwikkeling en validatie van drie verschillende analytische methodes wordt beschreven. Deze methodes zijn ontwikkeld om de activiteit van twee enzymen die belangrijk zijn voor het activeren en afbreken van capecitabine te kunnen meten. In **hoofdstuk 1 en 2** staat het enzym dihydropyrimidine dehydrogenase (DPD) centraal. Dit enzym is belangrijk voor het onschadelijk maken van 5-FU. Patiënten met een deficiëntie in DPD breken 5-FU minder snel af en lopen daarmee een groter risico om ernstige toxiciteit. Het is van belang om de fluoropyrimidine dosering aan te passen op basis van de individuele DPD activiteit. Om doseringsaanpassingen op basis van het DPD fenotype te realiseren, dient de DPD activiteit van patiënten nauwkeurig gemeten kunnen worden.

Een methode om DPD activiteit te bepalen is gebaseerd op kwantitatieve bepaling van het endogene DPD substraat uracil (U) en het reactieproduct dihydrouracil (UH_2) in het plasma van patiënten. In veel voorgaande studies wordt de ratio van UH_2 ten opzichte van U, de UH_2:U ratio, als maat voor DPD activiteit gebruikt. **Hoofdstuk 1** beschrijft de ontwikkeling en de validatie van een nieuwe analytische methode om U en UH_2 te meten in humaan plasma. Deze methode is gebaseerd op 'ultra performance' vloeistofchromatografie gekoppeld met massa spectrometrie (UPLC-MS/MS). U en UH_2

worden middels eiwitprecipitatie uit het plasma geïsoleerd. Deze opwerkmethode zorgt er, samen met een korte analysetijd, voor dat U en UH_2 snel bepaald kunnen worden. Middels validatie-experimenten werd aangetoond dat de ontwikkelde methode gevoelig en nauwkeurig is voor het bepalen van U en UH_2 in plasma.

Hoofdstuk 2 gaat over de ontwikkeling en validatie van een andere methode om DPD activiteit te meten. Bij deze methode wordt het DPD fenotype van een individu bepaald aan de hand van de hoeveelheid gevormde 5,6-dihydrothymine na *ex vivo* metabolisme van het DPD substraat thymine. Deze reactie wordt gekatalyseerd door het enzym DPD dat in het eiwitextract van witte bloedcellen voorkomt. De benodigde witte bloedcellen worden verkregen middels een centrifugetechniek waarbij de witte bloedcellen gescheiden worden van andere bloedcellen in volbloed op basis van dichtheid. We ontdekten dat de geïsoleerde witte bloedcellen vaak verontreinigd zijn met hemoglobine, wat een negatief effect heeft op de nauwkeurigheid van de DPD meting. Een simpele spectrofotometrische analysemethode is ontwikkeld om de mate van hemoglobine verontreiniging te meten, zodat we hiervoor kunnen corrigeren. Hierdoor kan de DPD activiteit nauwkeuriger bepaald worden. De methode werd verder verbeterd door de totale hoeveelheid radioactieve activiteit in de gemeten monsters te gebruiken als interne standaard. Resultaten van de validatie-experimenten toonden aan dat de methode specifiek, gevoelig en nauwkeurig is voor het bepalen van DPD activiteit in witte bloedcellen.

Het is bekend dat DPD belangrijk is voor het onschadelijk maken van 5-FU. Daarnaast is ook bekend dat het enzym thymidine fosforylase (TP) belangrijk is voor de activatie van 5-FU naar cytotoxische metabolieten. Een relatief hoge TP activiteit kan leiden tot grotere omzetting van capecitabine en 5-FU tot actieve metabolieten. Bij het voorspellen van ernstige toxiciteit door fluoropyrimidines zou het van belang kunnen zijn om meer informatie over het TP fenotype te hebben. De ontwikkeling en validatie van een methode voor het meten van TP activiteit in witte bloedcellen wordt beschreven in **hoofdstuk 3**. De TP activiteit werd bepaald aan de hand van de omzetting van het TP-substraat thymidine naar thymine. Op basis van de hoeveelheid thymine die gevormd werd, hetgeen gemeten werd met behulp van een vloeistofchromatografisch systeem met een ultraviolet detector, werd de TP activiteit vastgesteld. Middels validatie-experimenten werd aangetoond dat de juistheid en precisie van deze methode acceptabel was. Daarnaast werd de klinische toepasbaarheid van de methode aangetoond door de TP activiteit in witte bloedcellen van vijf patiënten succesvol te bepalen.

Variatie in de fenotypes van gezonde vrijwilligers en patiënten

In het tweede deel van dit proefschrift worden translationele en klinische studies beschreven waarin de ontwikkelde fenotypische methodes worden toegepast. In **hoofdstuk 4** onderzoeken we bij gezonde vrijwilligers of er een circadiaan ritme is in de enzymactiviteit van DPD en thymidylaat synthase (TS). Het enzym TS is belangrijk voor de synthese van DNA. Blokkade van TS door fluoropyrimidines wordt gezien als het belangrijkste werkingsmechanisme van deze geneesmiddelen. De activiteit van TS activiteit

&

werd ook gemeten in witte bloedcellen. Uit de studie blijkt dat de enzymactiviteit van DPD en TS onderhevig zijn aan circadiane variabiliteit. DPD activiteit in witte bloedcellen was het hoogst in het begin van de nacht. Op hetzelfde moment was TS activiteit in witte bloedcellen het laagst. In tegenstelling tot DPD activiteit in witte bloedcellen, was de UH_2:U ratio in plasma juist het laagst gedurende het begin van de nacht. Vooral DPD activiteit in witte bloedcellen vertoonde een sterk circadiaan ritme met een verhouding van de hoogste tot de laagste activiteit van 1.69. Het circadiaan ritme in de UH_2:U plasma ratio was minder sterk. Het verschil in circadiane variatie in DPD activiteit wordt mogelijk in de verschillende weefsels op een andere manier gereguleerd. Op basis van het sterke circadiaan ritme in DPD activiteit in witte bloedcellen zijn we een fase I studie gestart waarin we onderzoeken wat de rol van deze circadiane variatie is op de veiligheid van de behandeling met capecitabine (**hoofdstuk 10**).

Het enzym DPD komt sterk tot expressie in de lever. In **hoofdstuk 5** tonen we aan dat de UH_2:U plasma ratio in patiënten met colorectale levermetastasen verandert na resectie van de levermetastasen. De mediane UH_2:U plasma ratio verlaagde van 10.7, gemeten voor de resectie, naar 5.5 een dag na de partiële leverresectie. De daling in de UH_2:U ratio is mogelijk het gevolg van een de daling in hepatische DPD activiteit. Hoewel er een directe daling in de UH_2:U ratio was aangetoond, herstelde deze ratio 4-8 weken na de leverresectie. Deze studie toonde aan dat de UH_2:U ratio onderhevig is aan dynamische veranderingen na leverresectie. Op basis van deze resultaten werd geconcludeerd dat het bepalen van de UH_2:U plasma ratio een dag na leverresectie mogelijk tot onderschatting van de DPD activiteit leidt. Het is daarom af te raden om fluoropyrimidine dosisaanpassingen door te voeren op basis van de UH_2:U ratio in plasma dat kort na leverresectie is verzameld.

Behalve DPD deficiëntie is er ook meer wetenschappelijke bewijs voor een associatie tussen polymorfismen in het gen dat codeert voor TS, *TYMS*, en het optreden van ernstige bijwerkingen bij behandeling met fluoropyrimidines. In de studie die beschreven staat in **hoofdstuk 6** wordt de associatie tussen een genetisch polymorfisme, een G>C substitutie (rs183205964), dat ook wel bekend staat als het 2RC allel, in het 5' niet-getransleerde gebied van *TYMS* en ernstige bijwerkingen ten gevolge van behandeling met fluoropyrimidines onderzocht. In eerder onderzoek bleek de TS activiteit verlaagd te zijn door het 2RC allel. Op basis van een studiepopulatie bestaande uit 1605 patiënten bleek een associatie te bestaan tussen het 2RC allel en het optreden van ernstige toxiciteit en ziekenhuisopnames in een vroeg stadium van de behandeling met fluoropyrimidines. Een van de 1605 patiënten had het 2RC/2RC genotype. Deze patiënt was eerder opgenomen geweest in het ziekenhuis ten gevolde van ernstige toxiciteit. Het TS fenotype van deze patiënt werd door ons bepaald door de TS activiteit in witte bloedcellen te meten. De gemeten TS activiteit viel echter binnen de referentiewaardes die we eerder in gezonde vrijwilligers hadden bepaald. Verder onderzoek is nodig om een associatie tussen genetische variatie in *TYMS* en het TS fenotype vast te stellen bij patiënten die behandeld worden met fluoropyrimidines.

&

Farmacokinetiek van capecitabine

Het derde deel van dit proefschrift gaat over de farmacokinetiek van capecitabine na toediening van de geregistreerde en experimentele tablet formuleringen. In **hoofdstuk 7** presenteren we een populatie farmacokinetisch model van capecitabine, de eerste drie metabolieten 5'-deoxy-5-fluorocytidine (dFCR), 5'-deoxy-5-fluorouridine (dFUR) en 5-FU, en de laatst gevormde metaboliet fluoro-β-alanine (FBAL). Het model was ontwikkeld op basis van farmacokinetische data van een grote en heterogene patiëntenpopulatie. Capecitabine werd na inname van de commercieel beschikbare tabletten in het algemeen snel geabsorbeerd, maar dat verschilde sterk tussen patiënten en per innamemoment. Bij patiënten die eerder een partiële of totale gastrectomie hadden ondergaan voor de behandeling van kanker was de opname een factor 1.46 en 3.14 sneller ten opzichte van de andere patiënten in de populatie. Tevens vonden we dat de eliminatie van 5-FU met 21.5% was verlaagd bij patiënten die heterozygoot waren voor het *DPYD**2A allel. Dit *DPYD**2A allel leidt tot de formatie van niet-functioneel DPD enzym. Het ontwikkelde model geeft een nauwkeurige beschrijving van farmacokinetiek van capecitabine en de metabolieten.

De commercieel beschikbare capecitabine tabletten zorgen ervoor dat capecitabine na inname snel wordt opgenomen. Het farmacokinetische profiel van capecitabine laat zich kenmerken door een snelle absorptie en eliminatie. Door deze farmacokinetische eigenschappen is er een periode van ongeveer 6 uur binnen ieder doseerinterval van 12 uur waarin er geen blootstelling is aan capecitabine en de metaboliet 5-FU in plasma. Een nieuwe tabletformulering die zorgt voor gereguleerde afgifte van capecitabine zou ervoor kunnen zorgen dat er voor een langere periode blootstelling is aan capecitabine en 5-FU. Dit kan mogelijk leiden tot verbeterde effectiviteit en veiligheid van capecitabine. In **hoofdstuk 8** beschrijven we een fase 0 studie waarin we de farmacokinetische profielen van verschillende prototype gereguleerde afgifte tabletten onderzoeken. Het verschil tussen deze prototype tabletten was de hoeveelheid hulpstof, die gereguleerde afgifte dient te faciliteren, in de tablet matrix en coating. Uit het onderzoek bleek dat het verhogen van deze hulpstof in de tablet matrix geen verlengde afgifte van capecitabine teweeg bracht. De hoeveelheid hulpstof in de tablet coating had echter wel grote invloed op de afgifte van capecitabine. Door de hoeveelheid van de hulpstof in de tabletcoating te vergroten werd een steeds sterkere vertraagde afgifte van capecitabine in patiënten waargenomen. Op basis van dit onderzoek concludeerden we dat het mogelijk is om de capecitabine afgifte te moduleren met behulp van een tabletcoating. Verder farmaceutisch en klinisch onderzoek is nodig om de formulering voor verlengde afgifte van capecitabine te optimaliseren en het klinische effect ervan te onderzoeken.

Cytotoxische fluoropyrimidine metabolieten die een anti-kanker effect teweeg brengen worden pas gevormd nadat 5-FU in cellen wordt geactiveerd. Er is weinig bekend over de intracellulaire farmacokinetiek van deze cytotoxische metabolieten. De studie in **hoofdstuk 9** was uitgevoerd om meer informatie te verkrijgen over de intracellulaire farmacokinetiek van deze metabolieten. Bij 18 patiënten die behandeld werden met capecitabine werden witte bloedcellen geïsoleerd. In deze witte bloedcellen werd

bepaald hoeveel actieve metaboliet er intracellulair aanwezig was. De enige metaboliet waarvan de intracellulaire concentraties goed bepaald kon worden was 5-fluorouridine 5'-trifosfaat (FUTP). FUTP zorgt, door middel van blokkade van de RNA synthese, ervoor dat proliferatie van tumorcellen wordt geremd. In tegenstelling tot capecitabine en 5-FU concentraties in plasma, bleek dat FUTP concentraties accumuleerden bij patiënten die voor 14 dagen behandeld werden met capecitabine. Verdere klinische studies zijn nodig om de klinische relevantie van intracellulaire farmacokinetiek van FUTP te onderzoeken.

Capecitabine chronotherapie

In het laatste deel van dit proefschrift wordt een interim analyse van een fase I studie met capecitabine chronotherapie beschreven (**hoofdstuk 10**). In deze studie werd capecitabine twee maal per dag ingenomen, om 9:00 uur en om 24:00 uur, in een continu behandelschema. De dagdosering werd verdeeld tussen de ochtend- en avonddosis met een ratio van 3:5. De avonddosering diende om 24:00 uur ingenomen te worden, om maximale capecitabine en 5-FU plasmaconcentraties te bereiken rond de tijd dat de DPD activiteit op het hoogste punt van de dag is. Ten tijde van de interim analyse waren er vier dosisniveaus onderzocht, waarvan een dosering van 2000 mg/m^2/dag tot nu toe het hoogst was. Ernstige, ontoelaatbare, toxiciteit werd nog niet waargenomen. De dosisintensiteit in het vierde dosisniveau is ongeveer 20% hoger dan wat er bereikt wordt met het geregistreerde gebruik van capecitabine (tweemaal daags 1250 mg/m^2 op dag 1-14 van iedere 21-daagse cyclus). Capecitabine chronotherapie is veelbelovend en kan mogelijk leiden tot verbeterde capecitabine veiligheid en effectiviteit.

&

In conclusie, het realiseren van een veilige en effectieve behandeling met fluoropyrimidines blijft uitdagend. De studies die beschreven worden in dit proefschrift dragen bij aan een betere begrip van de farmacologie van fluoropyrimidines. Daarnaast worden er in dit proefschrift nieuwe methodes gepresenteerd die mogelijk bijdragen aan een veiligere behandeling met fluoropyrimdines.

DANKWOORD

Mijn periode als promovendus in het Antoni van Leeuwenhoek heb ik als ontzettend leerzaam en plezierig ervaren. Dit heeft voor een groot deel te maken met het interessante onderwerp waaraan ik heb mogen werken. Maar het eindresultaat, zoals beschreven in dit proefschrift, zou er niet geweest zijn zonder de inzet en begeleiding van vele anderen. Iedereen die een bijdrage heeft kunnen leveren aan dit werk ben ik ontzettend dankbaar.

Op de eerste plaats wil ik de patiënten bedanken die vrijwillig hebben deelgenomen aan de klinische studies. Zonder hen was het niet mogelijk geweest om het onderzoek naar nieuwe toedieningsvormen en behandelschema's van capecitabine uit te voeren. Verder wil ik ook graag de vrijwilligers die een nacht in het Slotervaartziekenhuis hebben doorgebracht voor het onderzoek naar circadiane ritmes bedanken.

In het bijzonder wil ik mijn promotoren, prof. dr. Jan Schellens en prof. dr. Jos Beijnen bedanken. Beste Jan, jouw enorme toewijding en ambitie hebben mij vanaf het begin van onze samenwerking erg geïnspireerd. Ik heb veel bewondering voor je grote expertise binnen het klinisch-farmacologische onderzoek en je manier van organiseren en motiveren. Bedankt voor de mogelijkheden die je me geboden hebt om dit onderzoek uit te voeren en het vertrouwen dat je me gegeven hebt tijdens deze leerzame periode. Beste Jos, ik heb grote waardering voor je ambitie om te innoveren in farmaceutische formuleringen en bioanalytische bepalingen. Ik heb erg veel gehad aan je kritische en leerzame commentaar op de diverse studieprotocollen, presentaties en manuscripten. Ontzettend bedankt voor jullie bijdrage.

&

Mijn co-promotor dr. Bastiaan Nuijen wil ik bedanken voor de goede begeleiding bij de onderzoeksprojecten die vanuit Modra zijn geïnitieerd. Ook buiten deze projecten heb ik je begeleiding en de samenwerking als zeer prettig ervaren.

Daarnaast wil ik prof. dr. Alwin Huitema bedanken. Beste Alwin, we hebben veelvuldig overleg gehad over de farmacokinetische analyses die in dit proefschrift zijn beschreven. Je enorme enthousiasme en je vermogen om razendsnel tot de kern van een onderzoeksprobleem te komen vind ik ontzettend inspirerend en leerzaam. Hartelijk dank voor de goede begeleiding.

Dr. Serena Marchetti, als hoofdonderzoeker van twee klinische studies was je zeer betrokken bij mijn projecten. Je hebt me erg geholpen bij de uitvoer van deze studies en het interpreteren van de data. Daarnaast heb je een kritische en leerzame bijdrage geleverd aan de manuscripten van deze studies. Ontzettend bedankt.

Dr. Hilde Rosing, het merendeel van de studies dat beschreven staat in dit proefschrift had niet plaats kunnen vinden zonder de verschillende bioanalytische bepalingen die onder jouw supervisie zijn ontwikkeld. Hartelijk dank voor je uitstekende hulp.

De leden van mijn leescommissie, prof. dr. R. Masereeuw, prof. dr. A. de Boer, prof. dr. A.J. Gelderblom, dr. A.B.P. van Kuilenburg en prof. dr. A.D.R. Huitema, wil ik bedanken voor de beoordeling van mijn proefschrift.

Prof. dr. Richard van Hillegersberg, dr. Miriam Koopman, dr. Nikol Snoeren, Morsal Samim van het UMCU wil ik bedanken voor de samenwerkingen bij het onderzoek naar de veranderingen in dihydrouracil:uracil ratio in patiënten na leverresectie.

Dr. Neeltje Steeghs en dr. Frans Opdam wil ik bedanken voor de betrokkenheid bij de klinische studies. De verpleegkundig specialisten, (kinetiek)verpleegkundigen, secretaressen en alle andere medewerkers van de afdeling Klinische Farmacologie wil ik bedanken voor de ondersteuning bij de klinische studies. Dankzij jullie inzet zijn deze studies uitstekend verlopen. Fijn dat jullie ervoor zorgden dat er altijd een bed voor me klaar stond tijdens mijn nachtelijke kinetieksessies. Marja, dank voor de organisatie van het klinische onderzoek.

Jolanda Slijkerman en Mirna Ekelschot - van Diermen, in de afgelopen jaren zijn jullie organisatorische talenten erg waardevol geweest. Dank voor jullie hulp en de gezelligheid.

De medewerkers van het laboratorium van de apotheek wil ik bedanken voor alle hulp bij de bioanalyse. Niels, dank voor de hulp bij het opzetten en valideren van de uracil assay en voor je hulp bij het meten van de capecitabine monsters. Matthijs en Abadi, ook jullie wil ik bedanken hulp bij de bioanalyse van capecitabine.

De CRA's Yvonne en Regina wil ik bedanken voor de ondersteuning bij de klinische studies.

De stagiaires Martin, Anna en Pia hebben een grote bijdrage geleverd aan verschillende projecten. Ik heb jullie met zeer veel plezier begeleid tijdens jullie onderzoeksstages. Dank voor de inzet en het enthousiasme.

Voor de mooie tijd op C2 wil ik mijn directe collega's, Robin, Dick, Artur, Geert, Rik, Vincent, Didier, Emilie, Bojana, Jill, Linda, Marit, Mark, Ruud en Sanne bedanken. Ook de OIO's uit 'de keet' wil ik bedanken voor de fijne tijd. De oud-OIO's Maarten, Didier en Ellen wil ik bedanken voor de samenwerking bij de verschillende projecten. Coen en Huixin, bedankt voor jullie hulp bij NONMEM.

Dick, van jou heb ik de kneepjes van het fenotyperen van DPD activiteit geleerd. Zelfs midden in de nacht heb je me nog eens geholpen bij isoleren van PBMCs. Dank voor al je hulp bij het bepalen van de enzymactiviteiten.

Beste vrienden, dank voor alle interesse die jullie getoond hebben en voor de gezelligheid en ontspanning!

Uiteraard wil ik mijn paranimfen in het bijzonder bedanken. Vincent, ooit zijn we samen begonnen met de studie biomedische wetenschappen. Drie jaar later besloten we allebei om farmacie te gaan studeren. Sinds die tijd zijn we ontzettend goed bevriend geraakt. Je bent altijd op zoek naar nieuw avontuur, wat onder meer heeft geleid in gezamenlijke trips naar Californië, Sint-Petersburg en Zwitserland. Waar gaat de volgende reis naar toe? Ik waardeer onze vriendschap zeer en fijn dat je mijn paranimf wilt zijn. Robin, het was ontzettend plezierig om een kleine vier jaar naast jou in kamertje 2047 te zitten. Het viel me op dat ik je in al die jaren niet een dag chagrijnig heb meegemaakt. Altijd positief. Naast de gezelligheid kon ik onze discussies over het onderzoek ook erg waarderen. Ik heb genoten van onze (soms wel wanhopige) avonturen op de Jaap Edenbaan. Bedankt voor deze mooie tijd en dank dat je mijn paranimf wilt zijn.

Lieve pap en mam, jullie onvoorwaardelijke steun heeft er toe geleid dat Niek en ik allebei onze ambities hebben na kunnen streven. Het valt met geen woord te beschrijven hoe trots ik ben dat jullie mijn ouders zijn. Dank voor alles!

Lieve Jet, toen ik begon als promovendus in Amsterdam leerden wij elkaar net wat beter kennen. Wat is er toch veel veranderd en wat ben ik ben ik daar ontzettend blij mee! Sinds een paar jaar wonen we samen en sinds kort genieten we iedere dag ons lieve zoontje Louis. Ontzettend veel dank voor al je steun, geduld, en liefde!

Bart

&

LIST OF PUBLICATIONS

Meulendijks D, Henricks LM, van Kuilenburg ABP, **Jacobs BAW**, Aliev A, Rozeman L, Meijer J, Beijnen JH, de Graaf H, Cats A, Schellens JHM. Patients homozygous for DPYD c.1129-5923C>G/haplotype B3 have partial DPD deficiency and require a dose reduction when treated with fluoropyrimidines. *Cancer Chemother Pharmacol. 2016 Aug 20; Epub ahead of print*

Jacobs BAW, Rosing H. de Vries N, Meulendijks D, Henricks LM, Schellens JHM, Beijnen JH.Development and validation of a rapid and sensitive UPLC-MS/MS method for determination of uracil and dihydrouracil in human plasma. *J Pharm Biomed Anal. 2016 Jul 15; 126:75-82*

Jacobs BAW, Deenen MJ, Pluim D, van Hasselt JGC, Krähenbühl MD, van Geel RM, de Vries N, Rosing H, Meulendijks D, Burylo AM, Cats A, Beijnen JH, Huitema ADR, Schellens JHM. Pronounced between-subject and circadian variability in thymidylate synthase and dihydropyrimidine dehydrogenase enzyme activity in human volunteers. *Br J Clin Pharmacol. 2016 Sep;82(3):706-16*

Jacobs BAW, Meulenaar J, Rosing H, Pluim D, Tibben MM, de Vries N, Nuijen B, Huitema ADR, Beijnen JH, Schellens JHM, Marchetti S. A phase 0 clinical trial of novel candidate extended-release formulations of capecitabine. *Cancer Chemother Pharmacol. 2016 Jun;77(6):1201-7*

Martial LC, **Jacobs BAW**, Cornelissen EAM, de Haan AFJ, Koch BCP, Burger DM, Aarnoutse RE, Schreuder MF, Brüggemann RJ. Pharmacokinetics and target attainment of mycophenolate in pediatric renal transplant patients. *Pediatr Transplant. 2016 Jun;20(4):492-9*

Derissen EJB, **Jacobs BAW**, Huitema ADR, Rosing H, Schellens JHM, Beijnen JH. Exploring the intracellular pharmacokinetics of the 5-fluorouracil nucleotides during capecitabine treatment. *Br J Clin Pharmacol. 2016 May;81(5):949-57*

Meulendijks D, **Jacobs BAW**, Aliev A, Pluim D, van Werkhoven E, Deenen MJ, Beijnen JH, Cats A, Schellens JHM. Increased risk of severe fluoropyrimidine-associated toxicity in patients carrying a G>C substitution in the first 28-bp tandem repeat of thymidylate synthase 2R allele. *Int J Cancer. 2016 Jan 1; 138(1):245-53*

Jacobs BAW, Opdam FL, Rodenhuis S, Baars JW. Reciverende luchtweginfecties tijdens en na rituximab. *Ned Tijdschr Geneeskd. 2015;159:A8546*

Pluim D, **Jacobs BAW**, Deenen MJ, Ruijter AEM, Van Geel RMJM, Burylo AM, Meulendijks D, Beijnen JH, Schellens JHM. Improved pharmacodynamic assay for dihydropyrimidine dehydrogenase activity in peripheral blood mononuclear cells. *Bioanalysis. 2015, Mar;7(5):519-29*

Pluim D, **Jacobs BAW**, Krähenbühl MD, Ruijter AEM, Beijnen JH, Schellens JHM. Correction of peripheral blood mononuclear cell cytosolic protein for hemoglobin contamination. *Anal Bioanal Chem. 2013, Mar; 405(7):2391-5*

Pluim D, Schilders KAA, **Jacobs BAW**, Vaartjes D, Beijnen JH, Schellens JHM. Pharmacodynamic assay of thymidylate synthase activity in peripheral blood mononuclear cells. *Anal Bioanal Chem. 2013, Mar; 405(8):2495-503*

&

CURRICULUM VITAE

Bart Jacobs was born in Winssen on September 27th, 1985. He graduated from high school at the Dominicus College in Nijmegen in 2004. Thereafter, Bart moved to Utrecht to study Biomedical Sciences. In 2008, he obtained his Bachelor's degree in Biomedical Sciences and completed the Pre-Master's programme for Pharmacy. In the same year, he started with the Master's programme Pharmacy. During this period, he performed a six-month research internship at the laboratory of dr. G. Gauvreau and prof. dr. P. O'Byrne at the Department of Medicine of McMaster University in Hamilton, Canada. There, Bart studied the role of the peroxisome proliferator-activator receptor gamma (PPAR-γ) agonist rosiglitazone on neutrophil activation and the immediate effect of fluticasone on the late allergic reaction and airway responsiveness in mild asthmatics. Directly after obtaining his Pharmacist degree in 2011, he started his PhD project at the Netherlands Cancer Institute – Antoni van Leeuwenhoek hospital under supervision of prof. dr. J.H.M. Schellens, prof. dr. J.H. Beijnen and dr. B. Nuijen. During the following years Bart was also trained as a clinical pharmacologist. In September 2015, he started as a hospital pharmacist in training at the Antoni van Leeuwenhoek hospital.

Bart Jacobs werd op 27 september 1985 geboren in Winssen. Hij behaalde zijn VWO diploma aan het Dominicus College in Nijmegen in 2004. Vervolgens verhuisde Bart naar Utrecht om daar Biomedische Wetenschappen te studeren. In 2008 behaalde hij het bachelordiploma en voltooide hij ook de premaster opleiding Farmacie. Aansluitend begon hij aan de masteropleiding Farmacie. Gedurende deze opleiding ging hij voor een stage van zes maanden naar McMaster University in Hamilton, Canada om onderzoek te doen in de groep van dr. G. Gauvreau en prof. dr. P. O'Byrne binnen de afdeling Geneeskunde. Daar onderzocht hij het effect van de 'peroxisome proliferating-activator receptor gamma' (PPAR-γ) agonist rosiglitazon op de activatie van neutrofielen en onderzocht hij het directe effect van fluticason op de late allergische reactie en luchtwegweggevoeligheid bij patiënten met milde astma. Na het behalen van zijn apothekersdiploma in 2011, begon hij zijn promotieonderzoek bij het Nederlands Kanker Instituut – Antoni van Leeuwenhoek ziekenhuis onder supervisie van prof. dr. J.H.M. Schellens, prof. dr. J.H. Beijnen en dr. B. Nuijen. Gedurende de jaren daarna volgde Bart tevens de opleiding tot klinisch farmacoloog. Vanaf september 2015 werkt hij als ziekenhuisapotheker in opleiding bij het Antoni van Leeuwenhoek ziekenhuis.

&